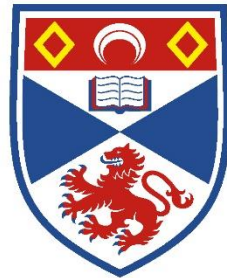


Gene knock-in as a tool to phenotype clinically
relevant variant alleles for studies on malaria
pathobiology: Proof of concept using the
Plasmodium knowlesi Normocyte Binding Protein
Xa gene

Scott Baxter Millar, BSc



University of
St Andrews

This thesis is submitted in partial fulfilment for the degree of PhD

at the

University of St Andrews

Date of Submission: 27-03-17

Declaration

1. Candidate's declarations:

I Scott Millar hereby certify that this thesis, which is approximately ..39700.. words in length, has been written by me, and that it is the record of work carried out by me, or principally by myself in collaboration with others as acknowledged, and that it has not been submitted in any previous application for a higher degree.

I was admitted as a research student in March, 2013 and as a candidate for the degree for the degree of PhD in March, 2013; the higher study for which this is a record was carried out in the University of St Andrews between 2013 and 2017.

(If you received assistance in writing from anyone other than your supervisor/s):

I,, received assistance in the writing of this thesis in respect of [language, grammar, spelling or syntax], which was provided by

Date signature of candidate

2. Supervisor's declaration:

I hereby certify that the candidate has fulfilled the conditions of the Resolution and Regulations appropriate for the degree of in the University of St Andrews and that the candidate is qualified to submit this thesis in application for that degree.

Date signature of supervisor

3. Permission for publication: *(to be signed by both candidate and supervisor)*

In submitting this thesis to the University of St Andrews I understand that I am giving permission for it to be made available for use in accordance with the regulations of the University Library for the time being in force, subject to any copyright vested in the work not being affected thereby. I also understand that the title and the abstract will be published, and that a copy of the work may be made and supplied to any bona fide library or research worker, that my thesis will be electronically accessible for personal or research use unless exempt by award of an embargo as requested below, and that the library has the right to migrate my thesis into new electronic forms as required to ensure continued access to the thesis. I have obtained any third-party copyright permissions that may be required in order to allow such access and migration, or have requested the appropriate embargo below.

The following is an agreed request by candidate and supervisor regarding the publication of this thesis:

PRINTED COPY

- a) ~~No embargo on print copy~~
- b) Embargo on all or part of print copy for a period of 2 years (maximum five) on the following ground(s):
 - Publication would be commercially damaging to the researcher, or to the supervisor, or the University
 - Publication would preclude future publication
 - ~~Publication would be in breach of laws or ethics~~
- e) ~~Permanent or longer term embargo on all or part of print copy for a period of ... years (the request will be referred to the Pro-Provost and permission will be granted only in exceptional circumstances).~~

Supporting statement for printed embargo request if greater than 2 years:

ELECTRONIC COPY

- ~~a) No embargo on electronic copy~~
- b) Embargo on all or part of electronic copy for a period of 2 years (maximum five) on the following ground(s):
 - Publication would be commercially damaging to the researcher, or to the supervisor, or the University
 - Publication would preclude future publication
 - ~~Publication would be in breach of law or ethics~~
- ~~e) Permanent or longer term embargo on all or part of electronic copy for a period of ... years (the request will be referred to the Pro-Vost and permission will be granted only in exceptional circumstances).~~

Supporting statement for electronic embargo request if greater than 2 years:

ABSTRACT AND TITLE EMBARGOES

An embargo on the full text copy of your thesis in the electronic and printed formats will be granted automatically in the first instance. This embargo includes the abstract and title except that the title will be used in the graduation booklet.

If you have selected an embargo option indicate below if you wish to allow the thesis abstract and/or title to be published. If you do not complete the section below the title and abstract will remain embargoed along with the text of the thesis.

- a) I agree to the title and abstract being published YES
- b) I require an embargo on abstract NO
- c) I require an embargo on title NO

Date signature of candidate signature of supervisor

Please note initial embargos can be requested for a maximum of five years. An embargo on a thesis submitted to the Faculty of Science or Medicine is rarely granted for more than two years in the first instance, without good justification. The Library will not lift an embargo before confirming with the student and supervisor that they do not intend to request a continuation. In the absence of an agreed response from both student and supervisor, the Head of School will be consulted. Please note that the total period of an embargo, including any continuation, is not expected to exceed ten years.

Where part of a thesis is to be embargoed, please specify the part and the reason.

Acknowledgements

Firstly, I would like to acknowledge my supervisor Dr Janet Cox-Singh. Thank you for all the advice and continual support throughout the project and for giving me the opportunity to work with you.

To Dr Miguel Pinheiro for assistance with Bioinformatics, you made everyone around you happier. A special thanks go to Dr Rob Moon for the *in vitro* culture, plasmids and allowing me to spend time in your Lab to perform transfection studies. I am incredibly grateful for your generosity. I would also like to extend my thanks and appreciation to Dr Franziska Mohring for monitoring transfections in my absence.

A particular thanks must go to the Tay Charitable Trust, and Elizabeth Mussen who provided crucial financial support to continue my work, for which I am extremely thankful.

I would also like to acknowledge my PhD committee for their encouragement and guidance and to all in the Infection Group for providing stimulating discussion and useful insight. My thanks are also extended to all our honours and summer medical students; Freddie, Dawnn, Joshua, Akash and Ben, it was a pleasure to teach and have you in the lab.

To Dr Laura Aitken, Dr Zoe Allen, Madhurima Dey, Sophie Ferguson, Dr Patrick Guest, Dr Robert Hammond, Kate Haley, Dr John Kennedy, Ben Reilly-O'Donnell, Gavin Robertson, Dr Robert Shore and Dr Andrew Tilston-Lunel, thank you for all the insightful discussions, wisdom and fun times in the lab as well as the constant borrowing of reagents. I will pay you all back in the pub (as long as it's Mennies!).

This thesis would not have been completed without the unwavering support from my friends, family and Lindsey. I am very appreciative of your encouragement and for not letting me give up when stress levels were high. You have been my constant source of motivation.

This thesis is dedicated to my Grandparents.

Abstract

The zoonotic parasite, *Plasmodium knowlesi*, is one of five human malaria species. *P. knowlesi* is geographically restricted to locations of the long-tailed and pig-tailed macaque, indigenous across South-East Asia (SEA). Initial research showed that *P. knowlesi* was present in the human population in Malaysian Borneo, with subsequent studies confirming *P. knowlesi* throughout SEA. *P. knowlesi* cases were shown to be both severe (10%) and lethal (2%), with hyperparasitaemia correlating with severe malaria. Recent work has identified a polymorphism in the essential *P. knowlesi* normocyte binding protein Xa (*Pknbpxa*) gene that associates with high parasitaemia. The aims of this study were firstly to enhance and standardise the isolation of parasite DNA from a Biobank of frozen clinical isolates. Alongside this we aimed to take *P. knowlesi* whole genome sequence data and identify further mutations in the *Pknbpxa* gene linked to severe disease and express these in an *in vitro* *P. knowlesi* experimental line.

Detailed here is the optimisation of the Whatman-Plasmodipur method to purify *P. knowlesi* DNA from a Biobank of frozen clinical samples. This resulted in 13/22 samples returning greater than 70% *P. knowlesi* DNA and within this, 8 samples were suitable for genome sequencing. Genome sequence data representing cluster type 2 was used to inform the synthesis and construction of a *Pknbpxa* synthetic gene representing clinical alleles. Single-crossover homologous recombination was used to replace the native *Pknbpxa* with this synthetic copy, containing polymorphisms associated with high parasitaemia. This was subsequently transfected into the *P. knowlesi* A.1-H.1 clone via nucleofection, resulting in an experimental line expressing clinically relevant mutations within the essential PkNBPXa invasion gene. The construction of this translational approach enables functional examination for mutation involvement in parasite erythrocyte invasion and contribution to severe disease.

Contents

Acknowledgements.....	4
Abstract	6
Abbreviations.....	17
Chapter 1: Introduction.....	20
1.1 Malaria General Information.....	21
1.1.1 Malaria: the statistics.....	21
1.1.2 A brief history of malaria	22
1.1.3 Plasmodium the causative agent.....	23
1.1.4 Global malaria distribution.....	24
1.1.5 Epidemiology of <i>P. knowlesi</i>	25
1.1.6 <i>P. knowlesi</i> natural hosts and mosquito vectors	26
1.1.7 Treatment and prevention of malaria	29
1.1.8 Pathology and classification of disease severity	31
1.2 <i>Plasmodium</i> Life Cycle.....	32
1.2.1 Clinical presentation of <i>P. knowlesi</i> malarial in humans	36
1.3 Severe Malaria Pathophysiology.....	37
1.3.1 Features of severe malaria	37
1.3.2 Sequestration in <i>P. falciparum</i>	37
1.3.3 Sequestration in <i>P. knowlesi</i>	40
1.3.4 Hyperparasitaemia and severe malaria.....	41
1.3.5 Parasite polymorphisms in severe malaria	41
1.4 Models to Study Malaria Pathophysiology	42
1.5 Invasion: How do Merozoites Invade Host Erythrocytes?.....	45
1.5.1 The merozoite	49
1.5.2 Merozoite attachment and reorientation	50
1.5.3 Junction formation.....	53
1.5.4 Actin-myosin mediated invasions	54
1.5.5 Shedding of the merozoite surface proteins	56
1.6 Egress	57
1.7 Invasion Blocking Vaccine Candidates.....	58
1.8 Merozoite Invasion Proteins.....	60

1.8.1	Duffy binding proteins	60
1.8.2	Reticulocyte binding protein family.....	63
	Project aims and objectives	70
	Chapter 2: Materials and Methods.....	72
Section 1:	List of Reagents.....	73
Section 2:	Cell Culture	77
2.1	Cell Culture Solutions	77
2.1.1	D-glucose.....	77
2.1.2	Heat inactivation of serum.....	77
2.1.3	Sodium hydroxide	77
2.1.4	Hypoxanthine	77
2.1.5	L-glutamine	78
2.1.6	Incomplete medium	78
2.1.7	Complete medium	78
2.1.8	Optiprep synchronisation solution.....	79
2.1.9	Histodenz stock solution.....	79
2.1.10	Histodenz synchronisation solution.....	79
2.1.11	Freezing solution	79
2.1.12	Cryoretrieval solution.....	80
2.1.13	Phosphate buffered solution pH 7.2	80
2.1.14	Cytomix transfection solution (pH 7.6).....	80
2.2	Cell Culture Techniques.....	81
2.2.1	Blood collection.....	81
2.2.2	Preparation of blood for parasite culture	81
2.2.3	Routine <i>in vitro</i> culture of the <i>P. knowlesi PkA1-H.1</i> clone in human erythrocytes	81
2.2.4	Parasite synchronisation using MACS LD column.....	82
2.2.5	Optiprep synchronisation.....	82
2.2.6	Histodenz gradient synchronisation	83
2.2.7	Cryopreservation	83
2.2.8	Cryoretrieval.....	84
2.2.9	Monitoring <i>in vitro PkA1-H.1</i> cultures.....	84
Section 3:	Microscopy.....	86

2.3.1	Permeabilisation solution	86
2.3.2	Blocking solution.....	86
2.4	Microscopy Techniques	87
2.4.1	Light microscopy.....	87
2.4.2	Immunocytochemistry	87
2.4.3	Fluorescence microscopy	88
Section 4:	Molecular Biology	89
2.5	Molecular Biology Reagents.....	89
2.5.1	Tris-Borate-EDTA (TBE) (1x).....	89
2.5.2	Sodium acetate pH 5, 3 M	89
2.5.3	Phosphate buffered saline (PBS) (1x concentration).....	89
2.5.4	Tris- buffered saline (TBS) 10x concentration.....	89
2.5.5	Tris-buffered saline (TBS) 1x concentration.....	89
2.5.6	Tris-buffered saline 0.1% Tween® 20 (TBS-T)	90
2.6	Molecular Biology Methods.....	91
2.6.1	Qubit DNA quantification	91
2.6.2	NanoDrop 2000	91
2.6.3	Gel electrophoresis	91
2.6.4	Restriction digestion of plasmid DNA	92
2.6.5	Gel extraction	92
2.6.6	Ligations	93
2.6.7	DNA extraction from blood samples.....	93
2.6.8	InstaGene DNA extraction	94
2.6.9	Ethanol precipitation	95
2.6.10	DNA sequencing to verify cloning steps.....	95
2.6.11	Restriction digestion of plasmid DNA for transfection.....	95
2.6.12	PCR.....	96
Section 5:	Microbiology.....	99
2.7	Reagents for Microbiology.....	99
2.7.1	Ampicillin stock	99
2.7.2	LB broth.....	99
2.7.3	LB agar plate preparation	99
2.8	Bacterial Culture Techniques	100

2.8.1	Heat shock bacterial transformation.....	100
2.8.2	Bacterial cell electroporation.....	100
2.8.3	Starter culture	101
2.8.4	Overnight culture.....	101
2.8.5	Glycerol stock.....	101
2.8.6	Plasmid DNA extraction from starter culture <i>E. coli</i>	101
2.8.7	Plasmid DNA extraction from overnight culture <i>E. coli</i>	102
Chapter 3: Purification of <i>P. knowlesi</i> DNA from Frozen Whole Blood Samples 104		
3.1	Introduction	105
3.2	Methods.....	108
3.2.1	Whole blood seeded with <i>PkA1-H.1</i> <i>in vitro</i> culture.....	108
3.2.2	TaqMan quantitative PCR of <i>P. knowlesi</i> and human DNA	108
3.2.3	<i>P. knowlesi</i> and human DNA standard curves	111
3.2.4	Whatman leukocyte depletion method	111
3.2.5	Plasmodipur leukocyte depletion method	112
3.2.6	Whatman-Plasmodipur leukocyte depletion method.....	112
3.2.7	Fold reduction of DNA following leukocyte depletion.....	114
3.3	Results	115
3.3.1	Generation of standard curves for <i>P. knowlesi</i> and human DNA....	115
3.3.2	Plasmodipur leukocyte depletion of seeded whole blood	117
3.3.3	Whatman-Plasmodipur leukocyte depletion of clinical samples.	119
3.4	Discussion	127
Chapter 4: <i>Plasmodium knowlesi</i> A1-H.1 transfection to knock-in a clinically relevant variant of the gene <i>Pknbpxa</i>		
4.1	Introduction	134
4.2	Methods.....	137
4.2.1	Next generation sequence alignment.....	137
4.2.2	Variant call analysis	137
4.2.3	<i>Pknbpxa</i> DNA sequence extraction.....	138
4.2.4	Nucleotide diversity calculation	138
4.2.5	Selection of <i>Pknbpxa</i> cluster 2 variation	139
4.2.6	Synthesis of the cluster 2 <i>Pknbpxa</i> gene	141
4.2.7	Restriction digestion of the <i>PkconGFP</i> plasmid	143

4.2.8	Sequential ligation of synthetic <i>Pknbpxa</i> Cluster 2 fragments 1-3 into the PkconGFP plasmid	146
4.2.9	Identification of further mutations in <i>Pknbpxa</i> cluster 2 linked with S200P	146
4.2.10	Site-directed mutagenesis	147
4.2.11	Transfection and drug selection.....	149
4.2.12	Transfection of the <i>P. knowlesi</i> <i>PkA1-H.1</i> experimental line with <i>Pk_{con}Pknbpxa_f1-3</i> plasmids	150
4.2.13	Limiting dilution to clone transfected parasite lines	153
4.2.14	Integration PCR to confirm Pk _{con} <i>Pknbpxa</i> integration at the <i>Pknbpxa</i> locus.....	154
4.3	Results	156
4.3.1	Assembly of full length <i>Pknbpxa</i> gene sequences from clinical isolates	156
4.3.2	Defining the <i>Pknbpxa</i> cluster 2 sequence.....	158
4.3.3	Synthesis of a cluster 2 type <i>Pknbpxa</i> gene.....	158
4.3.4	Constructing the <i>Pk_{con}Pknbpxa_f1-3</i> transfection plasmid	161
4.3.5	Transfecting the <i>P. knowlesi</i> <i>PkA1-H.1</i> experimental line.....	172
4.3.6	PCR to demonstrate construct integration in the Tf11.4 line	174
4.3.7	Identification and generation of mutations associated with high parasitaemia	177
4.3.8	Transfection of the <i>P. knowlesi</i> <i>A1-H.1</i> clone with <i>Pknbpxa</i> cluster 2 S200P, G420E and S733N	179
4.3.9	Immunofluorescence staining of the HA-tagged PkNBPXa in transfected parasite lines.....	183
4.3.10	Dilution cloning of the Tf13.1 line.....	184
4.4	Discussion	188
Chapter 5: Summary and future perspectives		195
Chapter 6: Appendices.....		202
Appendix A: Cytomix Transfection Buffer		203
Appendix B: Ethics, Information and Consent forms		204
Appendix C: PkDNA retrieval vs Trophozoite percentage		212
Appendix D: Amino Acids Defining Cluster 2 Type <i>Pknbpxa</i>		213
Appendix E: Synthetic <i>Pknbpxa</i> generation and validation		214
Appendix F: Cloning validation, Restriction digests and Sequencing results.....		218

Appendix G: Alignment of PkNBPXa clinical sequences	226
Appendix H: Site Directed Mutagenesis Validation	255
Appendix I: Growth Monitoring of Tf11.4 Pk _{con} <i>Pknbpxa_f1-3</i>	261
Appendix J: Uncropped Integration PCR gel images	261
Appendix K: Publications	264

List of Tables

Table 1.1.	Features of <i>Plasmodium</i> species causing malaria in humans.....	29
Table 1.2	Currently known RBP and DBP proteins in <i>P.falciparum</i> , <i>P. vivax</i> and <i>P. knowlesi</i>	69
Table 2.1	Restriction enzymes and compatible buffers.....	92
Table 2.2	Table of primers	97
Table 2.3.1	GoTaq® G2 Flexi PCR mastermix	98
Table 2.3.2	GoTaq® G2 Flex PCR cycling conditions	98
Table 3.1	Parasitaemia and percent life stage of seeded samples used for leukocyte depletion.....	108
Table 3.2	TaqMan probes used for qPCR.	110
Table 3.3	Mastermix for TaqMan multiplex qPCR.....	110
Table 3.4	TaqMan qPCR cycling conditions.....	111
Table 3. 5	Plasmodipur leukocyte depletion of frozen whole blood seeded with the <i>P. knowlesi PkAI-H.1</i> <i>in vitro</i> culture.	119
Table 3.6	Fold reduction and percent recovery of DNA following Plasmodipur leukocyte depletion of frozen whole blood seeded with the <i>P. knowlesi PkAI-H.1</i> <i>in vitro</i> culture.	121
Table 3.7	Post-Plasmodipur leukocyte depletion of clinical samples calculated by qPCR.....	123
Table 3.8	Fold reduction and percent recovery of Whatman-Plasmodipur depleted <i>P. knowlesi</i> frozen clinical samples.	126
Table 4.1	Site directed mutagenesis cycling conditions.....	148
Table 4.2	Primers used to create mutant copies of $Pk_{con}Pknbp_xa_f2$	148
Table 4.3	Genotyping PCR amplicons for the native and transfected <i>Pknbp_xa</i> locus*.....	155
Table 4.4	Nucleotide diversity, synonymous and non-synonymous mutations for clinical <i>Pknbp_xa</i> gene sequences.....	157

Table 4.5	Cloning Strategy for the cluster 2 type synthetic gene.....	163
Table 4.6	Transfection optimisation.....	167

Table of Figures

Figure 1.1	Global distribution of malaria in 2016.	23
Figure 1.2	Geographical distribution of the hosts and vectors of <i>P. knowlesi</i>	28
Figure 1.3	Plasmodium life cycle.	35
Figure 1.4	Schematic showing <i>P. falciparum</i> merozoite invasion of a susceptible erythrocyte.....	47
Figure 1.5	The structure of the invasive merozoite	48
Figure 1.6	Proposed mechanisms involving the Actin-Myosin motor complex.	55
Figure 1.7	Proposed model of PfRh5 binding to the merozoite and erythrocyte surface.....	66
Figure 3.1	Schematic of TaqMan probe qPCR.....	109
Figure 3.2	Standard curve of human DNA generated to accurately quantify hDNA in clinical samples.....	116
Figure 3.3	Standard curve of <i>P. knowlesi</i> DNA generated to accurately quantify PkDNA in clinical samples.	117
Figure 3.4	Total human DNA yield following Whatman-Plasmodipur depletion of frozen clinical samples.	124
Figure 3.5	Total <i>P. knowlesi</i> DNA yield following Whatman-Plasmodipur depletion of frozen clinical samples.	125
Figure 4.1	Haplotype network of the dimorphic 885 bp fragment of <i>Pknbpxa</i>	136
Figure 4.2	Schematic showing the locations of the residues in the <i>Pknbpxa</i> protein defining cluster 2.....	140
Figure 4.3	Schematic of the <i>Pknbpxa</i> gene fragments and location of restriction sites used for cloning.	143
Figure 4.4	Schematic of Pk _{con} <i>Pknbpxa</i> _f1-3 construct linearized at the KpnI restriction site.	144
Figure 4.5	Map of the PkconGFP and Pkconp230pGFP transfection plasmids.	145
Figure 4.6	Alignment of the region of homology in <i>Pknbpxa</i> _f1 and <i>Pknbpxa</i> _f2 codon optimized fragments representing cluster 2.....	159

Figure 4.7	Amino acid sequence alignment of the 3 clinical PkNBPXa sequences with the corrected <i>P. knowlesi</i> PkNBPXa reference sequence.....	160
Figure 4.8	Confirmation of <i>Pknbpaxa</i> fragment ligation by sequencing.....	162
Figure 4.9	Map of the Pk _{con} GFP <i>Pknbpaxa_f1</i> plasmid.	164
Figure 4.10	Map of the Pk _{con} <i>Pknbpaxa_f1-2</i> plasmid.	165
Figure 4.11	Map of the Pk _{con} <i>Pknbpaxa_f1-3</i> plasmid.	166
Figure 4.12	Comparison of synchronisation methods to isolate segmented schizonts prior to transfection.	173
Figure 4.13	Schematic for stable genomic integration of the cluster 2 type <i>Pknbpaxa</i>	175
Figure 4.14	Integration PCR showing failed Tf11.4 transfection.....	176
Figure 4.15	Creation of the S200P mutation in the pMA-RQ_ <i>Pknbpaxa_f2</i> construct.	178
Figure 4.16	Successful integration of the cluster 2 type construct at the <i>Pknbpaxa</i> locus.....	182
Figure 4.17	Successful integration of the GFP construct into the <i>p230p</i> locus...	183
Figure 4.18	Detection of the HA tagged <i>Pknbpaxa</i> cluster 2 type protein in schizonts isolated from the Tf13.1 experiment.	186

Abbreviations

Aa	Amino acid
AMA-1	Apical membrane antigen 1
bp	Base pairs
BSA	Bovine serum albumin
CD36	Cluster of differentiation 36
CR1	Complement receptor 1
CyRPA	Cysteine-rich protective antigen
DARC	Duffy antigen receptor for chemokines
DBL	Duffy binding like
DBP	Duffy binding protein
DNA	Deoxyribonucleic acid
DV	Digestive vacuole
EBA	Erythrocyte binding antigen
EMP1	Erythrocyte membrane protein 1
GAP	Glideosome associated protein
GPI	Glycosylphosphatidylinositol
HA	Hemagglutinin
hDNA	Human DNA
iRBCs	Infected red blood cells
ICAM-I	Intercellular adhesion molecule I
kb	Kilobasepairs
kDa	Kilodalton
MSP	Merozoite surface protein

MTIP	Myosin A tail interacting protein
MTRAP	Merozoite TRAP like protein
MyoXIV	Myosin XIV
NBP	Normocyte binding protein
nt	nucleotide
<i>Pf</i>	<i>Plasmodium falciparum</i>
PfDNA	<i>Plasmodium falciparum</i> DNA
PfEMP1	<i>P. falciparum</i> erythrocyte membrane protein 1
<i>Pk</i>	<i>Plasmodium knowlesi</i>
PkDNA	<i>P. knowlesi</i> DNA
<i>Pm</i>	<i>Plasmodium malariae</i>
<i>Po</i>	<i>Plasmodium ovale</i>
<i>Pv</i>	<i>Plasmodium vivax</i>
PV	Parasitophorous vacuole
RBC	Red Blood Cell
RBP	Reticulocyte-binding protein
rcf	Relative centrifugal force
Rh	Reticulocyte-binding protein homologue
PfRIPR	RH5-interacting protein
RNA	Ribonucleic acid
ROM	Rhomboid protease
RON	Rhoptry neck protein
SA	South America
SEA	South-East Asia
SERA	Serine repeat antigen

SSA	Sub-Saharan Africa
SICA	Schizont infected cell agglutination
SNP	Single nucleotide polymorphism
SP	Signal peptide
SUB	Subtilisin-like serine protease
T _a	Annealing temperature
TM	Transmembrane domain
TRAP	Thrombospondin-related adhesive protein
VCAM	Vascular cell adhesion molecule
v/v	Volume/volume
WHO	World Health Organisation
w/v	Weight/volume

Chapter 1: Introduction

1.1 Malaria General Information

1.1.1 Malaria: An introduction

Alarming statistics demonstrate malaria still remains one of the biggest global health issues in the world today. In 2016, there were over 3 billion people worldwide at risk of malaria, with an estimated 212 million cases and 429,000 deaths (WHO, 2016). Although the number of malaria cases has decreased over the last 16 years, there is still a large global burden with 91 malaria endemic countries, Figure 1.1 (WHO, 2016). As Figure 1.1 shows 90% of global malaria cases were in African regions, while only 7% of cases occurred in the South-East Asian region and the remaining 2% of cases reported in the Eastern Mediterranean region (WHO, 2016). When examining global malaria cases nine African countries feature in the top ten for percentage of global cases and Nigeria was estimated to have over 25% of global cases alone (WHO, 2016). It is reported that 70% of the global fatalities are of children under the age of 5 (WHO, 2016). The mortalities alone are predicted to cost malaria endemic countries 3.6% of their combined gross domestic product, without taking into account the much higher non-fatal case numbers (WHO, 2016). Currently treatment is available for malaria, yet drug-resistance is a concern and still the underlying mechanisms of disease pathology and parasite biology are not fully understood highlighting the requirement for further research on this devastating disease. However, considering the worldwide scale of this disease it is likely that a combined approach from governments, medical professionals and researchers will be required to eradicate malaria.

1.1.2 A brief history of malaria

One of the first descriptions of malaria came from an ancient Chinese medical textbook, the Nei Ching (Moss, 2008) which described periodic fever, a hallmark symptom of malaria (Cunha and Cunha, 2008, Cox, 2010). Fast-forwarding through time, further clinical observations were documented by Hippocrates in 400BC who recorded intermittent fever in combination with chills, sweating and enlargement of the spleen (Cox, 2010). The word malaria itself arose from the Romans who believed that poor air quality or “bad airs”, “mal’ aria” in Italian, around swamp and marsh land, was responsible for the characteristic fevers associated with malaria (Meshnick and Dobson, 2001). Although incorrect, the Romans had inadvertently connected the importance of stagnant water, the mosquito breeding grounds, with contracting malaria. However, the link between stagnant water, mosquitoes and fever was not connected until the late 19th century when the mosquito was implicated in transmitting malaria (Cox, 2010). Following publication of Louis Pasteur’s germ theory, Charles Laveran, a French military doctor, discovered the presence of parasites in the blood of a malaria patient (Laveran, 1982). Following this breakthrough discovery, research intensified identifying different parasite forms based on regularity of fever. This causative parasitic agent of malaria was termed *Plasmodium* (Cox, 2010).

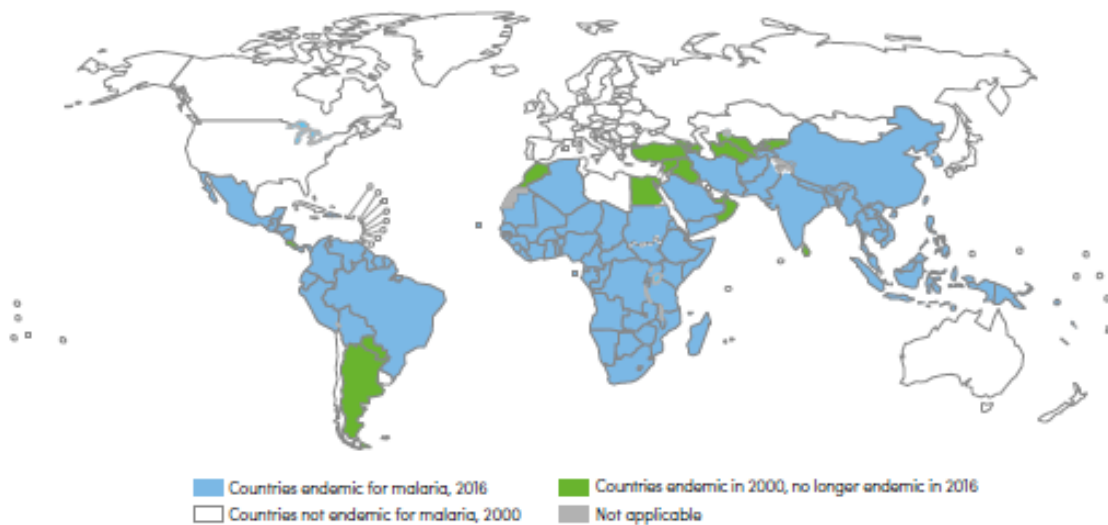


Figure 1.1 Global distribution of malaria in 2016.

A world map is shown highlighting the 91 countries in blue where malaria is endemic. Countries in green represent countries where malaria was endemic in 2000, but are no longer endemic in 2016. Countries with no colour were not endemic for malaria in 2000. No data is available for countries shaded in grey. Figure adapted from the World Malaria Report 2016 (WHO, 2016).

1.1.3 Plasmodium the causative agent

Malaria is caused by species of the genus *Plasmodium*, a member of the large Apicomplexan phylum. There are over 450 species of *Anopheles* mosquitoes (Cohuet *et al.*, 2010), capable of transmitting *Plasmodium* parasites responsible for causing malaria in a range of mammals, birds and reptiles. Of these Anopheline mosquitoes, approximately 60 species are capable of transmitting *Plasmodium* parasites that cause malaria in humans (Cohuet *et al.*, 2010). Currently 6 *Plasmodium* species have been reported in humans; *Plasmodium falciparum*, *P. vivax*, *P. knowlesi*, *P. malariae* and *P. ovale*, of which there are two subspecies, *P. ovale wallikeri* and *P. ovale curtisi* (Oguike *et al.*, 2011). Phylogenetically, the latter 5 species cluster with *Plasmodium* species that infect monkeys, while *P. falciparum* clusters with ape *Plasmodium* species. *P.*

falciparum is responsible for causing almost all deaths (99%) caused by malaria (WHO, 2016). In contrast, *P. vivax* is the second most common human malaria-causing species, and is responsible for only 0.7% of all malaria deaths (WHO, 2016). *P. vivax* is less likely to cause severe malaria as it is restricted to the invasion of reticulocytes, which comprise approximately 2% of all red blood cells. A naturally acquired human infection of the simian malaria *P. knowlesi* was reported but considered to be a rare event (Chin *et al.*, 1968). However, an important study revealed that there was a large number of human *P. knowlesi* cases in Kapit, Malaysian Borneo that were being microscopically misdiagnosed as *P. malariae* (Singh *et al.*, 2004). Morphologically *P. knowlesi* is similar to the early life stages of *P. falciparum* and the later stages of *P. malariae*, and PCR was required for accurate identification. Recently, a naturally acquired *P. cynomolgi* infection was reported (Ta *et al.*, 2014). This may suggest that *P. cynomolgi* is a zoonotic *Plasmodium* species.

1.1.4 Global malaria distribution

Over 3 billion people are at risk of malaria infection and transmission occurs in the tropical and sub-tropical belt (Figure 1.1, Table 1.1). Most of the reported cases (90%) occur in Sub-Saharan African countries and are caused by *P. falciparum*, the human malaria responsible for the highest prevalence of morbidity and mortality. *P. vivax* is distributed throughout the sub-tropical belt (Figure 1.1, Table 1.1), and contributes to approximately 41% of cases outside of Africa (WHO, 2016). *P. vivax* is rarely found in Africa as the majority of the African population lack the Duffy erythrocyte receptor required for *P. vivax* infection (Miller *et al.*, 1976). However recently cases of *P. vivax* have been reported in regions of Africa, suggesting invasion can occur independent of

the Duffy erythrocyte receptor (Mendes *et al.*, 2011, Ryan *et al.*, 2006, Wurtz *et al.*, 2011). *P. malariae* has the same distribution as *P. falciparum* and *P. ovale* and is primarily found in Sub-Saharan Africa (Figure 1.1, Table 1.1). *P. knowlesi*, as a zoonosis, is only found across areas of South-East Asia (SEA) where the geographical distribution of the natural host, the long-tailed or pig-tailed macaques, overlaps with mosquitoes belonging to the group *Anopheles leucosphyrus* (Lee *et al.*, 2011).

1.1.5 Epidemiology of *P. knowlesi*

P. knowlesi was previously believed to be a simian malaria that rarely infected humans, however, in 2004 it was identified that *P. knowlesi* malaria was being misdiagnosed as *P. malariae* (Singh *et al.*, 2004). *P. knowlesi* is unique compared to the other human malarias as it is zoonotic, naturally infecting *Macacca fascicularis* (long-tailed) and *Macacca nemestrina* (pig-tailed) (Coatney *et al.*, 1971, Garnham, 1966). The geographical distribution of these two macaque species can be seen in Figure 1.2 (Cox-Singh, 2012). This distribution shows that the natural hosts of *P. knowlesi* are found in areas of SEA, and since the discovery of *P. knowlesi* as a pathogen causing malaria in humans cases of *P. knowlesi* malaria have been reported in almost all countries within the boundaries of the natural host (Figure 1.2). Research has shown *P. knowlesi* to be the main cause of malaria in Malaysian Borneo, with relatively few *P. falciparum* and *P. vivax* cases, and few cases of *P. malariae* (Cox-Singh *et al.*, 2008, Singh *et al.*, 2004). Furthermore, the only country not to have reported human cases of *P. knowlesi* in SEA is Laos (Figtree *et al.*, 2010, Jiang *et al.*, 2010, Luchavez *et al.*, 2008, Jeslyn *et al.*, 2011, Jongwutiwes *et al.*, 2011, Sermwittayawong *et al.*, 2012, Khim *et al.*, 2011,

Marchand *et al.*, 2011, Maeno *et al.*, 2016). A recent study carried out in North Sumatra, Indonesia (Figure 1.2) showed that *P. knowlesi* was present in 11.8% of patients tested, levels similar to *P. vivax* and *P. falciparum* in that region (Lubis *et al.*, 2017). This result suggests that within this geographical region, *P. knowlesi* is important and occurs as frequently as *P. vivax* and *P. falciparum*. This suggests that as monitoring *P. knowlesi* infected macaques and humans increases, and in combination with more sensitive diagnostics, the exact range and prevalence of *P. knowlesi* infections across SEA will become clear.

1.1.6 *P. knowlesi* natural hosts and mosquito vectors

The geographical restriction of *P. knowlesi* to SEA (Figure 1.2) is determined by both the anopheline vectors responsible for transmitting *P. knowlesi*, and presence of either the long-tailed macaques or pig-tailed macaques indigenous to SEA (Lee *et al.*, 2011). Currently, transmission of *P. knowlesi* to humans is associated with entry or close proximity to the forest, the natural habitat of the macaques' (Daneshvar *et al.*, 2009). Human-to-human transmission of *P. knowlesi* has to date only been demonstrated under experimental transmission conditions (Chin *et al.*, 1965, Chin *et al.*, 1968). Only a small number of studies have been conducted to identify geographical locations in SEA where macaques are *P. knowlesi* positive. *P. knowlesi* infected long-tailed and pig-tailed macaques have been found in Singapore (Jeslyn *et al.*, 2011), Peninsular Malaysia (Vythilingam *et al.*, 2008), Malaysian Borneo (Lee *et al.*, 2011), Thailand (Jongwutiwes *et al.*, 2004), Palawan Island and the Philippines (Tsukamoto *et al.*, 1978).

The *Anopheles leucosphyrus* group of mosquitoes shows a similar distribution to that of the two macaque hosts (Figure 1.2). Both distributions overlap across the majority of

SEA with a few exceptions, such as southern regions of Indonesia (Figure 1.2). Presence of both the macaque hosts and the *Anopheles leucosphyrus* group of mosquito vectors are required for a geographical area to be classed as a potential *P. knowlesi* transmission area (Vythilingam and Hii, 2013). Within the *leucosphyrus* group of mosquitoes, there are a number of species reported to transmit *P. knowlesi*, including *A. cracens* (Jiram *et al.*, 2012), *A. dirus* (Marchand *et al.*, 2011, Maeno *et al.*, 2016), *A. balabacensis* (Vythilingam, 2010, Collins *et al.*, 1967), *A. latens* (Tan *et al.*, 2008) and *A. introlatus* (Vythilingam *et al.*, 2014). Interestingly, *A. cracens* was not observed in households, and feeding was exophagic, which in part might explain why human-to-human transmission has not been reported (Jiram *et al.*, 2012). Different members of the *Anopheles leucosphyrus* group have been implicated in *P. knowlesi* transmission in different geographical locations. Although only a handful of studies have examined the vectors of *P. knowlesi* however the geographical distribution of those that have been identified suggest further regions of transmission across SEA (Figure 1.2). An important observation made by Daneshvar and colleagues was that 87% of *P. knowlesi* patients had recently been in close proximity to a forest setting (Daneshvar *et al.*, 2009). This suggests that the primary transmission site is the forest setting, where both macaques and *Anopheles* mosquitoes are located (Lee *et al.*, 2011).

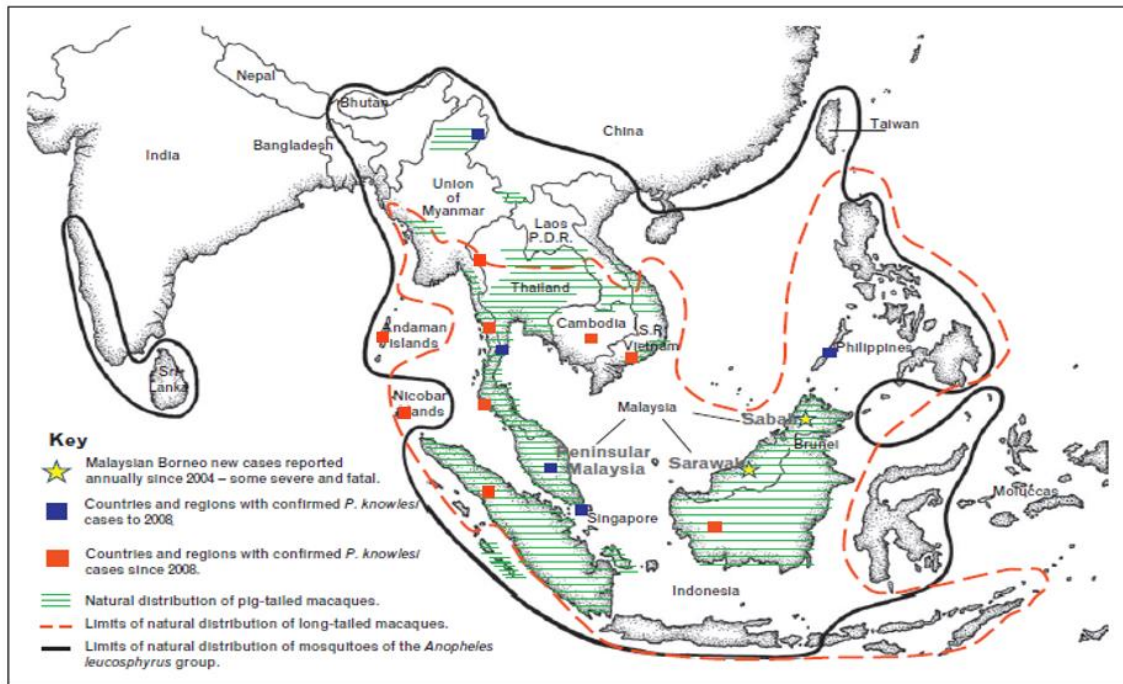


Figure 1.2 Geographical distribution of the hosts and vectors of *P. knowlesi*.

The map of SEA shows the countries that *P. knowlesi* vectors and macaque hosts are native to. The *A. leucosphyrus* group of mosquitoes (inside the black line) covers the majority of SEA, except some locations in Indonesia. The long-tailed macaques (orange dotted line) cover a similar range to the mosquito vector, although the range does not reach as far north, and the macaques are not found in India or Sri Lanka. The pig-tailed macaques (horizontal green lines) are less widespread, but are predominantly found in Borneo, Peninsular Malaysia, Thailand and Indonesia. Countries with cases of human *P. knowlesi* malaria reported before 2008 are shown by a blue square, while cases reported after 2008 are shown by an orange box. More recent data has also been added (Lubis *et al.*, 2017)(Figure adapted from Cox-Singh 2012).

Table 1.1. Features of *Plasmodium* species causing malaria in humans

<i>Plasmodium</i> sp.	Naturally Infects	Geographic distribution	Erythrocytes invaded	Causes Severe Malaria
<i>falciparum</i>	Humans	SSA, SEA, SA	Normocytes	High % in non-immune
<i>vivax</i>	Humans	SEA, SA	Reticulocyte	Rare
<i>knowlesi</i>	Humans, Macaque sp.	SEA	Predicted - Normocytes	~10 % of cases
<i>ovale</i>	Humans	SSA	Reticulocytes	rare
<i>malariae</i>	Humans	SSA, SEA, SA	Senescent RBCs	rare

SSA- Sub-Saharan Africa;SEA- South-East Asia;SA South America

1.1.7 Treatment and prevention of malaria

Traditionally the bark from the Chinchona tree, was used as a herbal remedy for treatment of malaria (Meshnick and Dobson, 2001). It was not until the early 19th century that quinine was identified as the active compound (Achan *et al.*, 2011). Although quinine was effective it was costly and poorly tolerated, but is still used today to treat severe malaria (WHO, 2016, Meshnick and Dobson, 2001). In 1934, the antimalarial chloroquine was synthesised, and quickly became adopted as the primary treatment of malaria due to its cost effective production compared to the extraction of quinine, (Giadom *et al.*, 1996). Chloroquine functions by inhibiting the formation of hemozoin in the parasite's food vacuole, producing toxic haem intermediates causing parasite death (Sullivan *et al.*, 1996). Chloroquine was primarily used as a monotherapy across the world for both uncomplicated and severe malaria (Achan *et al.*, 2011). Although extremely effective, during the 1950s and 60s reports of chloroquine

resistance were arising (Eyles *et al.*, 1963, Wellems and Plowe, 2001). The resistance to chloroquine spread to almost all worldwide transmission areas, with the guideline that suspected *P. falciparum* malaria in Africa no longer be treated with chloroquine (WHO, 2016). Following the widespread resistance to chloroquine, two novel compounds, sulfadoxine and pyrimethamine, targeting the folate pathway inhibiting nuclear replication, were introduced in 1967 as a replacement for chloroquine. However, resistance to sulfadoxine/pyrimethamine was detected in a refugee camp in Thailand (Hurwitz *et al.*, 1981). A similar story is seen with mefloquine. It was brought into use in the mid-1980s (Price *et al.*, 2004) and again a pattern of resistance emerged as within 6 years mefloquine-resistant *P. falciparum* was identified (Wongsrichanalai and Meshnick, 2008).

The discovery of the compound artemisinin, isolated from the Chinese plant qinghaosu, merited the Nobel Prize in 2015 (White *et al.* 2015, Qinghaosu Antimalaria Coordinating Research Group 1979). This important new compound was not only found to have antimalarial properties, but also had better parasite clearance compared to previous antimalarials (White, 2011). Additionally, artemisinin has been reported as being well tolerated and fast acting (White *et al.*, 2015). These drugs are currently being used as combination therapies with pre-existing drugs to delay the onset of drug resistance. However, recent studies in SEA have shown that resistance in *P. falciparum* is developing against these latest antimalarials (Ashley *et al.*, 2014). New antimalarial compounds such as cipargamin, a spiroindolone targeting all stages of the erythrocytic cycle have undergone clinical testing with results suggesting cipargamin has a higher parasite clearance compared to artemisinin (Chavchich *et al.*, 2016, White *et al.*, 2014, Rottmann *et al.*, 2010). The compound DDD107498 targets a broad spectrum of

parasite life stages, including liver stages, erythrocytic stages, gametocytes and the sexual stages to oocysts (Baragana *et al.*, 2015). A primary concern will be over reliance on specific antimalarials, driving selection pressures and increases in resistance.

1.1.8 Pathology and classification of disease severity

Malaria can present as asymptomatic, uncomplicated or severe disease. Patients can be infected with *Plasmodium spp.* but are asymptomatic with no clinical symptoms (Laishram *et al.*, 2012). Uncomplicated malaria is characterised by presence of any range of the following symptoms; fever, chills, nausea, diarrhea, headache, abdominal pain and malaise (Bartoloni and Zammarchi, 2012). Clinical presentation can include any number of these non-specific symptoms, which can result in misdiagnosis, especially if not in areas of high transmission (Mahdavi *et al.*, 2014). Failure to diagnose these symptoms can lead to delayed treatment and an increased likelihood of progression to severe malaria and death (Rajahram *et al.*, 2013, Allen *et al.*, 2013). Severe malaria is characterised by convulsions, respiratory distress, circulatory shock, organ dysfunction, hyperparasitaemia and, in *P. falciparum*, coma (WHO, 2016, World Health Organisation, 2012). Children under the age of 5 are most at risk of severe malaria. Immunity in areas of high transmission is obtained through repeated infections and children under the age of 5 have not acquired this immunity yet, putting them at risk of severe disease (Doolan *et al.*, 2009). Severe malaria can occur in adults who enter high transmission areas that are either from low areas of transmission or from non-endemic areas. *P. falciparum* is the primary cause of severe malaria although both *P.*

vivax and *P. knowlesi* can cause severe malaria although only *P. knowlesi* can reach parasitaemias similar to those associated with severe *P. falciparum* infection (World Health Organisation, 2012, Rahimi *et al.*, 2014, Naing *et al.*, 2014, Daneshvar *et al.*, 2009).

1.2 Plasmodium Life Cycle

The *Plasmodium* life cycle is complex as it requires both a vertebrate and mosquito host (Bray and Garnham, 1982). Infection of the vertebrate host begins when a blood meal is taken by an infected female Anopheline mosquito from a susceptible vertebrate host (Coatney *et al.*, 1971). Sporozoites residing in the salivary glands of the mosquito are injected into the host, (Figure 1.3) and migrate to the liver from the host dermis (Jin *et al.*, 2007, Menard *et al.*, 2013). The sporozoites are able to migrate by exhibiting a gliding motility from the dermis to the lymph nodes and blood stream with some remaining in the dermis (Sinnis and Zavala, 2012). In order to continue the life cycle the sporozoites exit the blood stream in the liver and invade hepatocytes via invagination creating a parasitophorous vacuole (PV) where they undergo asexual replication, forming thousands of merozoites capable of invading host erythrocytes, Figure 1.3 (Stanway *et al.*, 2011). In *P. vivax* and *P. ovale* rather than undergoing immediate asexual replication in the liver a portion of sporozoites differentiate into quiescent hypnozoites which can remain dormant for months or years before asexual replication begins, however the mechanisms controlling these conversions remain unknown (Wells *et al.*, 2010, Markus, 2015, Hulden and Hulden, 2011). Following asexual replication and merozoite formation, breakdown of the PV releases the merozoites into the

cytoplasm of the hepatocyte (Prudencio *et al.*, 2006). Subsequently the merozoites bud off into the host's blood stream in hepatocyte derived vesicles termed merosomes (Graewe *et al.*, 2011, Tawk *et al.*, 2013, Baer *et al.*, 2007, Burda *et al.*, 2017).

Once in the blood stream, merozoites can attach to erythrocytes via their protein coat to initiate erythrocyte invasion, involving adhesive proteins secreted from merozoite apical organelles (detailed further in section 1.5). Interestingly some species of malaria have adapted to invade specific invasion susceptible erythrocytes. *P. vivax* and *P. ovale* are adapted to invade reticulocytes (immature red blood cells) while *P. malariae* is adapted to invade senescent (older) erythrocytes. Both *P. falciparum* and *P. knowlesi* can invade all erythrocyte ages (Moreno-Perez *et al.*, 2013, Antinori *et al.*, 2012), although some data suggests that reticulocytes are preferred by long standing experimental lines of *P. knowlesi* during *in vitro* culture (Lim *et al.*, 2013, Moon *et al.*, 2016). The early trophozoite/ring stage parasite exists within the PV and is named so because of the ring-shaped morphology (Figure 1.3). As the parasite matures to a trophozoite, known as the feeding stage, the parasite digests host haemoglobin in the digestive vacuole (DV) using this as a nutrient source for energy metabolism and for incorporation into newly expressed parasite proteins (Francis *et al.*, 1997). As further haemoglobin is digested the inert by-product hemozoin can be seen within the digestive vacuole (DV) (Dluzewski *et al.*, 2008). During trophozoite stages the DV is dilated with hemozoin diffusely spread throughout the DV (Wunderlich *et al.*, 2012).

A trophozoite can have two fates; maturation to schizonts, where multiple copies of merozoites are produced asexually (8-12 copies *P. knowlesi*, 16-20 copies *P. falciparum*, (Coatney *et al.*, 1971), or to enter the sexual life stage of the life cycle. The

most common trophozoite fate is to continue with asexual development producing multiple merozoites which can go on to infect further erythrocytes (Figure 1.3). As the trophozoite matures it develops into a schizont, characterised by rounds of mitotic division producing a multinucleated syncytium (Francia and Striepen, 2014). Upon the last mitotic division, the synchronous formation of individual daughter merozoites takes place which are released from the erythrocyte via a process termed egress (detailed further in section 1.6). The newly released merozoites are released into the blood stream allowing further erythrocytes to be invaded, creating a mounting parasitaemia producing the symptoms of malaria. The full erythrocytic cycle time varies depending on *Plasmodium* species (*P. knowlesi* 24 hours; *P. falciparum*, *P. vivax*, *P. ovale* 48 hours; *P. malariae* 72 hours). Alternatively, a small proportion of parasites develop into sexual parasite forms known as gametocytes (Josling and Llinas, 2015). These trophozoites are able to produce both male and female gametocytes which remain in the S phase of cell cycle development until taken up by a female mosquito during a blood meal (Bray and Garnham, 1982). In the mosquito mid-gut the male gametocyte undergoes exflagellation and fertilises the female gametocyte producing a zygote (Coatney *et al.*, 1971). The zygote develops into a motile ookinete that traverses the mosquito's midgut epithelium, permitting oocyst formation beneath the basal lamina in the subepithelial space (Carter *et al.*, 2007). The oocyst cytoplasm increases in size over 10-15 days whilst undergoing mitotic divisions producing a sporoblast from which thousands of sporozoites bud asynchronously (Prudencio *et al.*, 2006, Nacer *et al.*, 2008, Wang *et al.*, 2005, Gerald *et al.*, 2011). The sporozoites then migrate from the oocyst on the basal epithelial membrane to the salivary glands of the mosquito host (Coatney *et al.*, 1971). Once at this stage of the life cycle, when a mosquito takes a blood meal the cycle can repeat.

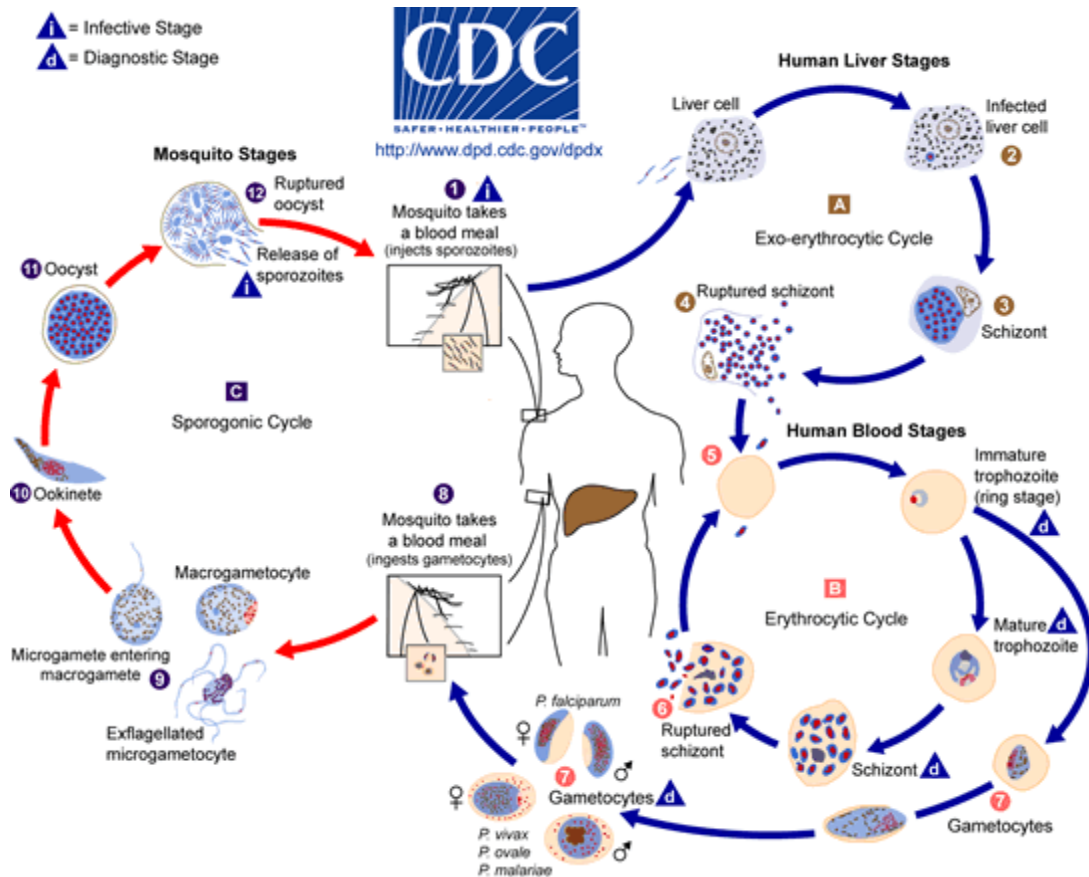


Figure 1.3 Plasmodium life cycle.

The asexual *Plasmodium* life cycle begins with inoculation of a human host by an Anopheline mosquito infected with *Plasmodium* sporozoites in the salivary glands (1). The sporozoites migrate to the liver via the blood stream and infect a liver cell (2), where multiple rounds of division produce thousands of merozoites contained within the liver cell (3). Rupture of the liver schizont (4) releases the merozoites into the blood stream (5) where they enter the erythrocytic cycle (B). Merozoites invade a susceptible RBC and are maintained in the asexual erythrocytic cycle where they digest host proteins using this as an energy source to grow and replicate producing anywhere between 8-30 merozoites depending on the *Plasmodium* species. Rupture of the schizont releases the merozoites which can remain in the erythrocytic cycle (B). Alternatively, newly invaded red blood cells (RBCs) can mature into male or female gametocytes (7), the early stage of sexual replication. The gametocytes are ingested by the mosquito (8) where the female gametocyte is fertilised by the male in the mosquito mid-gut (9). The zygote matures into an ookinete (10) which traversed the midgut epithelium and undergoes divisions beneath the basal lamina in the subepithelial space (11) creating an oocyst containing thousands of sporozoites. When the oocyst ruptures, the sporozoites migrate to the salivary glands where they can then be injected into a host upon the next blood meal (Centers for Disease, 2017).

1.2.1 Clinical presentation of *P. knowlesi* malarial in humans

Unlike other human *Plasmodium* species, *P. knowlesi* has a 24-hr life cycle. This results in fever every 24 hours, and can progress to severe disease rapidly if misdiagnosed, or treatment is delayed (Rajahram *et al.*, 2012). The majority of patients presenting with uncomplicated *P. knowlesi* malaria exhibit non-specific symptoms similar to uncomplicated *P. falciparum* malaria (Daneshvar *et al.*, 2009). The most common symptoms reported were fever/chills, rigors, headache, malaise, muscle pain and poor appetite (Daneshvar *et al.*, 2009). Laboratory results indicate that thrombocytopenia is a common feature of *P. knowlesi* malaria (Daneshvar *et al.*, 2009). Complications associated with severe *P. knowlesi* are as seen with severe *P. falciparum* malaria, but without coma (Cox-Singh *et al.*, 2010, Daneshvar *et al.*, 2009, Willmann *et al.*, 2012). The ranges on the proportion of *P. knowlesi* malaria cases that meet severe disease criteria varies drastically between study sites (9.5% - 39%) (Barber *et al.*, 2013, Willmann *et al.*, 2012, Cox-Singh *et al.*, 2011, William *et al.*, 2011). However, this is likely due to some study sites being based at referral hospitals (Barber *et al.*, 2013, William *et al.*, 2011). As with the reported disease severity rates, the fatality rates of *P. knowlesi* malaria vary between studies (1.8 - 10.7%) (Barber *et al.*, 2013, Willmann *et al.*, 2012, Cox-Singh *et al.*, 2011, William *et al.*, 2011, Daneshvar *et al.*, 2009).

1.3 Severe Malaria Pathophysiology

1.3.1 Features of severe malaria

A common feature of severe *P. falciparum* malaria is the sequestration of late stage parasites in the microvasculature resulting in removal infected RBCs (iRBCs) from peripheral blood circulation. This process prevents infected RBCs passing through the spleen preventing removal of iRBCs (Del Portillo *et al.*, 2012, White, 2017). Sequestration of iRBCs to different host tissues can result in different pathologies. For example sequestration and rosetting cause microvasculature obstruction in the brain that can produce cerebral malaria characterised by coma and death, while sequestration in the placenta of pregnant women can result in an increased risk of severe malaria, mortality and abortion (Kovacs *et al.*, 2015, Wahlgren *et al.*, 2017). The binding of iRBCs to microvasculature starves tissue of oxygen, resulting in increased lactate and a lower pH in the blood producing the symptoms of severe malaria discussed in section 1.1.8 (Wahlgren *et al.*, 2017).

1.3.2 Sequestration in *P. falciparum*

The PfEMP1 proteins are the primary cause of sequestration and are encoded by a multi-gene family termed the *var* genes. This antigenically variable gene family consists of approximately 60 copies (Gardner *et al.*, 2002). During the erythrocyte life cycle the parasite silences the majority of the *var* genes, resulting in mutually exclusive expression (Brancucci *et al.*, 2014, Perez-Toledo *et al.*, 2009, Guizetti and Scherf, 2013). The expressed *var* gene determines the cytoadherent properties of the iRBC as

the protein is anchored to knob structures on the erythrocyte surface enabling interactions with the endothelial cells to take place (Hviid and Jensen, 2015). Periodically a small number of parasites switch *var* gene expression, resulting in a PfEMP1 variant that has not been exposed to the immune system enabling immune evasion (Hviid and Jensen, 2015). The *var* genes that encode the PfEMP1 proteins can be grouped into 3 main groups (A-C) according to sequence similarity of the 5' upstream promoter that drives *var* gene transcription (Lavstsen *et al.*, 2003). Members of each group have a common chromosomal location, with group A encoded in the subtelomeric regions and group B are encoded in the telomeric regions while the group C *var* genes are located in central chromosomal regions (Tuikue Ndam *et al.*, 2017).

The PfEMP1 family consist of DBL domains, cysteine rich domain regions, transmembrane domains and an acidic terminal segment (Kraemer and Smith, 2006). Different domain combinations combined with variation within each domain enables variant PfEMP1 proteins to bind different endothelial surface receptors resulting in sequestration in different host tissues (Chakravorty *et al.*, 2008). PfEMP1 predominantly binds to the human CD36 receptor expressed across all endothelial cells except those in the brain (Kaestli *et al.*, 2006). PfEMP1 variants specific for chondroitin sulfate A (CSA) are responsible sequestration of infected erythrocytes to the placenta (Beeson *et al.*, 2002). The binding of PfEMP1 to intercellular adhesion molecule 1 (ICAM-1) on brain endothelium was implicated as the cause of cerebral malaria (Newbold *et al.*, 1999), however recent studies have implicated the presence of PfEMP1 variants containing the cysteine rich interdomain region in binding to host endothelial protein C receptor (EPCR) (Turner *et al.*, 2013). Additionally, an EPCR variant was identified to protect children in Thailand from severe malaria (Naka *et al.*, 2014).

In addition to PfEMP1 both RIFIN and STEVOR have been proposed to contribute to sequestration of iRBCs to endothelial cells (Bachmann *et al.*, 2009, Wahlgren *et al.*, 2017). The RIFIN proteins are encoded by a family of approximately 150 repetitive interspaced genes (*rif*) with 70% of these categorised as subgroup A (A-RIFIN) and remainder classified as subgroup B (B-RIFIN) (Goel *et al.*, 2015). As with PfEMP1, RIFINs have an extracellular N-terminal domain enabling interactions with the host (Goel *et al.*, 2015). Antibodies against A-RIFIN present in the FCR3S1.2 parasite clone were shown to disrupt rosettes specifically when cultured in blood group A RBCs (Goel *et al.*, 2015). However, rosetting was unchanged when parasites were cultured in blood group O RBCs in the presence of the same antibody, suggesting the specific A-RIFIN in this clone only bound the blood group A antigen on the RBC surface (Goel *et al.*, 2015). The rosetting as seen in parasites cultured with RBCs from blood group O has been attributed to the function of B-RIFIN binding glycophorin A on the erythrocyte surface (Goel *et al.*, 2015). Microvasculature sequestration was observed when iRBCs matured in blood group A were injected into rodents (Goel *et al.*, 2015, Wahlgren *et al.*, 2017). Although implicated in sequestration RIFINs are also expressed in merozoites and gametocytes, suggesting they may have a broader function (Wahlgren *et al.*, 2017).

The *stevor* gene family contain approximately 30 gene copies encoding the STEVOR proteins which are structurally similar to RIFINs (Wahlgren *et al.*, 2017). STEVORs bind to glycophorin C, similar to B-RIFINs that bind glycophorin A (Niang *et al.*, 2014). As with the RIFINs, STEVORs are expressed in merozoites and gametocyte stages, suggesting a wider ranging function (Wahlgren *et al.*, 2017). This may be the case, as Niang *et al.*, show that antibodies against STEVOR inhibited invasion by approximately 10-30%, and rosetting by approximately 50% (Niang *et al.*, 2014).

1.3.3 Sequestration in *P. knowlesi*

Although less thoroughly researched, *P. knowlesi* appears to exhibit cytoadhesion characteristics similar to those of *P. falciparum* infected erythrocytes. Sequestration has been documented in macaque infections (Miller *et al.*, 1971) but importantly it has also been observed in fatal human infections (Cox-Singh *et al.*, 2010). Post-mortem studies have shown that infected erythrocytes accumulated in the brain microvasculature in a patient that died of severe *P. knowlesi* malaria (Cox-Singh *et al.*, 2010). The schizont infected cell agglutination variant (*sicavar*) gene family is present in the genome of *P. knowlesi*, which show homology to the *var* genes in *P. falciparum* (Korir and Galinski, 2006) and homologues are not present in any other human malaria species (Galinski *et al.*, 2017). Unlike the *var* genes the *sicarvar* genes have not been classified or grouped according to the 5' upstream promoter region as in *P. falciparum*. Investigations into the functions of individual *sicavar* genes and SICA proteins may now accelerate with the annotations of the *sicavar* genes now complete (Lapp *et al.*, 2017). As seen with the *var* genes in *P. falciparum*, switching of *sicavar* genes occurs periodically resulting in the expression of different SICA antigens (Brown and Brown, 1965). Investigations into SICA endothelial receptor interactions has only been tested by incubating *ex vivo* matured schizonts on dishes coated with recombinant protein (Fatih *et al.*, 2012). Binding was variably to recombinant ICAM1 and vascular cell adhesion molecule (VCAM), but mature schizonts did not bind to CD36 (Fatih *et al.*, 2012). Further research is required to elucidate the contribution of the *sicavar* genes in severe malaria.

1.3.4 Hyperparasitaemia and severe malaria

In *P. falciparum*, the most widely studied human malaria, hyperparasitaemia is a feature of severe malaria and primarily affects children in Sub-Saharan African countries (Trampuz *et al.*, 2003, World Health Organisation, 2012). The laboratory marker for hyperparasitaemia is a parasitaemia greater than 100,000 para/ μ L for non-immune individuals, and greater than 250,000 para/ μ L for individuals residing in endemic countries (World Health Organisation, 2012). Recently, hyperparasitaemia was found to associate with an increased risk of progression to cerebral malaria in children under 5 (Sowunmi *et al.*, 2011). Severe complications of *P. knowlesi* malaria are also strongly linked with hyperparasitaemia (Daneshvar *et al.*, 2009). Parasite counts can reach 764,720 para/ μ L, densities similar to those seen in *P. falciparum* hyperparasitaemia (Cox-Singh *et al.*, 2008, Daneshvar *et al.*, 2009). The pathogenesis behind severe malaria in both *P. knowlesi* and *P. falciparum* remains unclear, although both host and parasite factors are thought to contribute to disease outcome (Cox-Singh *et al.*, 2010).

1.3.5 Parasite polymorphisms in severe malaria

A recent study performed by Ahmed *et al.*, (2014) identified an association between a single nucleotide polymorphism (913C) in the *P.knowlesi* invasion gene *Pknbpxa* and high parasitaemia (Ahmed *et al.*, 2014). *Pknbpxa* is essential to invasion of human erythrocytes (discussed further in section 1.8.2) suggesting that non-synonymous mutations in genes essential to the invasion process may affect merozoite invasion efficiencies (Moon *et al.*, 2016). Little research has been conducted on the contribution of parasite polymorphisms to severe malaria. However, polymorphisms were identified in the invasion genes EBA-140 and EBA-181 which affected the affinity of the protein

to erythrocytes (Maier *et al.*, 2009). Additionally, a case control study examining associations between severe malaria and polymorphisms in 6 virulence genes identified polymorphisms in both Rh1 and EBA-175 as associating with severe malaria (Chokejindachai and Conway, 2009). This suggests that polymorphisms in merozoite invasion proteins can potentially contribute to severe malaria, likely by an altered invasion phenotype. In order to conduct experiments on the contribution of invasion efficiencies or erythrocyte selection to the pathology of severe malaria would require an appropriate research model.

1.4 Models to Study Malaria Pathophysiology

During the 20th century, the tools and models available for malaria research have improved greatly and have become more accessible. One of the main developments was the ability to maintain the asexual erythrocytic stages in culture *in vitro* (Trager and Jensen, 1976, Haynes, 1976 #1312). Prior to this, studies were confined to *in vivo* and *ex vivo* work primarily using rodent and simian *Plasmodium* species (Brown *et al.*, 1968, Brown and Brown, 1965, Bannister *et al.*, 1975). *In vitro* cultures of *P. falciparum* are an important part of malaria research as this is the most deadly form of the disease. However, studies on pathophysiology are difficult to perform in *P. falciparum* as there is no natural *in vivo* model, although *P. falciparum* is infectious to several *Aotus* monkey species (Egan *et al.*, 2002, Herrera *et al.*, 2002). Currently, results from *P. falciparum* pathophysiology studies conducted *in vitro* must be translated to a *Plasmodium spp* with an appropriate *in vivo* model which may not comprehensively mirror *P. falciparum* pathophysiology in humans. Alternatively a host that is experimentally susceptible to *P. falciparum* can be used to model human disease

however often key features of human severe malaria are not mirrored in the chosen host (Schmidt, 1973). Recently, novel mechanisms such as humanized rodents (Kaushansky *et al.*, 2014) or the recreation of the human host tissue *in vitro* may provide alternative avenues of research into the pathology of severe malaria (Shelby *et al.*, 2003, Pehrson *et al.*, 2016). Although useful, many of these systems *P. falciparum* models have drawbacks.

The rodent malaria species *P. berghei*, *P. chabaudi*, and *P. yoelii* provide an opportunity to study malaria pathophysiology *in vivo* and are extremely useful for researching the sexual parasite stages of the life cycle (Figure 1.3c). The ability to conduct transmission studies is hugely important as this allows the entire life cycle to be studied, which cannot be performed *in vitro*. In addition, the pathology of disease can also be examined especially as *P. berghei* is amenable to genetic manipulation (Fonager *et al.*, 2011, Janse *et al.*, 2006, Orr *et al.*, 2012). However, features of human severe malaria such as iRBC sequestration in brain microvasculature are absent suggesting mechanisms that are specific to hosts (Craig *et al.*, 2012). This may be attributed to the differences in the subtelomeric regions between rodent malaria species and human parasite with a primate origin (Otto *et al.*, 2014a).

Prior to the establishment of the *P. falciparum in vitro* culture system simian *Plasmodium* species were used extensively both *in vivo* and *ex vivo*. Ground-breaking studies used *ex vivo* matured *P. knowlesi* schizonts to study both merozoite invasion and schizont rupture microscopically (Dvorak *et al.*, 1975), while *in vivo* work identified both agglutination and antigenic variation mediated by the schizont-infected cell agglutination proteins (SICA) (Brown and Brown, 1965), sequestration of schizont

infected cells (Miller *et al.*, 1971), and identification of the first erythrocyte receptor essential for merozoite invasion (Miller *et al.*, 1975) were studies that were all carried out in the simian malaria parasite *P. knowlesi*. Further simian malaria species can model features of *P. falciparum* and *P. vivax* malaria. Cerebral malaria and cytoadhesion can be modelled by *P. fragile* and *P. cynomolgi* (Craig *et al.*, 2012), and the latter can also model the dormant hypnozoite stage which is a feature of *P. vivax* malaria (Dembele *et al.*, 2014). The pathology of *P. knowlesi* severe malaria mirrors many features of severe *P. falciparum* malaria both in humans and several macaque species (Craig *et al.*, 2012, Cox-Singh and Culleton, 2015). Although these simian malaria species can be useful for pathophysiology studies, *P. knowlesi* is of particular interest for the study of severe malaria, as it is naturally zoonotic, enabling studies both *in vitro* and *in vivo* using the same species.

An important step in *P. knowlesi* research was the development of transfection methodology and the establishment of continuous *in vitro* cultures (Kocken *et al.*, 2002, Moon *et al.*, 2013). Kocken *et al.*, (2002) developed an *in vitro* *P. knowlesi* culture (H-strain) in Rhesus macaque erythrocytes and transfection methods to genetically manipulate the *P. knowlesi* genome (Kocken *et al.*, 2002). It was identified that the *P. knowlesi* H-strain *in vitro* culture reverted to an *in vivo* phenotype following passage in a Rhesus macaque enabling transmission studies to be performed (Kocken *et al.*, 2002). Following *A. stephensi* feeding on *P. knowlesi* infected Rhesus macaques oocysts were detected in the midgut demonstrating that the culture was capable of producing gametocytes (Kocken *et al.*, 2002) although completion of the life cycle was not achieved as *P. knowlesi* sporozoites are unable to invade the salivary glands of *A. stephensi* (Coatney *et al.*, 1971, Kocken *et al.*, 2002, Gruring *et al.*, 2014). A

requirement for culturing the H-strain *in vitro* is access to a source of macaque erythrocytes which restricts research to facilities with access to non-human primate animal units or with resources to purchase macaque erythrocytes. The adaptation of *P. knowlesi* to continuous *in vitro* culture in human erythrocytes has greatly increased the feasibility of conducting *P. knowlesi* research (Moon *et al.*, 2013). The generation of the *PkA1-H.1* clone was achieved via long term *in vitro* culture in 80% human erythrocytes and 20% cynomolgus erythrocytes (Moon *et al.*, 2013). The *PkA1-H.1* clone has not been tested *in vivo* although it remains invasive to cynomolgus erythrocytes *in vitro* (Moon *et al.*, 2013). Advantages of *in vitro* culture in human erythrocytes are that human erythrocytes are more readily available, the efficiencies of transfections have been reported as higher than in *P. falciparum* and mechanisms specific to human disease can now be studied (Moon *et al.*, 2013). *P. knowlesi* is unique as it is the only human *Plasmodium* species with both a natural host for *in vivo* studies and an accessible *in vitro* culture system which can be used to study the *P. knowlesi* erythrocytic cycle.

1.5 Invasion: How do Merozoites Invade Host Erythrocytes?

The invasion of merozoites into a susceptible erythrocyte is a highly structured process which is complete within approximately 30 seconds (Weiss *et al.*, 2015, Gilson and Crabb, 2009). The molecular interactions which take place during the invasion process are highly organised and sequential. The invasion process is conserved between *Plasmodium* species, suggesting common mechanisms which can be broken down into key steps (Gilson and Crabb, 2009). These consist of merozoite attachment; merozoite

apical reorientation; junction formation; actin-myosin mediated invasion and erythrocyte resealing (Figure 1.4).

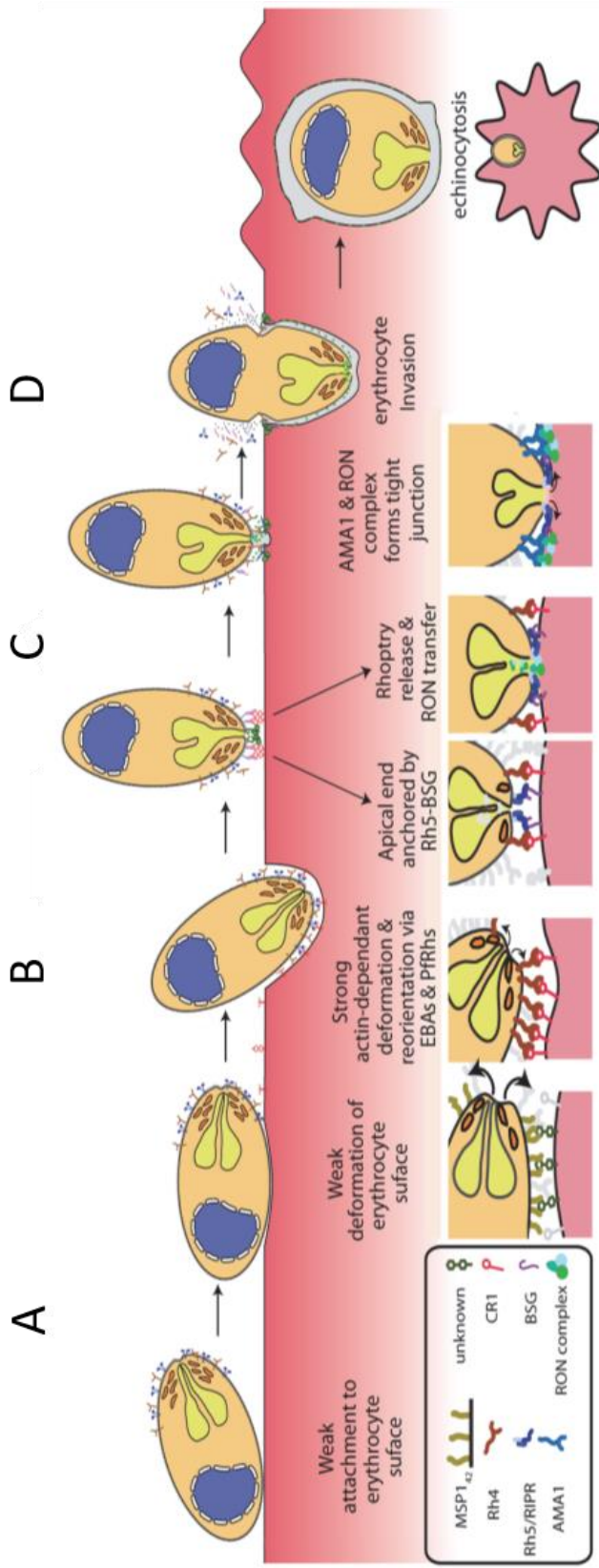


Figure 1.4 Schematic showing *P. falciparum* merozoite invasion of a susceptible erythrocyte.

A. the merozoite binds weakly to the erythrocyte surface via unknown interactions. The MSP proteins are proposed to bind to the erythrocyte causing weak deformations of the erythrocyte. **B.** Apical reorientation positions the apical end of the merozoite against the erythrocyte surface, proposed to be mediated by RBPs and DBPs binding to erythrocyte receptors. **C.** In *P. falciparum*, the membrane bound P113 protein binds the secreted Rh5 which in turn binds to the erythrocyte protein basigin. This binding is implicated in causing the release of proteins from the rhotrieries and micronemes facilitating tight junction formation. The tight junction consists of the AMA1, RON2, RON4 and RON5 proteins, of which, the latter 2 proteins are proposed to be inserted into the erythrocyte membrane. The RON2 protein contains multiple transmembrane domains allowing it to traverse the RBC membrane whilst linking the RON complex to the merozoite surface via binding to AMA1. An irreversible junction is created committing the merozoite to invasion. **D.** The actin-myosin motor is produces force to insert the merozoite into the erythrocyte creating the PV. The merozoite surface proteins are cleaved off enabling invasion and resealing of the erythrocyte membrane (Image adapted from Weiss *et al.*, 2015).

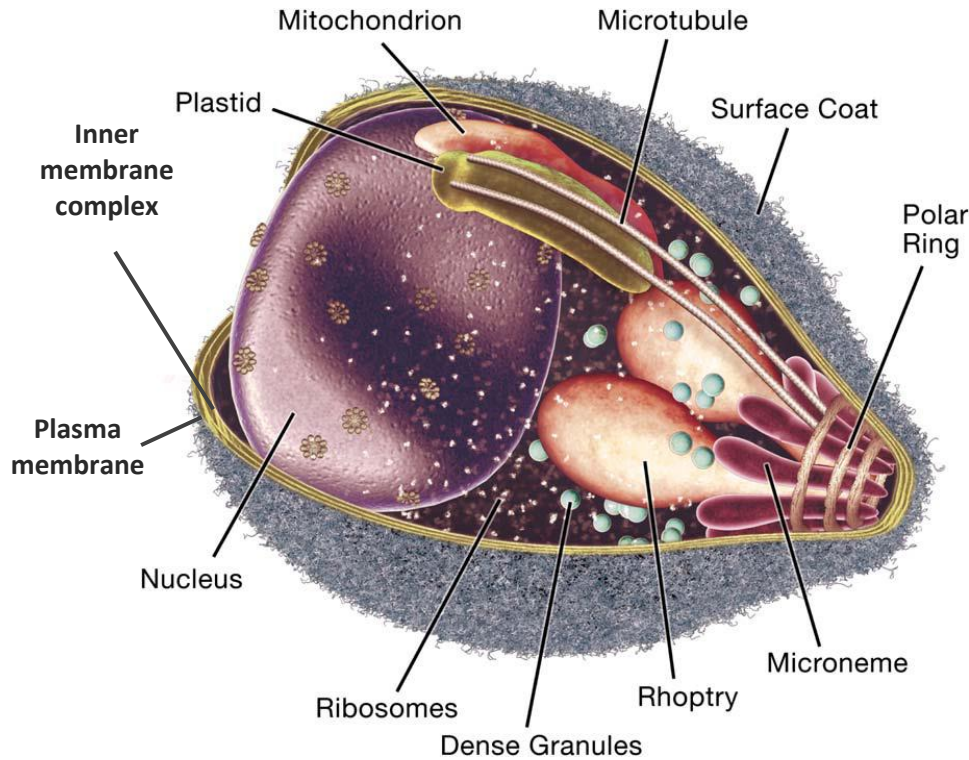


Figure 1.5 The structure of the invasive merozoite.

The invasive merozoite is spatially organised for invasion. Merozoites contain 2 membranes with the outermost membrane being covered in a dense protein coat, facilitating attachment to RBCs. The inner membrane complex (IMC) is located below the outer plasma membrane. Proteins involved in the actin myosin motor complex are located between these two membranes. The Rhoptries and the micronemes are secretory organelles which secrete proteins during the invasion process. The Rhoptries consist of two distinct regions, the rhoptry bulb and the rhoptry neck, which contain distinct protein subsets (Counihan *et al.*, 2013). Both organelles secrete the proteins at distinct time points during the invasion process. The dense granules are a secretory organelle dispersed throughout the cytoplasm and release their contents following the establishment of the PV (Culvenor *et al.*, 1991). The exoemes (not shown) are the smallest known secretory vesicles which secrete proteins required for efficient egress (Yeoh *et al.*, 2007, Janse and Waters, 2007, Collins *et al.*, 2017). The cytoskeleton consists of the microtubules extending from the polar rings located at the apical end of the merozoite towards the posterior of the merozoite, spanning two thirds the length of the merozoite. The microtubules and polar rings give structure and apical orientation to the merozoite (Morrissette and Sibley, 2002). The apicoplast is an essential organelle homologous to chloroplast, although no longer photosynthetic and is involved in the production of essential metabolites (Kalanon and McFadden, 2010, Amberg-Johnson *et al.*, 2017). (Image adapted Cowman *et al.*, 2006).

1.5.1 The merozoite

A merozoite is the *Plasmodium* parasite life stage which mediates invasion into host erythrocytes, initiating the symptomatic stages of infection. The merozoite is not only the smallest *Plasmodium* life stage, but it is also one of the smallest eukaryotic cells. Merozoites are approximately 1 μm in length in *P. falciparum*, and 2 μm in *P. knowlesi*. All *Plasmodium* species share a common structure, with the nucleus surrounded by endoplasmic reticulum (ER) towards the posterior of the merozoite. Unique apicomplexan secretory organelles are located at the merozoite's apical end (Figure 1.5). A characteristic feature of *Plasmodium* merozoites is the presence of an organelle thought to be a chloroplast relic termed the apicoplast (Figure 1.5). This organelle possesses its own circular genome encoding 30 putative genes (Goodman and McFadden *et al.*, 2014). The apicoplast is essential for parasite survival, and functions to synthesise metabolites unable to be synthesised or scavenged by the parasite (McFadden and Yeh, 2017, Gisselberg *et al.*, 2013, Ke *et al.*, 2014). The apicoplast has been identified to be involved in the synthesis of isopentenyl diphosphate, haem and fatty acids which are essential at different stages of the parasite life cycle (McFadden and Yeh, 2017).

Merozoites possess four types of apical organelle involved in the release of parasite proteins during the invasion process and egress; the rhoptries, micronemes, dense granules and exonemes (Mercier *et al.*, 2005). The rhoptries are the largest of the secretory organelles and consist of a neck and bulb region. The release of the rhoptry neck proteins occurs before release of the rhoptry bulb, suggesting organised structure within this organelle (Counihan *et al.*, 2013). Members of the *P. falciparum*

Reticulocyte-Binding-homologue (PfRh) proteins locate to the rhoptry neck prior to invasion. The micronemes (Figure 1.5) are another organelle containing proteins involved in red blood cell invasion, such as the Erythrocyte Binding Proteins (PfEBAs). The dense granules (Figure 1.5) differ from the rhoptries and micronemes as they are not localised to the apical pole of the merozoite and are found throughout the merozoite cytoplasm (Mercier *et al.*, 2005). Secretion of dense granule appears to follow invasion with the secreted proteins implicated in establishment of the parasitophorous vacuole (PV) and host cell modification (Culvenor *et al.*, 1991). Previously, the subtilisin-like protein 1 (SUB1) was predicted to be released by dense granules; however SUB1 has been shown to be secreted by the exosomes into the PV during egress (Collins *et al.*, 2017, Yeoh *et al.*, 2007, Collins *et al.*, 2013b).

1.5.2 Merozoite attachment and reorientation

When a liver schizont ruptures it releases thousands of merozoites into the blood stream. In order for merozoites to survive and replicate they must invade an erythrocyte. The initial stage of the invasion process is the attachment of a merozoite to an erythrocyte which can occur on any region of the merozoite surface (Bannister and Dluzewski, 1990) (Figure 1.4A). This initial interaction is thought to be a weak interaction causing deformation of the host erythrocyte (Dvorak *et al.*, 1975, Weiss *et al.*, 2015). The merozoite (Figure 1.5) has a dense protein surface coat consisting of many different proteins such as glycosylphosphatidylinositol (GPI) anchored membrane proteins, transmembrane anchored proteins or peripherally-associated surface proteins (Figure 1.4 A) (Beeson *et al.*, 2016). One of the most abundant proteins on the

merozoite surface is the GPI anchored merozoite surface protein (MSP) 1 (Gilson *et al.*, 2006). Proteolytic cleavage of MSP1 during schizont rupture results in the presence of 4 different fragments during the invasion process MSP₁₄₂, MSP₁₈₃, MSP₁₃₀ and MSP₁₃₈ (Stafford *et al.*, 1994), with the MSP₁₄₂ fragment being proteolytically cleaved during the invasion process into MSP₁₁₉ and MSP₁₃₃ (Blackman and Holder, 1992). The MSP1 fragments have been implicated in binding to the erythrocyte receptors Band 3 (Goel *et al.*, 2003, Kariuki *et al.*, 2005), and Glycophorin A (Baldwin *et al.*, 2015). Lin *et al.*, (2016) propose that fragments of MSP1 bind with MSP3, MSP6, MSP7, MSPDBL1 and MSPDBL2 individually, forming multiple different complexes (Lin *et al.*, 2016). Conversely, Baldwin and colleagues propose that MSPs form larger complexes comprising multiple different MSP proteins (Baldwin *et al.*, 2015). Blockage of MSP1 binding to the host erythrocyte surface using heparin, did not abolish binding to the erythrocyte but did prevent the weak deformation (Weiss *et al.*, 2015). This suggests MSP1 plays an early role in the attachment to erythrocytes, but is not responsible for the initial attachment with the initial interactions still unknown (Weiss *et al.*, 2015). Although MSP1 has been shown to bind the erythrocyte receptors as discussed here, further data suggests that MSP1 plays an important role in binding the host erythrocyte cytoskeleton during egress, further discussed in Section 1.6 (Das *et al.*, 2015).

Following initial attachment and MSP1 binding, a strong deformation is observed which coincides with apical reorientation (Figure 1.4 B) (Weiss *et al.*, 2015). The secondary interactions at the apical pole to the erythrocyte membrane involve two key protein families, the Reticulocyte binding-like protein family (RBP/Rh/NBP) (detailed in section 1.8.2) and the Duffy binding proteins (DBPs)/Erythrocyte binding antigens (EBAs) (detailed in section 1.8.1) (Cowman and Crabb, 2006). Both protein families are

conserved in all *Plasmodium* species, with multiple RBP and DBP/EBA members present in each species genome (Gunalan *et al.*, 2013). *P. knowlesi* contains 2 functional RBPs and 3 functional DBPs (Miller *et al.*, 1975), while *P. falciparum* contains 5 functional RBPs and 3 functional EBAs and *P. vivax* contains 2 RBP forms with multiple sub-types of each protein, and 2 DBPs (Meyer *et al.*, 2009, Li and Han, 2012, Carlton *et al.*, 2008, Adams *et al.*, 1990, Singh *et al.*, 2005, Gunalan *et al.*, 2016). The majority of RBP protein erythrocyte receptors remain unknown, with the interactions between PfRh5 with basigin and PfRh4 with Complement receptor 1 (CR1) being the only two reported for the Rh proteins in *P. falciparum* (Crosnier *et al.*, 2011, Tham *et al.*, 2010). The erythrocyte receptor DARC was identified as a binding partner for members of the *P. knowlesi* and *P. vivax* DBP family (Miller *et al.*, 1975, Miller *et al.*, 1976), while the glycophorins have been identified as erythrocyte receptors for the EBA proteins in *P. falciparum* (Maier *et al.*, 2003, Orlandi *et al.*, 1992, Lobo *et al.*, 2003). Members of the RBP and DBP/EBA protein families have been shown to be essential for merozoite invasion (Moon *et al.*, 2016, Baum *et al.*, 2009, Miller *et al.*, 1975, Miller *et al.*, 1976) although redundancy between RBPs and DBPs in *P. falciparum* appears to compensate for blocked invasion pathways (Stubbs *et al.*, 2005). PfRh5 is the only essential Rh protein in *P. falciparum* and in addition to binding basigin PfRh5 can also the micronemal protein PfCyRPA in complex with PFRIPR and the merozoite surface protein PfP113 (Galaway *et al.*, 2017). Although this is the model proposed for *P. falciparum*, the invasion process in *P. knowlesi* remains unclear, as no orthologue of PfRh5 is present in the *P. knowlesi* genome. However, PfP113, PfCyRPA and PFRIPR are all present in *P. knowlesi* (Pain *et al.*, 2008).

1.5.3 Junction formation

During the invasion process there is a release of intracellular protein stores from the rhoptry and microneme apical organelles functioning to secrete proteins involved in erythrocyte adhesion and formation of the PV (Figure 1.4) (Counihan *et al.*, 2013). The trigger for release is predicted to be caused by PfRh5-Basigin binding in *P. falciparum* and was visualised using erythrocytes loaded with a calcium sensitive fluorophore, although it is unknown if this mechanism is present in other species (Weiss *et al.*, 2015). Following rhoptry release (Figure 1.7 A) the apical membrane antigen 1 (AMA1) attaches to the merozoite surface enabling the binding to proteins secreted from the rhoptry neck (RON). This interaction has been shown to be essential for invasion of both *Plasmodium* and *Toxoplasma gondii* (Srinivasan *et al.*, 2013, Alexander *et al.*, 2005, Weiss *et al.*, 2015, Yap *et al.*, 2014). AMA1 binds to RON2 in a complex with both RON4 and RON5 that localised to the moving junction (Figure 1.7 B) (Counihan *et al.*, 2013, Srinivasan *et al.*, 2013). RON2 contains multiple transmembrane domains, allowing it to cross the erythrocyte membrane (Besteiro *et al.*, 2009, Shen and Sibley, 2012) while RON4 localises to the cytosolic side of the erythrocyte membrane (Srinivasan *et al.*, 2011). In *Toxoplasma gondii* members of the RON complex, including RON5 and RON8, traverses the host cell membrane linked to AMA1 on the merozoite surface via RON2 (Beck *et al.*, 2014) committing the merozoite to invasion (Chen *et al.*, 2011, Riglar *et al.*, 2011, Srinivasan *et al.*, 2013, Srinivasan *et al.*, 2011). To date, knockout studies in *P. berghei* have shown that RON2, RON4 and RON5 are refractory to genetic deletion suggesting an essential role in the erythrocyte stages, however conditional knockouts have not been performed to verify that they are essential for junction formation (Giovannini *et al.*, 2011, Bushell *et al.*,

2017). Data from a conditional AMA1 knockout in both *T. gondii* tachyzoites and *P. berghei* merozoites has challenged the role of AMA1 in tight junction formation as invasion was not abolished in the AMA1 knockout (Bargieri *et al.*, 2013). However, invasion was very low in an imperfect conditional knockout of AMA1 in *P. falciparum* (Yap *et al.*, 2014). This data may suggest that an additional protein present in *P. berghei* and *T. gondii* but absent in *P. falciparum* may compensate for the role of AMA1 during the invasion process (Bargieri *et al.*, 2013, Harvey *et al.*, 2014).

1.5.4 Actin-myosin mediated invasions

In order for invasion to take place, the merozoite uses the tight junction described above to anchor itself to the erythrocyte membrane and force its way into the erythrocyte creating the PV. Although the exact mechanism is still not understood for merozoite invasion, a schematic of the current proposed method can be seen in Figure 1.6 (Tardieux and Baum, 2016). The Glideosome Associated Protein (GAP) 50, GAP45, GAP40 and Myosin A tail domain interacting protein (MTIP) form a protein complex on the parasite IMC (Figure 1.6) (Cowman and Crabb, 2006). In turn MTIP binds to Myosin XIV (MyoXIV) which interacts with polymerising actin filaments between the IMC and the parasite membrane (Figure 1.6) (Douse *et al.*, 2012, Baum *et al.*, 2008). Recently, the roles of both aldolase and MTRAP (Figure 1.6) in the invasion process have been disproved (Shen and Sibley, 2014, Riglar *et al.*, 2016). Currently, the proteins involved in linking the actin filaments to the erythrocyte membrane are unknown (Tardieux and Baum, 2016). Additionally, the orientation of the glideosome machinery remains unknown. Tardieux and Baum propose 3 possible mechanisms (Figure 1.6),

whereby extension of the actin filament to the posterior of the merozoite produces movement of the merozoite in the opposite direction into erythrocyte creating the PV (Figure 1.6). The actin filament is proposed to sit between the parasite adhesion attached extracellularly to the erythrocyte surface and the MyoXIV protein linked to the IMC (Figure 1.6 panel A). Alternatively, the second model proposes that the actin filament extends in the same direction that force is exerted. This model proposes inversion of MyoXIV, MTIP and actin, with the actin filament closely associating closely with the GAP proteins on the IMC and MTIP binding to the unknown parasite adhesin possibly via a linker protein (Figure 1.6 panel B). The second model proposed that the direction of actin filament extension is the same as the direction of movement. The final proposed method mirrors the mechanism shown in Figure 1.6 panel A, however the actin filament interacts directly with multiple parasite adhesins rather than linked to the adhesin via a linker protein (Figure 1.6 panel C)(Tardieux and Baum, 2016).

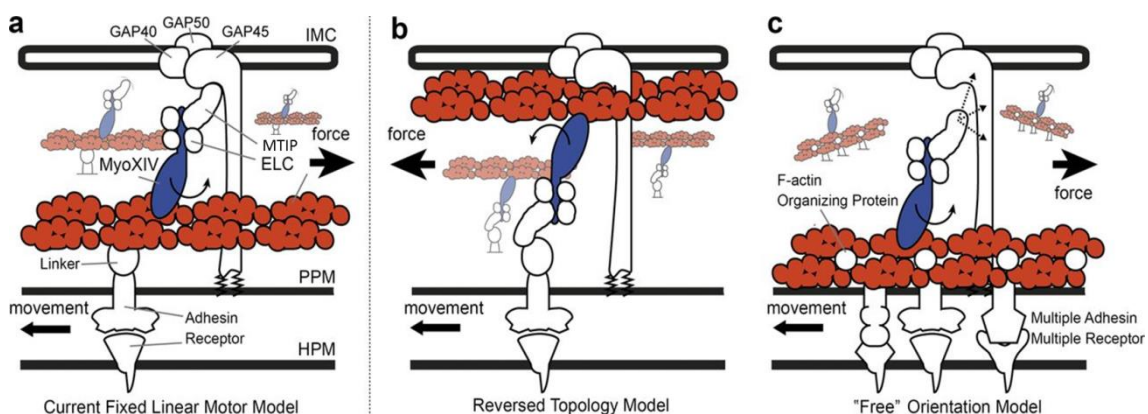


Figure 1.6 Proposed mechanisms involving the Actin-Myosin motor complex.

1. The Inner membrane complex binds GAP50, GAP45 and MTIP, which in turn binds MyoXIV (2). Polymerisation of the actin filament (3) causes MyoXIV to move backwards producing (4) backward force (5) Producing forward merozoite movement into the erythrocyte forming the PV (6) Rhomboid proteases cleave surface adhesins. (7-8) Depolarisation of actin is then recycled. (Image adapted from Tardieux and Baum 2016).

1.5.5 Shedding of the merozoite surface proteins

An important feature of the active invasion process is the cleavage of the merozoite surface proteins as the tight junction moves to the posterior of the merozoite. This process is predicted to disrupt the interactions between the merozoite and the erythrocyte allowing invasion to occur (Olivieri *et al.*, 2011). In *P. falciparum*, this process appears to be mediated by 2 Rhomboid proteases, ROM1 and ROM4, as well as the subtilisin-like protease SUB2 (Cowman *et al.*, 2012). The SUB2 protease is implicated in cleaving the AMA1 protein, involved in tight junction formation, at the transmembrane domain in a non-sequence specific manner (Olivieri *et al.*, 2011). Cleavage of AMA1 was also shown to be mediated by ROM1 (Baker *et al.*, 2006), while ROM4 cleaved the EBA-175 surface adhesin in a sequence specific manner (O'Donnell *et al.*, 2006). Interestingly, the ROM proteases were also shown to cleave the EBA proteins, the Rh proteins and other merozoite surface proteins showing their importance during the invasion process. The cleavage of specific merozoite surface proteins was able to be altered by producing a chimeric AMA1 and EBA-140 proteins by combining the extracellular domain of EBA-140 with the TM domain of AMA1 (Baker *et al.*, 2006). ROM4 was able to cleave native EBA-140 and ROM1 only demonstrated weak cleavage of EBA-140. However incorporation of the AMA1 TM domain resulted in a switch in ability to cleave EBA-140 containing the TM domain of AMA1, and was now able to be cleaved by ROM1 and was unable to be cleaved by ROM4 showing not only that cleavage occurs in a sequence specific manner but also reveals the level of complexity (Baker *et al.*, 2006).

1.6 Egress

In order to continue the life cycle, merozoites must escape the host erythrocyte. The exit of merozoites from a schizont occurs in a conserved manner across *Plasmodium* species. Initial observations in *P. knowlesi* identified that movement of merozoites can be visualised inside mature schizonts prior to swelling and rupture (Dvorak *et al.*, 1975). Detailed studies have subsequently been performed in *P. falciparum* showing that initially the release of 1-2 merozoites occurs before the erythrocyte membrane curls outwards from the location of initial merozoite release followed by buckling of the erythrocyte membrane expelling the remaining merozoites, all taking place in less than 400 ms (Abkarian *et al.*, 2011). Although this process appears violent morphologically, it is actually a highly structured process molecularly as inefficient egress impacts subsequent merozoite invasion.

As previously mentioned, serine proteases have been shown to process proteins involved in erythrocyte invasion but perhaps play a more important role in egress (Dowse *et al.*, 2008). Three subtilisin-like (SUB) serine proteases are present in the *P. falciparum*, *P. knowlesi* and *P. vivax* genomes (Carlton *et al.*, 2008, Pain *et al.*, 2008, Gardner *et al.*, 2002). A recently proposed mechanism for the initiation of egress demonstrates that the PV membrane is permeabilised 10-30 minutes prior to complete PV membrane rupture (Hale *et al.*, 2017). Following this the cGMP dependent kinase PKG triggers SUB1 release from exonemes into the PV (Hale *et al.*, 2017, Collins *et al.*, 2017, Collins *et al.*, 2013a, Hopp *et al.*, 2012). PfSUB1 was shown to have multiple substrates, including serine rich antigen (SERA) 4, 5 and 6 (Yeoh *et al.*, 2007, Silmon de Monerri *et al.*, 2011). Further SERA family members may also be processed by PfSUB1, as 9 are present in the *P. falciparum* genome. PfSERA5 and 6 were previously

shown to be essential, however a conditional knockout of SERA5 was viable (McCoubrie *et al.*, 2007). Conditional disruption of SERA5 shortened the time to egress however the membrane was ruptured early and incompletely, reducing the dispersal of merozoites upon egress (Collins *et al.*, 2017). Collins *et al.*, suggest that SERA5 has a regulatory role during egress ensuring efficient egress and reinvasion, as the parasites lacking functional SERA5 had a reduced replication rate (Collins *et al.*, 2017).

In addition to the role PfSUB1 plays in processing SERA5, it has also been shown to process MSP1 (Yeoh *et al.*, 2007, Koussis *et al.*, 2009, Stallmach *et al.*, 2015, Das *et al.*, 2015). Processing of MSP1 at specific sites as discussed previously results in 4 MSP1 fragments which form a complex following cleavage (Section 1.5.2) (Das *et al.*, 2015). The processing of MSP1 by SUB1 during egress activates the processed MSP1 to bind heparin and spectrin (Das *et al.*, 2015). Genetic disruption of MSP1 at sites cleaved by SUB1 and truncation of MSP1 identified a region of MSP1 able to bind spectrin that was required for parasite viability and absence of MSP1 processing resulted in egress defect (Das *et al.*, 2015).

1.7 Invasion Blocking Vaccine Candidates

As discussed above, the RBPs and DBPs play important roles during erythrocyte invasion. This has led to RBPs being the focus for vaccine studies. Specifically, PfRh5 is a current leading vaccine candidate against *P. falciparum* infection (Douglas *et al.*, 2011, Douglas *et al.*, 2014, Ord *et al.*, 2014, Osier *et al.*, 2014). PfRh5 appears to be more conserved than other RBPs and it is hoped that this will improve vaccine efficacy. Nine different *P. falciparum in vitro* lines, three of which contained non-synonymous

mutations in the PfRh5 gene, were challenged with antibodies raised against recombinant PfRh5 (3D7 line). Invasion was blocked in all 9 strains showing that the antibodies had activity against multiple PfRh5 variants (Bustamante *et al.*, 2013). *Aotus* monkeys are experimentally susceptible to *P. falciparum*, which presents with anaemia and death if untreated. Douglas *et al.*, showed that when *Aotus* monkeys were vaccinated with PfRh5 prior to challenge with *P. falciparum*, there were no fatalities and no primate required antimalarial treatment (Douglas *et al.*, 2015). This is a promising step forward in the steps to prevent *P. falciparum* malaria. However, as *P. falciparum* is the only human malaria species that expresses PfRh5, this vaccine would not be able to protect from any of the other human malaria species. A current target for a *P. vivax* vaccine is the PvDBP (Chen *et al.*, 2016). Blocking the PvDBP interaction with DARC would give a similar invasion phenotype to *P. vivax* infection of a Duffy negative individual. As the merozoite invasion ligands are essential to successful erythrocyte invasion and are expressed on the surface of merozoites they provide a good target for an invasion blocking vaccine. However, the RBPs and DBPs are not just important for vaccine studies; they function at a crucial point in the parasite life cycle which can determine the fate of the merozoite. The greater the number of successful invasions the higher the parasitaemia which is critical for survival of the parasite, but also important in disease pathology as hyperparasitaemia is associated with severe malaria.

1.8 Merozoite Invasion Proteins

1.8.1 Duffy binding proteins

The Duffy Binding Proteins (DBPs) are a multigene family responsible for binding to erythrocytes. The DBPs are predicted to function immediately prior to tight junction formation, and play a similar role to the RBPs (Lopaticki *et al.*, 2011). The *P. knowlesi* genome contains 3 *dbp* genes, the *P. falciparum* genome encodes 4 *eba* genes and *P. vivax* encodes 2 *dbp* genes (Pain *et al.*, 2008, Carlton *et al.*, 2008, Gardner *et al.*, 2002). The Duffy binding proteins, so called because of their erythrocyte receptor Duffy antigen receptor for chemokines (DARC), were first identified as being essential for the invasion of *P. knowlesi* and *P. vivax* (Miller *et al.*, 1976, Miller *et al.*, 1975). The DBPs function to attach merozoites to the erythrocyte surface, causing strong deformation prior to invasion (Weiss *et al.*, 2015).

1.8.1.1 *P. falciparum* erythrocyte binding antigens

Of the 4 *P. falciparum* Erythrocyte binding antigens (EBA), EBA-181, EBA-175, EBL-1 and EBA-140, erythrocyte receptors are known for the latter 3 parasite proteins, which bind to Glycophorin A, Glycophorin B and Glycophorin C respectively, Table 1.2 (Duraisingh *et al.*, 2003a, Maier *et al.*, 2003, Mayer *et al.*, 2009). The EBA proteins share a common structure consisting of an N-terminal signal sequence (RI) followed by the erythrocyte binding domain (RII). Within this binding domain there are two cysteine-rich DBL domains and a linking domain to a small cysteine-rich domain immediately prior to the transmembrane domain (Sim *et al.*, 1994). In *P. falciparum* the EBAs localise to the micronemes of merozoites prior to invasion (Treeck *et al.*, 2006). During the invasion process the EBA and PfRh proteins appear to function

cooperatively, as invasion is only inhibited by anti-Rh2a antibodies when EBA-181 is present, however if EBA-181 is present, invasion can be blocked suggesting a cooperative function (Lopaticki *et al.*, 2011). This is mirrored in other members of the protein families as knock-out of EBA-175 results in increased PfRh4 expression which has been reported in both clinical isolates and laboratory strains suggesting a compensatory role between EBA-175 and Rh4. The compensatory role is further enhanced as invasion via EBA-175 and its receptor Glycophorin A is a sialic acid dependent invasion pathway whilst invasion via Rh4 and its receptor CR1 is a sialic acid independent pathway (Gaur *et al.*, 2006, Nery *et al.*, 2006, Stubbs *et al.*, 2005). The benefit of being able to switch invasion pathways allows merozoites to invade a diverse range of RBCs.

The presence of multiple adhesive proteins enables merozoites to invade erythrocytes via different invasion pathways potentially overcoming blockage of single merozoite - erythrocyte interaction (Lopaticki *et al.*, 2011). Polymorphisms present in the EBA-181 and EBA-140 proteins have been shown to be responsible for altering the affinity of the EBA protein for the erythrocyte receptor (Maier *et al.*, 2009). This could suggest that the altered affinity for erythrocyte receptors could result in either an increased or decreased number of successful invasions however as *P. falciparum* uses multiple invasion pathways this would likely be masked by invasion via another pathway.

1.8.1.2 *P. vivax* duffy binding proteins

Previously it had been noted that black Africans appeared not to be susceptible to *P. vivax* infection (Miller *et al.*, 1976). Following ground breaking work in *P. knowlesi* it was identified that the erythrocyte Duffy antigen was essential for *P. vivax* erythrocyte invasion (Miller *et al.*, 1976, Miller *et al.*, 1975). It was later identified that PvDBP was

responsible for binding to the Duffy antigen, Table 1.2 (Adams *et al.*, 1992, Wertheimer and Barnwell, 1989). Recently the binding of PvDBP to the Duffy antigen was shown to occur as a dimer, with the initial PvDBP-Duffy interaction recruiting a second PvDBP receptor which associates and binds to the second Duffy antigen (Batchelor *et al.*, 2014). It remains unclear whether this binding pattern is unique to *P. vivax* or is present in other species. In addition to dimerization Batchelor *et al.*, showed that single amino acid changes in regions of PvDBP proteins resulted in decreased binding to RBCs suggesting that mutations in key protein-protein interactions could result in fewer interactions between merozoites and RBCs suggesting fewer RBC invasions (Batchelor *et al.*, 2014). Interestingly, *P. vivax* was found recently to have invaded Duffy-negative human erythrocytes at 3 geographically distinct regions in Africa (Angola and Equatorial Guinea, Mauritania and Kenya) (Mendes *et al.*, 2011, Ryan *et al.*, 2006, Wurtz *et al.*, 2011). This suggests there may be invasion pathways for *P. vivax* independent of the Duffy invasion pathway.

1.8.1.3 *P. knowlesi* duffy binding proteins

As with *P. vivax*, Duffy-negative individuals are resistant to *P. knowlesi* erythrocytic stages (Miller *et al.*, 1975). The *P. knowlesi* PvDBP orthologue was shown to be responsible for binding to the Duffy RBC surface antigen (Miller *et al.*, 1975). The *P. knowlesi* genome encodes three DBP genes *DBP α* , *DBP β* and *DBP γ* . Research showed that PkDBP α was able to bind both human and macaque erythrocytes while DBP β and DBP γ were able to bind macaque erythrocytes but not human erythrocytes (Chitnis *et al.*, 1996). Knockout studies have shown that PkDBP α was the parasite ligand that bound to the erythrocyte receptor DARC (Singh *et al.*, 2005).

1.8.2 Reticulocyte binding protein family

The Reticulocyte Binding proteins (RBPs) are a family of merozoite proteins that are thought to play important roles during invasion prior to junction formation. If some of the key RBP-RBC interactions are disrupted invasion can be blocked demonstrating their important role in the invasion process (Baum *et al.*, 2009, Moon *et al.*, 2016). The first member of this protein family was identified as a 235 kDa protein in the rodent malaria *Plasmodium yoelli* in the early 1980's (Freeman *et al.*, 1980, Holder and Freeman, 1981). Homologues of the 235 kDa protein were subsequently identified in other *Plasmodium* species, and termed the reticulocyte binding protein family, so named because in *P. vivax* the RBPs are implicated in selection of reticulocytes for invasion (Galinski *et al.*, 1992). In *P. falciparum* the proteins are termed the reticulocyte binding-like protein homology (PfRh), and in *P. knowlesi* they are termed the normocyte binding proteins (PkNBP). The number of genes present in each *Plasmodium* species varies, with pseudogenes also being present. Currently, 2 functional NBP proteins have been identified in *P. knowlesi*, 5 in *P. falciparum*, and approximately 11 were recently identified in *P. vivax* by *de novo* assembly of a field isolate genome sequence (Hester *et al.*, 2013). The RBP gene family share a common genomic organisation with two exons separated by a small intron (Gunalan *et al.*, 2013) and predominantly encode large proteins over 230 kDa (Gunalan *et al.*, 2013). The proteins all contain an N-terminal signal peptide along with a single C-terminal transmembrane domain, and a short cytoplasmic tail. The exception to this is PfRh5 in *P. falciparum*, which contains a signal peptide, but has neither a cytoplasmic domain nor a transmembrane domain, and is smaller (63 kDa) than other proteins in the family (Rodriguez *et al.*, 2008, Baum *et al.*, 2009).

1.8.2.1 *P. falciparum* reticulocyte-binding-homologue proteins

The *P. falciparum* Rh proteins are the most well characterised RBPs in all species. There are six genes in the *P. falciparum* genome, one of which is a pseudogene (*PfRh3*). The following rhoptry secretion the PfRh proteins (Rh1, Rh2a, Rh2b, Rh4 and Rh5) localise to the apical end of the merozoite consistent with a direct role for the Rh proteins in erythrocyte binding and invasion (Triglia *et al.*, 2009, Baum *et al.*, 2009). During this time, between schizont rupture and merozoite invasion, the PfRh1–4 proteins undergo proteolytic cleavage (Triglia *et al.*, 2009). The PfRh1 processed fragments were capable of binding to host erythrocytes, and both were detected inside newly invaded iRBCs and in the culture supernatant, suggesting that there may be more than one binding domain (Triglia *et al.*, 2009). A similar pattern of proteolytic cleavage has been reported for PfRh4 and PfRh2a/2b (Gunalan *et al.*, 2011).

The PfRh proteins share N-terminal homology (Sahar *et al.*, 2011, Rayner, 2008). However, the PfRh2a/Rh2b proteins are strikingly similar, with the first 8 kb at the 5' region of the genes identical and only differ in a short 3' region of the gene (Rayner *et al.*, 2000). This divergent 500 amino acids sequence at the C-terminus encompasses some of the ectodomain, the transmembrane domain and the cytoplasmic tail (Sahar *et al.*, 2011). Interestingly, the differences observed in cytoplasmic domain between PfRh2a and PfRh2b alter its invasion pathway, as shown by a chimeric PfRh2a parasite containing the PfRh2b cytoplasmic domain (Duraisingh *et al.*, 2003b, Dvorin *et al.*, 2010) (Table 1.2). This shows that the cytoplasmic domains of invasion proteins can be responsible for invasion phenotype (Dvorin *et al.*, 2010). In addition, phosphorylation of PfRh4 cytoplasmic tail residues by casein kinase 2 has been shown to be essential to erythrocyte invasion (Tham *et al.*, 2015). It is anticipated that further studies examining

intracellular signalling will reveal how merozoite – erythrocyte interactions trigger the subsequent stages of erythrocyte invasion (Tham *et al.*, 2015).

The erythrocyte receptors for two of the five PfRh5s have been identified, Table 1.2. PfRh4 was identified to bind to CR1 (Tham *et al.*, 2010) and PfRh5 was identified to bind basigin (Bartholdson *et al.*, 2013). Homologues of PfRh5 are absent from other human malaria species, and are only found in species of the *laverania* subgenus, such as the gorilla malaria species *P. reichenowi* which is phylogenetically the most closely related to *P. falciparum* (Sundararaman *et al.*, 2016, Wanaguru *et al.*, 2013, Wright *et al.*, 2014). Additionally, PfRh5 has a unique structure compared to other RBPs as it is the only family member which does not contain a C-terminal transmembrane domain (TM) (Baum *et al.*, 2009). In addition to PfRh5 binding via its C-terminal end it has recently been shown to bind PfP113 N-terminally (Bartholdson *et al.*, 2013, Galaway *et al.*, 2017). As discussed previously this interaction is proposed to be important for rhoptry release enabling the formation of the tight junction consisting of AMA-1, RON2, RON4 and RON5 complex (Galaway *et al.*, 2017) followed by microneme secretion to release a cysteine rich protein (PfCyRPA), and the PfRh5 interacting protein PfRIPR, Figure 1.7 (Reddy *et al.*, 2015, Galaway *et al.*, 2017). In this model PfCyRPA binds C-terminally to PfRh5 while PfRIPR does not bind directly to PfRh5 but is linked via PfCyRPA resulting in the N-terminal disruption of PfRh5 and PfP113 releasing the PfRIPR-PfCyRPA-PfRh5-Basigin complex from the merozoite surface (Crosnier *et al.*, 2011, Galaway *et al.*, 2017, Reddy *et al.*, 2015).

Although PfRIPR and PfCyRPA are both implicated in disrupting the PfP113-PfRh5-Basigin complex their function in other *Plasmodium spp.* lacking PfRh5 remains

unknown. However, both *P. knowlesi* and *P. vivax* contain homologues of PfRIPR and PfCyRPA (Carlton *et al.*, 2008, Pain *et al.*, 2008). Identifying the role of these proteins in other species lacking homologues of Rh5 could help to identify their role during the invasion process.

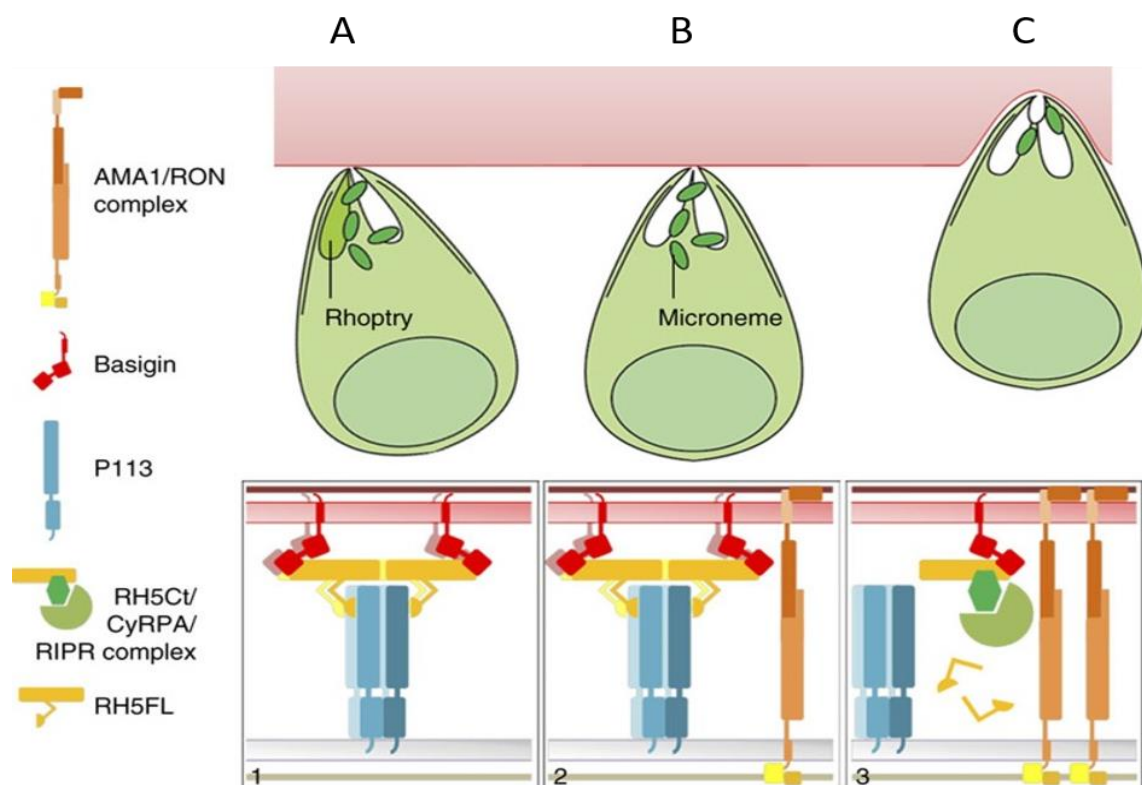


Figure 1.7 Proposed model of PfRh5 binding to the merozoite and erythrocyte surface.

The proposed PfRh5 interactions with the erythrocyte receptor Basigin, the merozoite surface protein P113 and the PfRh5 interacting proteins PfRIPR and PfCyRPA as detailed by Galaway *et al* (2017) **A.** Following initial attachment and rhoptry release (Panel A). PfRh5 is bound to the merozoite surface protein P113 via its N-terminal domain, allowing the C terminus of PfRh5 to bind Basigin on the erythrocyte surface (Panel A/1). **B.** This interaction is proposed to cause further rhoptry release (Panel B), allowing the tight junction to form through the interaction of the AMA1-RON complex (Panel B/2). **C.** Following tight junction formation and microneme secretion (Panel C) of the PfRh5 interacting proteins PfCyRPA and PfRIPR the PfRh5 protein is bound by PfCyRPA at the C terminus of PfRh5. PfCyRPA is predicted to bridge the interaction of PfRIPR and PfRh5, and upon PfRIPR binding causes disruption of the PfP113-PfRh5 interaction, resulting in the PfRIPR-PfCyRPA-PfRh5-Basigin complex no longer tethered to the merozoite surface (Panel C/3). Figure adapted from (Galaway *et al.*, 2017).

1.8.2.2 *P. vivax* reticulocyte binding proteins

Initial work suggested that *P. vivax* contained 2 PvRBP genes, *Pvrbp1* and *Pvrbp2*, responsible for selective invasion of reticulocytes (Wertheimer and Barnwell, 1989, Galinski *et al.*, 1992). However, completion of the *P. vivax* genome revealed that there are subtypes of both *Pvrbp1* and *Pvrbp2*, with the full repertoire consisting of 11 genes, 3 of which are pseudogenes and three are partial coding genes, Table 1.2 (Carlton *et al.*, 2008, Hester *et al.*, 2013, Hietanen *et al.*, 2015). In comparison to *P. falciparum*, relatively little is known about the PvRBP proteins, as the lack of an *in vitro* culture system has hampered further research. Hietanen and colleagues showed that the full length PvRBP proteins are of a similar size to RBPs from other species (>280 kDa), although the binding partners are yet to be determined (Hietanen *et al.*, 2015). Recently, the crystal structure of the PvRBP2a erythrocyte binding domain was solved, revealing that the N-terminal structure shared homology with PfRh5, suggesting a common structure between RBP proteins (Gruszczuk *et al.*, 2016).

1.8.2.3 *P. knowlesi* normocyte binding proteins

Publication of the *P. knowlesi* genome led to the identification of 2 novel NBPs and a single pseudo-gene (Meyer *et al.*, 2009, Pain *et al.*, 2008). Meyer *et al.*, showed that of the three genes present in the *P. knowlesi* genome (*nbp_{xa}*, *nbp_{xb}* and *nbp_l*), only the *Pknbp_{xa}* and *Pknbp_{xb}* produced proteins with masses (324 kDa and 334 kDa respectively) similar to the orthologues in other *Plasmodium* species (Meyer *et al.*, 2009). Immunofluorescence and electron microscopy confirmed that like the PfRh proteins the NBPs localise to the apical end of merozoites consistent with a role during invasion, although they are thought to locate to the microneme (Figure 1.5) and not the rhoptry (Meyer *et al.*, 2009). The PkNBPXb protein was found to bind erythrocytes

from Old World monkeys including Rhesus macaques and long-tailed macaques, but not New World monkeys such as the owl monkey (Meyer *et al.*, 2009, Semanya *et al.*, 2012). This suggests a common receptor specific to the invasion of Old World monkeys (Semanya *et al.*, 2012). Semanya *et al.*, (2012) showed that the PkNBPA protein but not the PkNBPB protein bound to human erythrocytes, suggesting PkNBPA is currently the only known PkNBP protein involved in human erythrocyte invasion (Semanya *et al.*, 2012).

Recent work has shown that the *Pknbpxa* gene is essential for *P. knowlesi* invasion of human erythrocytes (Moon *et al.*, 2016, Meyer *et al.*, 2009, Semanya *et al.*, 2012). The *Pknbpxa* gene was disrupted while cultured in macaque erythrocytes *in vitro*, allowing invasion of macaque erythrocytes using *Pknbpxb* (Moon *et al.*, 2016). When transferred to human erythrocytes merozoites lacking *Pknbpxa* were able to bind to the human erythrocyte surface but were unable to invade (Moon *et al.*, 2016). No erythrocyte receptor has been identified for PkNBPA binding is not restricted to Duffy positive erythrocytes (Semanya *et al.*, 2012). Recent evidence has shown that the *Pknbpxa* gene is dimorphic, and individual residues only present in the more diverse cluster 2 type *Pknbpxa* are associated with high parasitaemia (Ahmed *et al.*, 2014, Pinheiro *et al.*, 2015). Evidence of polymorphisms in invasion genes associating with high parasitaemia has not been reported for other RBPs. However this may be due to both the number of RBP members, and the redundancy shown between PfRhs and EBAs during invasion in *P. falciparum*. However, as *Pknbpxa* is essential for *P. knowlesi* invasion these individual residues may alter the affinity for the PkNBPA protein to, the as yet unknown, erythrocyte receptor resulting in a stronger binding or more interactions with erythrocytes which in turn could lead to a higher parasitaemia.

Table 1.2 Currently known RBP and DBP proteins in *P.falciparum*, *P. vivax* and *P. knowlesi*.

Species	Protein	RBC Receptor	Reference
<i>P. falciparum</i>			
	Rh1	Unknown– Receptor Y	Triglia <i>et al.</i> , 2005
	Rh2a	Unknown– Receptor Z	Gunalan <i>et al.</i> , 2011
	Rh2b	Unknown– Receptor Z	Gunalan <i>et al.</i> , 2011
Pseudogene	Rh3	-	
	Rh4	Complement receptor 1	Tham <i>et al.</i> , 2010
	Rh5	Basigin	Crosnier <i>et al.</i> , 2011
	EBA-175	Glycophorin A	Orlandi <i>et al.</i> , 1992
	EBA-181	Unknown– Receptor W	Mayer <i>et al.</i> , 2008
	EBA-140	Glycophorin C	Maier <i>et al.</i> , 2003
	EBL1	Glycophorin B	Mayer <i>et al.</i> , 2009
Pseudogene	EBA-165	-	Triglia <i>et al.</i> , 2001
<i>P. vivax</i>			
	RBP1a	Unknown	Hester <i>et al.</i> , 2013
	RBP1b	Unknown	Hester <i>et al.</i> , 2013
	RBP2a	Unknown	Hester <i>et al.</i> , 2013
	RBP2b	Unknown	Hester <i>et al.</i> , 2013
	RBP2c	Unknown	Hester <i>et al.</i> , 2013
Pseudogene	(PvRBP2) RBP2d	-	Kosaisavee <i>et al.</i> , 2012
Pseudogene	RBP3	-	Kosaisavee <i>et al.</i> , 2012
	DBP1	DARC	Miller <i>et al.</i> , 1976, Wertheimer <i>et al.</i> , 1989
	DBP2	unknown	Gunalan <i>et al.</i> , 2016
<i>P. knowlesi</i>			
	NBPXa	Unknown	Meyer <i>et al.</i> , 2009
	NBPXb	Unknown	Meyer <i>et al.</i> , 2009
Pseudogene	NBP3	-	Meyer <i>et al.</i> , 2009
	DBP α	DARC	Singh <i>et al.</i> , 2005
	DBP β	Unknown	Singh <i>et al.</i> , 2005
	DBP γ	Unknown	Singh <i>et al.</i> , 2005

Project aims and objectives

The hypothesis of this work is that point mutations present in clinical *Pknbpaxa* sequences are responsible for an increased parasite fold increase resulting in high parasitaemia, a marker of severe malaria. The aim was to develop a translational approach, testing clinical associations with severe malaria *in vitro*. This would be achieved by replacing *Pknbpaxa* in the *PkA1-H.1* clone with a dimorphic copy containing mutations with putative associations with high parasitaemia.

In order to achieve this, further genome sequencing of clinical sequences will be required. As our Biobank of patient samples are frozen without leukocyte depletion the parasite DNA will only compose a small proportion of the total DNA. In order to produce *P. knowlesi* DNA samples suitable for whole genome sequencing, we require an improved and more standardised leukocyte depletion method for frozen clinical samples. By introducing the Plasmodipur filter to the workflow of Ahmed *et al.*, (2014) we aim to test the leukocyte depletion of mock clinical samples, analysing the quantities of human and *P. knowlesi* DNA pre and post leukocyte depletion using TaqMan qPCR. Following optimisation of the leukocyte depletion method we aim to progress to the leukocyte depletion of clinical samples, which if suitable would be genome sequenced.

Following on from this, the clinical genome sequence data from the above aims will be added to the current 6 genome sequences already available. The genome data will be mapped to the reference genome sequence, and variant positions identified. Using this data, the full length cluster 2 *Pknbpaxa* gene sequences will be established and analysed for mutations associated with high parasitaemia. The cluster 2 *Pknbpaxa* sequence will be recreated as a codon optimised synthetic *Pknbpaxa* gene, with putative residues

associated with high parasitaemia introduced singly to the cluster 2 *Pknbpxa* sequence. Using published transfection methods different lines will be created replacing the parental *Pknbpxa* gene with the cluster 2 type sequences with and without residues with a putative association with high parasitaemia. Phenotyping clones of each line will be carried out analysing growth rate using flow cytometry, and competition assays to establish if clones containing single residue changes dominate the parasite population showing a growth advantage.

Chapter 2: Materials and Methods

Section 1: List of Reagents

Reagent	Manufacturer	Product Code
Agarose	Bioline	BIO-41026
AlbuMAX™ II	Gibco®, Invitrogen™	11021029
Ampicillin	Sigma-Aldrich	10835242001
Antarctic Phosphatase	New England Biolabs	M0289S
Anti-HA (Mouse)	Sigma-Aldrich	H9658
Anti-Mouse (Goat) Alexa®-568	Invitrogen™	A1104
Anti-HA (Mouse)	Abcam	18181
Basic Parasite Nucleofector® Kit 2	Lonza	VAMI-1021
B-Mercaptoethanol	Sigma-Aldrich	M3148
Buffered Tablets pH 7.2	VWR	36310W
Bovine Serum Albumin	Sigma-Aldrich	A9647-100
Calcium Chloride (CaCl ₂)	Sigma-Aldrich	C3881
CO ₂ :O ₂ : N ₂ , L cylinder	BOC	509965719
D-(+)-Glucose	Gibco®, Invitrogen™	15023021
Dimethyl sulfoxide	Sigma-Aldrich	D5879
di-Potassium hydrogen orthophosphate 3-hydrate (K ₂ HPO ₄)	VWR (BDH chemicals)	BDH9266
<i>DpnI</i>	Thermo-Scientific	FD1703
Distilled water, DNase/RNase free	Gibco® Invitrogen™	10977-035
D-Sorbitol	Sigma-Aldrich	85529
EDTA BD Vacutainer®	Becton, Dickinson and Company	366643
Efficiency™ Dh5α™ <i>E. coli</i>	Invitrogen™	18265017
EGTA	Sigma-Aldrich	E3889
ElectroTen-Blue Electroporation Competent <i>E. coli</i>	Agilent	200159
Ethanol absolute	VWR Chemicals	20821.330

FluorSave™	Calbiochem® Millipore	345789
Gentamicin Reagent (50 mg/mL)	Gibco®, Invitrogen™	15750-060
Glacial Acetic acid	Fisher Scientific	A/0360/PB17
Glycerol	Sigma-Aldrich	G2025
GoTaq® G2 Flexi DNA polymerase	Promega	M7801
Gurr® Giemsa's improved R66 solution	VWR Chemicals	350864X
HA-tagged Positive Control	Thermo Scientific	26180X
HEPES (4-(2-hydroxyethyl)-1- piperazineethanesulfonic acid)	Gibco®, Invitrogen™	15630-080
Hoechst 33342	Thermo Scientific	62249
Horse serum	Gibco®, Invitrogen™	11510516
Histodenz™	Sigma-Aldrich	D2158
Human AB serum	Interstate Blood Banks	N/A
Hydrochloric acid (HCl)	Sigma-Aldrich	71826
Hyperladder™ 1kb	Bioline	BIO-33053
Hyperladder™ 50bp	Bioline	BIO-33054
Hypoxanthine	Sigma-Aldrich	H9377
Immersion Oil	Sigma-Aldrich	5178650
Instagene™ Matrix	Bio-Rad	7326030
<i>Kpn</i> I restriction enzyme	Promega	R6341
LB broth	Sigma-Aldrich	L3022
LB broth with lennox agar	Sigma-Aldrich	L2897
L-glutamine	Sigma-Aldrich	G8540
MACs LD column	MACs, Miltenyi Biotec	130-042-901
Magnesium Chloride (MgCl ₂)	VWR	25108260
MidiMACs	MACs, Miltenyi Biotec	130-042-302
Methanol	Fisher Scientific	M/4000/17

<i>NotI</i> restriction enzyme	New England Biolabs	R0189S
NucleoBond® Xtra Maxi	Macherey-Nagel	740414.10
NucleoSpin® Gel and PCR Clean-up	Macherey-Nagel	740609.50
NuPAGE LDS Sample buffer (4x)	NuPAGE® Novex®	NP0008
P3 Primary Cell solution	Lonza	PBP3-02250
Paraformaldehyde	Fisher	P/0840/53
Phosphate buffered saline, 10x	Gibco®, Invitrogen™	70011-036
Phusion®	New England Biolabs	M0530L
Plasmodipur	Europroxima	8011Filter10u
Potassium dihydrogen orthophosphate (KH ₂ PO ₄)	VWR (BDH chemicals)	BDH153184u
Pyrimethamine	Sigma-Aldrich	P4200000
QIAamp® DNA Blood Mini Kit	Qiagen	51104
QIAamp® DNA Mini Kit	Qiagen	51304
QIAprep® Spin Miniprep Kit	Qiagen	27104
RPMI 1640 with GlutaMAX™	Gibco®, Invitrogen™	61870-010
<i>SacII</i> restriction enzyme	Promega	R6221
Saponin	Sigma-Aldrich	47036-50G-F
Sodium Acetate	Sigma-Aldrich	S8750
Sodium Chloride	Fisher Scientific	S/3160/60
Sodium Hydroxide	Fisher Scientific	S/4920/53
<i>SpeI</i> restriction enzyme	Promega	R6591
SYBR® Green I	Invitrogen™	S7563
SYBR® Safe	Invitrogen™	S33102
T4 ligase	Thermo-Scientific	M1801
TaqMan® Control Genomic DNA (Human)	Applied Biosystems® Invitrogen™	4312660
TaqMan® Universal PCR Master Mix	Applied Biosystems® Invitrogen™	4304437
Thermo Scientific™ Pierce™ Hoechst 33342 Stain	Thermo Scientific	62249
Tris EDTA Buffer	Sigma-Aldrich	93283

Triton X-100	Sigma-Aldrich	T8787
Trizma® Base	Sigma-Aldrich	T1503
Tween® 20	Sigma-Aldrich	P2287
UltraPure™ 10x Tris-Borate-EDTA (TBE) Buffer	Gibco®, Invitrogen™	15581044
Whatman paper, 11 µm	Sigma-Aldrich	Z274852
Whatman paper, 6 µm	Sigma-Aldrich	Z240478
<i>Xma</i> I restriction enzyme	New England Biolabs	R0180S

Section 2: Cell Culture

2.1 Cell Culture Solutions

2.1.1 D-glucose

Four grams of D-glucose (Invitrogen™) was dissolved in 40 mL of RPMI 1640 GlutaMAX (Invitrogen™) to obtain a 0.1 g/mL solution. Aliquots of 10 mL were frozen at -20°C.

2.1.2 Heat inactivation of serum

Horse serum (Invitrogen™) was heat inactivated in a water bath at 56°C for 30 minutes. The serum was divided into aliquots and stored at -40°C.

2.1.3 Sodium hydroxide

A 1M sodium hydroxide (Fisher Scientific) solution was made by dissolving 4 g of sodium hydroxide in 100 mL of distilled H₂O.

2.1.4 Hypoxanthine

A 25 mg/mL solution of hypoxanthine (Sigma-Aldrich) was made by dissolving 0.1 g of hypoxanthine (Sigma-Aldrich) in 4 mL sodium hydroxide 1M. Aliquots of 1 mL were frozen at -20°C.

2.1.5 L-glutamine

A 15 mg/mL solution of L-glutamine (Sigma-Aldrich) was made by dissolving 0.6 g of L-glutamine (Sigma-Aldrich) in 40 mL of RPMI 1640 GlutaMAX® (Invitrogen™). Aliquots of 1 mL were frozen at -20°C.

2.1.6 Incomplete medium

RPMI 1640 containing GlutaMax® (Invitrogen™) was by supplemented with 10 mL 0.1 g/mL D-glucose stock (Sigma-Aldrich) (2 g/L), 12.5 mL HEPES buffer (Invitrogen™) (5.957 g/L), 1 mL 25 mg/mL hypoxanthine stock (Sigma-Aldrich) (50 mg/L) and 250 µL 50 mg/mL gentamicin sulphate (Invitrogen™) (25 mg/L) to give 500 mL final volume. Incomplete medium was filter sterilised and stored at 4°C for 4 weeks.

2.1.7 Complete medium

Complete medium was made by adding 10 mL 15 mg/mL L-glutamine stock solution (Sigma-Aldrich) (0.3 g/L) and 2.5 g AlbuMAX® (Invitrogen™) (5 g/L) to incomplete medium to give a final volume of 450 mL. Medium was warmed to dissolve the AlbuMAX® (Invitrogen™) before filtration through a 0.22 µm PES/PVDF 500 mL filter unit (Millipore/Nalgene). 50 mL of heat inactivated horse serum (Invitrogen™) was added to the sterile medium for a 10% (v/v) concentration of horse serum in complete medium. Complete medium was stored at 4°C for 2 weeks.

2.1.8 Optiprep synchronisation solution

Briefly, 1.25 mL of Optiprep was added to 4.75 mL sterile PBS pH 7.4. for a 25% v/v solution. The 25% solution was filter sterilised using a 0.22 µm PES filter.

2.1.9 Histodenz stock solution

A 27.6% w/v Histodenz solution was made by dissolving 27.6 g of Histodenz powder (Sigma-Aldrich) in 80 mL distilled H₂O and heating to 60°C until in solution. 1 mL of 1 M HEPES (Invitrogen™) was added for a 10 mM concentration and adjusted to pH 7. The solution was adjusted to 100 mL using distilled H₂O and filter sterilised through a 0.22 µm PES filter. The Histodenz stock solution was stored as a 27.6% stock solution at 4°C

2.1.10 Histodenz synchronisation solution

A 55% (v/v) Histodenz synchronization solution was made by adding 55 mL of the 27.6% (w/v) Histodenz solution to 45 mL sterile incomplete medium. The 55% (v/v) Histodenz synchronization solution was stored at 4°C.

2.1.11 Freezing solution

The freezing solution was made by combining 14 mL of 100% glycerol (Sigma-Aldrich), 0.324 g sodium chloride (110.9 mM) (Fisher Scientific), 1.512 g of D-sorbitol (166 mM) (Sigma-Aldrich) and 36 mL distilled H₂O. The freezing solution was filter sterilised through a 0.22 µm PES filter and stored at 4°C.

2.1.12 Cryoretrieval solution

A 3.5% (w/v) sodium chloride solution was made by adding 3.5 g of sodium chloride (Fisher Scientific) to 100 mL of distilled H₂O. The cryoretrieval solution was filter sterilised through a 0.22 µm PES filter and stored at 4°C.

2.1.13 Phosphate buffered solution pH 7.2

One phosphate buffer tablet (VWR), pH 7.2, was dissolved in 1 L of distilled H₂O.

2.1.14 Cytomix transfection solution (pH 7.6)

Cytomix transfection solution was made using the stock buffers detailed in Appendix A. A 100 mL working solution was made in distilled H₂O consisting of; 120 mM KCl, 0.15 mM CaCl₂, 2 mM EGTA, 5 mM MgCl₂, 25 mM HEPES, 10 mM KH₂PO₄/K₂HPO₄. The pH was adjusted to pH 7.6 then filter sterilized through a 0.22 µm PES filter and stored at 4°C.

2.2 Cell Culture Techniques

2.2.1 Blood collection

Ethical approval was obtained from the University of St Andrews Teaching and Research Ethics Committee (UTREC) to collect whole blood from volunteers with signed consent. Ethics forms, information form and consent form can be found in Appendix B.

2.2.2 Preparation of blood for parasite culture

Ten mL of whole blood collected into EDTA vacutainer tubes (Becton, Dickinson and Company) was transferred to a sterile centrifuge tube (Greiner) and centrifuged at 611 rcf for 8 minutes with brake removed. The top plasma layer and the concentrated leukocyte layer, the buffy coat, on top of the red blood cell layer were removed by gentle aspiration. The remaining RBC lower fraction was washed twice by adding an equal volume of incomplete medium (section 2.1.6), mixing by gentle inversion and centrifuged as above. Following the final wash step, the RBCs were resuspended in an equal volume of incomplete medium (section 2.1.6) giving a 50% haematocrit. The RBCs were stored at 4°C for up to 3 weeks.

2.2.3 Routine *in vitro* culture of the *P. knowlesi*

***PkA1-H.1* clone in human erythrocytes**

The *P. knowlesi* *PkA1-H.1* clone (kindly donated by Dr Moon, LSHTM) was maintained in human RBCs following buffy coat removal (section 2.2.2) at a 2% haematocrit in complete medium (section 2.1.7). Medium was replaced every second

day and fresh RBCs were added to dilute the culture and keep the parasitaemia below 5% for routine culture.

2.2.4 Parasite synchronisation using MACS LD column

An LD MACs column (Miltenyi Biotec) attached to a MidiMACs (Miltenyi Biotec) magnet was equilibrated with 3 mL of incomplete medium (section 2.1.6) and allowed to drip through. A *PkAI-H.1* culture (> 100 μ L of packed RBCs) containing mostly pigmented parasites was pelleted at 181 rcf, and resuspended in 4.5 mL incomplete medium (section 2.1.6). The infected RBC (iRBC) suspension was applied to the LD column and allowed to drip through. The pigmented iRBCs bind to the magnetised column if they contain hemozoin, allowing the uninfected RBCs and early stage parasites to pass through the column and be collected in a 50 mL tube. The column was washed three times with 5 mL incomplete medium (section 2.1.6) until the flow through was no longer red. The LD column was detached from the MACs magnet and 5 mL incomplete medium (section 2.1.6) was added and pushed through the column to flush out the pigmented iRBCs that were collected in a fresh tube. The recovered iRBCs were then pelleted at 181 rcf for 5 minutes.

2.2.5 Optiprep synchronisation

Briefly, cultures of *PkAI-H.1* were centrifuged at 181 rcf and supernatant removed. The pelleted *PkAI-H.1* culture was resuspended to a 50 % haematocrit and 2 mL was gently layered onto 5 mL of 25% sterile Optiprep in a 15 mL centrifuge tube. The tubes were centrifuged at 920 rcf for 12 minutes with brake removed. The upper brown layer containing schizonts was removed and added to 5 mL of incomplete medium (section

2.1.6) to neutralize the gradient. The resuspended schizonts were centrifuged at 181 rcf for 5 minutes. The supernatant was removed and the schizont pellet was resuspended in complete medium (section 2.1.7) and transferred to a 1.5 mL centrifuge tube. The schizont suspension was centrifuged briefly and the packed cell volume was estimated. The schizonts were resuspended in 1 mL complete medium (section 2.1.7) and divided for transfections or added to fresh RBCs and complete medium (section 2.1.7) for culturing.

2.2.6 Histodenz gradient synchronisation

For each gradient synchronisation, 5 mL of a Histodenz synchronisation solution (section 2.1.9) was added to 15 mL centrifuge tubes. Cultures of *PkA1-H.1* were centrifuged at 181 rcf and supernatant removed. Pelleted cells were resuspended at a 50% haematocrit and 2 mL of this was gently transferred to the top of the 5 mL 55% Histodenz density gradient. Tubes were centrifuged at 920 rcf for 12 minutes with no brake. The upper brown layer enriched with schizonts was removed and added to incomplete medium (section 2.1.6). The schizont suspension was then centrifuged at 181 rcf for 5 minutes. The supernatant was removed and the schizont pellet was resuspended in complete medium (section 2.1.7) and transferred to a 1.5 mL centrifuge tube which was pulse centrifuged for 30 seconds. The schizont packed cell volume was estimated, resuspended in 1 mL complete medium and divided into aliquots for transfection or added to fresh RBCs and complete medium (section 2.1.7) for culturing.

2.2.7 Cryopreservation

For cryopreservation of the *P. knowlesi* line *PkA1-H.1*, 15 mL cultures at a 2% haematocrit (300 µL) containing predominantly ring stage parasites (>5% parasitaemia) were centrifuged at 611 rcf and the supernatant was removed. The 300 µL of pelleted *PkA1-H.1* culture were combined with 700 µL of warm freezing solution (section 2.1.10). The 1 mL suspension was transferred to cryovials and immediately stored in LN₂.

2.2.8 Cryoretrieval

Cryovials containing the cryo-preserved *PkA1-H.1* culture were removed from LN₂, thawed rapidly at 37°C and resuspended in 1 mL of pre-warmed cryoretrieval solution (section 2.1.12). Cells were pelleted via centrifugation at 181 rcf for 5 minutes. The supernatant was removed and the cells resuspended in 1 mL cryoretrieval solution. Two further wash steps in cryoretrieval solution were performed. The pelleted *PkA1-H.1* infected RBCs were resuspended in complete medium (section 2.1.7) and fresh RBCs at a 2% haematocrit. The *PkA1-H.1* culture was then gassed and returned to 37°C.

2.2.9 Monitoring *in vitro* *PkA1-H.1* cultures

Blood films were made daily for monitoring the growth of *P. knowlesi* A1-H.1 cultures in human RBCs. Approximately 30 µL of the culture was removed from the flask (T-25 or T-75) and centrifuged in a 1.5 mL centrifuge tube at 900 rcf for 1 minute. The supernatant was removed and the RBC pellet was gently mixed using a pipette tip. Approximately 1 µL of resuspended cells were placed onto a glass microscope slide and, using the edge of another microscope slide a monolayer created. The monolayer – thin blood film, was air dried and fixed with 100% methanol (Fisher Scientific), and

stained with a 5% Gurr Giemsa's improved R66 solution (VWR Chemicals) in buffered H₂O (pH 7.2) for 30 minutes.

Section 3: Microscopy

2.3.1 Permeabilisation solution

The permeabilisation solution for immunofluorescence studies was prepared by adding 50 μL of Triton X-100 to 50 mL 1x PBS to give a 0.1% (v/v) Triton X-100 solution in PBS.

2.3.2 Blocking solution

A 3% (w/v) bovine serum albumin (BSA) blocking solution as per (Ruecker *et al.*, 2012) was made by dissolving 1.5 g of BSA in 50 mL 1x PBS.

2.4 Microscopy Techniques

2.4.1 Light microscopy

Thin blood films were examined by light microscopy for parasitaemia and determining the parasite lifecycle stages. Parasitaemia was determined by examining a monolayer of the thin film using a Miller reticle, counting all RBCs inside the inner square and touching the lower and right edges and iRBCs in the larger square and those touching the lower and right edges. The parasitaemia was determined by using the following

$$\text{equation } \frac{iRBCs \text{ in Large Square}}{RBCs \text{ in Small Square} \times 9} \times 100 = \% \text{ parasitaemia}$$

2.4.2 Immunocytochemistry

Immunofluorescence was performed as per Ruecker et al, 2012 (Ruecker *et al.*, 2012). Briefly, thin blood films were dried and placed at -80°C in zip-lock bags. Slides were removed from -80°C and allowed to come to room temperature. Thin films were fixed with 4% paraformaldehyde in PBS for 30 minutes. Cells were permeabilised with 0.1% Triton X-100 in PBS for 10 minutes at room temperature followed by three 10 minute PBS washes. Slides were blocked at room temperature in 3% BSA in PBS for 1 hour. Immediately following this the slides were incubated at room temperature with 1:200 mouse anti-HA (Sigma-Aldrich), Table 2.4, containing 1% BSA for 1 hour. Three 10 minute washes in 1x PBS containing 0.1% Tween-20. Slides were stained with 1:1,000 goat anti-mouse Alexafluor[®] 568 (Thermo Fisher) diluted in 1% BSA for 1 hour at room temperature. Slides were washed three with PBS and immediately stained with 1 ug/mL Hoechst 33342 for 15 minutes. Coverslips were mounted with FluorSave[®] reagent and imaged using the Leica DM5500 B.

2.4.3 Fluorescence microscopy

Transfected parasites with the *Pk_{con}p230pGFP* plasmid were resuspended in 15 μ L incomplete medium (Section 2.1.6) and stained with 1 μ g/mL Hoechst 33342 for 10 minutes. The cell suspension was mounted on Vaseline edged slides sealed with a coverslip. Slides were imaged using the Leica DM5500 B.

Section 4: Molecular Biology

2.5 Molecular Biology Reagents

2.5.1 Tris-Borate-EDTA (TBE) (1x)

UltraPure TBE 10x (Gibco) was diluted with distilled H₂O for a 1x working concentration.

2.5.2 Sodium acetate pH 5, 3 M

A 3M sodium acetate solution was prepared by dissolving 20.4 g of sodium acetate (Sigma-Aldrich) in 50 mL of distilled H₂O. The pH was adjusted to 5.3 using glacial acetic acid (Fischer Scientific).

2.5.3 Phosphate buffered saline (PBS) (1x concentration)

PBS 10x (Invitrogen™) was diluted with distilled H₂O for a 1x working concentration.

2.5.4 Tris- buffered saline (TBS) 10x concentration

A 10x Tris-Buffered saline solution was made by dissolving 12 g of Trizma® Base (20 mM) (Sigma-Aldrich) and 44 g NaCl (150 mM) (Fisher Scientific) in 480 mL of distilled H₂O. The pH was adjusted to pH 7.6 using concentrated HCl before adjusting the volume to 500 mL.

2.5.5 Tris-buffered saline (TBS) 1x concentration

A 1x TBS solution was made by diluting 100 mL 10x TBS with 900 mL distilled water.

2.5.6 Tris-buffered saline 0.1% Tween® 20 (TBS-T)

One millilitre of Tween®-20, 1.095 g/mL (Sigma-Aldrich) was added to 1 L of 1x TBS for a 0.1% Tween®-20 concentration.

2.6 Molecular Biology Methods

2.6.1 Qubit DNA quantification

DNA was quantified using the Qubit 2.0 system. A master-mix solution was created by adding High Specificity (HS) buffer and HS dye at a ratio of 189:1 respectively. 10 μL of either 10 ng/ μL or 0 ng/ μL standards were added to 190 μL of master-mix, vortexed for 2 seconds and incubated at room temperature for 2 minutes. Standards were then read on the Qubit 2.0 to create a standard curve. For experimental samples, 2 μL of DNA was added to 198 μL of the HS mastermix, and processed as previously for the standards.

2.6.2 NanoDrop 2000

The NanoDrop 2000 spectrophotometer was used to measure the DNA concentrations of samples. Briefly, 1 μL of DNase free water was used as a blank before 1 μL of DNA was measured. DNA quantity was measured in ng/ μL and DNA purity represented as 260/280.

2.6.3 Gel electrophoresis

Agarose (Bioline) was added to 1x Tris-borate-EDTA buffer (Gibco 10x stock) to make 0.8-2% agarose gels. The agarose solution was heated until the solution was clear. The gel was allowed to cool and 3.5 μL of SYBR Safe (Invitrogen) was added per 50 mL gel. The gel was allowed to set in an electrophoresis cassette and submerge with 1x TBE buffer. Samples were prepared in 5 x loading dye (Bioline, BIO-37045) and then

electrophoresed at 110 V for 1 hour. Molecular ladders used were Hyperladder 1 kb (Bioline) and Hyperladder 50 bp (Bioline).

2.6.4 Restriction digestion of plasmid DNA

Plasmid DNA was digested as per the manufacturer's instruction. Briefly, plasmid DNA was purified using Miniprep or Maxiprep (section 2.8.6 and 2.8.7) and added to 1x restriction digest buffer, 0.1 mg/mL BSA (for Promega enzymes) and 5-50 units of restriction enzyme, Table 2.1. The reaction was incubated at 37°C for 1 hour per microgram of plasmid DNA. Incubation time varied depending on quantity of DNA and units of enzyme. The digestion was then heat inactivated at 65°C for 20 minutes.

Table 2.1 Restriction enzymes and compatible buffers.

<i>Restriction Enzyme</i>	<i>Source</i>	<i>Buffer</i>
<i>NotI</i> (NEB)	<i>E. coli</i>	Cutsmart
<i>XmaI</i> (NEB)	<i>E. coli</i>	Cutsmart
<i>SpeI</i> (Promega)	<i>S. natans</i>	B / C
<i>SacII</i> (Promega)	<i>S. achromogenes</i>	C
<i>KpnI</i> (Promega)	<i>E. coli</i>	J

2.6.5 Gel extraction

Size separated DNA was extracted from Gels using the NucleoSpin® Gel and PCR Clean-up, as per the Macherey-Nagel instructions. Briefly, 200 µL of NTI buffer was added per 100 mg of excised agarose gel and incubated for 5-10 minutes at 50°C. Samples were centrifuged in the silica columns provided at 11,000 rcf for 30 seconds followed by two 700 µL washes with NT3 buffer using the same centrifugation

conditions. The column was then centrifuged at 11,000 rcf for 1 minute to remove residual NT3 buffer. Target DNA was eluted using 20 μ L of nuclease free water (Gibco) pre-warmed to 50°C and incubated for 5 minutes at room temperature. DNA concentration and quality was analysed using the NanoDrop 2000 spectrophotometer.

2.6.6 Ligations

Insert DNA and vector plasmid DNA were digested as described previously (Section 2.6.4). The digested vector was incubated with 1 μ L of Antarctic Phosphatase (NEB) and 1x Antarctic phosphatase buffer for 1 hour at 37°C and heat inactivated at 70°C for 5 minutes. Digested DNA was separated by gel electrophoresis as described previously (section 2.6.3). DNA was visualised using a dark reader transilluminator (Clare Chemical Research) and the linear fragment extracted (section 2.6.3 - 2.6.6). The DNA concentration was measured using a NanoDrop 2000 spectrophotometer (section 2.6.2) and the fragment ligated into the vector plasmid at insert:vector (I:V) molar ratios of either 3:1 or 5:1. The reactions were carried out in a 10 μ L volume in 1.5 mL microcentrifuge tubes. Ligation buffer was used at a 1x concentration and 5 units of T4 Ligase were used per reaction (ThermoFisher). The ligation mixture was then incubated at room temperature for 16 – 48 hours.

2.6.7 DNA extraction from blood samples

DNA was extracted from whole blood and *PkA1-H.1* culture using the QIAgen DNA Blood Mini as per the Qiagen whole blood protocol. Briefly, 20 μ L proteinase K and 4 μ L of RNase A (100 mg/ml stock) was added to 200 μ L of whole blood or *PkA1-H.1* culture. Cells were lysed with the addition of 200 μ L of AL buffer and vortexed for 15

seconds. Samples were incubated at 56°C for 10 minutes. Microcentrifuge tubes containing the lysed samples were centrifuged briefly to collect the solution and 200 µL of ethanol (96-100%) added prior to agitation via vortexing for 15 seconds. Samples were added to a DNA purification column and centrifuged at 6,000 rcf for 1 minute. The column was then washed with 500 µL of AW1 buffer, and subsequently washed with 500 µL AW2 centrifuging at 20,000 rcf 3 minutes. The column was centrifuged for 1 minute to remove residual solution and then 50 – 200 µL of DNase- and RNase-free water, pre-warmed to 50°C, was added to the column and incubated for 5 minutes at room temperature. Eluate was collected into a 1.5 mL Eppendorf via centrifugation at 6,000 g. DNA was quantified using the NanoDrop 2000 spectrophotometer.

2.6.8 InstaGene DNA extraction

DNA was extracted from 3-10 µL of *P. knowlesi* A1-H.1 *in vitro* culture packed cell volume. Pelleted cells were incubated for 30 minutes in 1 mL DNase- and RNase-free water (Gibco). Microcentrifuge tubes were centrifuged at 13,500 rcf for 3 minutes. All but approximately 20 µL of supernatant was removed. Pelleted lysed RBC material and 20 µL supernatant were combined with 100 µL InstaGene matrix and incubated at 56°C for 30 minutes. Following the incubation the suspension was vortexed vigorously for 10 seconds and boiled at 100°C for 8 minutes. Boiled samples were vortexed as before and centrifuged as previously. The DNA containing supernatant was removed and 10 µL used for PCR or stored at -20°C.

2.6.9 Ethanol precipitation

Sodium acetate (3 M) at pH 5.2 was added to a DNA solution for 10% final concentration. Three volumes of >96% ethanol was added to the DNA sodium acetate solution. The solution was vortexed and incubated at -20°C for 1 hour. The DNA ethanol solution was centrifuged at 16,000 rcf for 10 minutes at 4°C. The supernatant was decanted and 1 mL of 70% ethanol added and the centrifugation repeated. The supernatant was decanted and the DNA pellet was air dried. The DNA was resuspended in DNase- and RNase-free water or TE buffer (10 mM TrisHCl, 1mM EDTA, pH 8).

2.6.10 DNA sequencing to verify cloning steps

To validate ligations and mutagenesis based experiments, miniprep extracted DNA was sequenced using the facilities offered by the Dundee Sequencing Unit. Greater than 600 ng of DNA at 20 ng/uL was submitted along with 15 µL of primer at 3.2 µM was submitted for sequencing. The DNA was sequenced on the applied Biosystems 3730 DNA analyser (or the Applied Biosystems 3730XL DNA analyser).

2.6.11 Restriction digestion of plasmid DNA for transfection

Briefly, 100 µg of *Pk_{con}pknbpxa_{f1}-3* or *Pk_{con}p230pGFP* plasmid was suspended in 500 µL of DNase- and RNase-free water (Gibco) containing 10x CutSmart™ Buffer (NEB), and 50 units (5 µL) of the restriction enzyme *KpnI*. The restriction digest mixture was incubated at 37°C for 5 hours followed by immediate ethanol precipitation of the linearised DNA (section 2.6.9). The linearised DNA pellet was resuspended in 20-40 µL of DNase- and RNase-free water (Gibco) or TE buffer (10 mM TrisHCl, 1

mM EDTA, pH 8). A 1 μ L sample was removed and diluted 1:10 to quantify the DNA concentration using the NanoDrop 2000 spectrophotometer (section 2.6.2).

2.6.12 PCR

Transfections were validated using PCR with primers specific for the $Pk_{con}pknbpxa_{f1-3}$ plasmid, the native *pknbpxa* gene and the flanking regions of the *Pknbpxa* gene (Table 2.2). Briefly, PCR reagents were used according to the manufacturer's instructions and optimised cycling conditions (Table 2.3.1 and 2.3.2). Annealing temperature and elongation time were dictated by primer sequence and amplicon length. DNA extracted from cultured *PkA1-H.1 in vitro* transfected lines were used as template.

Table 2.2 **Table of primers**

<i>Primer ID</i>	<i>5'→3' Nucleotide Sequence</i>
F-A1H1Xa	CTCTTGTGGAATTGGTTCTGTTG
R-A1H1Xa	CGAATTGCACTCCTTAGGGC
F-NotI	CAATACGCAAACCGCCTCTC
R-NotI	CTTGTTCCCAGCTTGACCT
F-XmaI	GGAAGGAAGCCATCACGCTAT
R-XmaI	GCCGTA CTCTTCGATGCT
F-SpeI	GATGCGATTGCCGAACGTG
R-SpeI	CTGACGCAGATTGCTTTCCA
F-SacII	GCAGCAGGTATTACCGTGG
F ag382-3cc	CCGGGATAATccCGGTGATGATGATC
R ag382-3cc	CATCATCACCGggATTATCCCGGG
F- gt1043/4ag	CCCTGGTTGagAAAAGCCTGGATC
R- gt1043/4ag	CCAGGCTTTTctCAACCAGGGTTT
F- g1982a	GCATTGATAaCAGCAGCAGCGCAG
R- g1982a	GCTGCTGCTGtTATCAATGCTATCGG
SDM-Xaf2-1043ag	CGCCAAAAGCATTGTGAGCA
SDM-Xaf2-1982a	GGGTACACCGCTGGATATGG
R-XaTf-2706	GTCGTCGTATTTTCATGCTTTTG
Plasmo1	GTTAAGGGAGTGAAGACGATCAGA
Plasmo2	AACCCAAAGACTTTGATTTCTCATAA
Klaassen F	GGGCAACGTGCTGGTCTG
Klaassen R	AGGCAGCCTGCACTGGT
ol144	GCCATTCAGGCTGCGCAACTGT
ol145	GAATACTTCGAGGAAGAAATTCAATTTTCCTG
ol146	AACAGTATCTTTGATTAGAACCCCTGGAATCA
hDNA probe	YAKYE -CTGGCCCATCACTTTGGCAAAGAA-BHQ1
Pk probe	FAM-CTCTCCGGAGATTAGAACTCTTAGATTGCT-BHQ1

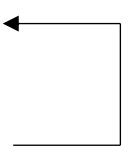
All primers were obtained from Eurofins Genomics MWG Operon

Table 2.3.1 GoTaq® G2 Flexi PCR mastermix

<i>Reagent</i>	<i>Stock concentration</i>	<i>Volume (μL)</i>	<i>Final concentration</i>
F-Primer	10 μM	0.5	0.25 μM
R-Primer	10 μM	0.5	0.25 μM
Buffer	5x	4	1x
MgCl ₂	25 mM	1.6	2 mM
Nucleotide mix (dNTPs)	1 M	0.4	0.2 mM
GoTaq Flexi G2 Polymerase	10 U/μL	0.1	0.05 U/μL
DNA	-	2	>1ng
H ₂ O	-	To 20 μL	-

Table 2.3.2 GoTaq® G2 Flex PCR cycling conditions

<i>Temperature (°C)</i>	<i>Time (minutes)</i>	<i>Cycles</i>
94	4	1
94	0.5	x35
55-65	1.5	
72	0.5-3	
72	5	1



Section 5: Microbiology

2.7 Reagents for Microbiology

2.7.1 Ampicillin stock

A 100 mg/mL ampicillin (Sigma-Aldrich) was created by dissolving 1 g of ampicillin in 10 mL of distilled H₂O. The 100 mg/mL ampicillin stock solution was filter sterilised using a 0.22 µm PES filter and stored at -20°C.

2.7.2 LB broth

LB broth was made by dissolving 2 g of LB broth powder (Sigma-Aldrich) per 100 mL of distilled H₂O. The LB broth was autoclaved and stored at room temperature.

2.7.3 LB agar plate preparation

LB agar was made by dissolving 3.5 g of LB broth powder containing Lennox agar (Sigma-Aldrich) in 100 mL of double distilled H₂O. The LB agar solution was autoclaved and cooled to solidify and stored at room temperature. When required, stock LB agar was heated until fully melted and cooled prior to antibiotic addition. 100 µL of 100 mg/mL ampicillin (Sigma-Aldrich) was added to the molten LB agar to a final concentration of 100 µg/ml. Approximately 10 mL of LB agar was poured into 10 cm petri dishes and allowed to set. LB agar plates were sealed in parafilm and stored at 4°C.

2.8 Bacterial Culture Techniques

2.8.1 Heat shock bacterial transformation

DH5 α *Escherichia coli* (Invitrogen) cells were thawed on ice and 25 μ L transferred to fresh microcentrifuge tubes as required. Plasmid DNA less than 10 kb and less than 200 ng was added to the bacterial cells on ice. The bacteria/DNA mixture was then heated at 42°C for 45 seconds and then placed on ice for 2 minutes. 500 μ L of LB broth (Section 2.6.2) was added to the transformed cells and incubated shaking at 210rpm for 1 hour at 37°C. The transformed Dh5 α *E. coli* cells were then spread onto LB agar plates (Section 2.6.3) containing 100 ug/mL ampicillin and incubated at 37°C overnight.

2.8.2 Bacterial cell electroporation

For plasmids >10 kb, bacterial electroporation was used. Briefly, ElectroTen-Blue (Agilent) electro-competent *E. coli* cells were thawed on ice and 35 μ L transferred into microcentrifuge tubes as required. For any ligation, 5 μ L of StrataClean resin was added per 10 μ L of ligation mixture. The ligation-resin mixture was vortexed for 15 seconds and centrifuged at 2,000 rcf for one minute. The supernatant was transferred to a fresh microcentrifuge tube and the wash step with the resin was repeated. Following the second wash step 5 μ L of the supernatant containing the washed DNA from the ligation mix was added to 35 μ L of ElectroTen-Blue electrocompetent *E. coli*. The DNA - *E. coli* mixture was then added to a chilled cuvette with a 1 mm gap, tapped to collect the solution to the bottom of the cuvette and then pulsed at 2250 Volts (Eppendorf Electroporator 2510). Transformed cells were immediately resuspended in 0.5 mL of pre-warmed LB broth, transferred to a microcentrifuge tube and incubated shaking at

210 rpm for 1 hour at 37°C. The entire cell suspension was then plated out on LB agar plates containing the 100 µg/mL ampicillin (Section 2.6.3) and incubated at 37°C overnight.

2.8.3 Starter culture

Bacterial colonies were selected from an LB agar plate or from a glycerol stock using a sterile pipette tip which was ejected into 10 mL of LB broth (Sigma-Aldrich) containing 100 µg/mL ampicillin (Sigma-Aldrich) (section 2.6.1). The bacterial starter culture was grown at 37°C overnight (16-18 hrs) at 210 rpm.

2.8.4 Overnight culture

Approximately 1-5 mL of the starter culture was added to 200 - 400 mL of LB broth containing 100 µg/mL ampicillin (section 2.6.1). The bacterial cultures were grown at 37°C overnight (16 – 18 hrs) at 210 rpm.

2.8.5 Glycerol stock

Glycerol stocks of transformed bacteria were made by mixing 750 µL bacterial culture with 250 µL 80% sterile glycerol in a microcentrifuge tube giving a final glycerol concentration of 20% and stored at -80°C.

2.8.6 Plasmid DNA extraction from starter culture *E. coli*

Plasmid minipreps (Section 1) were performed according to the manufacturer's instructions. Briefly, 5 – 10 mL of transformed bacterial starter culture was centrifuged at 3,200 rcf and the pellet resuspended in 250 µL of buffer A1 before transferring to a

microcentrifuge tube. Buffer A2 (250 μ L) was added to each sample and incubated at room temperature for 5 minutes to lyse the bacteria. Following incubation, 300 μ L of buffer A3 was added to neutralise the lysis solution and the microcentrifuge tube was inverted 5 times. The microcentrifuge tube was then centrifuged at 11,000 rcf for 10 minutes at room temperature. The plasmid containing supernatant was removed and added to the miniprep spin column and centrifuged at 11,000 rcf for 1 minute. 500 μ L of buffer AW was then added to the spin column and centrifuged at 11,000 rcf for 1 minute, then 600 μ L of buffer A4 was added to the spin column and centrifuged at 11,000 rcf for 1 minute. The spin column was then centrifuged at 11,000 rcf for 2 minutes without the addition of any buffer to remove residual solution. The spin column was placed inside a microcentrifuge tube and 30 μ L of nuclease-free water (Gibco) pre-warmed to 50°C was added and incubated for 5 minutes at room temperature to elute the plasmid DNA. The eluate was collected by centrifugation at 11,000 rcf for 1 minute. Plasmid DNA was analysed for concentration and quality on the NanoDrop 2000 spectrophotometer. Plasmid DNA was stored at 4°C for short term storage or -40°C for long term storage.

2.8.7 Plasmid DNA extraction from overnight culture

E. coli

Plasmid maxipreps (Section 1) were performed according to the manufacturer's instructions. Maxipreps was performed as per Macherey-Nagel instruction. Briefly, a 200 – 400 mL overnight bacterial culture with an OD₆₀₀ over 2 was collected by centrifugation at 6,000 rcf for 15 minutes at 4°C and the supernatant removed. The Bacterial pellet was resuspended in 12 mL of RES buffer containing RNase A, 67

$\mu\text{g/mL}$, and transferred to a 50 mL centrifuge tube. 12 mL of LYS buffer was added to the centrifuge tube, inverted 5 times and incubated for 5 minutes at room temperature. The lysis buffer was neutralised with the addition of 12 mL of NEU buffer and inverted 5 times. The maxiprep filter and column was equilibrated with 35 mL of EQU buffer before the lysed bacterial solution was added and allowed to drip through the filter and column into a waste centrifuge tube. The filter and column was washed with 15 mL of buffer EQU and allowed to drip through into the waste tube. The filter above the column was discarded and 25 mL of Wash buffer was added to the column and allowed to drip through. Plasmid DNA was eluted from the column by adding 15 mL of Buffer ELU and allowed to drip into a Nalgene round bottomed centrifuge tube (Nalgene, 3119-0050). 10.5 mL of isopropanol was added and the mixture vortexed thoroughly. The plasmid containing eluate and isopropanol mixture was centrifuged at 15,000 rcf for 30 minutes at 4°C to pellet the DNA. The supernatant was removed and 5 mL of 70% ethanol was added to the plasmid DNA pellet and centrifuged at 15,000 rcf for 5 minutes at room temperature. The supernatant was carefully removed and the DNA pellet was allowed to air dry for approximately 15 minutes. The DNA pellet was reconstituted in 300 μL of nuclease-free water (Gibco), and the concentration and quality were analysed using the NanoDrop 2000 spectrophotometer.

Chapter 3: Purification of *P. knowlesi* DNA from Frozen Whole Blood Samples

3.1 Introduction

Since the first *Plasmodium* genome was sequenced in 2002 there has been an explosion of data arising from genome sequencing (Gardner *et al.*, 2002). This has facilitated avenues of research and discoveries that previously would not have been possible, such as the discovery of novel proteins, further investigation of variant protein families, important epidemiological studies and tracking resistance to antimalarial drugs. To date genome sequences are available for all five human malaria species, *P. falciparum*, *P. vivax*, *P. knowlesi* and more recently *P. malariae* and *P. ovale* (Gardner *et al.*, 2002, Carlton *et al.*, 2008, Pain *et al.*, 2008, Rutledge *et al.*, 2017). Furthermore, genome sequences are available for the parasite species; *P. reichenowi*, *P. coatneyi*, *P. cynomolgi*, *P. yoelii*, *P. berghei*, *P. gaboni* (Tachibana *et al.*, 2012, Carlton *et al.*, 2002, Otto *et al.*, 2014a, Otto *et al.*, 2014b, Sundararaman *et al.*, 2016).

The reference genomes of the majority of *Plasmodium* species originate from experimental lines maintained *in vitro* or *in vivo* where high quantities of pure parasite DNA can be obtained. However, the sequencing of *Plasmodium* clinical whole blood samples requires the removal of leukocytes and host genomic DNA. The human genome is over 100 times larger than the parasite genome (Boissiere *et al.*, 2012) resulting in much higher quantities of human DNA (hDNA) in clinical samples compared to the parasite genome. If clinical samples are not leukocyte depleted prior to DNA extraction, the resulting DNA mixture will primarily consist of hDNA with a very small portion of parasite DNA. This in turn results in a low number of reads that map to the parasite reference genome, and low read coverage making sequence reliability problematic (Bright *et al.*, 2012). There are several published methods for leukocyte

depletion on fresh whole blood samples. The methods use a variety of different techniques such as; leukocyte depletion using hand packed CF-11 columns (Auburn *et al.*, 2011, Chan *et al.*, 2012, Sriprawat *et al.*, 2009, Venkatesan *et al.*, 2012); Plasmodipur filters (Grech *et al.*, 2002, Hunt *et al.*, 2004, Hunt *et al.*, 2010, Janssen *et al.*, 2001, Otto *et al.*, 2014b, Pain *et al.*, 2008, Roobsoong *et al.*, 2015, Sriprawat *et al.*, 2009); Lymphoprep density gradient (Venkatesan *et al.*, 2012); anti-HLA antibodies (Auburn *et al.*, 2011); and Flow cytometry (Boissiere *et al.*, 2012). Alternative methods have been developed to isolate parasite DNA, or remove the human DNA from a non-leukocyte depleted sample (Bright *et al.*, 2012, Melnikov *et al.*, 2011, Oyola *et al.*, 2016).

However, few of the techniques have been trialled on frozen whole blood clinical samples. To date, only one filtration method has been used to leukocyte deplete and recover parasite material from frozen whole blood (Pinheiro *et al.*, 2015). The frozen clinical whole blood samples contain intact leukocytes that have survived freezing along with lysed leukocyte, RBC and infected RBC (iRBC) material from the freezing process. The filtration method uses layered Whatman filter papers of different pore sizes to selectively remove intact leukocytes which have survived the freezing process. The eluate containing RBCs, iRBCs and free parasite material is then pelleted and washed free of contaminating hDNA (Pinheiro *et al.*, 2015). The authors had access to a biobank of clinical frozen whole blood samples from patients infected with *P. knowlesi* which were not leukocyte depleted prior to freezing. Pinheiro *et al.*, (2015) trialled various methods of leukocyte depletion on the frozen clinical samples including CF-11 filtration, but no material was recovered (Personal correspondence Dr Atique Ahmed). The final method consisted of three Whatman filter circles each with an 11 µm pore size

layered above three Whatman paper circles with pore a size of 6 µm inside the same 10 mL syringe to create a column. The pore sizes were selected to remove both small and large lymphocytes that had survived freezing, but to allow the iRBCs or free parasite material to pass through. Although parasite DNA was recovered and *P. knowlesi* genome sequences were obtained, there was consistently a substantial presence of hDNA in all samples, demonstrated by only two samples having a PkDNA purity >70% (Pineiro *et al.*, 2015). This work suggests that only high parasitaemia samples would be suitable for processing, due to the consistent hDNA presence after depletion. Furthermore, replication of the method with clinical samples with lower parasitaemias showed that insufficient hDNA was removed. This would limit the number of suitable samples available for leukocyte depletion.

The aim of this work was to enhance the hDNA depletion ability of the Whatman method for clinical frozen whole blood samples, while recovering maximum parasite material and to improve standardisation by incorporating a Plasmodipur filter. The Plasmodipur filter is a commercially available filter unit which contains two membranes. The Plasmodipur filter has been used extensively for leukocyte depletion, including leukocyte depletion of *P. knowlesi* to generate the *P. knowlesi* reference genome (Pain *et al.*, 2008). However, there has been no reported use of the Plasmodipur filters on frozen whole blood samples.

3.2 Methods

3.2.1 Whole blood seeded with *PkA1-H.1 in vitro* culture

Mock patient samples were created by mixing equal packed cell volumes of the *P. knowlesi PkA1-H.1 in vitro* culture (parasitaemias 1% to 1.5%) and non-leukocyte depleted donor whole blood (section 2.2.2). Following mixing, thin blood films were prepared to determine the percent parasitaemia and parasite life stage differential counts. The mixed seeded whole blood samples were divided into 200 µL packed iRBCs aliquots and frozen at -80°C to represent archived clinical samples. Percent parasitaemia and life stage of seeded samples are given, see Table 3.1.

Table 3.1 Parasitaemia and percent life stage of seeded samples used for leukocyte depletion.

Seeded Sample (SS)	Parasitaemia (%)	% Parasite Life stage (Rings : Trophs : Schizonts)*
SS1	0.75	32 : 59 : 10
SS2	0.56	48 : 44 : 07
SS3	0.54	72 : 22 : 06

*Parasite life stage was determined using giemsa stained blood films and categorised as ring, trophozoite or schizont. The percentage of ring stages, trophozoites and schizonts was counted for each seeded sample.

3.2.2 TaqMan quantitative PCR of *P. knowlesi* and human DNA

The TaqMan quantitative PCR system allows for accurate quantification of DNA. TaqMan probes specific for hDNA and for *P. knowlesi* DNA (PkDNA) were used as in Figure 3.1. Quantitative PCR (qPCR) was used to determine the concentration of

parasite and human DNA in seeded or clinical blood samples. Primers were specific for the *P. knowlesi* 18S rRNA gene (Rougemont *et al.*, 2004) and the β -globin gene in hDNA (Klaassen *et al.*, 2003), primer sequences given in Table 3.2. The *P. knowlesi* TaqMan probe was from (Divis *et al.*, 2010) and the human TaqMan probe from (Klaassen *et al.*, 2003), and the sequences are given in Table 3.2. The reagents and volumes required for a single 20 μ L qPCR reaction are given in Table 3.3. The qPCR cycling conditions were an initial denaturation step of 95°C for 10 minutes, followed by 55 cycles of: 95°C for 15 seconds and 60°C for 1 minute using the Rotor-Gene Q (QIAGEN). Primer and probe concentrations were optimised across a range of concentrations, and the final concentrations can be seen in Table 3.3.

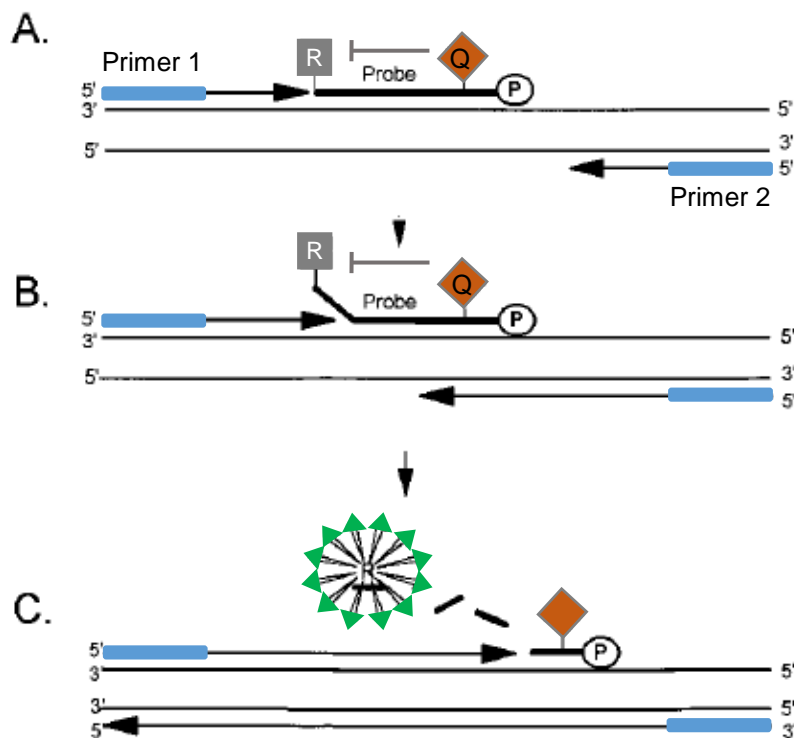


Figure 3.1 Schematic of TaqMan probe qPCR.

A. The TaqMan probe (P) containing a 5' fluorophore (R grey box) and 3' quencher (Q orange box) binds to single stranded DNA after the template DNA has been denatured. Primers (blue rectangles) bind to the template DNA and extension is facilitated by a DNA polymerase. The close proximity of the quencher (Q) to the fluorophore (R) quenches fluorophore fluorescence. **B.** The strand displacement properties of the polymerase causes the fluorophore (R grey box) on the 5' end of the probe to be dissociated from the DNA. **C.** Replaced of the 5' end of the probe with dNTPs causes cleavage of the fluorophore (R) from the

probe, which results in the fluorophore no longer being quenched. One fluorescent fluorophore is released for every amplicon produced, enabling accurate quantification of DNA. Figure adapted from (Morris *et al.*, 1996).

Table 3.2 TaqMan probes used for qPCR.

<i>TaqMan probe</i>	<i>Sequence (5'-3')</i>
Plasmo1	GTTAAGGGAGTGAAGACGATCAGA
Plasmo2	AACCCAAAGACTTTGATTTCTCATAA
Klaassen-F	GGGCAACGTGCTGGTCTG
Klaassen-R	AGGCAGCCTGCACTGGT
hDNA probe*	YAKYE -CTGGCCCATCACTTTGGCAAAGAA-BHQ1
Pk probe*	FAM-CTCTCCGGAGATTAGAACTCTTAGATTGCT-BHQ1

*Probes were obtained from Eurofins Genomics MWG Operon. (Divis *et al.*, 2010, Klaassen *et al.*, 2003)

Table 3.3 Mastermix for TaqMan multiplex qPCR

<i>Reagent</i>	<i>Stock concentration (μM)</i>	<i>Volume (μL)</i>	<i>Final concentration (nM)</i>
Klaassen-F	10	0.5	250
Klaassen-R	10	0.5	250
Plasmo 1	10	0.5	250
Plasmo 2	10	0.5	250
hDNA probe	10	0.2	100
PkDNA probe	10	0.16	80
TaqMan	2x	10	1x
Mastermix			
DNA extracted from whole blood	-	5	-
H ₂ O	-	2.64	-

(Divis *et al.*, 2010, Klaassen *et al.*, 2003)

Table 3.4 TaqMan qPCR cycling conditions.

<i>Temperature (°C)</i>	<i>Time</i>	<i>Cycles</i>
95	10 min	1
95	15 sec	55 cycles
60	1 min	

3.2.3 *P. knowlesi* and human DNA standard curves

Standard curves of both hDNA and PkDNA were generated using TaqMan[®] control genomic hDNA and PkDNA extracted from the *P. knowlesi* *PkA1-H.1* *in vitro* culture (Section 2.6.7). DNA concentrations of the standards were measured using Qubit 2.0 (Section 2.6.1). Serial dilutions of hDNA resulted in 9 dilutions ranging from 10 ng/μL to 39.1 pg/μL and similarly 10 dilutions of PkDNA ranging from 3.5 ng/uL to 6.8 pg/μL. Triplicate qPCR reactions were used to prepare each species DNA standard curve, see Table 3.3. The qPCR conditions were as given in Table 3.4. A fluorescent threshold value was calculated by the Qiagen Rotor-Gene Q (Qiagen) software to convert fluorescence to DNA concentration. QPCR for all whole blood DNA samples were analysed using the Rotor-Gene Q (Qiagen).

3.2.4 Whatman leukocyte depletion method

Leukocyte depletion was carried out as described in Pinheiro *et al.*, (2015). Briefly, diluted clinical whole blood samples were passed through three 6 μm Whatman filters below three 11 μm Whatman filters inside a 10 mL syringe by gentle centrifugation (125 rcf). The filter membranes were washed with ice cold PBS until the Whatman filters were no longer red. All eluate was combined and centrifuged at 2,021 rcf at 4°C

for 20 minutes. The pelleted intact RBCs and free parasite material were washed three times at 14,000 rcf for 2 minutes at 4°C with 1 mL PBS to remove soluble hDNA. The washed pellet was resuspended in a total volume of 200 µL PBS and DNA extraction performed as per section 2.6.7 (Pinheiro *et al.*, 2015).

3.2.5 Plasmodipur leukocyte depletion method

Plasmodipur leukocyte depletion to remove surviving leukocytes that remained after freezing was carried out by diluting 200 µL of seeded whole blood samples (SS1 – SS3, Table 3.1) in 10 mL of cold PBS pH 7.4. The diluted sample was loaded into a 10 mL syringe with a Plasmodipur filter attached, and gently passed through into a 50 mL centrifuge tube. The filter unit was detached from the syringe and the plunger was removed. The filter was subsequently washed three times with 10 mL cold PBS pH 7.4. The eluate and PBS washes containing iRBCs, RBCs and parasite material were centrifuged at 2,021 rcf at 4 °C. The pelleted intact RBCs and free parasite material was washed three times at 14,000 rcf for 2 minutes at 4°C with 1 mL PBS to remove soluble hDNA. The washed parasite pellet was resuspended in a total volume of 200 µL PBS and DNA extraction performed as per section 2.6.7.

3.2.6 Whatman-Plasmodipur leukocyte depletion method

Briefly, clinical samples stored at -80°C were thawed on ice and resuspended in 10 mL cold PBS pH 7.4 per 200 µL of frozen patient whole blood. Two 11 µm Whatman filter paper circles the diameter of a 10 mL syringe were placed inside a 10 mL syringe, with one syringe being used per 10 mL of dilute clinical sample. Each syringe was then

placed into a 50 mL centrifuge tube and pre-wet with 2 mL cold PBS pH 7.4. The PBS was passed through the Whatman filters by centrifugation at 11 rcf for 2 minutes at 4°C. Ten mL of the dilute clinical sample was added to each 10 mL Whatman constructed syringe and centrifuged at 20 rcf for 20 minutes at 4°C. Flow through was collected, stored on ice and 10 mL fresh PBS pH 7.4 was added to each syringe and centrifuged as before to wash the Whatman filter to collect any remaining parasite material. The second flow through containing retrieved material from the Whatman filter was combined to the first flow through on ice. A Plasmodipur filter (EuroProxima) for leukocyte removal was attached to a 20 mL syringe and pre-wet with 10 mL PBS. The flow through from the Whatman filtration step was added to the syringe and gently pushed through the Plasmodipur filter into a centrifuge tube. Gentle pressure was maintained evenly. The Plasmodipur filter was detached from the syringe, the plunger was removed, and the syringe reattached to the Plasmodipur filter. The Plasmodipur filter was washed with 20 mL PBS and collected into the same centrifuge tube. Plasmodipur filter was then washed three times in the same manner or until any red colouring had disappeared. The Plasmodipur flow through containing RBCs, iRBCs and free parasite material was centrifuged at 2,000 rcf at 4°C for 20 minutes. The supernatant was removed and the pellet resuspended in 1 mL PBS pH 7.4. The cell suspension was then centrifuged at 14,000 rcf for 2 minutes at 4°C. The supernatant was removed and parasite/RBC pellet resuspended in PBS. The PBS wash step was repeated 5 times or until the supernatant was clear. The pellet was resuspended in 200 µL PBS for DNA extraction, see section 2.6.7.

3.2.7 Fold reduction of DNA following leukocyte depletion

The fold change of both hDNA and *Pk* DNA was calculated by dividing post-leukocyte depletion total hDNA by the pre-leukocyte depletion total hDNA. For example, if the total pre leukocyte depletion hDNA concentration was 2000 ng and the post leukocyte depletion hDNA total was 5 ng then $5/2000 = 0.0025$ fold change. However, for ease each fold change value has been converted by using 1 as the dividend and the fold change value as the divisor. For example, $1/0.0025$ (fold change) = 400 fold reduction.

3.3 Results

Upon examination of the clinical data associated with the biobank of clinical samples it was evident that each sample differed greatly when comparing, white blood cell count, parasitaemia, whole blood haematocrit, and parasite life stage. In addition, it was unknown how promptly samples had been frozen. Because of this, it was decided that to produce a more standardised leukocyte depletion method, replicate samples would be required for testing prior to progression to clinical samples. In order to achieve this, fresh whole blood would be seeded with *P. knowlesi* *in vitro* culture of known parasitaemias to create a mock clinical sample which would then be frozen, mirroring the samples in our biobank prior to leukocyte depletion. It was decided that TaqMan qPCR would be used to quantify both *P. knowlesi* and human DNA, as it would be more accurate and more informative than iRBC and WBC counts pre and post-leukocyte depletion. In addition, it would provide accurate quantification of each DNA population at low nanogram levels, enabling samples suitable for genome sequencing to be identified.

3.3.1 Generation of standard curves for *P. knowlesi* and human DNA

In order to accurately quantify both *P. knowlesi* DNA (PkDNA) and human DNA (hDNA) known quantities of DNA were required to create standard curve for both PkDNA and hDNA. This would allow samples with unknown DNA concentrations to be identified by analysing how many cycles were required to reach a threshold

fluorescence value which can then be converted to a DNA concentration using the standard curve which would be maintained between experiments. DNA was extracted from the *PkA1-H.1 in vitro* culture (section 2.6.7) and TaqMan® Control Genomic hDNA was used to create standard curves (section 3.2.3). TaqMan qPCR was carried out as in section 3.2.2 and Figures 3.2 and 3.3 respectively. A cycle threshold was applied to give the most predictive concentration for each curve. R² squared values for PkDNA and for hDNA were 0.9927 and 0.996 respectively.

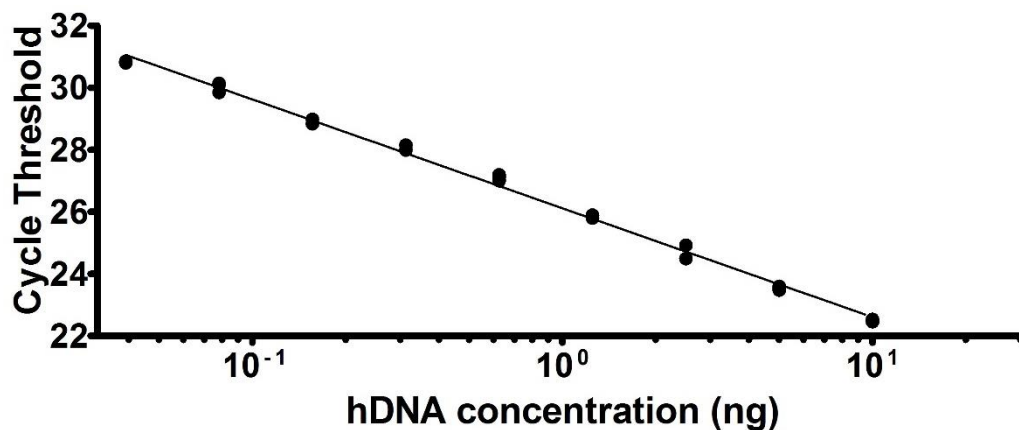


Figure 3.2 Standard curve of human DNA generated to accurately quantify hDNA in clinical samples.

A standard curve was generated for hDNA in order to quantify the hDNA in clinical samples containing a mixture of hDNA and PkDNA. A known concentration (10 ng/μL) of TaqMan control hDNA was serially diluted from 10 ng/μL to 0.04 ng/μL. hDNA was amplified using human specific primers and a human specific TaqMan probe (Klaassen *et al.*, 2003). Quantification of hDNA was carried out using the cycling conditions as detailed in Table 3.4 using the Rotor-Gene Q (Qiagen) qPCR machine. A cycle threshold (CT) was applied to the standard curve data in order to best represent fluorescence value for each data point with the given DNA concentration, allowing for unknown hDNA concentrations to be calculated using the following equation, concentration (ng/μL) = $10^{(-0.285 \cdot CT + 7.439)}$.

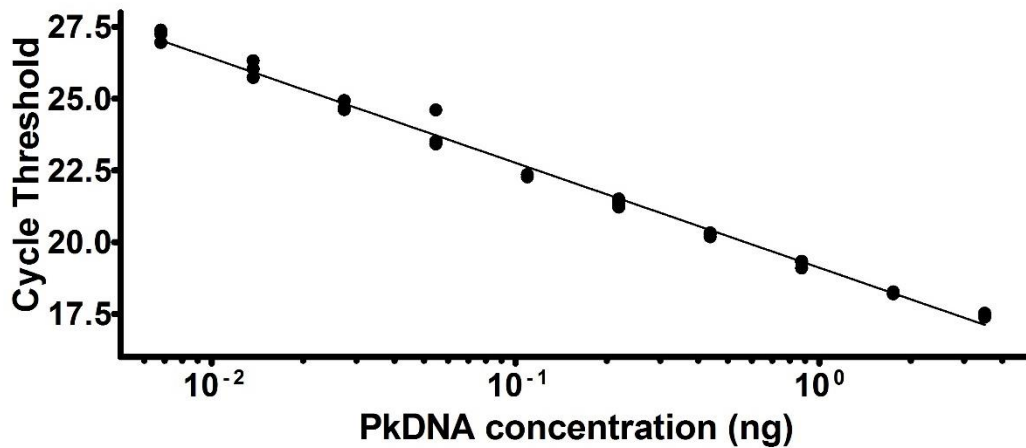


Figure 3.3 Standard curve of *P. knowlesi* DNA generated to accurately quantify PkDNA in clinical samples.

A standard curve was generated for PkDNA in order to quantify the PkDNA in clinical samples containing a mixture of hDNA and PkDNA. A known concentration (3.5 ng/μL) of PkDNA, isolated from the Pk A1-H.1 *in vitro* culture using the QIAgen DNA blood mini kit, were serially diluted from 3.5 ng/μL to 0.0068 ng/μL. PkDNA was quantified using PkDNA specific primers and a PkDNA specific TaqMan probe (Divis *et al.*, 2010). Quantification of PkDNA was carried out using the cycling conditions as detailed in Table 3.4 using the Rotor-Gene Q (Qiagen) qPCR machine. A cycle threshold (CT) was applied to the standard curve data in order to best represent fluorescence value for each data point with the given DNA concentration, allowing for unknown PkDNA concentrations to be calculated using the following equation, concentration (ng/μL) = $10^{(-0.274 \cdot CT + 5.228)}$.

3.3.2 Plasmodipur leukocyte depletion of seeded whole blood

In order to optimise the leukocyte depletion method a set of replicate samples were required that mirrored the frozen samples in our biobank. Donor whole blood was mixed with the *PkA1-H.1* culture at a 1:1 ratio and frozen, providing a stock of replicate samples to optimise leukocyte depletion with. The frozen seeded samples (SS1 to SS3) were depleted using solely Plasmodipur filtration.

Three aliquots of seeded sample 1 (SS1) were selected, two of these (SS1-1 and SS1-3) were leukocyte depleted using three 10 mL PBS pH 7.4 washes as in section 1.2.5, and

SS1-2 was processed with 5 mL PBS pH 7.4 washes. The ratio of human to parasite DNA in SS1 represented clinical isolates with high proportions of hDNA (mean total hDNA 3 ug and mean percentage of hDNA 88.9%) and low levels of PkDNA (mean total PkDNA 405 ng and mean percentage of PkDNA 11%, Table 3.5). Depletion of hDNA was seen in all three of these initial experiments, but to varying degrees. The depleted SS1-1 and SS1-3 samples had greater than 99.8% of hDNA removed, showing a fold reduction greater than 860 for both. The SS1-2 depletion had greater than 98.4% of hDNA removed with a 64 fold reduction in hDNA. The levels of post depletion PkDNA were similar for SS1-1 and SS1-3, however SS1-2 had lower levels of PkDNA, resulting in a lower percentage of PkDNA in the post-depletion sample compared with samples pre-depletion SS1-1 and SS1-3, see Table 3.5.

Table 3. 5 Plasmodipur leukocyte depletion of frozen whole blood seeded with the *P. knowlesi* PkA1-H.1 in vitro culture.

	Pre-Depletion		Post-Depletion	
	PkDNA ng (%)	hDNA ng (%)	PkDNA ng (%)	hDNA ng (%)
SS1-1	161.1 (7.4)	2026.2 (92.6)	69.5 (96.9)	2.2 (3.1)
SS1-2	398.3 (10.0)	3595.2 (90.0)	23.8 (29.8)	56.1 (70.2)
SS1-3	657.1 (15.8)	3495.2 (84.2)	69.7 (94.5)	4.1 (5.5)
Mean	405.5 (11.1)	3038.8 (88.9)	54.3 (73.7)	20.8 (26.3)
SS2-1	93.8 (0.8)	11737.1 (84.2)	9.5 (95.7)	0.4 (4.3)
SS2-2	54.9 (0.7)	8308.5 (99.3)	15.9 (97.0)	0.5 (3.0)
SS2-3	56.4 (0.7)	7786.0 (99.3)	38.6 (95.2)	1.9 (4.8)
SS2-4	58.8 (0.7)	8195.7 (99.3)	19.0 (99.0)	0.2 (1.0)
SS2-5	27.6 (0.9)	2967.5 (99.1)	6.4 (94.1)	0.4 (5.9)
SS2-6	56.9 (0.8)	6883.4 (99.2)	35.4 (99.0)	0.4 (1.0)
SS2-7	82.3 (1.0)	7874.0 (99.0)	44.0 (91.0)	4.4 (9.0)
Mean	61.5 (0.8)	7678.9 (99.2)	24.1 (95.9)	1.2 (4.1)
SS3-1	152 (2.1)	7041.6 (97.9)	57.0 (98.4)	0.9 (1.6)
SS3-2	101.8 (1.7)	5825.1 (98.3)	48.6 (95.8)	2.1 (4.2)
Mean	126.9 (1.9)	6433.3 (98.1)	52.8 (97.1)	1.5 (2.9)

A further two whole blood samples seeded (SS2 and SS3, Table 3.1) with *PkA1-H.1* culture were used to validate the reproducibility and success of the Plasmodipur leukocyte depletion method. The seeded samples were homogenised thoroughly by pipetting prior to aliquoting and freezing. Seven replicates were used for seeded sample 2 and a duplicate used for seeded sample 3. The Plasmodipur method was carried out as previously described (section 3.2.5), with the alteration that all seeded samples were diluted in 20 mL PBS pH 7.4 for Plasmodipur depletion, and 20 mL PBS wash steps were used. As seen with SS1, the SS2 pre-leukocyte depletion samples had high totals of hDNA (mean 7.6 ug, 99.2%) and low PkDNA (61.5 ng, 0.8%, Table 3.5). Following leukocyte depletion, the mean total hDNA was lower in samples receiving a 20 mL wash step (SS2) compared to a 5 mL or 10 mL wash step (SS1). Additionally, there was a higher recovery of parasite DNA in samples receiving a 20 mL wash step (SS2)

compared to the 5 mL or 10 mL wash steps used for SS1, suggesting the 20 mL wash step produced both greater hDNA depletion and greater recovery of PkDNA from the original starting material.

The SS3 samples were processed as per the SS2 samples, diluting the seeded sample in 20 mL PBS and using 20 mL wash steps. The purpose of the SS3 samples was to test whether the purification using 20 mL dilutions and wash steps was replicable with a different seeded sample. As with the SS1 and SS2 pre leukocyte depletion samples, the SS3 samples had high levels of hDNA and low levels of PkDNA (Table 3.5). The percentages of hDNA and PkDNA post-leukocyte depletion were similar to the post-leukocyte depletion percentages of SS2 depleted samples (Table 3.5), and the percentage of hDNA and PkDNA recovered were also comparable to SS2 (Table 3.6). The optimisation of the Plasmodipur method enabled the progression to clinical samples.

Table 3.6 Fold reduction and percent recovery of DNA following Plasmodipur leukocyte depletion of frozen whole blood seeded with the *P. knowlesi* PkA1-H.1 *in vitro* culture.

	Pre-Leukocyte Depletion, ng		Post-Leukocyte Depletion, ng		Fold Reduction		Percent Recovered	
	PkDNA	hDNA	PkDNA	hDNA	PkDNA	hDNA	PkDNA	hDNA
SS1-1	161.11	2026.2	69.53	2.22	2.3	912.7	43.2	0.11
SS1-2	398.28	3595.2	23.81	56.11	16.7	64.1	6.0	1.56
SS1-3	657.09	3495.2	69.69	4.05	9.4	863.0	10.6	0.12
SS1 Mean	405.49	3038.9	54.34	20.79	9.5	613.3	19.9	0.60
SS2-1	93.75	11737	9.51	0.43	9.9	27295.5	10.1	0.003
SS2-2	54.85	8308.5	15.93	0.5	3.4	16617.0	29.0	0.01
SS2-3	56.39	7786	38.63	1.93	1.5	4034.2	68.5	0.02
SS2-4	58.79	8195.7	19.01	0.19	3.1	43135.3	32.3	0.002
SS2-5	27.63	2967.5	6.38	0.4	4.3	7418.8	23.1	0.01
SS2-6	56.93	6883.4	35.37	0.35	1.6	19666.8	62.1	0.01
SS2-7	82.3	7874	43.99	4.36	1.9	1806.0	53.5	0.06
SS2 Mean	61.52	7678.9	24.12	1.17	3.7	17139.1	39.8	0.02
SS3-1	151.95	7041.6	57.02	0.91	2.7	7738.0	37.5	0.01
SS3-2	101.75	5825.1	48.59	2.13	2.1	2734.8	47.8	0.04
SS3 Mean	126.85	6433.4	52.81	1.52	2.4	5236.4	42.7	0.03

3.3.3 Whatman-Plasmodipur leukocyte depletion of clinical samples

Leukocyte depletion of clinical samples was performed as for seeded samples SS2 and SS3. However, the Plasmodipur leukocyte depletion of the initial clinical sample was not as successful as with the seeded samples. When processed, the Plasmodipur filter retained a brown discolouration that was unable to be washed through the filter and no material was recovered following centrifugation. This prompted a pre-filtration step incorporating 3 of the larger 11 µm Whatman circles, as used in the Whatman method. This was introduced to remove debris from the clinical sample in order to prevent

blockage of the Plasmodipur filter. The modified syringe filter was constructed, and leukocyte depletion carried out as in section 3.2.6.

Clinical samples were selected for newly modified Whatman-Plasmodipur leukocyte depletion based on the PkDNA content (greater than 100 ng, by qPCR section 3.2.2) or where available a parasite count greater than 35,000/ μ L based on reported parasitaemias from patient data. In total, 22 clinical samples were selected based on these criteria. The initial four clinical sample depletions using the combined Whatman-Plasmodipur method used three 11 μ m Whatman filters per syringe. Two of these four depletions were unsuccessful, due to damaged Whatman filter papers and subsequent blockage of the Plasmodipur filter. For the remaining 18 samples two 11 μ m Whatman filter papers were used in subsequent depletions to prevent clogging in the Whatman filter column before Plasmodipur leukocyte depletion.

Following Whatman-Plasmodipur depletion, a parasite pellet was present in 15 out of the 22 clinical samples processed. The DNA quantities and purities following DNA extraction (section 2.6.7) can be seen in Table 3.7. As with the seeded samples, the pre-depletion clinical samples contained high quantities of hDNA (median 96.5%) and low quantities of PkDNA (median 3.5%). Following Whatman-Plasmodipur depletion, the hDNA was a low proportion in thirteen of the fifteen depletions (median 8.2%). The resulting PkDNA percentage was high in 13 of the 15 samples (median 91.8%) although some of the samples had low quantities of PkDNA (Table 3.7). The fold reduction of hDNA was high with a median percent retention of 0.02%. The retention of PkDNA was lower (median 17.2%) than was seen with seeded samples (Table 3.6 and 3.8).

Thirteen of the fifteen samples contained PkDNA purities greater than 70 %, 9 of which had purities greater than 90 % PkDNA (Table 3.7). Eight of the fifteen depleted clinical samples contained greater than 100 ng of PkDNA as shown by the threshold in Figure 3.5, with 100 ng PkDNA being the requirement for genome sequencing on HiSeq and MiSeq Illumina machines. Two samples, SKS069 and SKS225, had no leukocyte depletion (Figure 3.4) and had post-depletion hDNA percentages of 97% and 87.8% respectively (Table 3.7). The remaining five samples (SKS308, SKS339, SKS313, SKS132 and SKS352) all had purities of PkDNA greater than 80%, with PkDNA quantities below 75 ng, and hDNA quantities below 5 ng (Figure 3.5 and Table 3.7).

Table 3.7 Post-Plasmodipur leukocyte depletion of clinical samples calculated by qPCR.

	Pre-Depletion		Post-Depletion	
	PkDNA ng (%)	hDNA ng (%)	PkDNA ng (%)	hDNA ng (%)
SKS325*	357 (3.7)	9355 (96.3)	290 (99.7)	0.9 (0.3)
SKS343*	324 (6.4)	4738 (93.6)	169.3 (82.2)	36.7 (17.8)
SKS069	235 (3.9)	5740 (96.1)	42.2 (3)	1350.5 (97)
SKS071	1357 (9.3)	13201 (90.7)	163.2 (71.8)	64 (28.2)
SKS074a	546 (11.4)	4258 (88.6)	216.3 (99.7)	0.8 (0.3)
SKS132	182 (1.1)	16548 (98.9)	24 (96.6)	0.8 (3.4)
SKS139	850 (5.8)	13882 (94.2)	139.0 (91.8)	12.4 (8.2)
SKS201a	5842 (24.6)	17947 (75.4)	2287.1 (99.9)	2.9 (0.1)
SKS225	505 (2.2)	22750 (97.8)	447.3 (12.2)	3227 (87.8)
SKS231	716 (3.1)	22353 (96.9)	641.9 (99.4)	3.8 (0.6)
SKS308	N/A	N/A	74.5 (99.2)	0.6 (0.8)
SKS313	151 (1.2)	12544 (98.8)	7.2 (80.8)	1.7 (19.2)
SKS339	518 (2.9)	17292 (97.1)	43 (91.3)	4.1 (8.7)
SKS344	1516 (4.5)	31852 (95.5)	161 (94.2)	9.9 (5.8)
SKS352	110 (1.2)	8788 (98.8)	3.7 (84.4)	0.7 (15.6)
Mean	935.86 (5.7)	14375 (94.3)	314 (80.4)	314.4 (19.6)
Median	511.5 (3.5)	13542 (96.5)	161 (91.8)	3.8 (8.2)
1st IQR	370 (2.3)	12873 (93.8)	42.6 (81.5)	0.8 (0.7)
3rd IQR	1103.5 (6.2)	20150 (97.7)	253.1 (99.3)	24.6 (18.5)

*denotes samples were processed with three 11 µm filter paper

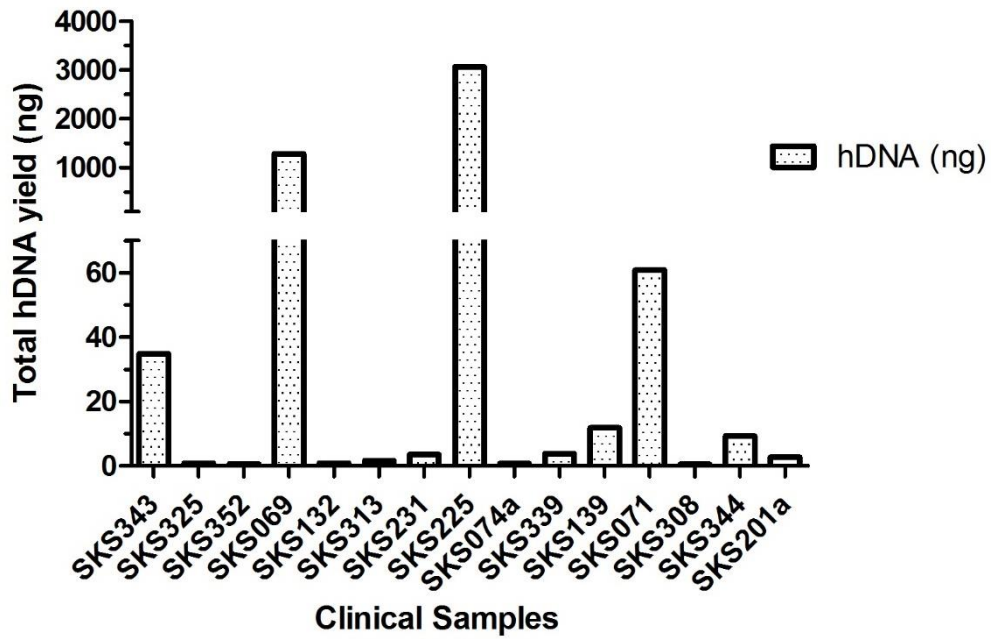


Figure 3.4 Total human DNA yield following Whatman-Plasmodipur depletion of frozen clinical samples.

Clinical samples were processed using the Whatman-Plasmodipur leukocyte depletion and the DNA was extracted using the Qiagen DNA blood mini kit. The hDNA was quantified using the Klaassen-F and Klaassen-R primers in combination with the hDNA TaqMan probe (Klaassen *et al.*, 2003) and cycled as in Table 3.4. Data shown is the mean qPCR reading of technical triplicates.

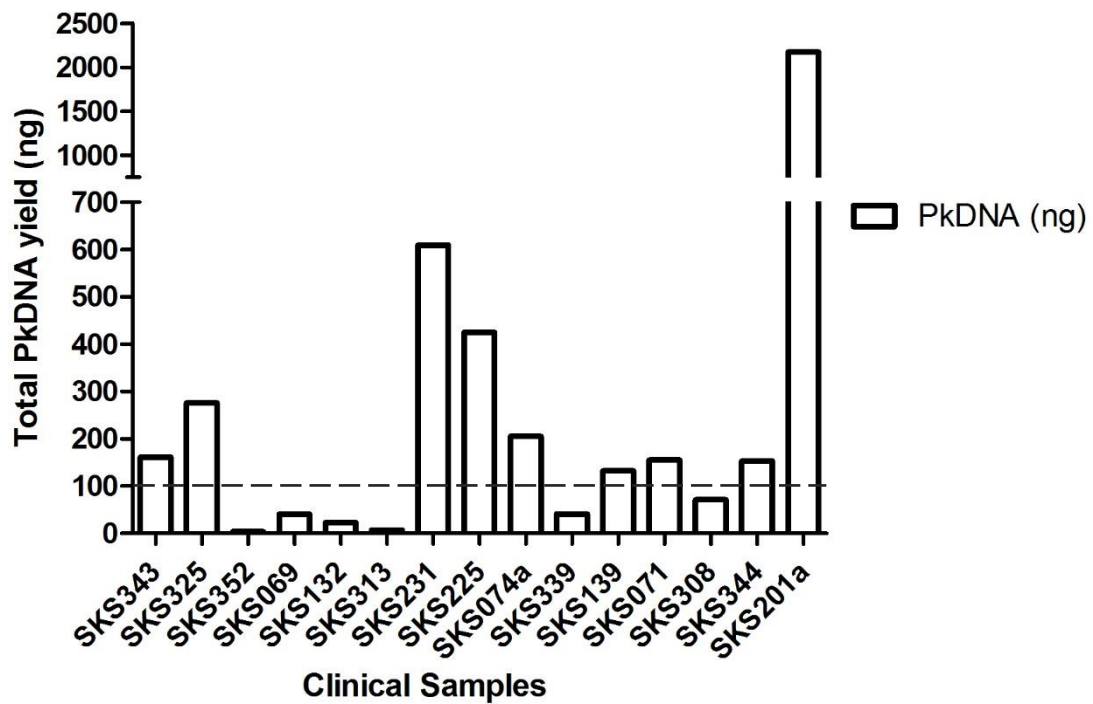


Figure 3.5 Total *P. knowlesi* DNA yield following Whatman-Plasmodipur depletion of frozen clinical samples.

Clinical samples were processed using the Whatman-Plasmodipur leukocyte depletion and the DNA was extracted using the Qiagen DNA blood mini kit. The PkDNA was quantified using the Plasmo1 and Plasmo2 primers in combination with the PkDNA probe (Divis *et al* 2010) and cycled as in Table 3.4. Data shown is the mean qPCR reading of technical triplicates. The dotted line denotes 100 ng of DNA, the minimum total DNA required for Illumina sequencing.

Table 3.8 Fold reduction and percent recovery of Whatman-Plasmodipur depleted *P. knowlesi* frozen clinical samples.

	Fold DNA Reduction		Percentage of DNA Retained	
	PkDNA	hDNA	PkDNA	hDNA
SKS325*	1.2	11005.9	81.2	0.01
SKS343*	1.9	129.1	52.3	0.77
SKS069	5.6	4.3	18.0	23.53
SKS071	8.3	206.2	12.0	0.49
SKS074a	2.5	5677.3	39.6	0.02
SKS132	7.6	19700.0	13.2	0.01
SKS139	6.1	1118.6	16.4	0.09
SKS201a	2.6	6188.6	39.1	0.02
SKS225	1.1	7.0	88.6	14.18
SKS231	1.1	5944.9	89.6	0.02
SKS313	21.0	7335.7	4.8	0.01
SKS339	12.0	4238.2	8.3	0.02
SKS344	9.4	3230.4	10.6	0.03
SKS352	29.8	12923.5	3.4	0.01
Mean	7.9	5550.7	34.1	2.8
Median	5.8	4957.8	17.2	0.02

*denotes samples were processed with three 11 µm filter paper

3.4 Discussion

The Whatman-Plasmodipur method successfully leukocyte depleted frozen *P. knowlesi* clinical samples to hDNA levels suitable for Illumina sequencing. Clinical samples were diluted in 20 mL PBS and filtered through two 11 µm Whatman filter papers per 10 mL syringe. The eluate was then filtered through a Plasmodipur filter and washed repeatedly with 20 mL PBS. The eluate was centrifuged and the parasite pellet was washed of soluble hDNA. Filtration through the two 11 µm Whatman filter papers was designed to remove debris from the frozen sample and prevent blocking the Plasmodipur filter. The Plasmodipur filter was more efficient compared to the 6 µm Whatman leukocyte depletion as in Pinheiro *et al.*, (2015). The adapted method was devised to enhance hDNA removal, while endeavouring to maximise recovery of PkDNA. The Plasmodipur filter was selected due to the standardisation of the filters, in comparison to the homemade CF-11 columns, which have been reported to be variable (Auburn *et al.*, 2011) and debate over retention of specific life stages (Janse *et al.*, 1994, Sriprawat *et al.*, 2009). Plasmodipur filters had previously been used to successfully leukocyte deplete fresh whole blood from a Rhesus macaque infected with *P. knowlesi*, with the purified parasites being used for DNA extraction and sequencing (Pain *et al.*, 2008), but until now have not been used on frozen whole blood samples.

Here the results show that Plasmodipur filtration alone performed well for seeded samples, depleting 98% of hDNA. However, processing of a clinical sample using the Plasmodipur filter alone resulted in a brown colouration of the filter and no recovery of RBCs, iRBCs or parasite material. The adapted method depleted greater than 99% of hDNA from 13 clinical samples, which was greater than the depletion reported by (Pinheiro *et al.*, 2015). However, two samples did not show sufficient removal of

hDNA. In addition, a parasite pellet was unable to be retrieved from 7 samples during leukocyte depletion. The reasons for this ranged from extensive lysis of the clinical sample, blockage in the Plasmodipur filter and blockage or damage to the 11 µm Whatman filter papers. The 13 successful purifications resulted in 8 samples with PkDNA quantities and purities suitable for genome sequencing on Illumina platforms. Additionally, as per Boissiere *et al.*, (2012) whole genome amplification could be incorporated to amplify the DNA content of the 5 samples below 100 ng of total PkDNA, all of which had greater than 80% PkDNA (Boissiere *et al.*, 2012).

The clinical data for the samples which failed to produce a parasite pellet following leukocyte depletion were analysed for any feature which associated with the recovery of *P. knowlesi* DNA. The parasite life stage was analysed by plotting the percentage of parasites in each life stage (ring, trophozoite, schizont or gametocyte) for each clinical sample against the percent recovery of PkDNA. A negative correlation (-0.56) was identified when the percentage of trophozoites in clinical samples was plotted against the percentage of PkDNA retained following leukocyte depletion (Appendix C). This may be a result of either; late stage parasites being prone to agglutination causing clumping and blockage of filters, or, increased lysis of late stage parasites during storage at -80°C producing more cell debris, increasing the risk of blockages (Jeffery, 1962, Wilson *et al.*, 1977). It would be useful to test this with further samples to give some indication of the potential for using the Whatman-Plasmodipur method on particular frozen clinical isolates, as success may be dictated by parasite asexual life stage. Testing would require synchronous cultures to be sampled throughout the life cycle and stored at -80°C. This would provide samples which have identical

parasitaemias, but with each replicate containing progressively more mature parasites enabling a direct comparison between retrieval of PkDNA and parasite life stage.

To date, there are a variety of filtration methods used for leukocyte depletion of malaria samples, such as cellulose packed syringes, commercially available Plasmodipur filters, non-woven filters and the Whatman filtration method (Janse *et al.*, 1994, Tao *et al.*, 2011, Fulton and Grant, 1956, Pinheiro *et al.*, 2015, Venkatesan *et al.*, 2012, Auburn *et al.*, 2011). However, only the Whatman filtration method has reported purification of parasite material from frozen clinical whole blood samples and subsequent genome sequencing using filtration. One method previously described the isolation of *P. falciparum* from frozen clinical samples (Boissiere *et al.*, 2012), where flow cytometry was used to isolate 200 *P. falciparum* nuclei, followed by whole genome amplification. This process yielded genome sequence data for *P. falciparum* where 62% of reads mapped to the *P. falciparum* reference genome. Although not sequenced, the mean PkDNA percentage for clinical samples presented here was greater than 80%. The difference between the two methods may be because the target region for flow cytometry is based on fluorescence intensity of propidium iodide stained nuclei and cell size (Boissiere *et al.*, 2012). This could result in debris containing human nuclear material being incorrectly sorted as parasite nuclei. Additionally, this technique requires access to a flow cytometer with cell sorting abilities which is not common lab equipment. Conversely, the Whatman-Plasmodipur methods described here requires only a centrifuge making it not only more efficient but more readily accessible for the research community.

The whole genome amplification described by Boissiere *et al.*, could be a pivotal inclusion to the Whatman-Plasmodipur method obtaining samples suitable for genome sequencing. The median hDNA removal for the method presented here is greater than 99%, however there are samples which contain less than 100 ng of PkDNA and less than 20% hDNA, therefore the incorporation of whole genome amplification for low PkDNA recovery samples could enable them to be sequenced. If the amplification is not biased towards species, these high percentage PkDNA fractions should remain but with a greater quantity. Further research has shown that if leukocyte depletion was not performed on clinical samples prior to long term storage, the parasite DNA is able to be isolated from the mixed DNA population using biotin tagged RNA probes. Briefly, control genomic DNA is sheared to approximately 250 bp and is used as the template DNA for creating the baits. The sheared ends were repaired and dA tailed prior to the ligation of an adapter oligonucleotide sequence. PCR was then carried out using primers specific for the adapter sequence followed by amplification of the PCR product using a primer containing a T7 promoter. The PCR product is then amplified using T7 RNA polymerase in the presence of biotinylated uracil, producing biotinylated RNAs complimentary to regions throughout the genome (Melnikov *et al.*, 2011). Following this the biotinylated RNA baits can be incubated with a mixed DNA population, and pulled down using streptavidin coated beads (Melnikov *et al.*, 2011). The streptavidin beads are washed to remove any unbound DNA, and the genomic parasite DNA can be eluted. Whole genome amplification can then be performed to increase the total yield of parasite DNA to levels suitable for genome sequencing (Melnikov *et al.*, 2011). However, this process seems to enrich for regions of the genome where the RNA-baits are targeted which could result in bias read coverage to RNA bait regions of the

genome, although it appears this did not affect the genome sequencing outputs (Melnikov *et al.*, 2011). However, Bright *et al.*, show that selection of *P. vivax* DNA using RNA baits, resulted in genome sequence outputs that biased against GC % rich areas of the genome, compared against a leukocyte depleted sample (Bright *et al.*, 2012). Oyola *et al.*, 2016 describe a method to selectively amplify *P. falciparum* genomic DNA using primers specific to the *P. falciparum* genome. However, the subtelomeric regions, which contain variable gene families such as *var*, *rif stevor* and *phist* gene families, were not covered (Oyola *et al.*, 2016, Gardner *et al.*, 2002, Witmer *et al.*, 2012). Also, the element of bias toward specific regions of the genome where primers are located, is not fully addressed. This suggests that leukocyte depletion would be preferable for: (a) high GC content genomes like *P. knowlesi*; and (b) subsequent genome analysis of repeat gene families.

In order to further develop the Whatman-Plasmodipur method, testing of sample selection parameters could have been performed. The mock clinical samples were frozen immediately following homogenisation, and when processed they did not cause blockages of the Whatman or Plasmodipur filters. However, the clinical samples used in this study may not have been stored as rapidly as in this study. In order to recreate the variability of frozen clinical *P. knowlesi* whole blood samples, the seeded samples could have been incubated at room temperature prior to freezing. Additionally, clinical samples may have undergone freeze-thaw events, and this too could have been tested with seeded samples. The parasite life stage could also have been analysed by obtaining synchronous cultures of rings, trophozoites and schizonts to analyse the retrieval of parasite material following the freezing process.

The Whatman-Plasmodipur method presented here improved upon the hDNA depletion published by Ahmed *et al.*, (2014) using archived frozen clinical samples. The method results in low quantities of hDNA, and high purity *Pk*DNA, important for genome sequencing, enabling genomic research to be conducted on archived clinical samples.

**Chapter 4: *Plasmodium knowlesi* A1-H.1
transfection to knock-in a clinically
relevant variant of the gene *Pknbpxa***

4.1 Introduction

Severe malaria is a highly complex disease involving variable parasite and host factors (Miller *et al.*, 2002). A common theme in severe *P. knowlesi* and *P. falciparum* malaria is high parasitaemia (Daneshvar *et al.*, 2009). The accessibility of new rapid genome sequence platforms has opened novel opportunities to explore the role for parasite genetic variability in severe malaria (Pinheiro *et al.*, 2015, Chokejindachai and Conway, 2009). Genetic variation at invasion gene loci may affect the specificity or affinity of merozoite invasion proteins for RBC receptors. An experimental cross of two *P. falciparum* lines exhibiting differing abilities to invade and replicate in *Aotus nancymaae* erythrocytes was performed (Hayton *et al.*, 2008). Only progeny with specific inherited markers from the parent able to invade *A. nancymaae* erythrocytes were able to invade *A. nancymaae* erythrocytes. Further analysis revealed that a single amino acid substitution in the *P. falciparum* reticulocyte binding-like homologue 5 (PfRh5) protein was responsible for this change in phenotype in parasite tropism and also parasite invasion rate (Hayton *et al.*, 2008, Mayer *et al.*, 2002, Mayer *et al.*, 2004). This suggests that small differences in invasion proteins can have profound effects on invasion characteristics, thereby altering parasite invasion phenotypes. An association between markers of severe malaria and the PfRh proteins has not yet been reported, but variants of the *P. knowlesi* normocyte binding protein Xa (*pknbpxa*), a protein essential for the invasion of human RBCs by *P. knowlesi* (Meyer *et al.*, 2009, Semanya *et al.*, 2012, Moon *et al.*, 2016), were recently implicated in progression to severe disease in *P. knowlesi* malaria in Malaysian Borneo (Ahmed *et al.*, 2014). Ahmed and colleagues identified that a dimorphism was present in an 885 bp 5' region of the *P. knowlesi*

Pknbpxa gene, with one of the dimorphic clusters being more diverse (cluster 2) (Figure 4.1). In addition, 34% of *P. knowlesi* clinical isolates with cluster 2 type *Pknbpxa* sequences contained a proline at amino acid 200 which was found to be associated with clinical markers of severe disease, including high parasitaemia ($p = 0.02$) (Figure 4.1, Ahmed *et al.*, 2014), suggesting that mutations in the *Pknbpxa* gene may be involved in virulence. Development of the *P. knowlesi in vitro* culture in human RBCs has provided a model where the association with high parasitaemia can be carried out. However, phylogenetically the PkNBPXa protein sequence in the *PkAI-H.1* clone does not cluster with either dimorphic cluster 1 or 2 and instead appears ancestral to both clusters meaning that the *Pknbpxa* sequence does not represent either cluster 1 or cluster 2.

The work presented here employs whole genome sequence data, generated from *P. knowlesi* clinical isolates (Pinheiro *et al.*, 2015), to assemble the full-length sequence of *Pknbpxa* cluster 2 variants. This sequence data was subsequently used to guide the construction of a transfection plasmid to knock-in and replace the wild-type *Pknbpxa* gene with a clinically relevant *Pknbpxa* isoform. The experimental line, *P. knowlesi* *PkAI-H.1*, which has been adapted to *in vitro* culture in human erythrocytes was employed for this purpose (Moon *et al.*, 2013).

4.2 Methods

4.2.1 Next generation sequence alignment

Fastq files containing HiSeq and MiSeq reads previously generated from *P. knowlesi* clinical isolates (Pineiro *et al.*, 2015) with study accession code PRJEB1405 and accession codes ERR274221, ERR274222, ERR274223, ERR274224, ERR274225, ERR366425 and ERR366426, were downloaded from the EMBL-EBI European Nucleotide Archive (<http://www.ebi.ac.uk/ena/data/view/PRJEB1405>). The *P. knowlesi* reference genome (version 11.1) was downloaded from PlasmoDB (www.plasmodb.org/plasmo/). The *Pknbp_{xa}* locus of interest was incorrectly annotated with 3 exons on chromosome 14 in the original reference genome (Pain *et al.*, 2008). The genomic *Pknbp_{xa}* coding sequence was replaced with the Meyer *et al.*, (2009) published *Pknbp_{xa}* sequence (PKNH_1472300) enabling the *P. knowlesi* clinical genome sequences to be aligned correctly at this locus (Meyer *et al.*, 2008, Pineiro *et al.*, 2015). The Bowtie 2 program was used to align paired end reads (100bp) to the edited reference genome. Files were output as *.sam* files and converted to *.bam* files before sorting and indexing. BEDtools was then used to measure the coverage for each alignment to the reference.

4.2.2 Variant call analysis

The samtools mpileup function (Li *et al.*, 2009) was used in combination with BCFtools to identify variant positions. Only bases with a base alignment quality (BAQ) score above 13 were called as variant bases to remove possible sequencing errors from further analysis. The BCFtools (Li, 2011) VarFilter command was used to remove single

nucleotide polymorphisms (SNPs) with an allele frequency less than 0.9. In combination with the removal of sequencing errors, inserts and deletions were also removed from further analysis.

4.2.3 *Pknbpxa* DNA sequence extraction

The *Pknbpxa* gene is located at 3,176,653 bp on chromosome 14 of the corrected Pinheiro *et al.*, (2015) *P. knowlesi* reference genome sequence. Chromosome 14 from the previously mentioned clinical genome sequences were aligned to the reference genome sequence using the genome browser software Artemis (Carver *et al.*, 2012). Alignment to the reference, and visualisation of the *Pknbpxa* locus enabled the *Pknbpxa* genes sequences from the clinical isolates to be extracted and saved as fasta files. The seventh genome sequence (ERR274223) was not analysed as this was a post-treatment sample isolated from a patient where a pre-infected sample was obtained (ERR274222) (Pinheiro *et al.*, 2015). The full-length *Pknbpxa* gene sequences from all 6 isolates were extracted as FASTA files with insertions and deletions removed. Three of the sequences were in *Pknbpxa* cluster 1 (ERR274224, ERR274225 and ERR366425) and three in cluster 2 (ERR274221, ERR274222 and ERR366426).

4.2.4 Nucleotide diversity calculation

Nucleotide diversity in the *Pknbpxa* gene was calculated using DnaSP with a step size of 25 bp and a sliding 400 bp window (Librado and Rozas, 2009).

4.2.5 Selection of *Pknbpxa* cluster 2 variation

The *Pknbpxa* gene sequence in the *PkA1-H.1* line contained SNPs present in both cluster 1 and 2, suggesting it is ancestral to both clusters. In order to examine the impact of the S200P mutation, only present in cluster 2, the residues defining cluster 2 were identified. This would allow a *Pknbpxa* sequence containing only the cluster 2 sequence to be transfected into the *PkA1-H.1* line, followed by the *Pknbpxa* cluster 2 sequence containing the S200P mutation. The cluster 2 sequence was defined as SNPs present in all three *Pknbpxa* cluster 2 sequences that resulted in a non-synonymous amino acid changes as seen in Figure 4.2 (all mutations detailed in Appendix D). Where there was not 100% consensus on amino acid positions between the three sequences in cluster 2, the most frequently occurring amino acid between both clusters was selected. Alignments of both DNA and amino acid sequences were performed using Clustal Omega (Sievers *et al.*, 2011) and Jalview software (Waterhouse *et al.*, 2009).

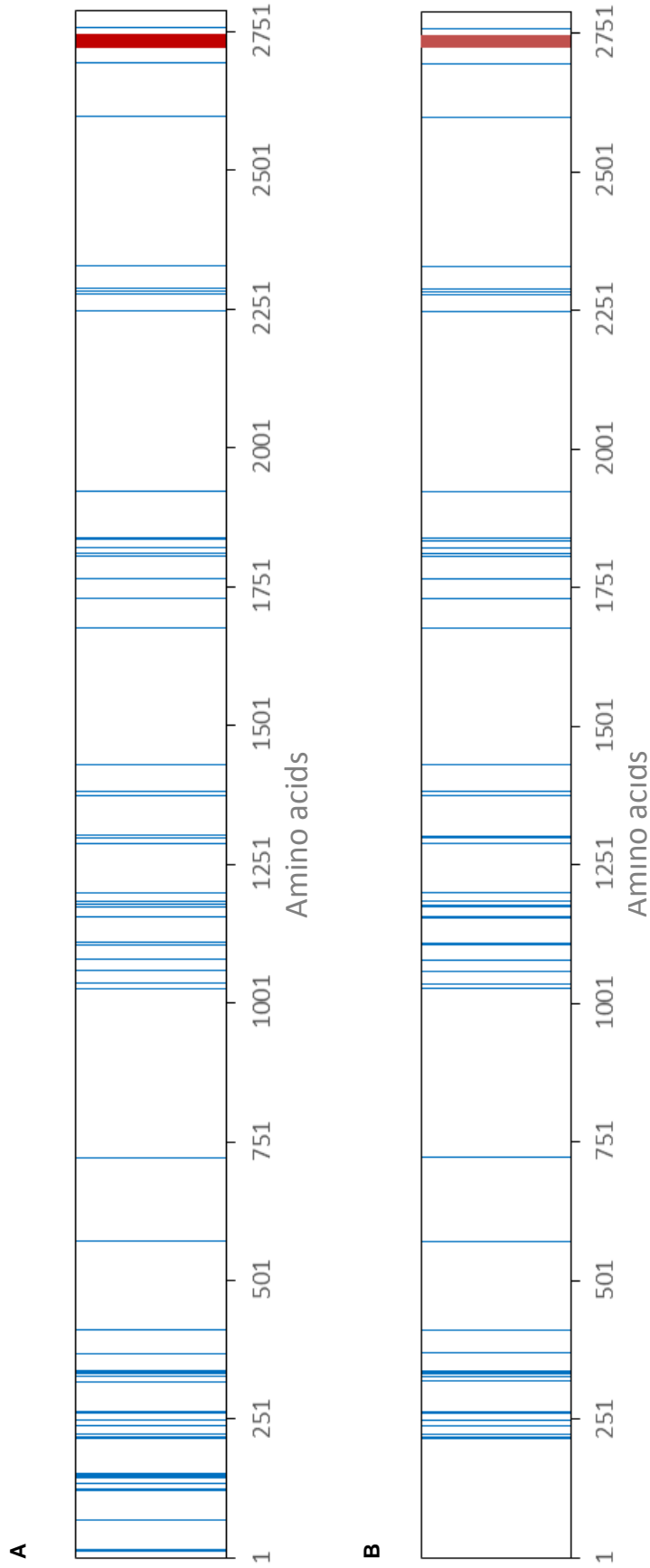


Figure 4.2 Schematic showing the locations of the residues in the *Pknbpxa* protein defining cluster 2.

A. The locations of all 65 residues defining cluster 2 have been mapped on the *Pknbpxa* protein (blue). The transmembrane domain has also been annotated (red); showing that one cluster 2 specific residue is on the Cytoplasmic tail, while the remaining 64 residues are located in the ectodomain of transmembrane protein. All 65 cluster 2 specific amino acids in the PkNBPXa protein can be found in Appendix D.

B. Thirteen of the cluster 2 specific residues were located within the first 160 amino acids at the N-terminal region of the *Pknbpxa* protein. These 13 cluster 2 specific residues were removed from the *Pknbpxa* cluster 2 gene coding sequence, as it was essential for this sequence to be to be homologous to the parental *Pknbpxa* sequence in the *PkA1-H.1* clone for later transfection studies.

4.2.6 Synthesis of the cluster 2 *Pknbpxa* gene

The following assignment of the *Pknbpxa* gene sequence to represent cluster type 2 was performed *in silico*. Positions identified as defining cluster type 2 were used to inform the construction of the synthetic *Pknbpxa* cluster type 2 gene for transfection experiments using single-crossover homologous recombination with the Pk_{con}GFP plasmid (Figure 4.5) developed for *P. knowlesi* transfection by Moon *et al.*, (2013) (Figure 4.13). The *Pknbpxa* gene sequence from the corrected *P. knowlesi* reference genome was extracted along with the 186 bp intron separating exon 1 and exon 2, and 243 bp of the 5' non-coding region Figure 4.3. A 3x HA tag (5' TAC CCA TAC GAT GTT CCA GAT TAC GCT 3', 84 bp) was added to the 3' end of the *Pknbpxa* coding region and immediately prior to the stop codon. The restriction site motifs *NotI*, *XmaI* and *SacII* in the Pk_{con}GFP plasmid were selected to remove the Pk HSP70 promoter and the GFP coding sequence (Figure 4.3 A), The *NotI* restriction site was added to the 5' end of the synthetic *Pknbpxa* sequence and the *SacII* restriction site was added to the 3' end of the sequence. A 1 kb region of homology was retained in the synthetic gene sequence to direct plasmid integration into the genomic *Pknbpxa* locus. Synonymous mutations were introduced at position 1010 bp in the synthetic *Pknbpxa* sequence to create the *XmaI* restriction site (5' cccggg 3'), and at position 4931 bp creating the *SpeI* restriction site (5' actagt 3'). The *NotI* and *XmaI* restriction sites flanked the region of homology in the *Pknbpxa* synthetic fragment *I(f1)* (Figure 4.3). This region was synthesized by GeneArt™ (Invitrogen™) and was delivered in a pMA-RQ vector (Plasmid map Appendix E).

Non-synonymous mutations to represent *Pknbpxa* cluster 2 (Section 4.2.5) and additional restriction sites to facilitate cloning were introduced into the remaining *Pknbpxa* 7874 bp fragment that was flanked by *Xma*I (5' end) and *Sac*II (3' end) (Figure 4.2, and Appendix D). The 7874 bp region was synthesised as two fragments (Figure 4.3). Synonymous mutations were introduced 4514 bp (4940 bp, including non-coding region and intron) into the remaining *Pknbpxa* sequence to create the *Spe*I restriction site (5' actagt 3'), and forming *Pknbpxa_f2* flanked by *Xma*I and *Spe*I and the final fragment *Pknbpxa_f3* was flanked by *Spe*I and *Sac*II. A 16 bp link sequence containing the *Sac*II restriction site was added immediately following the *Spe*I restriction site on the 3' end of *Pknbpxa_f2* to allow ligation of the *Pknbpxa_f3* fragment during transfection plasmid construction. The *Pknbpxa_f2* and *Pknbpxa_f3* fragments were codon optimized ensuring that the *Not*I, *Kpn*I, *Xma*I, *Spe*I and *Sac*II restriction site motifs were not disrupted at any position. The *Pknbpxa_f2* and *Pknbpxa_f3* sequences were synthesized by GeneArt™ (Invitrogen™).

Briefly, the GeneArt™ synthesis process involved *de novo* synthesis of overlapping short oligonucleotides covering the 3 *Pknbpxa* sequences individually (*Pknbpxa_f1*, *Pknbpxa_f2* and *Pknbpxa_f3*). The overlapping oligonucleotides were ligated using rounds of PCR to construct each *Pknbpxa* fragment (GeneArt™). The *Pknbpxa* fragments were flanked by the *Sfi*I restriction site and cloned into the pMA-RQ plasmid (Appendix E).

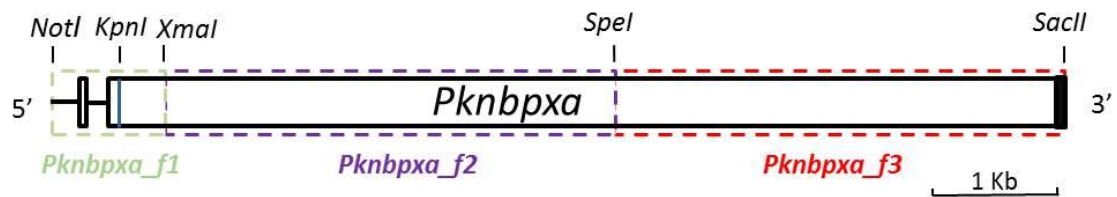


Figure 4.3 Schematic of the *Pknbpxa* gene fragments and location of restriction sites used for cloning.

The *Pknbpxa* gene from the corrected *P. knowlesi* genome consists of a short non-coding region (291 bp), a small exon1 (54 bp) and a much larger exon2 (8398 bp) separated by a short intron (186 bp). *Pknbpxa* was divided into three fragments as follows; fragment 1 (green box) representing the region of homology' Fragment 2 *Pknbpxa_f2* (purple box) and *Pknbpxa_f3* (red box) were codon optimized for *E. coli* codon usage to alter the DNA sequence but code for the same protein. Cluster 2 mutations were created in the *Pknbpxa_f2* and *Pknbpxa_f3* coding sequences thereby introducing the amino acid substitution associated with cluster 2. A 3xHA tag (black box) was introduced at the 3' end of *Pknbpxa_f3* fragment. Synonymous mutations were used to create *XmaI* and *SpeI* restriction enzyme sites at 1010 bp and 4938 bp respectively for subsequent cloning steps. A naturally occurring *KpnI* restriction enzyme motif (blue line, 578 bp) was located centrally in *Pknbpxa_f2*, towards the 5' end of exon2.

4.2.7 Restriction digestion of the *PkconGFP* plasmid

The *Pk_{con}GFP* and the *Pk_{con}p230pGFP* plasmids were kind gifts from Dr Moon (NIMR/LSHTM) (Figure 4.3). The *Pk_{con}GFP* plasmid contained the human dihydrofolate reductase selection marker (hDHFR), used for stable integration, (Figure 4.5a) under the control of a *P. knowlesi* specific promoter (*PkEF1a* 5' UTR, Figure 4.5a). Additionally, the *Pk_{con}GFP* plasmid contained the restriction sites *NotI*, *XmaI* and *SacII*, all required for cloning the *Pknbpxa_f1*, *Pknbpxa_f2* and *Pknbpxa_f3* fragments sequentially. The *Pk_{con}GFP* Plasmid was digested using the restriction enzymes *NotI* and *XmaI* as per the manufacturer's instructions (section 2.6.4). This removed the HSP70 5'UTR and GFP coding regions not required for *Pk_{con}Pknbpxa_f1-3* plasmid construction.

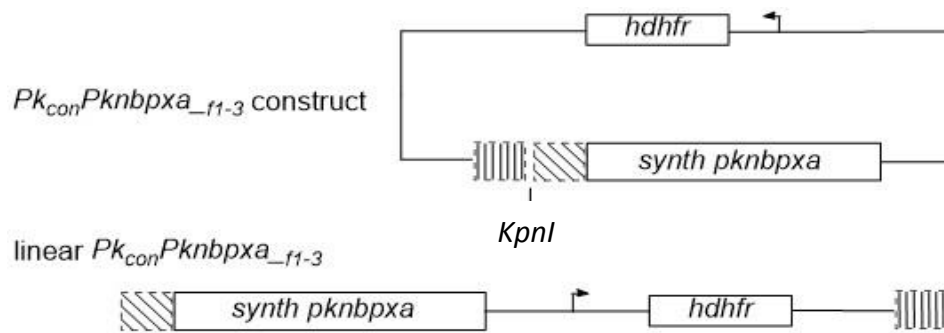


Figure 4.4 Schematic of *Pk_{con}Pknbpxa_{f1-3}* construct linearized at the *KpnI* restriction site. Restriction digest at the *KpnI* (578 bp) motif linearizes the construct in the middle of the 1010 bp region of homology, resulting in ends flanked with ~500 bp *Pknbpxa* homologous sequence. Human Dihydrofolate reductase (*hDHFR*) gene was included to select for transfected cells.

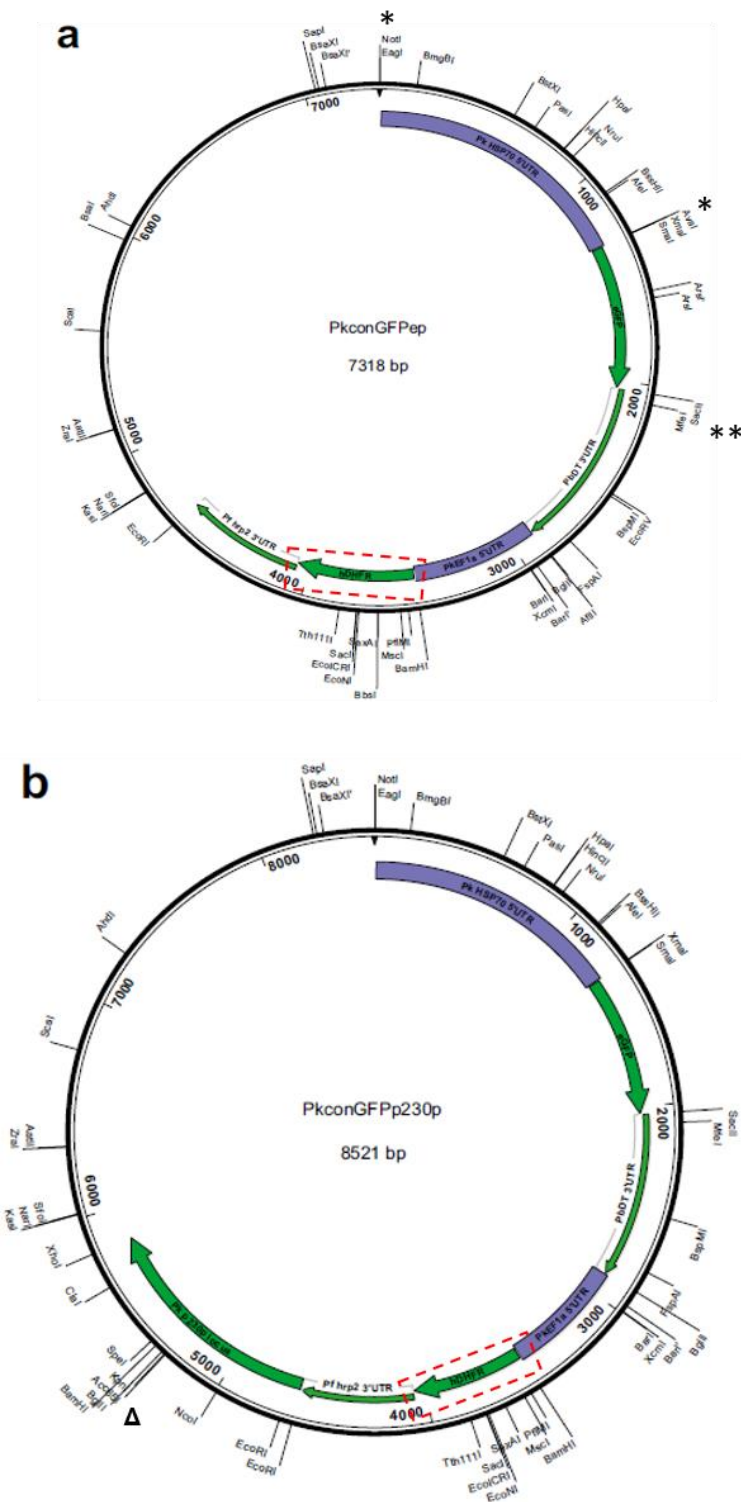


Figure 4.5 Map of the PkconGFP and Pkconp230pGFP transfection plasmids. **(A)** The PkconGFP and **(B)** the Pkcon p230pGFP plasmids were a kind gift from Dr Moon (LSHTM). Both plasmids contained the PKHSP70 5' UTR (purple box) followed by the GFP coding region (thick green arrow), and the PbDT3'UTR (thin green arrow). The PkEF1a 5' UTR promoter (purple) at the 5' end of the Human Dihydrofolate reductase (hDHFR) gene (thick green arrow highlighted in the red box) followed by the Pfhpr2 3'UTR (thin green arrow). **(A)** Digestion of the PkconGFP construct at the *NotI* and *XmaI* sites

(*) (1.3 kb) allowed for the removal of the 5' HSP70 promoter and the subsequent ligation steps of the *Pknbpxa_f1* fragment, followed by digestion at (**) *SacII* and *XmaI* (*) for *Pknbpxa_f2* and *Pknbpxa_f3* ligation steps **(B)** In the *Pk_{con}p230pGFP* plasmid the *Pkp230p* locus was situated immediately adjacent to the 3' end of the *Pfhrp2* 3'UTR. Restriction digest site *KpnI* (Δ) allows the plasmid to be linearised centrally in the *p230p* locus prior to transfection for stable integration into the *p230p* genomic locus. Plasmid maps adapted from Moon *et al.*, 2013.

4.2.8 Sequential ligation of synthetic *Pknbpxa* Cluster 2 fragments 1-3 into the *PkconGFP* plasmid

The synthetic *Pknbpxa* fragments 1-3 (Insert) and *Pk_{con}GFP* plasmid (Vector) were digested using restriction enzymes (see section 2.6.4 and 4.2.7). Restriction enzymes were selected based on the unique sites within the region to be removed from the *Pk_{con}GFP* plasmid (Figure 4.5A), or to excise the *Pknbpxa* fragment from the pMA-RQ plasmid. This allowed sequential ligation of all three *Pknbpxa* synthetic fragments (Figure 4.3) using T4 ligase (section 2.6.6).

4.2.9 Identification of further mutations in *Pknbpxa* cluster 2 linked with S200P

The previously described 913C mutation described by Ahmed *et al* (2014) and here termed S200P is found 598 bp into the *Pknbpxa* gene sequence. This was a non-synonymous SNP that encoded a proline (P) at amino acid position 200. The other clinical sequences encoded a serine (S) at this position. The amino acid change S200P is associated with high parasitaemia. *In silico* protein alignments using Clustal omega and Jalview were used to highlight further mutations that were linked with the S200P mutation in cluster 2.

4.2.10 Site-directed mutagenesis

Site directed mutagenesis (SDM) was conducted following the Quikchange II kit manufacturer's instructions (Agilent). Briefly, clinically relevant mutations were introduced into the pMA-RQ *Pknbpxa_f2* plasmid (6 kb) using the primers detailed in Table 4.2. SDM primers were designed to have the desired mutations located centrally in both the forward and reverse primers, but otherwise to be complementary to the target sequence at all other positions. A Phusion[®] high-fidelity enzyme was used so that no additional mutations were incorporated into the gene sequence. The primers were used at a concentration of 250 nM combined with 0.4 U of Phusion[®] high-fidelity DNA polymerase (NEB), 1x GC buffer and 200 μ M dNTPs in a 20 μ L reaction volume. A total of 20 ng of template DNA (pMA-RQ *PkNBPXa_frag2*) was used for each SDM PCR. Cycling conditions are given in Table 4.1, with annealing temperature T_m approximately 5°C lower than the calculated T_m to allow for the primer containing the mismatch mutation to anneal. The pMA-RQ_ *Pknbpxa_f2* (Appendix E plasmid map) template DNA was digested with 1 μ L (10 U) of *DpnI*. The *DpnI* digestion was incubated at 37°C for 30 minutes followed by heat inactivation at 80°C for 20 minutes. The SDM PCR product (5 μ L) was analysed by gel electrophoresis (section 2.6.3) on a 1% agarose gel to identify if a DNA band was present at the expected size of 6 kb. The remaining PCR product was transformed into DH5 α *E. coli*, as detailed in section 2.8.1, and spread onto LB agar plates containing ampicillin (100 μ g/mL) and incubated at 37°C overnight. Colonies were selected and inoculated in LB broth with ampicillin for starter cultures (section 2.8.3). Minipreps were performed as in section 2.8.6 and DNA sequencing (as described in section 2.6.10) was used to confirm the presence of the

introduced mutation in the pMA-RQ_ *Pknbpxa_f2* plasmid (section 2.6.10, Appendix E Plasmid map; Appendix H SDM sequencing verification).

Table 4.1 Site directed mutagenesis cycling conditions.

Temperature (°C)	Time	Cycles
98	5 min	1
98	30 s	x25
-5 from Tm	30 s	
72	30 s/Kb	
72	5 min	1
4	Hold	1

Table 4.2 Primers used to create mutant copies of *Pk_{con}Pknbpxa_f2*.

Amino Acid Change	SDM Primer	Primer sequence (5' – 3')
S 200 P	F-ag382cc	CCGGGATAAT <u>cc</u> CGGTGATGATGATC
	R-ag382cc	CATCATCACCG <u>gg</u> ATTATCCCGGG
G 420 E	F-gt1043ag	CCCTGGTTG <u>ag</u> AAAAGCCTGGATC
	R-gt1043ag	CCAGGCTTTT <u>ct</u> CAACCAGGGTTT
S 733 N	F-g1982a	GCATTGATA <u>a</u> CAGCAGCAGCGCAG
	R-g1982a	GCTGCTGCTG <u>t</u> TATCAATGCTATCGG

Lower case and underlined denotes the mismatch bp to the *Pknbpxa_f2* sequence

4.2.11 Transfection and drug selection

4.2.11.1 WR99210 drug selection for transfected parasites

A 0.4 mg/mL (1 mM) WR99210 stock solution in DMSO was made and stored at -80°C. A 250 nM working solution was made by sequentially diluting the 1 mM stock 40 times (25 µM) and then 1 in 100 volumes of RPMI 1640 for a 250 nM concentration. The working solution was filter sterilised using a 0.22 µm PES syringe filter and stored at 4°C. The 250nM WR99210 working solution was used at a 1:100 ratio, to obtain a final concentration of 2.5 nM of WR99210 in complete medium.

4.2.11.2 Pyrimethamine drug selection for transfected parasites

A 2 mg/mL pyrimethamine stock solution in DMSO was made and stored at -80°C. A 20 µg/mL working solution was made in RPMI 1640 medium by diluting 50 µL of the stock solution in 4.95 mL of RPMI 1640. The working solution was filter sterilised using a 0.22 µm PES syringe filter and stored at 4°C. The 20 µg/mL pyrimethamine working solution was used at a 1:800 ratio, to obtain a final concentration of 25 ng/mL of pyrimethamine in complete medium.

4.2.12 Transfection of the *P. knowlesi* PkA1-H.1 experimental line with *Pk_{con}Pknbpxa_f1-3* plasmids

4.2.12.1 Amaxa I transfection system

The *PkA1-H.1* clone was grown for transfection studies as per (Moon *et al.*, 2013). Once the culture contained a high proportion of schizonts the culture was synchronised using either LD MACs synchronisation (section 2.2.4), Optiprep synchronisation (section 2.2.5) or Histodenz™ synchronisation method (sections 2.2.6), allowing the separation of multinucleated schizonts from ring stages and trophozoites. The isolated late stage parasites were re-cultured with fresh RBCs for a 1% parasitaemia and allowed to reinvade. Synchronisation was repeated over several days to progressively produce a stage specific synchronous culture (as described in sections 2.2.4-2.2.6). Once the culture reached a parasitaemia greater than 4% and a volume greater than 2 mL packed RBCs, the culture was monitored to assess the synchronicity and life stage of the parasites. Thin blood films were taken and analysed to assess the maturity of the culture, staging the parasites using the following 5 categories: ring stage (R), early trophozoite (ET), late trophozoite (LT), early schizont (ES) and late schizont (LS). A parasite would be defined as an early schizont if there were 4 or less nuclei present and as a late schizont if there were greater than 4 nuclei. When the culture was enriched for late stage schizonts the culture was synchronised as previously described (section 2.2.6). The size of the schizont cell pellet volume was estimated by visually comparing with RBC pcv pellets ranging from 40 µL to 150 µL. The pelleted schizonts were resuspended in 1 mL of complete medium (section 2.1.7) and divided to obtain 10 µL of schizonts per 1.5 mL centrifuge tube. Individual aliquots were centrifuged briefly, the

supernatant was removed and the schizont pellet resuspended in 100 μ L of the following mixture; the linear *Pk_{con}Pknbpxa_{f1-3}* or *Pk_{con}p230pGFP* transfection efficiency control (Figure 4.5 B) (20 - 40 μ g) plasmids, previously linearised at the *KpnI* site (sections 2.6.9 and 2.6.11), were resuspended in 10 μ L DNase free water, added to 100 μ L of basic parasite nucleofector[®] solution 2 supplemented with P2 (Lonza). The schizont/linear plasmid mix (100 μ L) was transferred to an electroporation cuvette, inserted into the Amaxa nucleofector 1 and pulsed using the U-033 setting. The electroporated cells (100 μ L) were then transferred to a 1.5 mL microcentrifuge tube containing 500 μ L of pre-warmed complete medium (section 2.1.7) supplemented with 150 μ L of packed, fresh, uninfected RBCs, 750 μ L final volume. All of the aliquots were electroporated individually in the same manner. Following electroporation, cells were transferred to a microcentrifuge tube and agitated at 37°C at 650 rpm for 30 minutes to promote parasite reinvasion following transfection. Following the incubation period, the cell suspensions (750 μ L) were transferred to a T-25 tissue culture flask containing 4.5 mL of complete medium and cultured as in section 2.2.3. Pyrimethamine drug selection at a final concentration of 25 ng/mL was added 20 hours post-electroporation. Thin blood films (section 2.2.9) were used to monitor the cultures from approximately 20 hours post-transfection until iRBC's were seen.

4.2.12.2 Bio-Rad transfection system

The schizont pellets were prepared for electroporation as per section 4.2.12.1. The Optiprep[™] synchronisation method was used as per section 2.2.5 in replacement of the LD synchronisation method. Individually, aliquots of 10 μ L schizonts in complete medium were gently centrifuged in a benchtop mini centrifuge and the supernatant removed. Pelleted schizonts were resuspended in 480 μ L of cytomix pH 7.6 (see section

2.1.14), containing 20-40 µg of *Pk_{con}Pknbpxa_f1-3* or *Pk_{con}p230pGFP* plasmids previously linearised at the *KpnI* site (sections 2.6.9 and 2.6.11). The schizont cytomix solution was transferred to an electroporation cuvette (4 mm gap) and electroporated at 2500 V, 25 µF (7 - 12 ms), or transferred to an electroporation cuvette (2 mm gap) and electroporated at 310 V, 950 µF (0.7 - 0.9 ms). The electroporated cell suspension was then transferred to a 1.5 mL microcentrifuge tube containing 500 µL of pre-warmed complete medium (section 2.1.7). The steps taken following electroporation were as described in section 4.2.12.1.

4.2.12.3 Lonza 4D transfection system

The *PkA1-H.1* clone was grown to a parasitaemia greater than 4% in greater than 4 mL RBCs as in section 2.2.3. The schizont preparation differed from section 4.2.12.1, with the multinucleated cells being isolated by Histodenz™/Nycodenz® synchronisation (section 2.2.6). The schizonts were resuspended in complete medium (section 2.1.7) containing 10% human serum (Interstate Bloodbank). RBCs were added to produce a 2% haematocrit and incubated at 37°C for 1 - 3 hours with gentle rocking, in culture conditions as in section 2.2.3. Thin blood films (section 2.2.9) were made, stained and counted hourly starting at 1 hour to monitor reinvasion, counting only the ring stage parasites. Once ring stages were observed at a parasitaemia greater than 1%, the cultures (1 - 3 hours) were Histodenz™ synchronised (section 2.2.6) to remove the remaining schizonts. The lower fraction of the synchronisation containing the ring stage parasites were then re-cultured in complete medium containing 10% human serum until mature schizonts were visible in the thin films, approximately 24 - 27 hrs post-synchronisation. The schizonts were monitored until segmented schizonts were observed (Figure 4.12). The schizont rich cultures were then Histodenz™ synchronised (section 2.2.6) and the

pelleted schizont volume estimated as above. The schizonts were resuspended in 1 mL complete medium containing 10% human serum and divided to obtain approximately 10 μ L of pcv schizonts per aliquot and incubated at 37°C. Individual aliquots were centrifuged briefly and the supernatant was removed. The pelleted schizont iRBCs were resuspended using 100 μ L of P3 solution supplemented with solution A (Lonza), containing 20 μ g of Pk_{con}*Pknbpxa_f1-3* or Pk_{con}*p230pGFP* (10 μ L in TE buffer), previously linearised at the *KpnI* site (sections 2.6.9 and 2.6.11). The schizont/P3 solution/linear plasmid solution (100 μ L) was transferred to an electroporation cuvette, inserted into the Lonza 4-D Nucleofector and pulsed using the FP-158 setting. The electroporated cell suspensions were cultured as described in section 4.2.12.1 with alterations of culturing in 6 well plates with 10% human serum used in place of 10% horse serum.

4.2.13 Limiting dilution to clone transfected parasite lines

Accurate parasite counts (section 2.4.1) were performed for the *PkA1-H.1 in vitro* culture transfected with the Pk_{con}*Pknbpxa_f1-3* plasmid. Transfected lines were sequentially diluted to achieve approximately 3 iRBCs per mL in 5 mL volume of complete medium. Fresh uninfected RBCs were added to the diluted iRBCs to give a 2% haematocrit. The diluted culture was divided between wells of a 96 well flat bottom plate (100 μ L per well). Plates for limiting dilution were incubated at 37°C in an air tight chamber gassed with 5:5:90 (O₂:CO₂:N₂). Spent complete medium was exchanged with fresh complete medium every 3-4 days and 1 μ L (1%) of fresh RBCs was added once every 7 days. After 2 weeks, thin blood films were generated to identify wells containing iRBCs. The wells containing iRBCs were maintained in culture and split

regularly to bulk up parasitaemia and RBC volume. Once greater than 200 μ L of RBCs and 2% parasitaemia has been reached, half of each culture was removed for Instagene DNA extraction and insert detection (section 2.6.8).

4.2.14 Integration PCR to confirm $Pk_{con}Pknbpxa$ integration at the *Pknbpxa* locus

PCR was used to validate integration of the *Pk_{con}Pknbpxa_{fl-3}* plasmid in transfected lines at the native *Pknbpxa* locus. Briefly, primers were designed to specifically amplify only the transfected *Pknbpxa* locus at 3 locations (Primer pair B, C and D, Table 4.3 and Figure 4.13), and the untransfected *Pknbpxa* locus (Primer pair A, Table 4.3 and Figure 4.13). DNA was extracted for PCR as described in section 2.6.7 and PCR conditions are given in Tables 2.3.1 and 2.3.2. PCR products were analysed by gel electrophoresis as in section 2.6.3. Validation of the *Pk_{con}p230pGFP* plasmid integration was carried out as per Moon *et al.* (2013). Briefly, primer pair E o1145 and o1144 amplified a 1.4 kb region of the transfected *p230pGFP* locus and primer pair F o1145 and o1146 amplified a 1.3 kb region of the native *p230p* locus (Moon *et al.*, 2013). Primer sequences can be found in Table 2.2.

Table 4.3 Genotyping PCR amplicons for the native and transfected *Pknbpxa* locus*.

Primer pair	Forward Primer	Reverse Primer	Native <i>Pknbpxa</i> locus amplicon	Integrated <i>Pknbpxa</i> cluster 2 locus amplicon
A	F-A1-H.1	R-A1-H.1	1.6 kb	1.6 kb *
B	F- <i>NotI</i>	R-A1-H.1	-	1.6 kb (Pk _{con} backbone to the native <i>Pknbpxa</i>)
C	F- <i>SpeI</i>	R- <i>SpeI</i>	-	500 bp (internal region of synthetic <i>Pknbpxa</i>)
D	F-A1-H.1	R-XaTf-2706	-	3 kb (genomic loci to <i>Pknbpxa_f1-3</i> cluster 2)
	Forward Primer	Reverse Primer	Native <i>p230p</i> locus amplicon	Integrated <i>p230pGFP</i> locus amplicon
E	ol145	ol146	1.3 kb	-
F	ol145	ol144	-	1.45 kb (<i>p230p</i> genomic loci to the <i>p230pGFP</i> backbone)

*In these assays native *Pknbpxa* DNA will be present in any untransfected cells remaining in the transfected cell population as transfections efficiencies are not 100%.

Locations for each primer Figure 4.13

4.3 Results

The ability to transfer DNA sequences from clinical isolates into *in vitro* culture for the testing of associations with severe malaria is an important tool to help dissect the role of parasite factors involved in pathogenesis. The aim of this chapter was to identify the SNPs defining the cluster 2 sequence of the *Pknbpxa* gene using the sequence outputs from Chapter 3 and introduce these into the *PkA1-H.1* clone using a synthetic copy of the *Pknbpxa* gene. Following this, the previously identified S200P mutation and further mutations conserved to sequences containing the S200P would be introduced into the synthetic *Pknbpxa* gene and transfected into the *PkA1-H.1* clone. Achieving this would enable direct comparison of parasites expressing the *Pknbpxa* cluster 2 amino acid sequence with those containing the same sequence with the addition of residues changes associated with high parasitaemia, with the rationale being that mutations in the essential *Pknbpxa* gene are altering the invasion and/or growth rate of the parasite.

4.3.1 Assembly of full length *Pknbpxa* gene sequences from clinical isolates

Six *P. knowlesi* genome sequences from clinical isolates were available from the European Nucleotide Archive (ERR274221, ERR274222, ERR274224, ERR274225, ERR366426 and ERR366425). All sequences had greater than 88% of the genome covered at a read depth greater than 10 reads and *Pknbpxa* was represented. The genome data were used to assemble full-length *Pknbpxa* (8367 bp) from the six clinical *P. knowlesi* isolates sequenced (see section 4.2.3). Of the six *Pknbpxa* sequences available 3 were cluster 1 type (ERR274224, ERR274225 and ERR366425) and 3 were cluster 2 type (ERR274221, ERR274222 and ERR366426). The 885bp haplotype has

been highlighted on Figure 4.1 to give greater information as to the position of these sequences in the population structure. The nucleotide diversity of the assembled full length *Pknbpxa* sequences are given in Table 4.4. The nucleotide diversity of cluster 1 is lower than the diversity seen in cluster 2. Cluster 1 is less variable in the 5' region of the *Pknbpxa* gene (Figure 4.1) however the nucleotide diversity calculated here only represents 3 full length cluster 1 *Pknbpxa* sequences, 2 of which are found in the same 885 bp *Pknbpxa* haplotype (Figure 4.1). Cluster 2 sequences have more synonymous and non-synonymous mutations compared with cluster 1, resulting in a cluster 2 dN/dS ratio greater than 2. The dN/dS ratio for the cluster 1 sequences is lower than cluster 2, but is still greater than 1. This suggests that cluster 2 is under a greater selection pressure at the *Pknbpxa* locus compared with cluster 1. When both clusters are compared together (Table 4.4), the nucleotide diversity, dN/dS, synonymous and non-synonymous mutations all increase. This is due to the dimorphic positions which are conserved within each cluster now being included in the analysis. In order to analyse the population structure more accurately, further *Pknbpxa* gene sequences from cluster 1 and 2 would be required.

Table 4.4 Nucleotide diversity, synonymous and non-synonymous mutations for clinical *Pknbpxa* gene sequences.

<i>Pknbpxa</i> cluster (no. sequences)	Nucleotide Diversity (Pi)	Synonymous Mutations	Non-Synonymous Mutations	dN/dS
Cluster 1 (3)	0.0051	26	38	1.46
Cluster 2 (3)	0.00861	35	73	2.08
Cluster 1 and 2 (6)	0.01436	78	174	2.23

4.3.2 Defining *Pknbpxa* cluster 2 sequence

Pknbpxa alignment identified 65 non-synonymous cluster 2 specific SNPs (section 4.2.5). In total, 91 cluster 2 SNPs were identified, 3 in exon 1 and 88 in exon 2. *Pknbpxa* cluster 2-specific SNPs informed the synthesis of the clinically relevant codon-optimised *Pknbpxa* gene to include 52 of 65 amino acid changes specific to *Pknbpxa* cluster 2 type parasites for subsequent plasmid construction and knock-in transfection (Figure 4.2 and Appendix D). Thirteen cluster 2 specific SNPs occurring in the first 160 amino acids of the *Pknbpxa* protein were removed, as these were located within the region of homology required to be identical to *Pknbpxa* in the *PkA1-H.1* clone to enable recombination into the *Pknbpxa* locus. This left 52 residues specific for cluster 2 in the *Pknbpxa* cluster 2 type gene (Figure 4.2 and Appendix D).

4.3.3 Synthesis of a cluster 2 type *Pknbpxa* gene

To knock-in a *Pknbpxa* gene containing the cluster 2 specific variation identified in section 4.3.2, a synthetic *Pknbpxa* gene containing codon optimized regions was synthesized (section 4.2.4). The *Pknbpxa* gene sequence from the corrected *P. knowlesi* reference genome sequence was used, and mutations encoding the 52 cluster 2 non-synonymous mutations were incorporated *in silico*. A 1 kb region of homology (section 4.2.4) was synthesized by GeneArt™ Invitrogen™, flanked by *NotI* and *XmaI* restriction sites (Figure 4.3). The *XmaI* restriction site (1010 bp, Figure 4.3) was introduced *in silico* to facilitate subsequent *Pknbpxa_f1* cloning steps without disrupting the coding region (Figure 4.6 and Figure 4.7). The remaining *Pknbpxa* cluster 2 sequence (7872 bp) containing the 52 non-synonymous mutations was divided into two

segments (*Pknbpxa_f2* and *Pknbpxa_f3*; Figure 4.3) and cloning facilitated using synonymous mutations to create the *SpeI* (4938 bp, Figure 4.3) restriction site linking *Pknbpxa_f2* and *Pknbpxa_f3* gene fragments. The *Pknbpxa_f2* and *Pknbpxa_f3* fragments were codon optimized (Figure 4.7). Restriction digestion and gel electrophoresis of each plasmid confirmed the desired *Pknbpxa* fragment sizes prior to cloning (Appendix E).

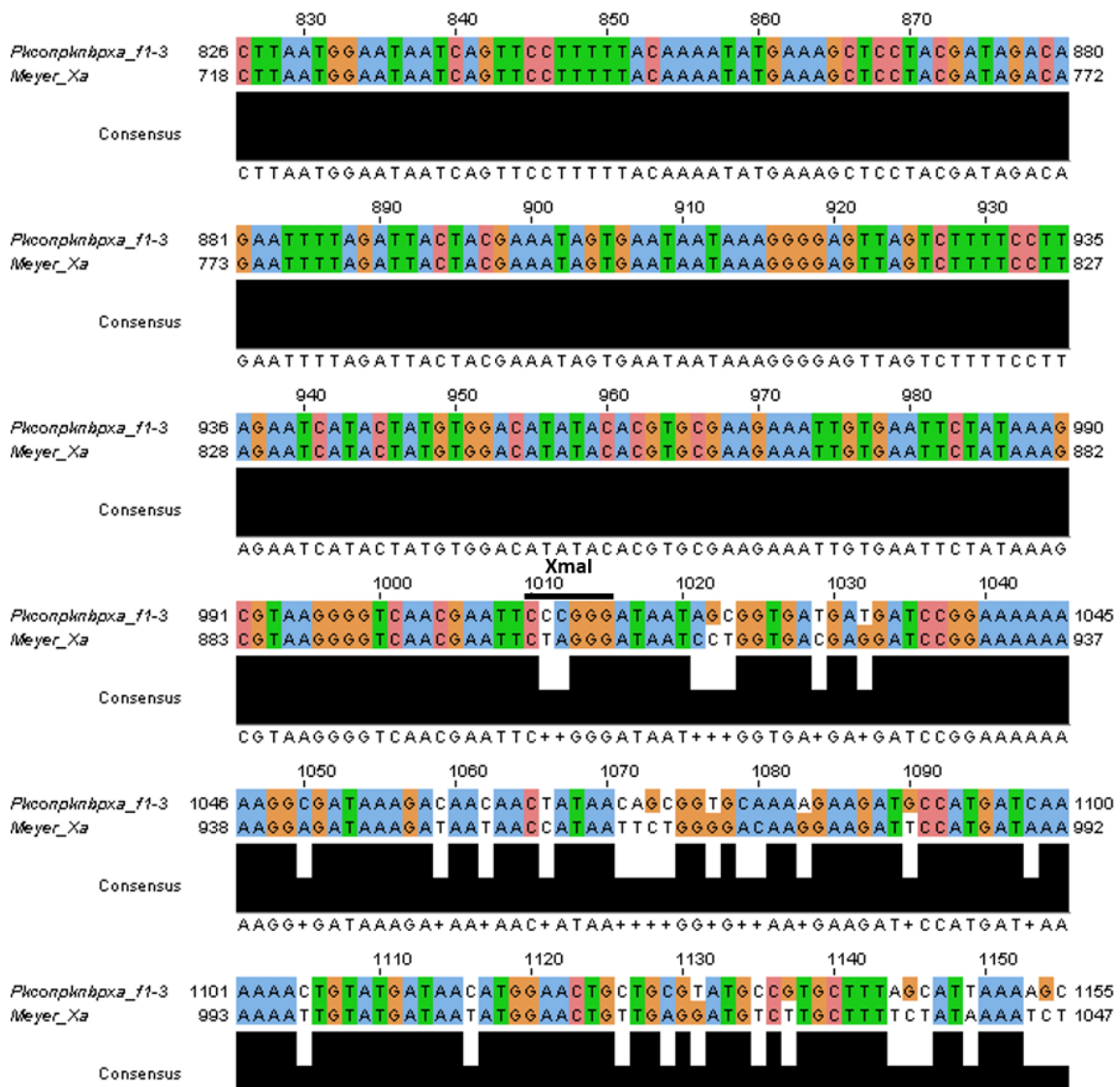


Figure 4.6 Alignment of the region of homology in *Pknbpxa_f1* and *Pknbpxa_f2* codon optimized fragments representing cluster 2.

The top sequence represents the *Pk_{con}Pknbpxa_f1-3* transfection plasmid, the bottom sequence represents the *Pknbpxa* sequence extracted from the corrected *P. knowlesi* genome sequence. The *Xmal*

restriction enzyme motif is highlighted and separates the *Pknbpxa_f1* region of homology and the codon optimized *Pknbpxa_f2* fragment.

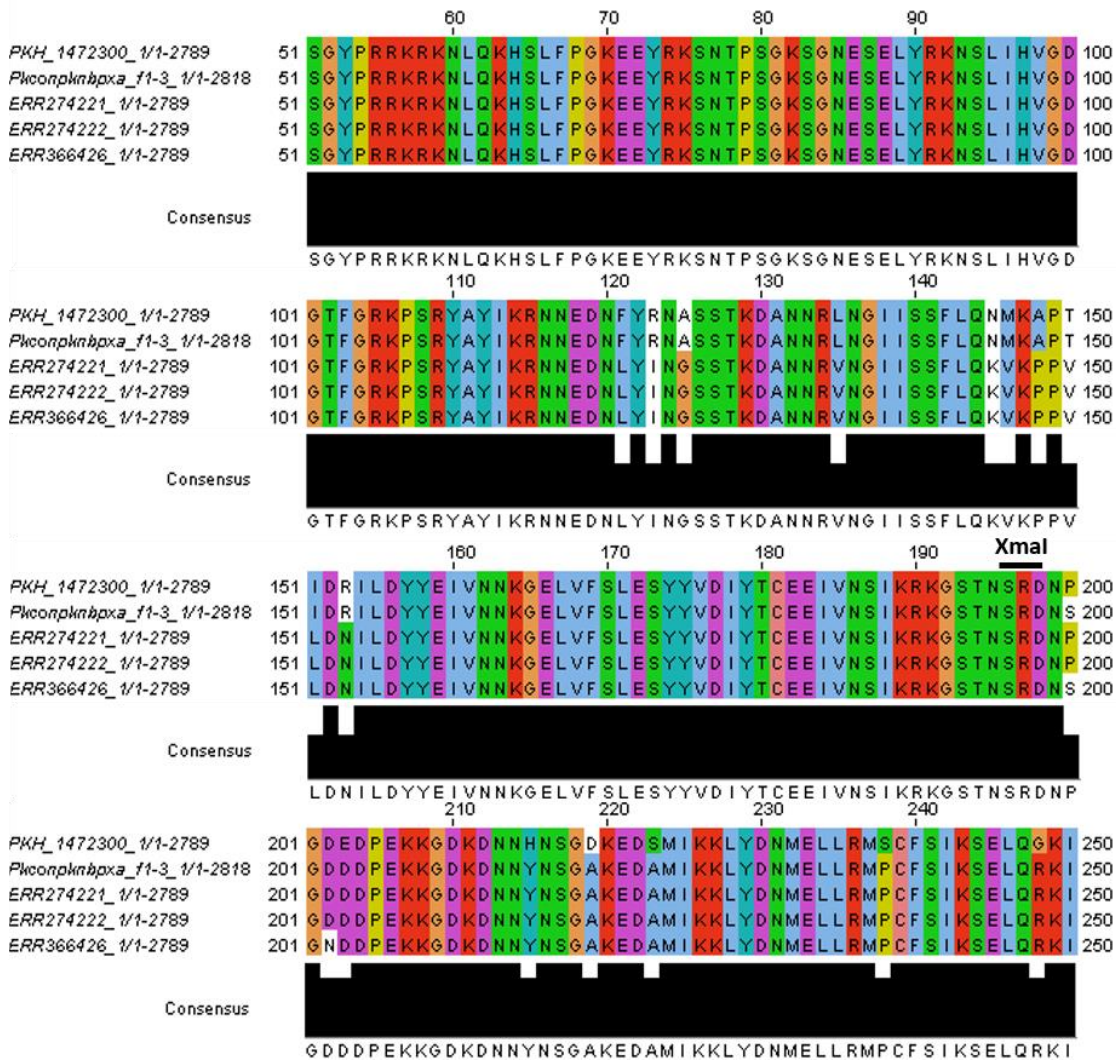


Figure 4.7 Amino acid sequence alignment of the 3 clinical PkNBPA sequences with the corrected *P. knowlesi* PkNBPA reference sequence.

The top sequence (PKH_1472300) is the PkNBPA amino acid sequence from the corrected *P. knowlesi* *Pknbpxa* genome sequence. The second top sequence is the amino acid sequence of the Pk_{con}*Pknbpxa_f1-3* plasmid. The bottom 3 sequences are the amino acid sequences from the 3 cluster 2 type genome sequences. The *Xma*I restriction site codes for amino acids 196-198, showing the separation of the *Pknbpxa_f1* region of homology and codon optimized *Pknbpxa_f2* sequence. The Pk_{con}*Pknbpxa_f1-3* amino acid sequence (second top) is identical to the corrected PkNBPA sequence (Top) until the SRD motif encoded by the *Xma*I restriction site tCCCGGgat.

4.3.4 Constructing the *Pk_{con}Pknbpxa_f1-3* transfection plasmid

The *Pknbpxa_f1* gene fragment representing the region of homology (Figure 4.5A) was ligated into the adapted *Pk_{con}GFP* plasmid (Figure 4.5a) containing the *GFP* coding sequence and the *hDHFR* resistance gene (Section 4.2.7), using the *NotI* and *XmaI* sites (green, Figures 4.3 and 4.9). The resulting *Pk_{con}GFP_Pknbpxa_f1* construct was validated by Sanger sequencing, and restriction enzyme digestion (sections 2.6.3 and 2.6.10, Figure 4.8; Appendix F alignment of sequencing and restriction digests).

The validated *Pk_{con}GFP_Pknbpxa_f1* construct was digested with the *XmaI* and *SacII* restriction enzymes to remove the *GFP* coding sequence (Figure 4.9 and 4.10), leaving the linearized *Pk_{con}Pknbpxa_f1* plasmid prepared for ligation with the codon optimised *Pknbpxa_f2* fragment (purple, Figure 4.3), also digested at the *XmaI* and *SacII* sites (Figure 4.9 and 4.10). The *Pknbpxa_f2* fragment was ligated immediately adjacent to *Pknbpxa_f1* coding sequence and the resultant construct validated as above, Figure 4.9 and Figure 4.8 (Appendix F alignment of sequencing and restriction digests).

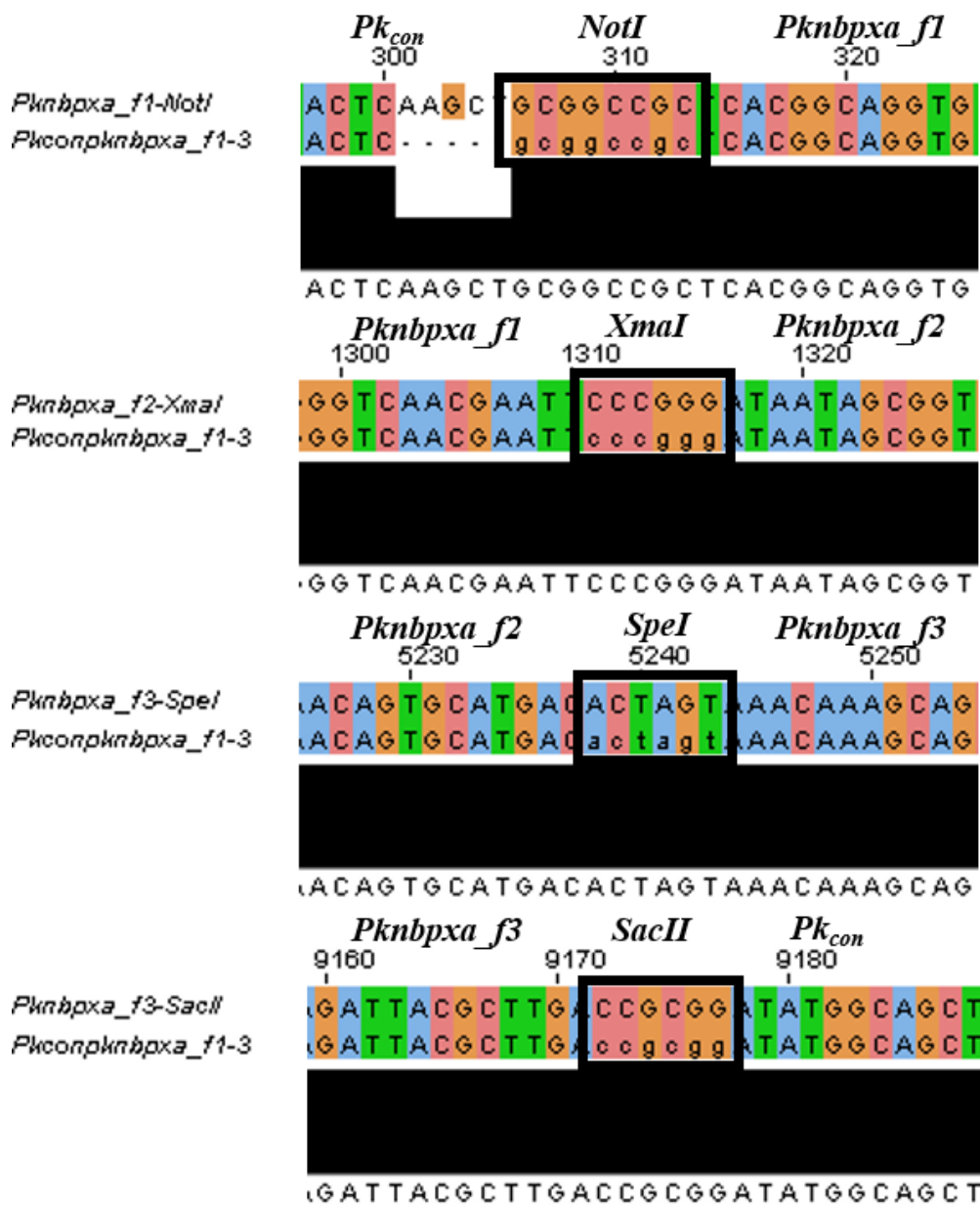


Figure 4.8 Confirmation of *Pknbpxa* fragment ligation by sequencing.

The ligation mixture was transformed into competent *E. coli* and grown in the presence of ampicillin (100 µg/mL), and plasmid DNA extracted by Miniprep. Successful cloning of all restriction sites was validated by sequencing, using the following primers F-*NotI*, F-*XmaI*, R-*XmaI*, F-*SpeI*, R-*SpeI* and F-*SacII*. Each primer was designed to produce an amplicon which traversed the ligation site. Sequencing was carried out by Dundee sequencing & services using Sanger Sequencing. Each panel shows the alignment of the sequencing read against the *in silico* predicted ligation product. The bottom track in each panel, *Pkconpknbpxa_f1-3*, is the sequence of the plasmid constructed *in silico* while the top track is the sequencing read produced using primers for each restriction motif. The box in each alignment highlights the correctly aligned sequence demonstrating successful ligation.

The $Pk_{con}Pknbpxa_f1-2$ plasmid, containing the *Pknbpxa_f1* and *f2* fragments (Figure 4.3 green and purple respectively) was digested using the restriction enzymes *SpeI* and *SacII*, removing a 16 bp sequence separating the two restriction sites (Figure 4.10). The *Pknbpxa_f3* (red in Figure 4.3) fragment, also cut at *SpeI* and *SacII* motifs, was ligated into the $Pk_{con}Pknbpxa_f1-2$ plasmid generating the $Pk_{con}Pknbpxa_f1-3$ 14kb *P. knowlesi* transfection plasmid (Figure 4.11). The ligation product was validated by Sanger sequencing (Appendix F) to ensure each fragment was correctly orientated and no insertions or deletions were introduced during the cloning steps (Figures 4.8 and 4.11).

Table 4.5 Cloning Strategy for the cluster 2 type synthetic gene.

<i>Pknbpxa</i> fragments	Fragment size (bp)	5' restriction site in $Pk_{con}Pknbpxa_f1-3$ (bp)	3' restriction site in $Pk_{con}Pknbpxa_f1-3$ (bp)
<i>Pknbpxa_f1</i>	1015	<i>NotI</i> (1-8)	<i>XmaI</i> (1010-1015)
<i>Pknbpxa_f2</i>	3950	<i>XmaI</i> (1010-1015)	<i>SpeI</i> (4937-4943), <i>SacII</i> (4953-4959)*
<i>Pknbpxa_f3</i> with 3x Haemagglutinin (HA) tag	3940	<i>SpeI</i> (4937-4943)	<i>SacII</i> (8871-8877)

*a 16 bp spacer sequence was used to introduce the *Pknbpxa_f2* fragment using *SacII*. The introduced *SpeI* and *SacII* sites were then used to ligate the *Pknbpxa_f3*.

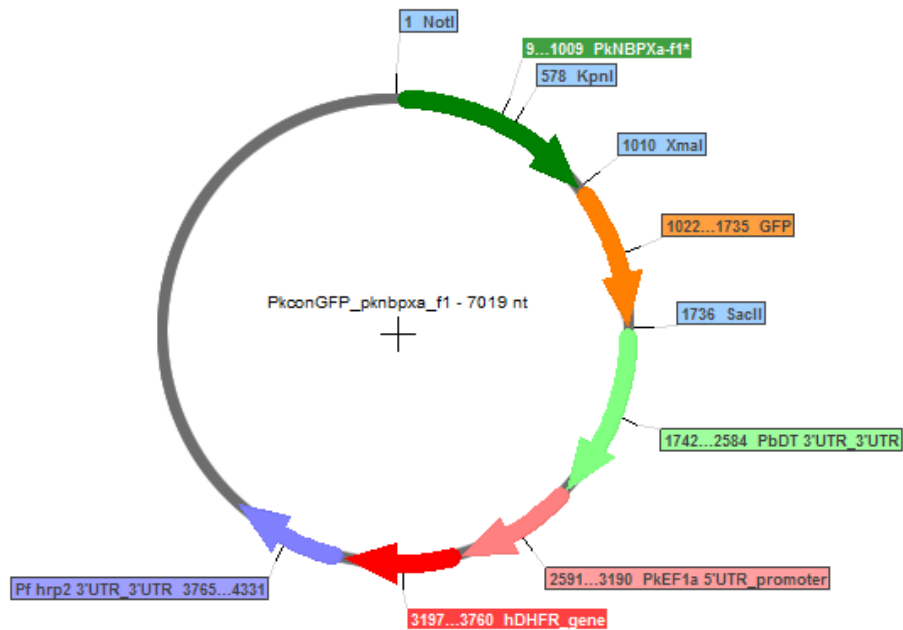


Figure 4.9 Map of the Pk_{con}GFP*Pknbpxa_f1* plasmid.

The PkHSP70 promoter at the 5' end of the GFP coding sequence in the Pk_{con}GFP plasmid was removed using the *NotI* and *XmaI* restriction sites. The *Pknbpxa_f1* homology region was ligated into the plasmid using the *NotI* and *XmaI* restriction sites. Digestion at the *XmaI* and *SacII* sites removed the GFP coding sequence allowing for the ligation of the *Pknbpxa_f2* codon optimised sequence.

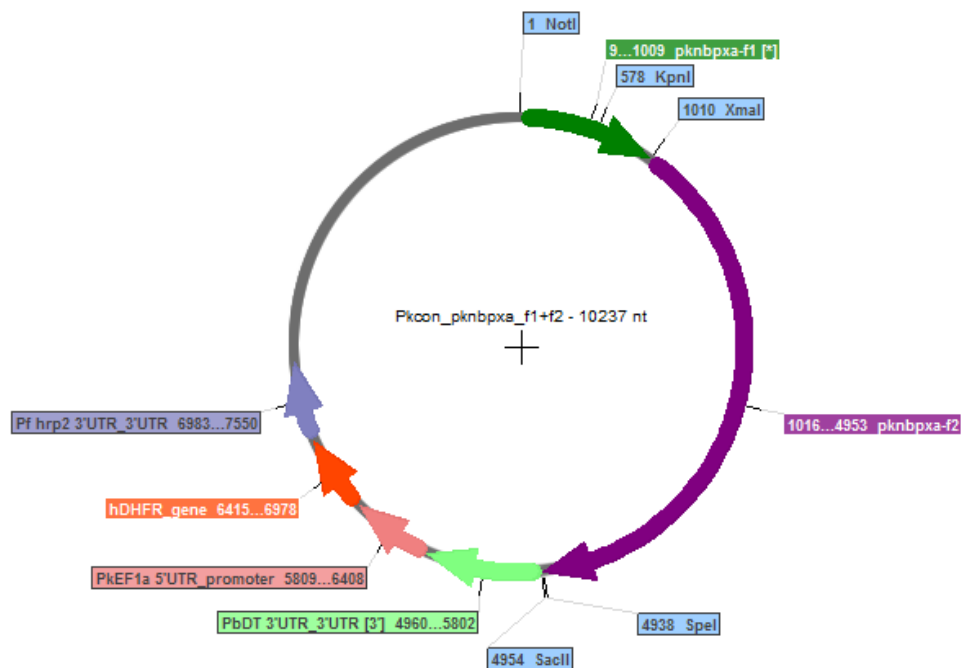


Figure 4.10 Map of the *Pk_{con}Pknbpxa_f1-2* plasmid.

The successful ligation of the codon optimised fragment *Pknbpxa_f2* using the *XmaI* and *SacII* restriction sites introduced the *SpeI* restriction site. An *SpeI* restriction site at the 3' end of the *Pknbpxa_f2* coding region was followed by a 16 bp linker sequence and the *SacII* restriction site. This enabled subsequent cloning of the *Pknbpxa_f3* fragment using the *SpeI* and *SacII* restriction sites.

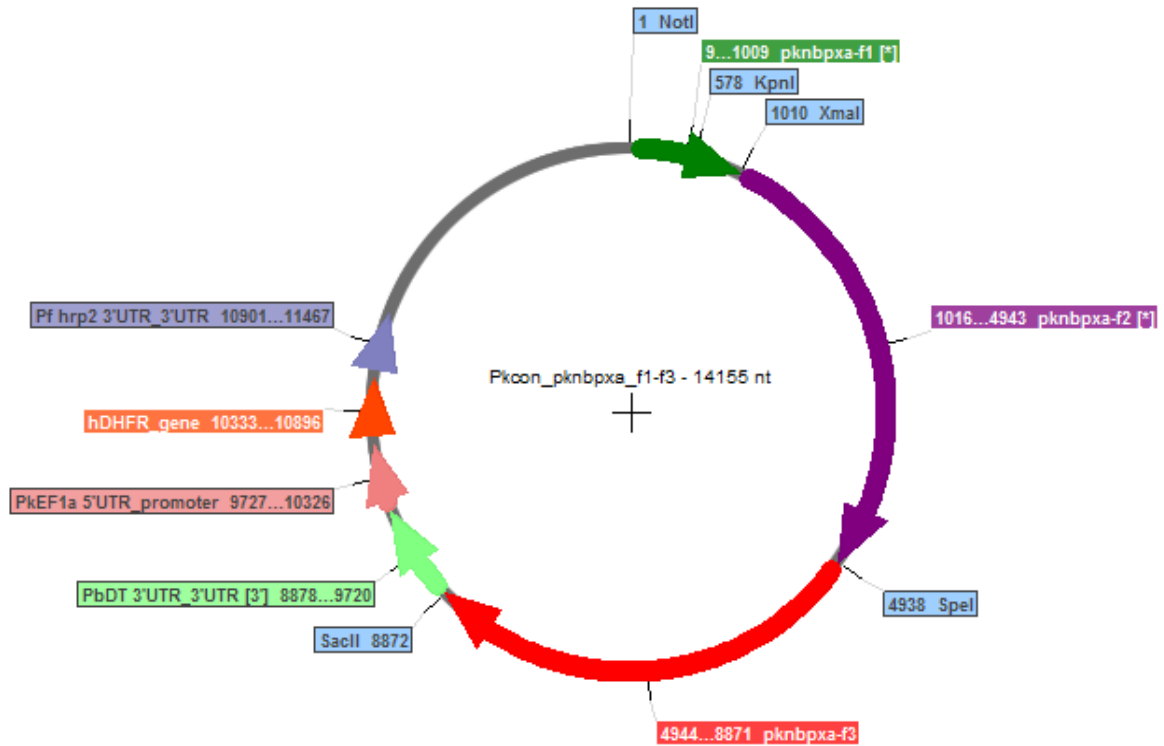


Figure 4.11 Map of the $Pk_{con}Pknbp_xa_f1-3$ plasmid.

Restriction digestion of the $Pk_{con}Pknbp_xa_f1-2$ with the restriction enzymes *SpeI* and *SacII* removes the 16 bp linker sequence between the two restriction enzyme motifs, enabling the ligation of the 3939 bp $Pknbp_xa_f3$ sequence into the $Pk_{con}Pknbp_xa_f1-2$ plasmid.

Table 4.6 Transfection optimisation.

	Plasmid (µg)	Synchronisation method	Pre-Synch Differential (R:ET:LT:ES:LS)*	Post-Synch Differential (R:ET:LT:ES:LS)*	Transfection solution	Transfection method	Pyrimethamine/WR99210 added at 20hrs (P/W)	Growth within 4 weeks
Tf 1								
1	Pk _{con} <i>Pknbpxa_f1-3</i> (20)	LD MACs	30:12:25:20:13		kit2	Amaya I (U-033)	W+	N
2	Pk _{con} <i>p230pGFP</i> (20)**	LD MACs	30:12:25:20:13		kit2	Amaya I (U-033)	W+	N
Tf 2								
1	Pk _{con} <i>Pknbpxa_f1-3</i> (30)	LD MACs	8:9:47:16:21		Kit1	Amaya I (U-033)	W+	N
2	Pk _{con} <i>p230pGFP</i> (20)**	LD MACs	8:9:47:16:21		Kit1	Amaya I (U-033)	W+	N
3	Pk _{con} <i>p230pGFP</i> (20)**	LD MACs	8:9:47:16:21		Kit2	Amaya I (U-033)	W+	N
4	No Plasmid DNA	LD MACs	8:9:47:16:21		Kit1	Amaya I (U-033)	W+	N
Tf 3								
1	Pk _{con} <i>Pknbpxa_f1-3</i> (20)	Optiprep	30:12:25:20:13	2:5:61:18:13	Kit2	Amaya I (U-033)	P+	N
2	Pk _{con} <i>Pknbpxa_f1-3</i> (20)	Optiprep	30:12:25:20:13	2:5:61:18:13	Kit2	Amaya I (U-033)	P+	N
3	Pk _{con} <i>p230pGFP</i> (20)**	Optiprep	30:12:25:20:13	2:5:61:18:13	Kit1	Amaya I (U-033)	P+	N
4	Pk _{con} <i>p230pGFP</i> (20)**	Optiprep	30:12:25:20:13	2:5:61:18:13	Kit1	Amaya I (U-033)	P+	N
Tf 4								
1	Pk _{con} GFP (20)**	Optiprep	0:1:55:47:32		Kit2	Amaya I (U-033)	P+	N
2	Pk _{con} <i>p230pGFP</i> (20)**	Optiprep	0:1:55:47:32		Kit2	Amaya I (U-033)	P+	N
3	Pk _{con} <i>Pknbpxa_f1-3</i> (40)	Optiprep	0:1:55:47:32		Kit2	Amaya I (U-033)	P+	N
4	Pk _{con} <i>Pknbpxa_f1-3</i> (40)	Optiprep	0:1:55:47:32		Kit1	Amaya I (U-033)	P+	N
5	No Plasmid DNA	Optiprep	0:1:55:47:32		Kit2	Amaya I (U-033)	P+	N

	Plasmid (μ g)	Synchronisation method	Pre-Synch Differential (R:ET:LT:ES:LS)*	Post-Synch Differential (R:ET:LT:ES:LS)*	Transfection solution	Transfection method	Pyrimethamine/ added at 20hrs	Growth within 4 weeks
Tf 5								
1	Pk _{con} <i>Pknbp_{xa}_f1-3</i> (20)	Optiprep	3:0:11:20:66		Kit1	Amaxa I (U-033)	P+	N
2	Pk _{con} <i>Pknbp_{xa}_f1-3</i> (30)	Optiprep	3:0:11:20:66		Kit1	Amaxa I (U-033)	P+	N
3	Pk _{con} <i>Pknbp_{xa}_f1-3</i> (40)	Optiprep	3:0:11:20:66		Kit1	Amaxa I (U-033)	P+	N
4	Pk _{con} <i>p230pGFP</i> (20)**	Optiprep	3:0:11:20:66		Kit1	Amaxa I (U-033)	P+	N
5	No Plasmid DNA	Optiprep	3:0:11:20:66		Kit1	Amaxa I (U-033)	P+	N
Tf 6								
1	Pk _{con} <i>p230pGFP</i> (50)**	Optiprep	24:11:22:26:17	0:1:25:43:32	CytoMix	BioRad (310 V)	P+	N
2	Pk _{con} <i>Pknbp_{xa}_f1-3</i> (50)	Optiprep	24:11:22:26:17	0:1:25:43:32	CytoMix	BioRad (310 V)	P+	N
3	Pk _{con} <i>p230pGFP</i> (50)**	Optiprep	24:11:22:26:17	0:1:25:43:32	CytoMix	BioRad (2500 V)	P+	N
4	Pk _{con} <i>Pknbp_{xa}_f1-3</i> (50)	Optiprep	24:11:22:26:17	0:1:25:43:32	CytoMix	BioRad (310 V)	P+	N
Tf 7								
1	Pk _{con} GFP (20)**	Histodenz		6:1:17:55:23	CytoMix	BioRad (310 V)	P+	N
2	Pk _{con} <i>p230pGFP</i> (20)**	Histodenz		6:1:17:55:23	CytoMix	BioRad (310 V)	P+	N
3	Pk _{con} <i>Pknbp_{xa}_f1-3</i> (40)	Histodenz		6:1:17:55:23	CytoMix	BioRad (310 V)	P+	N
4	No Plasmid DNA	Histodenz		6:1:17:55:23	CytoMix	BioRad (310 V)	P+	N
5	No Plasmid DNA	Histodenz		6:1:17:55:23	CytoMix	BioRad (310 V)	-	Y
Tf 8								
1	Pk _{con} GFP (20)**	Histodenz		0:0:21:53:26	CytoMix	BioRad (310 V)	P+	N
2	Pk _{con} <i>p230pGFP</i> (20)**	Histodenz		0:0:21:53:26	CytoMix	BioRad (310 V)	P+	N
3	Pk _{con} <i>Pknbp_{xa}_f1-3</i> (40)	Histodenz		0:0:21:53:26	CytoMix	BioRad (310 V)	P+	N
4	No Plasmid DNA	Histodenz		0:0:21:53:26	CytoMix	BioRad (310 V)	P+	N

	Plasmid (μ g)	Synchronisation method	Pre-Synch Differential (R:ET:LT:ES:LS)*	Post-Synch Differential (R:ET:LT:ES:LS)*	Transfection solution	Transfection method	Pyrimethamine/ at 20hrs	Growth within 4 weeks
Tf 9								
1	Pk _{con} GFP (50)**	Histodenz		0:0:11:45:44	CytoMix	BioRad (2.5 kV)	P+	N
2	Pk _{con} p230pGFP (50)**	Histodenz		0:0:11:45:44	CytoMix	BioRad (2.5 kV)	P+	N
3	Pk _{con} Pknbp _{xa} _f1-3 (100)	Histodenz		0:0:11:45:44	CytoMix	BioRad (2.5 kV)	P+	N
4	Pk _{con} GFP (50)**	Histodenz		0:0:11:45:44	CytoMix	BioRad (310 V)	P+	N
5	Pk _{con} p230pGFP (50)**	Histodenz		0:0:11:45:44	CytoMix	BioRad (310 V)	P+	N
6	Pk _{con} Pknbp _{xa} _f1-3 (100)	Histodenz		0:0:11:45:44	CytoMix	BioRad (310 V)	P+	N
7	No Plasmid DNA	Histodenz		0:0:11:45:44	CytoMix	BioRad (2.5 kV)	P+	N
Tf 10								
1	Pk _{con} p230pGFP (20)**	Histodenz		6:0:24:43:26	P3	4-D Nucleofector	P+	N
2	Pk _{con} Pknbp _{xa} _f1-3 (40)	Histodenz		6:0:24:43:26	P3	4-D Nucleofector	P+	N
3	Pk _{con} GFP (20)**	Histodenz		6:0:24:43:26	P3	4-D Nucleofector	P+	N
4	Pk _{con} Pknbp _{xa} _f1-3 (40)	Histodenz		6:0:24:43:26	P3	4-D Nucleofector	P+	N
5	Pk _{con} GFP (20)**	Histodenz		6:0:24:43:26	P3	4-D Nucleofector	P+	N
6	Pk _{con} p230pGFP (20)**	Histodenz		6:0:24:43:26	P3	4-D Nucleofector	P+	N
7	Pk _{con} p230pGFP (10)**	Histodenz		6:0:24:43:26	P3	4-D Nucleofector	P+	N
8	Pk _{con} Pknbp _{xa} _f1-3 (20)	Histodenz		6:0:24:43:26	P3	4-D Nucleofector	P+	N
9	No Plasmid DNA	Histodenz		6:0:24:43:26	P3	4-D Nucleofector	P+	N

	Plasmid (µg)	Synchronisation method	Pre-Synch Differential (R:ET:LT:ES:LS)*	Post-Synch Differential (R:ET:LT:ES:LS)*	Transfection solution	Transfection method	Pyrimethamine/ at 20hrs	Growth within 4 weeks
Tf11								
1	No Plasmid DNA 1	Histodenz		0:0:19:42:39	-	-	-	Y
2	No Plasmid DNA 2	Histodenz		0:0:19:42:39	P3	4-D Nucleofector	-	Y
3	No Plasmid DNA 3	Histodenz		0:0:19:42:39	P3	4-D Nucleofector	P+	N
4	Pk _{con} <i>Pknbpxa_f1-3</i> (40)	Histodenz		0:0:19:42:39	P3	4-D Nucleofector	P+	Y
5	Pk _{con} <i>p230pGFP</i> (20)**	Histodenz		0:0:19:42:39	P3	4-D Nucleofector	P+	Y
6	Pk _{con} <i>Pknbpxa_f1-3</i> (40)	Histodenz		0:0:19:42:39	P3	4-D Nucleofector	P+	N
7	Pk _{con} <i>p230pGFP</i> (20)**	Histodenz		0:0:19:42:39	P3	4-D Nucleofector	P+	N
Tf12 – LSHTM								
1	Pk _{con} <i>Pknbpxa_f1-3</i> (20)	Nycodenz			P3	4-D Nucleofector	P+	Y
2	Pk _{con} <i>Pknbpxa_f1-3 S200P</i> (20)	Nycodenz			P3	4-D Nucleofector	P+	Y
3	Pk _{con} <i>p230pGFP</i> (20)**	Nycodenz			P3	4-D Nucleofector	P+	Y
Tf13 – LSHTM								
1	Pk _{con} <i>Pknbpxa_f1-3</i> (20)	Nycodenz			P3	4-D Nucleofector	P+	Y
2	Pk _{con} <i>Pknbpxa_f1-3 S200P</i> (20)	Nycodenz			P3	4-D Nucleofector	P+	Y
3	Pk _{con} <i>p230pGFP</i> (20)**	Nycodenz			P3	4-D Nucleofector	P+	Y
Tf14 – LSHTM								
1	Pk _{con} <i>Pknbpxa_f1-3</i> (20)	Nycodenz			P3	4-D Nucleofector	P+	Y
2	Pk _{con} <i>Pknbpxa_f1-3 S200P</i> (20)	Nycodenz			P3	4-D Nucleofector	P+	Y
3	Pk _{con} <i>p230pGFP</i> (20)**	Nycodenz			P3	4-D Nucleofector	P+	Y
Tf15 – LSHTM								
1	Pk _{con} <i>Pknbpxa_f1-3 G420E</i> (20)	Nycodenz		0:0:12:43:45	P3	4-D Nucleofector	P+	Y
2	Pk _{con} <i>Pknbpxa_f1-3 S733N</i> (20)	Nycodenz		0:0:12:43:45	P3	4-D Nucleofector	P+	N
3	Pk _{con} <i>p230pGFP</i> (20)**	Nycodenz		0:0:12:43:45	P3	4-D Nucleofector	P+	Y

	Plasmid (μg)	Synchronisation method	Pre-Synch Differential (R:ET:LT:ES:LS)*	Post-Synch Differential (R:ET:LT:ES:LS)*	Transfection solution	Transfection method	Pyrimethamine/ at 20hrs	Growth within 4 weeks
Tf16 – LSHTM								
1	Pk _{con} <i>Pknbpxa_f1-3 G420E</i> (20)	Nycodenz			P3	4-D Nucleofector	P+	N
2	Pk _{con} <i>Pknbpxa_f1-3 S733N</i> (20)	Nycodenz			P3	4-D Nucleofector	P+	N
3	Pk _{con} <i>p230pGFP</i> (20)**	Nycodenz			P3	4-D Nucleofector	P+	N

* For transfections the parasite life stages were assessed more thoroughly by categorising as Ring (R), early trophozoite (ET), late trophozoite (LT), early schizont (ES, <4 nuclei) and late schizont (LS, >4 nuclei). Life stages were assessed either prior to synchronisation (Pre-Synch) or a sample was removed following synchronisation but immediately prior to transfection (Post-Synch).

**The Pk_{con}GFP (circular plasmid DNA) or Pk_{con}*p230pGFP* (plasmid DNA linearized at *KpnI*) plasmid was used during the optimisation process or as a positive control.

4.3.5 Transfecting the *P. knowlesi* *PkA1-H.1* experimental line

In order to replace the *Pknbpxa* locus in the *PkA1-H.1 in vitro* clone with the $Pk_{con}Pknbpxa_{f1-3}$ plasmids, an electroporation based transfection system was used. The $Pk_{con}Pknbpxa_{f1-3}$ plasmids were linearized at the *KpnI* restriction site to promote single crossover homologous recombination (Figure 4.13). A range of transfection optimisation experiments were performed in an attempt to obtain successful transfections with the $Pk_{con}Pknbpxa_{f1-3}$ plasmid as detailed in Table 4.6. Parameters tested included; varying DNA concentration, parasite synchronization methods and schizont enrichment, different electroporation conditions and equipment, and transfection buffer (Table 4.6). In particular, the synchronisation method was changed from LD MACs magnetic (Section 2.2.4) and Optiprep (section 2.2.5) to use Histodenz/Nycodenz density gradient synchronisation (section 2.2.6), as this produced a tighter synchronisation and fewer uninfected RBCs in the schizont preparation prior to transfections (Table 4.6 and Figure 4.12). Growth within 4 weeks represents presence of parasites resistant to pyrimethamine, suggesting successful transfection.

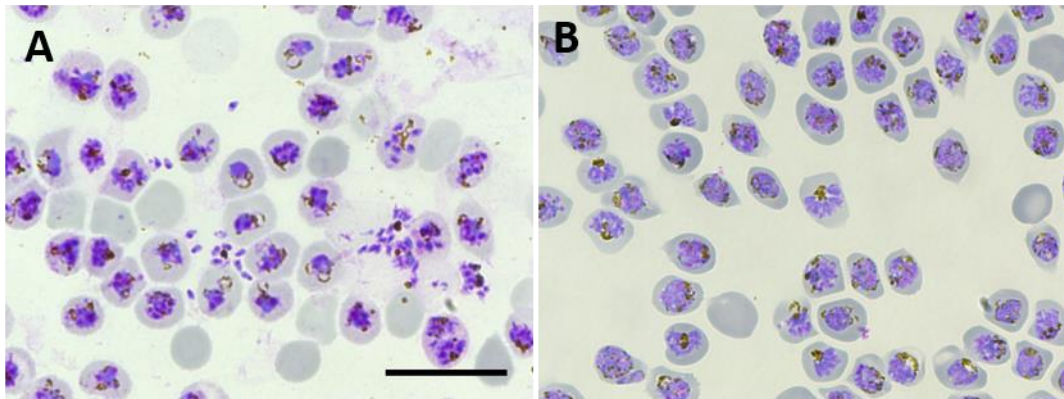


Figure 4.12 Comparison of synchronisation methods to isolate segmented schizonts prior to transfection.

Brightfield images of Giemsa stained thin blood films (section 2.2.9) showing multinucleated schizonts purified via **A.** an Optiprep density gradient (section 2.2.5, Tf6 - Table 4.6) where parasites were allowed to mature until the point of rupture before synchronisation, and **B.** a Nycodenz density gradient (Section 2.2.6) where synchronisation was performed prior to the bulk of the culture reaching the point of having multiple fully formed daughter merozoites. The harvested schizonts were incubated gently shaking at 37°C in complete medium until segmented schizonts were visible in thin blood films. The segmenter schizonts were then gently pelleted and resuspended in transfection buffer. As shown, the Nycodenz synchronisation produced a tighter schizont population and fewer uninfected RBCs compared to the Optiprep density gradient. Sides were imaged on an Olympus U-TV1X-2 and captured using a Leica DFC450C camera (Leica). Scale bar = 20 µm.

Transfection experiments TF 1 - 10 were not successful (Table 4.6). Parasite growth was observed in transfections TF11–4 ($Pk_{con}Pknbp_xa_{f1-3}$) and TF11–5 ($Pk_{con}p230pGFP$). These transfections were conducted using the 4-D nucleofector (Lonza) in combination with Histodenz synchronised schizonts that contained 39% late stage schizonts, containing greater than 4 nuclei (Table 3.6), which were then grown in complete medium with horse serum (Table 4.6, Section 4.2.12.3). However, there was no increase in parasitaemia above 0.1% by day 7 post transfection suggesting that a small population of the parasites may have been transfected. In order to capture this population the cultures were purified using an LD MACs column (Section 2.2.4) and

were added to 300 µL of complete medium containing 6 µL of red blood cells. The parasitaemia was carefully monitored and the cultures were gradually bulked up. TF11.4 transfected with *Pk_{con}Pknbpxa_f1-3* was successfully recovered, bulked up to 6% parasitaemia in 1.2 mL PCV and cryopreserved (see growth monitoring Appendix I) but TF11-5 was lost (see Immunofluorescence Appendix I, prior to loss).

4.3.6 PCR to demonstrate construct integration in the Tf11.4 line

A PCR assay was developed to confirm that the *Pk_{con}Pknbpxa_f1-3* plasmid in TF11.4 had integrated correctly into the *Pknbpxa* locus (Figure 4.13). Primer pair A (F-A1-H.1 & R-A1-H.1, Table 4.3) was designed to amplify a 1.6 kb region of the parental *Pknbpxa* locus. The F-A1-H.1 bound to a non-coding region outside the *Pknbpxa* gene at the 5' end, and the R-A1-H.1 primer bound to a region of the parental *Pknbpxa* gene which differed sufficiently from the cluster type 2 *Pknbpxa* sequence (Figure 4.13). Primer pair B (F-*NotI*&R-A1-H.1, Table 4.3) was designed to amplify a 1.6 kb sequence specific to the 3' end of the transfected *Pknbpxa* locus (Figure 4.13). The F-*NotI* primer was specific for a unique region in the backbone of the *Pk_{con}Pknbpxa_f1-3*, 300 bp away from the *NotI* restriction site at the beginning of *Pknbpxa_f1*. As previously mentioned the R-A1-H.1 primer was specific for the parental *Pknbpxa* sequence (Figure 4.13). Primer pair C (F-*SpeI*&R-*SpeI*) was designed to amplify a 500 bp central region of the transfection plasmid (Table 4.3). DNA was extracted from the parental *PkA1-H.1* clone and the Tf11.4 transfection experiment (Tf11.4, Table 4.6) for PCR analysis to validate integration of the construct into the *Pknbpxa* locus (Section 4.2.14 and Table 2.3.1 and 2.3.2). A 1.6 kb amplicon was detected in the DNA extracted

from the *PkA1-H.1* clone (Figure 4.14, panel A lane 2) and the Tf11.4 transfection (Tf11.4, Figure 4.14 panel A lane 3) when primers designed to detect the untransfected locus were used (Figure 4.13). Primers specific for the transfected *Pknbpaxa* locus (F-*NotI* & R-A1-H.1Xa) failed to produce any amplicon from template DNA extracted from the parental *PkA1-H.1* clone (Figure 4.14, panel B lane 2) or from the Tf11.4 transfection (Figure 4.14, panel B lane 3) suggesting there had been no integration of the construct into the *Pknbpaxa* locus. However, a 500 bp PCR product was present when DNA from both the Tf11.4 transfection (Figure 4.14, panel C lane 3) and the neat *Pk_{con}Pknbpaxa_f1-3* construct (Figure 4.14, panel C lane 4) were amplified using primers specific to a central region of the cluster 2 *Pknbpaxa* sequence. This shows that the construct was present in the parasites from the Tf11.4 transfection experiment, however episomal maintenance of the plasmid opposed to integration into the *Pknbpaxa* locus was predicted

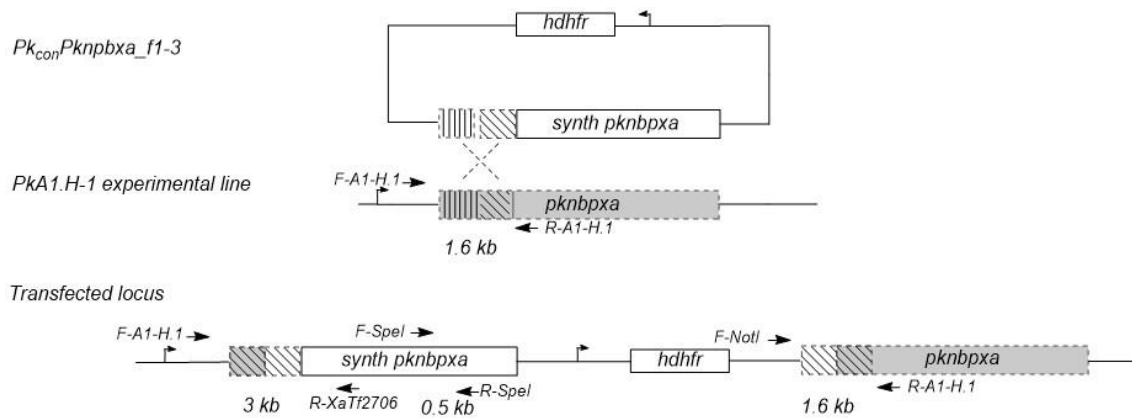


Figure 4.13 Schematic for stable genomic integration of the cluster 2 type *Pknbpaxa*.

Single crossover homologous recombination occurring in the region of homology between the linearised *Pk_{con}Pknbpaxa_f1-3* construct (white), and the *Pknbpaxa* genomic locus (grey). The mechanism of single crossover homologous recombination by a linear construct promotes recombination at the region of homology (marked by horizontal lines) which results in insertion of the construct (white) into the homologous region in the parental locus (grey and white boxes). This creates a second *Pknbpaxa* copy downstream of the cluster 2 type *Pknbpaxa* and importantly not under the control of a promoter. Integration of the full construct at this site should result in a transfected locus containing the synthetic *Pknbpaxa* cluster

type 2 sequence under the control of the natural promoter at the 5' end of the gene. Four primer sets were designed to amplify regions of the transfected or parental line. Primers F-A1-H.1 & R-A1-H.1 specifically amplified a 1.6 kb region of the parental *Pknbpxa*. Primers F-NotI & R-A1-H.1 amplified a 1.6 kb region from the backbone of the construct into the parental *Pknbpxa* copy. Primers F-SpeI & R-SpeI amplified a 3 kb region from a non-coding region outside the *Pknbpxa* locus to the synthetic cluster type 2 *Pknbpxa* sequence. Primers F-A1-H.1 & R-XaTf2706 amplified a central 0.5 kb region of the synthetic *Pknbpxa*. Primer sequences can be found in Table 2.2.

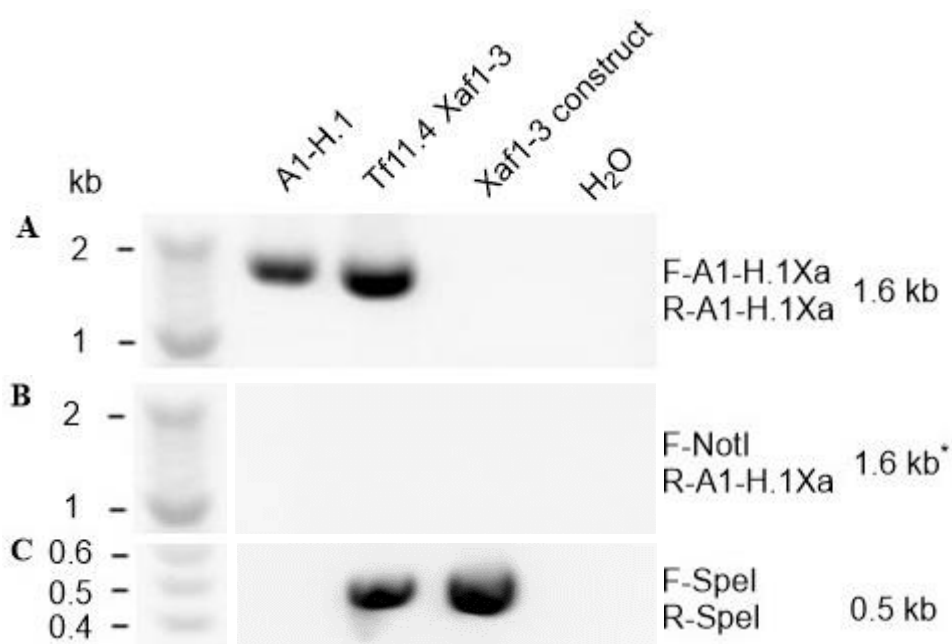


Figure 4.14 Integration PCR showing failed Tf11.4 transfection.

PCR analysis carried out on DNA extracted from the *PkA1-H.1* clone, the Tf11.4 *Pk_{con}Pknbpxa_f1-3*, and the circularised *Pk_{con}Pknbpxa_f1-3* construct failed to confirm integration of the construct at the *Pknbpxa* locus. Adjacent to each panel is the primer pair and expected amplicon, with * denoting that the primer set is specific for the transfected *Pknbpxa* locus. **A.** A PCR product was only produced from reactions containing DNA extracted from the *PkA1-H.1* clone and the Tf11.4 line. **B.** No PCR product was produced in any reaction for the transfected locus. The absence of a 1.6 kb PCR product suggests that the construct has not integrated into the *Pknbpxa* locus following transfection of Tf11.4. **C.** A 0.5 kb PCR product was produced from the Tf11.4 and the transfection construct extracted DNA, confirming presence of the plasmid in the Tf11.4 line, but suggests the construct is episomally maintained. No amplicon was detected in the negative control (lane 5). Lane 1 is the DNA marker hyperladder 50 bp (Bioline). The gel image has been cropped for presentation and the corresponding ladder is inserted next to panels B and C. A gap has been left to signify the ladder was not run adjacent to lanes in panel B or C. The full gel image can be found in appendix J.

4.3.7 Identification and generation of mutations associated with high parasitaemia

As only the initial 885bp of the *Pknbpxa* sequence had previously been analysed, the six full length *Pknbpxa* amino acid sequences were aligned and the S200P (913C) amino acid position was identified, with only 2 of the six clinical sequences (ERR274221 and ERR274222) encoding a proline (Black box, Appendix G). Using this information, the rest of the *Pknbpxa* protein was analysed for any amino acid positions that were conserved in the sequences that contained a proline at amino acid 200. Two additional amino acid changes were identified, consisting of a Glutamic acid at amino acid 420, (Blue box, Appendix G) and a Serine at amino acid 733 (Red box, Appendix G). Along with the S200P mutation the G420E and S733N mutations were also introduced into the pMA-RQ_ *Pknbpxa_f2* plasmid independently by site directed mutagenesis (section 4.2.10). Mutations were introduced into the pMA-RQ_ *Pknbpxa_f2* plasmid and subsequently cloned into the Pk_{con}*Pknbpxa_f1-3* plasmid, as the transfection plasmid was too large to obtain efficient amplification with the SDM primers (Plasmid map Appendix H). The SDM primers for each mutation are given in Table 4.2. The 6 kb pMA-RQ_ *Pknbpxa_f2* plasmid was amplified using primer pair ag382cc (S200P, Table 4.2) in both GC buffer and HF buffer. A 6 kb band was present for all annealing temperatures for GC buffer (lanes 6-9, Figure 4.15) but not the High Fidelity (HF) buffer (lanes 2-5, Figure 4.15). The PCR product from lanes 6-9 were bacterially transformed to increase copy number and presence of the ag382cc mutation, representing the S200P amino acid change, was validated by direct PCR sequencing (see PCR sequencing alignment Appendix H). The gt1043ag (G420E, Table 4.2) and g1982a (S733N, Table 4.2) mutations were generated in the same manner using GC

buffer and validated by direct PCR sequencing (see G420E and S733N PCR and sequencing results Appendix H). The three mutated pMA-RQ_ *Pknbpxa_f2* plasmids (pMA-RQ_ *Pknbpxa_f2*_S200P, pMA-RQ_ *Pknbpxa_f2*_G420E and pMA-RQ_ *Pknbpxa_f2*_S733N) were digested with *Xma*I and *Spe*I to isolate the *Pknbpxa_f2* mutated fragments, and the Pk_{con}*Pknbpxa_f1-3* transfection plasmid was digested with *Xma*I and *Spe*I to remove the *Pknbpxa_f2* fragment without the mutation. The three mutant *Pknbpxa_f2* fragments were then individually ligated into the Pk_{con}*Pknbpxa_f1-3* transfection plasmid, creating the following three transfection plasmids; Pk_{con}*Pknbpxa_f1-3*_S200P, Pk_{con}*Pknbpxa_f1-3*_G420E and Pk_{con}*Pknbpxa_f1-3*_S733N.

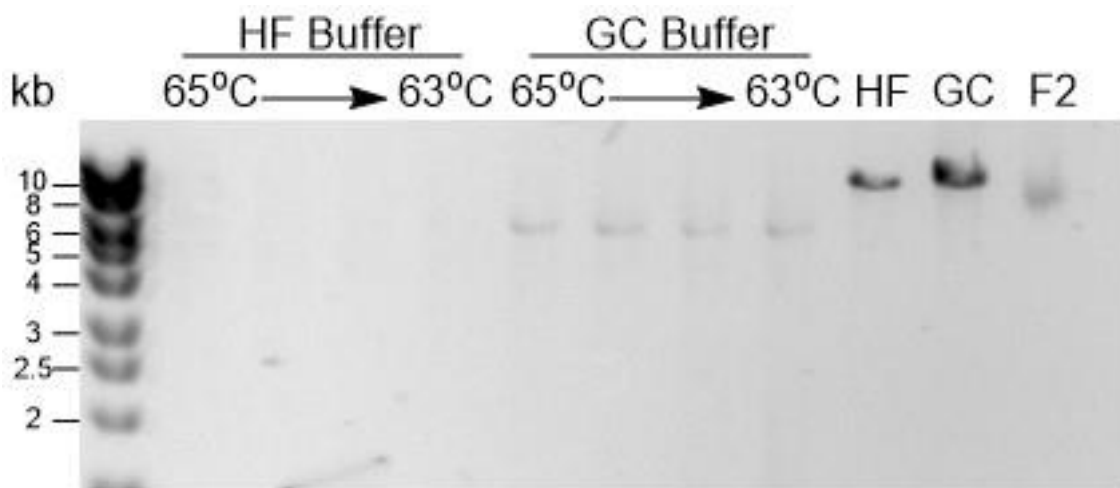


Figure 4.15 Creation of the S200P mutation in the pMA-RQ_ *Pknbpxa_f2* construct.

The pMA-RQ *Pknbpxa_f2* plasmid was PCR amplified using primers (F-ag382cc; CCGGGATAATccCGGTGATGATGATC and R-ag382cc; CATCATCACCGggATTATCCCGGG) specifically designed to introduce two mismatch mutations into the *Pknbpxa_f2* gene sequence. The high fidelity Phusion enzyme (NEB) was used in combination with either the high fidelity (HF) (lanes 2 – 5) or GC rich buffer (lanes 6 – 9). A thermal gradient was used (65 – 63°C) for the annealing temperature to allow primers containing mismatch mutations to bind to the template DNA construct. Primers to amplify a 10 kb region of Lambda DNA were used as a positive control using both HF buffer (lane 10) and GC buffer (lane 11). Uncut the pMA-RQ_ *Pknbpxa_f2* construct Lane 12 was uncut pMA-RQ *Pknbpxa_f2* plasmid that was used as plasmid template for the PCR. Lane 1 is the DNA marker hyperladder 1 kb (Bioline).

4.3.8 Transfection of the *P. knowlesi* A1-H.1 clone with *Pknbpxa* cluster 2 S200P, G420E and S733N

Transfection experiments Tf12, Tf13 and Tf14 (Table 4.6) were conducted in Dr Robert Moon's Laboratory at the London School of Hygiene and Tropical Medicine. $Pk_{con}Pknbpxa_{f1-3}$, $Pk_{con}Pknbpxa_{f1-3_S200P}$, $Pk_{con}Pknbpxa_{f1-3_G420E}$ and $Pk_{con}Pknbpxa_{f1-3_S733N}$ were used to transfect the *PkA1-H.1* clone (See section 4.2.12.3 and Table 4.6).

Parasites transfected with the $Pk_{con}Pknbpxa_{f1-3}$ (Tf12.1, Tf13.1 and Tf14.1) and $Pk_{con}Pknbpxa_{f1-3_S200P}$ (Tf12.2, Tf13.2 and Tf14.2) constructs all grew to produce drug resistant populations within 4 weeks (Table 4.6). The $Pk_{con}p230pGFP$ control plasmid was used to calculate transfection efficiency (Tf12.3, Tf13.3 and Tf14.3, Table 4.6) 1 day after electroporation using live cell microscopy (section 2.4.3) by counting the ratio of GFP-positive parasites to the number of parasites stained with the Hoechst DNA stain. Transfection efficiencies ranged from 16% in Tf13.3 to 34% for Tf14.3.

The drug resistant parasite lines produced in transfection experiments Tf13.1, Tf12.1 ($Pk_{con}Pknbpxa_{f1-3}$) and Tf13.2 ($Pk_{con}Pknbpxa_{f1-3_S200P}$) (Table 4.6) were assayed using the integration PCR and primer pairs A and B as previously described (Table 4.3, Section 4.14). PCR was conducted as in section 2.6.12 and 4.2.14 on DNA extracted from the *in vitro* cultures (section 2.6.7) and from the *PkA1-H.1* untransfected control. An additional primer pair F-A1-H.1 and R-XaTf-2706 was designed to amplify a 3 kb region at the 5' end of the transfected *Pknbpxa* locus (Figure 4.13). The F-A1-H.1 forward primer bound in the non-coding region at the 5' end of the native *Pknbpxa* locus, and the R-XaTf-2706 reverse primer was specific for a unique region of the

cluster 2 type *Pknbpxa* sequence, making the primer pair transfection specific (Figure 4.13). Using this primer pair specific for the transfected locus, produced a 3 kb PCR product from the Tf13.1 template DNA (Figure 4.16, panel A lane 6). Additionally, a faint 3 kb band was detected for the Tf13.2 experiment transfected with the $Pk_{con}Pknbpxa_fl-3$ S200P construct (Figure 4.16, panel A lane 5). Importantly, no amplicon was detected in PCRs using the parental *PkAI-H.1* clone as template DNA (Figure 4.16, lane 2). The PCR primer pair F-A1-H1 & R-A1-H.1, specific for the untransfected *Pknbpxa* locus produced an amplicon of the expected size (1.6 kb) in the parental clone (Figure 4.16, panel B lane 2) and all transfected lines (Figure 4.16 panel B, Tf12.1 lane 3; Tf13.2; lane 4; Tf13.2 lane 5; Tf13.1 lane 6). The primers F-*NotI* & R-A1-H.1 (specific for the transfected *Pknbpxa* locus) produced a 1.6 kb amplicon DNA extracted from the Tf13.1 transfection experiment (Figure 4.16, panel C lane 6) (Table 4.6). Additionally, a faint band at 1.6 kb was seen in PCRs with template DNA from the Tf12.2, and Tf13.2 experiments, transfected with the $Pk_{con}Pknbpxa_fl-3$ S200P construct (Figure 4.16, panel C lanes 3-5). These amplicons were not generated in PCR analysis of untransfected control DNA (Figure 4.16, panel C lane 2). Due to time constraints Tf14, 15, and 16 were not assayed.

Transfections using the control $Pk_{con}p230pGFP$ plasmid (Tf13.3) were assayed using integration PCR. Primer pairs were designed to amplify a 1.4 kb region of the transfected *p230p* locus (ol145 & ol144), and a 1.3 kb region of the untransfected *p230p* locus (ol145 & ol146). The PCR product of expected size for the transfected *p230p* locus (1.45 kb) was detected only in the $Pk_{con}p230pGFP$ transfection experiment Tf13.3 (Figure 4.17, panel A lane 4) (Table 4.8). A 1.3 kb amplicon was detected in both the untransfected parental clone (Figure 4.17, panel B lane 5). Using the ol145 & ol146

primer pair which amplifies the untransfected *p230p* locus produced bands of 1.3 kb when PCRs were carried out on DNA extracted from both transfected lines and the untransfected parental clone (Figure 4.17, panel B lanes 2-5).

These results collectively suggest that the parasites transfected with the $Pk_{con}Pknbpxa_f1-3$ construct successfully integrated this DNA into the *Pknbpxa* locus in experiment Tf13.1. Additionally; parasites transfected with the $Pk_{con}Pknbpxa_f1-3$ *S200P* construct may also have integrated the plasmid into the *Pknbpxa* locus, albeit at a low level. All transfected lines were cryopreserved and the Tf13.1 line was used for dilution cloning and immunofluorescence studies to validate protein expression.

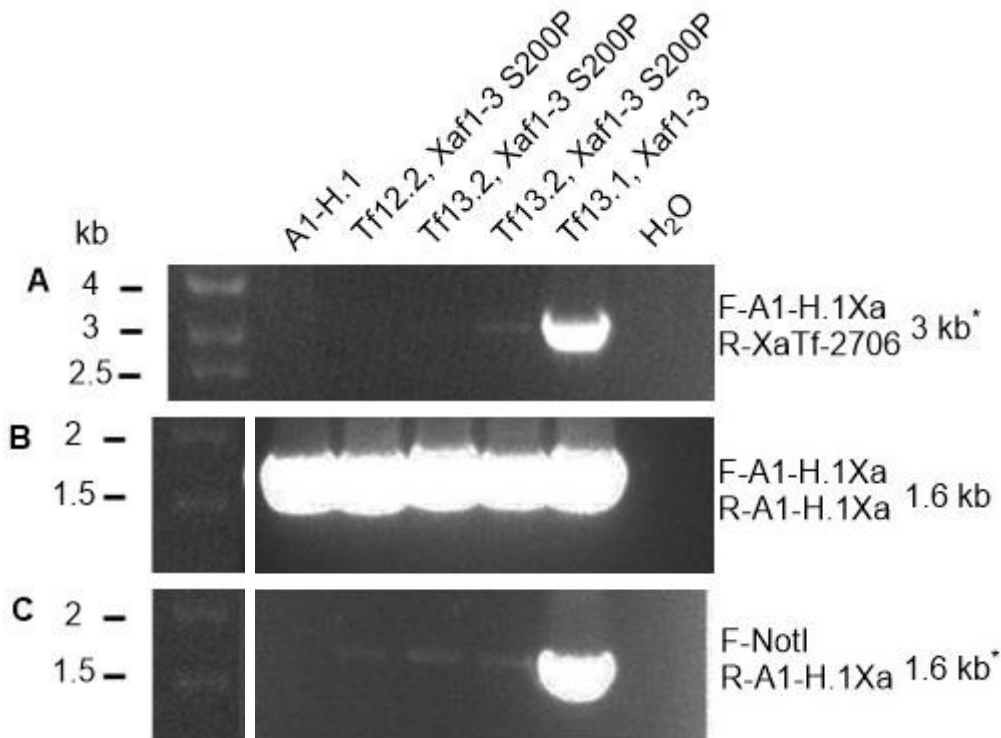


Figure 4.16 Successful integration of the cluster 2 type construct at the *Pknbpxa* locus.

Agarose gel electrophoresis of a PCR to confirm integration of transfection constructs into the *Pknbpxa* locus. PCR analysis was performed on DNA extracted from the *Pka1-H.1* clone along with 3 independent transfections Tf12.2_S200P, Tf13.2_S200P and Tf13.1. Adjacent to each panel is the primer pair and expected amplicon, with * denoting that the primer set is specific for the transfected *Pknbpxa* locus.

A. A 3 kb PCR product was produced from reaction containing DNA extracted from the Tf13.1 line, strongly suggesting integration of the construct into the *Pknbpxa* locus. **B.** PCR product was present in all lanes except the negative control, as this primer pair was specific for the parental *Pknbpxa* locus. **C.** A 1.6 PCR product was produced from the PCR using DNA from transfection Tf13.1, again suggesting successful integration of the construct at the *Pknbpxa* locus. Additionally, faint bands are visible for the transfections Tf12.2 and Tf13.2, but no PCR product is visible from the PCR containing the *Pka1-H.1* DNA. This may suggest that these lines are transfected, albeit at an extremely low level. No amplicon was detected in the negative control (lane 7). Lane 1 is the DNA marker hyperladder 1 kb (Bioline). The gel image has been cropped for presentation and the corresponding ladder is inserted next to panels B and C. A gap has been left to signify the ladder was not run adjacent to lanes in panel B or C. The full gel image can be found in appendix J.

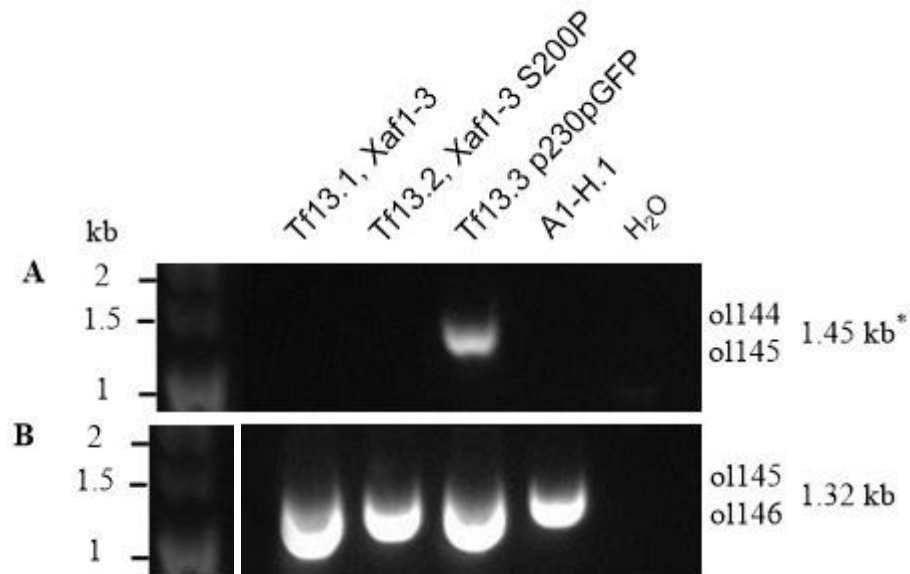


Figure 4.17 Successful integration of the GFP construct into the *p230p* locus.

DNA extracted was extracted from the parental *PkA1-H.1* clone (lane 5) and transfected lines; Tf13.1 (lane 2), Tf13.2 (lanes 3), Tf13.3 (lane 4) for PCR analysis to validate integration of the *p230pGFP* plasmid into the *p230p* locus. Adjacent to each panel is the primer pair and expected amplicon, with * denoting that the primer set is specific for the transfected *p230pGFP* locus. **A.** Template DNA was amplified with the primers ol145&ol144 designed to amplify the *p230pGFP* transfected locus. A 1.4 kb amplicon was observed only in the PCR using template DNA from the Tf13.3 transfection experiment (panel A, lane 4). **F:** Template DNA was amplified with the primers ol145&ol146 designed to amplify a 1.32 kb amplicon from the parental *p230p* locus. A 1.32 kb amplicon was observed in all transfected lines (lanes 2-4) and the parental clone (lane 5). No amplicon was detected in the negative control (lane 6). Lane 1 is the DNA marker hyperladder 1 kb (Bioline). The gel image has been cropped for presentation and the corresponding ladder is inserted next to panels B and C. A gap has been left to signify the ladder was not run adjacent to lanes in panel B. The full gel image can be found in appendix J.

4.3.9 Immunofluorescence staining of the HA-tagged PkNBPXa in transfected parasite lines

Immunocytochemistry was carried out on the Tf13.1 uncloned line. Due to the lack of a commercial antibody against the PkNBPXa protein, a triple HA tag was incorporated at the 3' end of the synthetic *Pknbpaxa* gene sequence prior to the stop codon (section 4.2.6). Transfected protein expression was detected within the Tf13.1 transfected line (Table 4.8) (section 2.4.2) using an anti-HA antibody (Sigma). If the transfected

Pknbpxa_f1-3 plasmid is expressed, the positive HA staining would be detected, confirming the expression of the transfected plasmid. The HA specific staining was visualised with a goat anti-mouse Alexafluor[®]568 secondary antibody (Invitrogen). Punctate anti-HA fluorescence was detected in the *P. knowlesi* Pk_{con}*Pknbpxa_1-3* Tf13.1 line, suggesting expression of the *Pknbpxa_f1-3* protein (Figure 4.18, panel B). Positive HA staining was predominantly on the outer periphery of the stained parasite cell body (Figure 4.18, panel D). Furthermore, this punctate HA staining was in close proximity to the Hoechst stained nuclei suggesting that the HA staining was of parasite origin and not artefact (Figure 4.18, panel C red and blue arrows). In addition, hemozoin pigment appears as dense black material surrounded by individual merozoites suggestive of a mature segmented schizont (Panel A) although contrast for brightfield is poor (Figure 4.18, panel A). A very low proportion of schizonts in the transfected line contained punctate HA stained, suggesting that only a small proportion of the parasites were successfully transfected (Figure 4.18, panel C green arrow). Untransfected control schizont infected cultures, *PkAI-H.1* clone, were negative for HA-staining and positive for Hoechst staining (Figure 4.18, panels B, C and F).

4.3.10 Dilution cloning of the Tf13.1 line

In order to obtain a clone of the Tf13.1 line transfected with Pk_{con}*Pknbpxa_f1-3*, dilution cloning was used. The Pk_{con}*Pknbpxa_f1-3* (Tf13.1) line was serially diluted until there were approximately 3 parasites/mL in 10 mL complete medium (section 2.1.7). Packed RBCs (200 µL) were added and the culture was divided between 100 wells in 96 well plates, and cultured for 2 weeks (Section 4.2.13). After 2 weeks of culture, thin blood films were made and stained to examine the presence of cells in all

100 diluted cultures, of which 33 wells had visible cell growth. The culture of the 33 wells continued for a further 3 weeks until Instagene DNA extractions were able to be performed (section 2.6.8). Integration PCR primers (section 4.2.14) specific for the transfected and untransfected lines were used to detect if the *Pknbpxa* locus was transfected. No clones were positive for the transfected locus, and the control DNA extracted from the T13.1 line was positive for the transfected *Pknbpxa* locus (Section 2.6.7). The primers for the native locus were not positive in all lanes, suggesting the DNA extraction was inefficient or the culture parasitaemia was too low. Repeats of these PCRs could not be performed as cultures became contaminated preventing a repeat DNA extraction.

Dilution cloning of the transfection experiment Tf13.1 failed to produce a transfected clone, suggesting a high percentage of parasites maintained the plasmid episomally. As per Triglia *et al.*, (1998) drug selection was removed from the cultured Tf13.1 transfection experiment for 3 weeks, followed by further pyrimethamine selection until drug resistant parasites were detected in the culture. Parasites recovered and were grown under pyrimethamine selection until able to be cryopreserved. Due to time constraints the dilution cloning of the transfection experiment Tf13.1 cycled in pyrimethamine was not repeated.

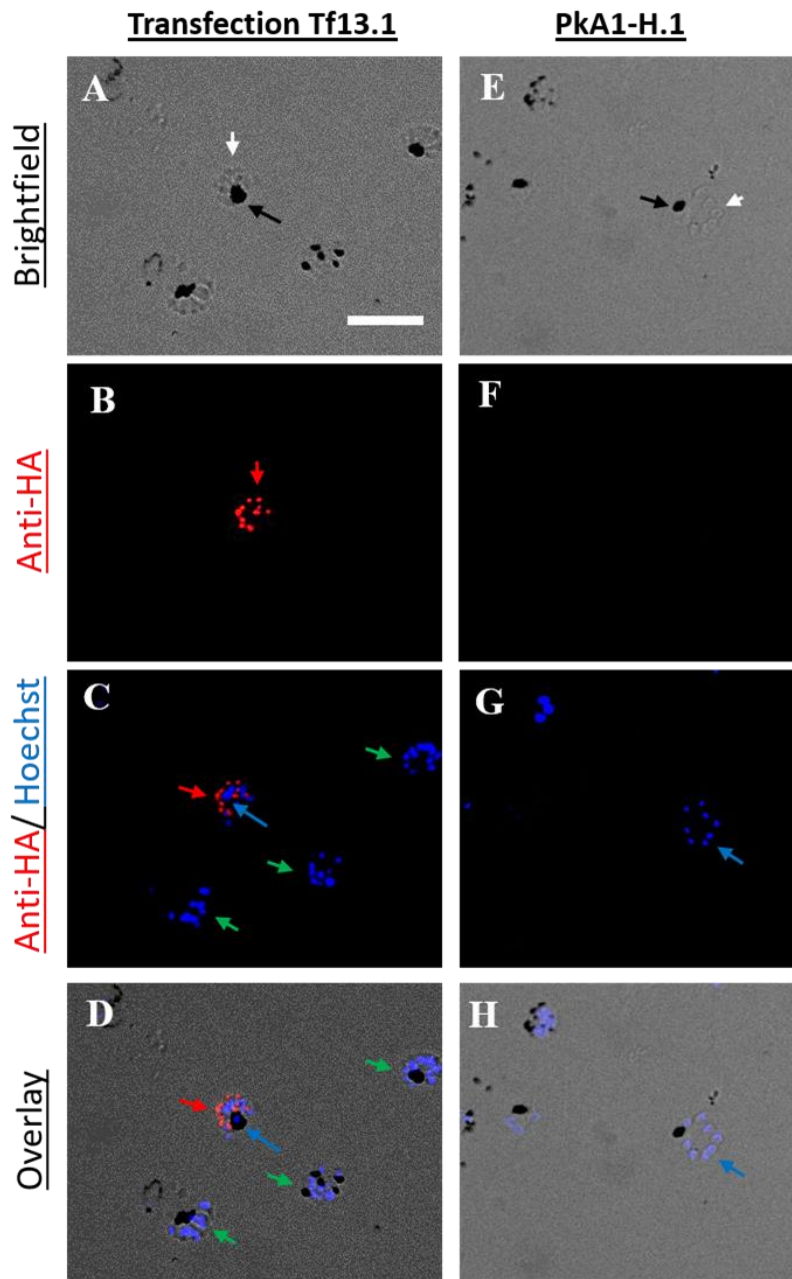


Figure 4.18 Detection of the HA tagged *Pknbpaxa* cluster 2 type protein in schizonts isolated from the Tf13.1 experiment.

Panels A-D are purified schizonts from the $Pk_{con}Pknbpaxa_{f1-3}$ transfection Tf13.1. Panels E-H are purified schizonts from the parental *PkA1-H.1* clone. Schizonts were stained as in section (2.4.2) with an Anti-HA antibody (Sigma), and detected using the Alexafluor®-568 secondary antibody. Schizonts were then stained with Hoechst 33342 (section 4.2.2). Brightfield images shows presence of late stage schizonts containing hemozoin and individual merozoites in panels A, D, E and H (black and white arrows, respectively). Red fluorescence (red arrows) can be seen in panels B, C, and D but is absent in panels F, G and H. Red fluorescence shows positive HA staining of HA-tagged *Pknbpaxa* protein. Parasite DNA stained blue with Hoechst dye (blue arrows) was present in panels C, D, G and H. Panels D is an overlay

of panels A-C and panel H is an overlay of panels E-G. Scale bar = 10 μm . Parasites were imaged using a Leica epifluorescent DM5500 microscope equipped with a Leica DFC550 digital camera.

4.4 Discussion

Single cross over homologous recombination was used to replace the homologous *Pknbpxa* gene in the *PkA1-H.1* clone with clinically relevant variants defining *Pknbpxa* cluster 2. Full-length *Pknbpxa* sequences (approx 9kb) were assembled from six *P. knowlesi* genome sequences generated from clinical isolates (Pineiro *et al.*, 2015). Variation at this locus was further informed by 75 *Pknbpxa* haplotypes identified in clinical isolates reported by Ahmed *et al.*, (2014). Using codon optimisation and *Pknbpxa* variation occurring in contemporary clinical isolates, a synthetic *Pknbpxa* gene sequence was derived to represent *Pknbpxa* cluster 2 (Pineiro *et al.*, 2015). The synthetic sequence included a region of homology and was otherwise codon optimised to ensure that recombination had a high chance of occurring at the correct position in the *Pknbpxa* locus and that the clinically relevant *Pknbpxa* cluster 2 sequence was superimposed on the *P. knowlesi* A1-H.1 clone.

The *PkA1-H.1* clone is reported to be derived from the original Human (H strain) infection with *P. knowlesi* (Chin *et al.*, 1965, Moon *et al.*, 2013, Moon *et al.*, 2016). Prior to adaptation of this line to human erythrocytes, it was cultured *in vivo* using Rhesus macaques (Moon *et al.*, 2013). However, the *P. knowlesi* genome sequence (Pain *et al.*, 2008), believed to be the H strain is in fact likely to be a distinct Malaysian isolate (Butcher and Mitchell, 2016, Assefa *et al.*, 2015). It is unknown how well the reference *Pknbpxa* sequence (Meyer *et al.*, 2009, Pain *et al.*, 2008), and the *PkA1-H.1* *Pknbpxa* gene sequence (Moon *et al.*, 2013) represent current clinical isolates. Therefore, replacing the *Pknbpxa* sequence in the *PkA1-H.1* clone with a clinically relevant cluster 2 *Pknbpxa* sequence would allow characterisation and invasion phenotyping of previously identified associations with virulence. Thereby, introducing a

sequence common to *Pknbpxa* cluster type 2 allowed individual mutations associated with high parasitaemia to be introduced.

Using the full length *Pknbpxa* sequence extracted from clinical genome sequences it was established that the published 913C mutation from the 885bp sequence of *Pknbpxa* (Ahmed *et al.*, 2014) encoded a proline at residue 200 (S200P). This residue was conserved in the two sequences that associated with high parasitaemia (Appendix G). Using the information that two sequences (ERR274221 and ERR274222) had an association with high parasitaemia the entire *Pknbpxa* protein sequence was examined identifying only 2 further residues conserved in the clinical isolates ERR274221 and ERR274222, G420E and S733N.

The substitution of a single lysine at residue 204 in PfRh5 has been shown to result in a switch in host tropism (Hayton *et al.*, 2008). Although PfRh5 and PkNBPXa only share small amounts of homology at the N-terminus, both are essential to erythrocyte invasion (Baum *et al.*, 2009, Semanya *et al.*, 2012, Moon *et al.*, 2016). This suggests that single non-synonymous mutations in essential adhesive genes could play an important role in erythrocyte invasion. In addition to the proline at residue 200 in the *Pknbpxa* protein we have identified two further residues (Glutamic acid at residue 420 and Asparagine at residue 733) in the *Pknbpxa* sequences which are confined to those that associate with high parasitaemia. Although the structure of PkNBPXa is unknown, a region of PkNBPXb (184 – 531 aa) has been shown to bind to Rhesus macaque erythrocytes (Meyer *et al.*, 2009, Semanya *et al.*, 2012). This PkNBPXb binding region encompasses two out of the 3 mutations identified in PkNBPXa protein (S200P and G420E). In addition, the residues in Rh5 that interact with basigin cluster between residues 197 – 449 aa (Wright *et al.*, 2014), a region where two out of the three mutations identified

here are located. The hypothesis that single residue substitutions in the cluster 2 type *Pknbp_{pxa}* protein result in an increased parasitaemia could be interrogated using the lines created here. Phenotypic analysis of these lines would be performed by analysing growth rates of the cluster 2 sequence compared with the cluster 2 sequence containing single residue substitutions. Analysis would be performed by counting parasitaemias via flow cytometry to ensure the parasitaemias are counted accurately and reliably. Following this, and depending on flow cytometry results, competition assays would be used to determine whether the clone expressing the cluster 2 sequence with single residue substitutions exhibited an invasion advantage over the cluster 2 type sequence. Samples would be taken at weekly time points to quantify the proportion of each clone in the mixed culture. By using TaqMan qPCR we could show how quickly, one clone begins to dominate the parasite population in the culture. The clones would also be phenotyped for differences in selection for human RBC blood groups and RBC maturity, to identify if the association with high parasitaemia in clinical isolates can be attributed to a larger proportion of RBCs able to be invaded. In addition, a pulldown study using an HA tagged *Pknbp_{pxa}* clone would have been carried out. In order to maximise the possible interactions of PkNBPXa with an RBC erythrocyte receptor, purified merozoites would have been incubated with RBCs in the presence of the cytochalasin D, an inhibitor of actin polymerisation. This would have halted the merozoites mid invasion, enabling the cross linking of the merozoites adhered to the erythrocyte surface, and subsequent pulldown of the HA tagged PkNBPXa.

By using single crossover homologous recombination, along with codon optimised synthetic DNA containing the cluster 2 variation, and the Lonza-4D nucleofector, a line

transfected with the *Pk_{con}Pknbpxa_f1-3* plasmid was obtained. Although the optimisation steps for transfection were thorough, transfections were not 100% effective, even when transfections were performed using the exact Moon *et al.*, (2013) protocol. The size of the plasmid, 14 kb, in combination with the relatively short 500 bp homology arms may have impacted upon the efficiency of homologous recombination (Kung *et al.*, 2013, Pfander *et al.*, 2011). However, the homologous arm lengths could not be increased, as this may have included the promoter region causing the transfected gene and the native gene to both be expressed. Additionally, consistent gene expression between transfected lines would be required for comparisons of growth rate. Single cross over homologous recombination had previously been used in the *P. knowlesi* *PkA1-H.1* *in vitro* culture for both knock-in and knock-out studies (Moon *et al.*, 2013, Tarr *et al.*, 2014, Moon *et al.*, 2016, Yusuf *et al.*, 2015). However, only partial gene sequences were used to tag genes, rather than replace a full copy and all plasmids were below 10 kb. Here we demonstrate that the *P. knowlesi* A1-H.1 culture adapted to human erythrocytes and the *P. knowlesi* transfection system developed by Moon *et al.*, (2013) supported whole gene knock-in for disease phenotyping experiment.

Use of the 4-D nucleofactor resulted in recovery of parasites containing the *Pk_{con}Pknbpxa_f1-3* plasmid in the presence of horse serum. However it took over 30 days for the parasites to recover under drug selection and no integration of the construct was detected by PCR. Transfection specific amplicons were produced from the DNA of transfections carried out in the presence of human serum opposed to horse serum. The increased parasite growth in human serum (Moon *et al.*, 2013) may have aided the growth of transfected cells, therefore shortening the duration of drug selection before parasites were detectable. Alternatively, a tighter synchronisation containing more late

stage parasites may have resulted in the successful growth of the Tf12-15 transfections, as segmented schizonts are the desired life stage for transfections (Janse *et al.*, 2006). Importantly, the transfection efficiencies calculated in this study were performed using the $Pk_{con}p230pGFP$ plasmid and were similar to those reported by Moon *et al.*, (2013). However, using a larger GFP construct targeted to the *p230p* locus would have provided a more appropriate control for the transfections carried out here with the $Pk_{con}Pknbpxa_fl-3$ construct.

Integration PCR experiments revealed that the $Pk_{con}Pknbpxa_fl-3$ (Tf13.1) plasmid was correctly inserted in the *Pknbpxa* locus in the transfected line Tf13.1. The transfection of the $Pk_{con}Pknbpxa_fl-3_S200P$ (Tf13.2) was analysed by integration PCR and a faint band representing the transfected locus was detected suggesting a low integration efficiency. The reason for this remains unclear, as transfections were performed and maintained at the same time, with the plasmid differing at only 2 nucleotides.

The Tf13.1 line showing positive integration of the $Pk_{con}Pknbpxa_fl-3$ plasmid at the *Pknbpxa* locus was taken forward for validation of protein expression. Due to the addition of the HA tag in the *Pknbpxa_fl-3* gene, the transfected PkNBPXa protein was able to be detected using an anti-HA antibody. Positive anti-HA staining of Tf13.1 schizonts suggests that the *Pknbpxa_fl-3* protein was expressed. This staining appeared as a punctate fluorescent pattern which overlaid onto single merozoites as visualised with Hoechst DNA staining in the same preparation. Nuclear staining had a similar pattern showing merozoites but was located slightly differently to the anti-HA signal (figure 4.18) which was more peripheral in the same merozoites. The HA staining pattern is consistent with the position of an apical organelle in outward facing merozoites in a segmented schizont with the nucleus to the posterior end of the

merozoites. The apical orientation has been reported for other RBP proteins with the PfRh proteins localising to the rhoptries (Taylor *et al.*, 2002). Additionally, Meyer *et al.*, (2009) report the localisation of *Pknbpxa* to the microneme as shown by electron microscopy (Meyer *et al.*, 2009). The results from this lay the groundwork for invasion phenotyping of these transfected lines.

The association between invasion efficiency and growth rate in the transfected lines containing *Pknbpxa* variants associated with high parasitaemia has yet to be determined. In order to identify whether the $Pk_{con}Pknbp\textit{xa}_{f1-3}$ transfected lines expressing the S200P, G420E or S733N mutations exhibit any growth change, all transfected lines will require limiting dilution cloning. Once cloned, these lines can be characterised for growth efficiency and invasion phenotype. In addition, *in vitro* competition assays between the transfected lines and the parent *P. knowlesi* A1-H.1 culture in human and macaque red blood cells, differing by type and age, would determine any changes in parasite growth and invasion efficiency *in vitro*. These results would add context to the studies by Ahmed *et al.*, (2014) where an association between *Pknbpxa* and disease severity was suggested.

Since starting this project a new transfection system using CRISPR Cas9 transfection plasmids has been developed (Ghorbal *et al.*, 2014, Wagner *et al.*, 2014, Zhang *et al.*, 2014) and may support gene-knock-in more efficiently. In the case of reproducing clinically relevant *P. knowlesi* loci, longer homology arms consisting of the upstream and downstream regions flanking the *Pknbpxa* gene would have been possible in the CRISPR system. This is because the Cas9 directed by the guide RNA creates two double strand breaks, removing the parental *Pknbpxa* gene. However, longer homology arms could not have been utilised whilst using single crossover homologous

recombination, as this method disrupts the *Pknbpxa* gene creating a duplicated copy, but importantly without a promoter at the 5' end. If longer homology arms had been used the parental *Pknbpxa* duplicate may have been expressed, as the promoter region at the 5' end of *Pknbpxa* would also have been duplicated. Therefore by using CRISPR it would have allowed the whole gene to be replaced as the homology arm could have entirely comprised non-coding regions outside the *Pknbpxa* locus (Ghorbal *et al.*, 2014, Wagner *et al.*, 2014, Zhang *et al.*, 2014). In addition to potential increases in efficiency, replacement of the *Pknbpxa* gene using CRISPR technologies would prevent the requirement for a codon optimised *Pknbpxa* synthetic gene. This could result in clinically relevant genes being directly amplified by PCR for CRISPR –CAS 9 transfection, substantially reducing time and costs currently required for codon-optimization and gene synthesis using the single homologous crossover system. Incorporation of CRISPR into this work flow would increase the ability to assay clinically relevant alleles *in vitro*.

Chapter 5: Summary and future perspectives

The aim of this project was to optimise a translational approach to studying genomic associations with severe malaria. By analysing the genome sequence data along with the patient clinical data, candidate genes and mutations associated with high parasitaemia could be identified. Recreating these mutations *in vitro* would allow for in-depth analysis to assess their role in severe disease. With access to a Biobank of frozen clinical isolates improved methods were required to isolate parasite DNA from frozen whole blood using a cost effective and simple method. Once *P. knowlesi* DNA was obtained and whole genome sequencing performed full length *Pknbpxa* gene sequence data along with clinical data would be available. This would enable residues associated with severe malaria to be introduced into the *in vitro* culture enabling associations with severe malaria to be studied. This translational approach, recreating clinical loci within an *in vitro P. knowlesi PkA1-H.1* experimental line, allowed for further investigations into mutations associated with severe malaria.

Previous work had shown that parasite DNA can be retrieved from frozen patient whole blood samples, although the efficiency of human DNA depletion was variable and not as efficient as required in some samples (Pinheiro *et al.*, 2015). Following optimisation steps, frozen patient whole blood was successfully leukocyte depleted using the Whatman-Plasmodipur method followed by parasite pellet washing to remove soluble hDNA. Although parasite DNA was not enriched in all clinical samples that were processed using the Whatman Plasmodipur method, those that did show enrichment for parasite DNA predominantly had minimal human DNA contamination. PkDNA was purified by the removal of hDNA in 13 of the 22 samples processed, producing 8 samples with DNA concentrations suitable for whole genome sequencing. Other samples contained PkDNA levels too low for genomic sequencing, but whole genome

amplification was suggested as a last resort method to increase the overall DNA concentration. The purified samples contained low enough hDNA and high enough quantities of PkDNA to enable MinION long read sequencing.

Genome sequence data was available from six recently sequenced *P. knowlesi* clinical isolates (Pinheiro *et al.*, 2015). Of these, two sequences contained previously reported variation in the dimorphic invasion gene, *Pknbpxa* (cluster 2), shown to associate with high parasitaemia in *P. knowlesi* infections (Ahmed *et al.*, 2014). Using the 6 available clinical genome sequences, alongside previously published haplotype analysis (Ahmed *et al.*, 2014), the full length cluster 2 *Pknbpxa* sequences were codon optimised and synthesised. The *Pknbpxa* cluster 2 sequences were sequentially cloned into a *P. knowlesi* specific transfection vector. Single crossover homologous recombination (Moon *et al.*, 2013) was used to replace the native *Pknbpxa* in the *PkAI-H.1* clone producing a transgenic line expressing clinically relevant variation for use in studies associated with high parasitaemia.

The effect of non-synonymous mutations on the binding of RBP proteins to erythrocyte receptors is not well characterised. As previously discussed a single residue substitution in PfRh5 resulted in an altered host tropism with merozoites capable of invading *Aotus* monkey erythrocytes (Hayton *et al.*, 2008). Furthermore, research shows single mutations within the *P. vivax* Duffy binding protein (DBP) can change binding efficiency (Batchelor *et al.*, 2014). Together this work highlights the impact of single amino acid mutations within essential parasite invasion proteins. Like the PfRh5 and PvRBP proteins, the *P. knowlesi* NBPXa protein has an essential role in erythrocyte invasion. Therefore, non-synonymous mutations within this gene may have an impact on parasite invasion and virulence.

In vitro work in *P. knowlesi*

One commonly used method to analyse the effects of single amino acid mutations on protein function is to analyse the mutated parasite proteins *in vitro*. Presented here is one such method, allowing our clinically relevant mutations of interest to be analysed for their association with severe disease. As shown in this study, the *P. knowlesi in vitro* culture in human erythrocytes is capable of genetic manipulation involving the replacement of large genes. Our results suggest the size of the transfection construct may affect the transfection efficiencies. Replacement of large genes could be improved using CRISPR technologies opposed to single crossover homologous recombination (Ghorbal *et al.*, 2014, Wagner *et al.*, 2014, Zhang *et al.*, 2014, Lu *et al.*, 2016, Mogollon *et al.*, 2016).

An advantage of working with *P. knowlesi* experimental models is that studies can be applied to both *in vitro* and *in vivo* systems. This is because *P. knowlesi* is a zoonotic parasite and naturally infects macaques, now a widely employed animal model for human disease. The *in vitro* cultured *P. knowlesi* lines can be genetically manipulated and the H-strain, adapted to long term *in vitro* culture in Rhesus erythrocytes, is infective to non-human primates (Kocken *et al.*, 2002, Moon *et al.*, 2013). The H-strain *in vivo* and *in vitro* line is amenable to genetic manipulated, and retains the ability to produce gametocytes *in vivo* enabling transmission studies to be carried out (Murphy *et al.*, 2014, Kocken *et al.*, 2002). *P. falciparum* is the most widely used *in vitro* cultured species. *P. falciparum* can experimentally infect *Aotus* monkeys, but without sequestration in brain microvasculature, a key features of severe *P. falciparum* malaria seen in human disease (Voller *et al.*, 1969). Additionally, there is no *in vivo* transmission model for *P. falciparum*. The rodent malarial species *P. berghei* is also

widely used as an *in vivo* model, and literature suggests that it can be maintained *in vitro* for short periods of time (Jambou *et al.*, 2011). Recent controversy regarding the suitability of *P. berghei* *in vivo* studies has shown that it cannot model crucial human aspects of severe *P. falciparum* malaria, such as cytoadhesion (Craig *et al.*, 2012).

In vivo work in *P. knowlesi*

As *P. knowlesi* is the only malaria species to naturally infect both macaques and humans, it also allows researchers a unique opportunity to monitor the effects of genetic manipulations within a non-human primate *in vivo* model. This information could reveal potential parasite invasion mechanisms in human severe disease. In particular, the lines generated from this work could be phenotyped *in vivo* to validate associations between *Pknbpxa* polymorphisms and high parasitaemia. Furthermore, *P. knowlesi* could be used to model aspects of *P. falciparum* malaria *in vivo*. For example, *P. knowlesi* expresses the SICA antigens, proposed to have a significant amount of common sequence with the *P. falciparum* erythrocyte membrane proteins (PfEMP1) when compared at the protein level (Korir and Galinski, 2006). Variants of PfEMP1 are linked to different aspects of severe malaria, such as cerebral sequestration, placental sequestration and iRBC rosetting (Pasternak and Dzikowski, 2009, Claessens *et al.*, 2014, Rowe *et al.*, 1995). Importantly, as with *P. falciparum*, *P. knowlesi* has been shown to sequester in brain microvasculature, as identified in a fatal case of *P. knowlesi* infection, but importantly, does not produce coma (Cox-Singh *et al.*, 2010). This suggests a common function between these two protein families, one which could be studied *in vivo* using *P. knowlesi*. The rodent malaria causing parasite *P. berghei* has been used to model cerebral malaria however, it does not express orthologues of the PfEMP1 or SICA proteins, and does not sequester in the brain (Franke-Fayard *et al.*, 2005). This suggests

that *P. knowlesi* would be a more suitable model for investigations into iRBC sequestration linked with *P. falciparum* malaria.

Non-Human Primates and *P. knowlesi*

A number of non-human primates, such as the Olive baboon, marmoset and Rhesus macaque, have been experimentally infected with *P. knowlesi* (Ozwarra *et al.*, 2003, Langhorne and Cohen, 1979, Coatney *et al.*, 1971), although few of these have been fully assessed for clinical features of severe malaria. From these studies, it is apparent that a wide array of non-human primates are susceptible to *P. knowlesi*. One species which has been characterised for modelling severe malaria is the Olive baboon (*Papio anubis*). When Olive baboons were challenged with *P. knowlesi*, sequestration was observed in brain microvasculature and in the placenta of pregnant females (Ozwarra *et al.*, 2003, Onditi *et al.*, 2015). This mirrored the sequestration present in brain microvasculature of both *P. falciparum* and *P. knowlesi* human infections (Cox-Singh *et al.*, 2008, Miller *et al.*, 2002). If specific parasite-host interactions are implicated in causing brain microvasculature and placenta sequestration in the olive baboons, this could have important implications for human disease.

Concluding remarks

In this project we have initiated a translational approach to test genetic associations with severe malaria *in vitro*. We have validated the use of the Whatman-Plasmodipur method for the enrichment of parasite DNA from frozen whole blood, producing quantities suitable for whole genome sequencing. This work has opened new avenues of investigation with the ability to obtain whole genome sequence data from archived samples. Following this, methods to replace whole genes in the *P. knowlesi* genome

with a clinically relevant copy were developed and would have led to *in vitro* testing, validating SNP associations with severe malaria. Furthermore, by using *P. knowlesi* the progression to *in vivo* modelling of associations with severe disease can be achieved. This is an important requirement for understanding severe malaria pathobiology.

Chapter 6: Appendices

Appendix A: Cytomix Transfection Buffer

Buffer stocks, and dilutions for CytoMix Transfection reagent

CytoMix					
Stock solution				For 100 mL	
Reagent	Grams	Volume	Concentration	Added	CytoMix conc
KCl	4.47 g	50 mL	1.2 M	10 mL	120 mM
CaCl ₂	83.2 mg	50 mL	0.15 M	0.1 mL	0.15 mM
EGTA	0.76 g	10 mL	0.2 M	1 mL	2 mM
MgCl ₂	825 mg	50 mL	0.5 M	1 mL	5 mM
HEPES	N/A	N/A	1 M	2.5 mL	25 mM
K ₂ HPO ₄ / KH ₂ PO ₄	N/A	N/A	1 M	1 mL	10 mM

For 1 M K ₂ HPO ₄ /KH ₂ PO ₄					
Stock solution					
Reagent	Grams	Volume	Concentration	Added	
K ₂ HPO ₄	8.7g	50mL	1M	40.1 mL	50 mL (1 M)
KH ₂ PO ₄	6.8g	50mL	1M	9.9 mL	

Appendix B: Ethics, Information and Consent forms



University of St Andrews

University Teaching and Research Ethics Committee
Sub-committee

26th June 2014

Dr Janet Cox-Singh
School of Medicine

Ethics Reference No: <i>Please quote this ref on all correspondence</i>	MD11076
Project Title:	Plasmodium Knowlesi Pathobiology
Researchers Name(s):	Janet Cox-Singh
Supervisor(s):	

Thank you for submitting your application which was considered by the School of Medicine Ethics Convener on the 26th June 2014. The following documents were reviewed:

- | | |
|----------------------------------|-----|
| 1. Ethical Application Form | YES |
| 2. Participant Information Sheet | YES |
| 3. Consent Form | YES |
| 4. External Permissions | YES |

The University Teaching and Research Ethics Committee (UTREC) approves this study from an ethical point of view. Please note that where approval is given by a School Ethics Committee that committee is part of UTREC and is delegated to act for UTREC.

Approval is given for three years. Projects, which have not commenced within two years of original approval, must be re-submitted to your School Ethics Committee.

You must inform your School Ethics Committee when the research has been completed. If you are unable to complete your research within the 3 three year validation period, you will be required to write to your School Ethics Committee and to UTREC (where approval was given by UTREC) to request an extension or you will need to re-apply.

Any serious adverse events or significant change which occurs in connection with this study and/or which may alter its ethical consideration, must be reported immediately to the School Ethics Committee, and an Ethical Amendment Form submitted where appropriate.

Approval is given on the understanding that the 'Guidelines for Ethical Research Practice' <https://www.st-andrews.ac.uk/utrec/guidelines/> are adhered to.

Yours sincerely

Dr Morven Shearer
Convener of the School Ethics Committee



27th November 2014

Janet Cox-Singh
School of Medicine

Ethics Reference No: <i>Please quote this ref on all correspondence</i>	MD12671
Project Title:	Malaria parasite pathobiology - donor blood is required to culture malaria parasites as part of a PhD by Mr Scott Millar
Researchers Name(s):	Janet Cox-Singh, Scott Millar (PhD student)
Supervisor(s):	Janet Cox-Singh

Thank you for submitting your application which was considered by the Convener of the School Ethics Committee on the 27th November 2014. The following documents were reviewed:

- | | |
|----------------------------------|-----|
| 1. Ethical Application Form | YES |
| 2. Participant Information Sheet | YES |
| 3. Consent Form | YES |
| 4. Study Description | YES |

The University Teaching and Research Ethics Committee (UTREC) approves this study from an ethical point of view. Please note that where approval is given by a School Ethics Committee that committee is part of UTREC and is delegated to act for UTREC.

Approval is given for three years. Projects, which have not commenced within two years of original approval, must be re-submitted to your School Ethics Committee.

You must inform your School Ethics Committee when the research has been completed. If you are unable to complete your research within the 3 three year validation period, you will be required to write to your School Ethics Committee and to UTREC (where approval was given by UTREC) to request an extension or you will need to re-apply.

Any serious adverse events or significant change which occurs in connection with this study and/or which may alter its ethical consideration, must be reported immediately to the School Ethics Committee, and an Ethical Amendment Form submitted where appropriate.

Approval is given on the understanding that the 'Guidelines for Ethical Research Practice' <https://www.st-andrews.ac.uk/utrec/guidelines/> are adhered to.

Yours sincerely

Dr Morven Shearer
Convener of the School Ethics Committee



Participant Information Sheet

Project Title

Parasite culture for malaria pathobiology study.

What is the study about?

We invite you to participate in a research project to understand pathobiology in malaria. For the study we need to culture malaria parasites in the laboratory. Malaria parasites grow inside red blood cells and therefore we need a supply of human red blood cells to maintain our parasite cultures. The blood will not be tested.

This study is being conducted as part of a PhD project on malaria pathophysiology.

Do I have to take Part?

No your participation is completely voluntary.

This information sheet has been written to help you decide if you would like to take part. It is up to you and you alone whether or not to take part. If you do decide to take part you will be free to withdraw at any time without providing a reason.

What would I be required to do?

You will be required to donate 20mls of blood (approximately 1 - 2 table spoons equivalent). The blood will be washed and the red cell fraction will be used to culture malaria parasites under varying conditions to measure parasite growth.

Exclusion - We will not be able to include you in the study if you have ever had malaria or if you have taken anti-malarials or antibiotics during the past 4 weeks.

Will my participation be Anonymous and Confidential?

Your participation will be anonymous - your participation will be coded as healthy donor, male or female and age.

Only the researcher(s) and supervisor(s) will have access to your data which will be kept strictly confidential. Your permission maybe sought in the Participant Consent

form for the data you provide, which will be anonymised, to be used for future scholarly purposes.

Storage and Destruction of Data Collected

Data gathered during this research project will be coded and kept confidentially by the researcher with only the researcher and supervisor having access. It will be securely stored in an excel spread sheet for the duration

of the study and kept for 15 years. Signed consent forms will be stored as hard copy in a secure filing cabinet for 15 years. .

What will happen to the results of the research study?

In vitro parasite culture will support various studies in malaria research.

Reward

N/A

Are there any potential risks to taking part?

No risk is anticipated. The blood will be collected by a trained phlebotomist in an area designated for sample collection in the School of Medicine.

Questions

You will have the opportunity to ask any questions in relation to this project before giving completing a Consent Form.

Consent and Approval

What should I do if I have concerns about this study?

A full outline of the procedures governed by the University Teaching and Research Ethical Committee is available at <http://www.st-andrews.ac.uk/utrec/Guidelines/complaints/>

Contact Details

Researcher:

Name Scott Millar (PhD student)

School of Medicine,
University of St Andrews,
Medical and Biological Sciences Building,
North Haugh,
ST ANDREWS,
Fife, KY16 9TF
Scotland
email sbm3@st-andrews.ac.uk

Supervisors Name

Dr Janet Cox-Singh,
School of Medicine,
University of St Andrews,
Medical and Biological Sciences Building,
North Haugh,
ST ANDREWS,
Fife, KY16 9TF
Scotland
Tel: 01334461896
email: **jcs26@st.andrews.ac.uk**



Participant Consent Form

Anonymous Data

Project Title: Malaria parasite pathobiology

Researcher(s) Name(s)

Scott Millar (PhD student)

School of Medicine,
University of St Andrews,
Medical and Biological Sciences Building,
North Haugh,
ST ANDREWS,
Fife, KY16 9TF
Scotland
email sbm3@st-andrews.ac.uk

Supervisors Names

Dr Janet Cox-Singh,
School of Medicine,
University of St Andrews,
Medical and Biological Sciences
Building,
North Haugh,
ST ANDREWS,
Fife, KY16 9TF
Scotland
Tel: 01334461896
email: **jcs26@st.andrews.ac.uk**

The University of St Andrews attaches high priority to the ethical conduct of research. We therefore ask you to consider the following points before signing this form. Your signature confirms that you are happy to participate in the study.

What is Anonymous Data?

THE TERM 'ANONYMOUS DATA' REFERS TO DATA COLLECTED BY A RESEARCHER THAT HAS NO IDENTIFIER MARKERS SO THAT EVEN THE RESEARCHER CANNOT IDENTIFY ANY PARTICIPANT. CONSENT IS STILL REQUIRED BY THE RESEARCHER, HOWEVER NO LINK BETWEEN THE PARTICIPANT'S SIGNED CONSENT AND THE DATA COLLECTED CAN BE MADE.

Consent

The purpose of this form is to ensure that you are willing to take part in this study and to let you understand what it entails. Signing this form does not commit you to anything you do not wish to do.

Material gathered during this research will be anonymous, so it is impossible to trace back to you. It will be securely stored. Data gathered during this research project will be coded, anonymised and kept confidentially by the researcher with only the researcher and supervisor having access. The data will be securely stored in an excel spread -sheet and kept for 15 years. Signed consent forms will be stored as hard copy in a secure filing cabinet for 15 years.

The balance of the blood sample may be kept by the researcher and archived and used for further related research projects or by other bona fide researchers.

Please answer each statement concerning the collection and use of the research data.

I have read and understood the information sheet. Yes No

I have been given the opportunity to ask questions about the study. Yes No

I have had my questions answered satisfactorily. Yes No

I understand that I can withdraw from the study without having to give an explanation. Yes No

I understand that my data once processed will be anonymous and that only the researcher(s) (and supervisors) will have access to the raw data which will be kept confidentially. Yes No

I understand that my data will be stored for a period of 15 years before being destroyed. Yes No

I have been made fully aware of the potential risks associated with this research and am satisfied with the information provided. Yes No

I agree to take part in the study Yes No

Participation in this research is completely voluntary and your consent is required before you can participate in this research.

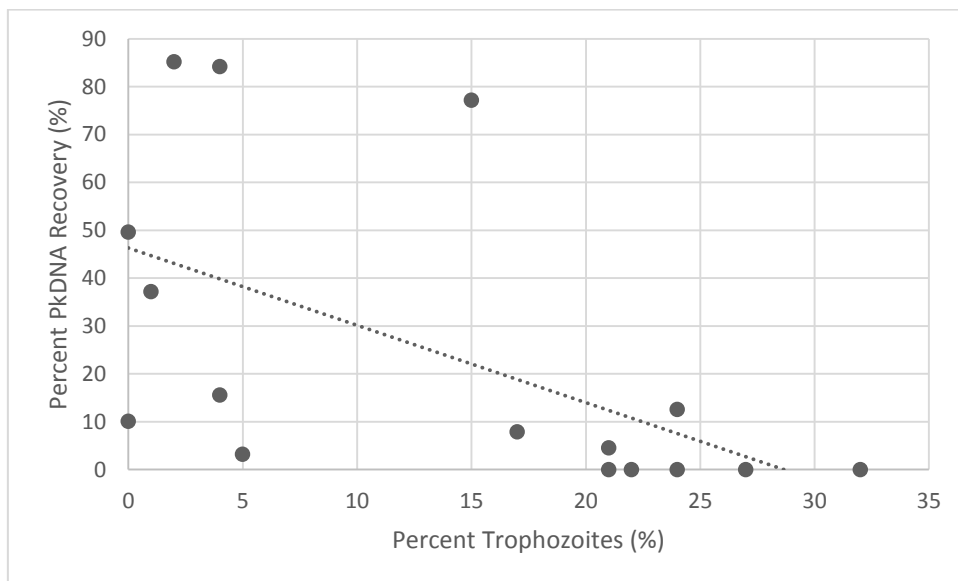
Name in Block Capitals

Signature

Date

Appendix C: PkDNA retrieval vs Trophozoite percentage

The percentage recovery of PkDNA was plotted against the percentage of Trophozoites (where available in patient data set) in each clinical sample processed. A negative correlation of - 0.56 was observed. However, all samples plotted that produced no material for a DNA extraction was assigned a 0% recovery of PkDNA.



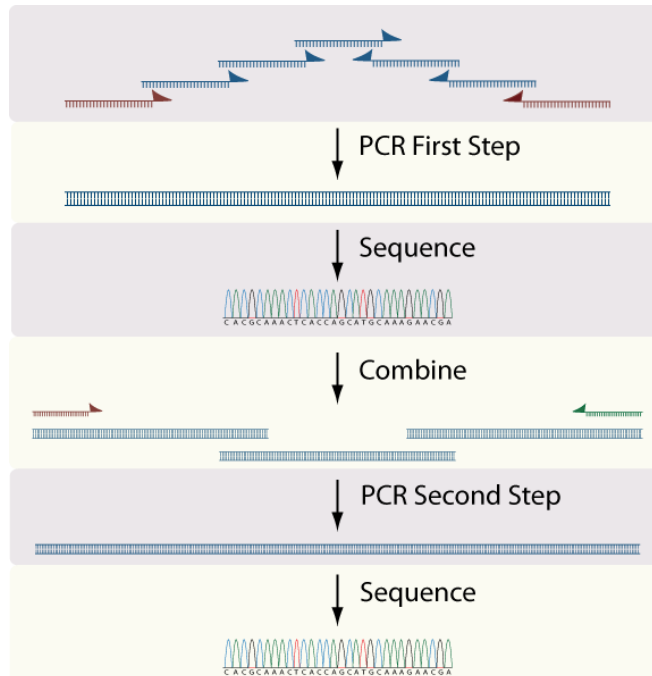
Appendix D: Amino Acids Defining Cluster 2 Type *Pknbpxa*

Amino acid locations and non-synonymous differences between cluster 1 type and cluster 2 type PkNBPXa protein.

AA position	Cluster 1 type	Cluster 2 type	AA position	Cluster 1 type	Cluster 2 type
12 *	G	A	1105	S	G
15 *	V	I	1109	V	M
67 *	S	F	1155	N	S
121 *	F	L	1156	Q	E
123 *	R	I	1174	M	T
125 *	A	G	1177	R	K
135 *	L	V	1184	Q	K
145 *	N	K	1199	L	F
146 *	M	V	1288	A	S
148 *	D	P	1298	E	G
150 *	T	V	1302	S	I
151 *	I	L	1374	A	V
153 *	G	N	1382	E	A
215	H	Y	1430	E	Q
219	D	A	1677	L	R
223	S	A	1729	M	K
238	S	P	1765	K	N
248	G	R	1805	A	E
260	G	D	1810	S	N
263	Q	E	1821	Q	K
318	D	A	1835	T	A
328	L	I	1838	F	Y
332	N	S	1923	S	N
335	S	T	2248	F	L
338	L	W	2279	N	K
369	M	I	2282	D	E
410	P	L	2289	K	N
571	N	K	2329	R	Q
722	Q	R	2597	A	E
1026	N	D	2694	D	G
1035	T	K	2695	A	D
1058	D	E	2757	K	R
1078	L	I			

*denotes that these sites were removed from further analysis, as this region was designed as the region of homology

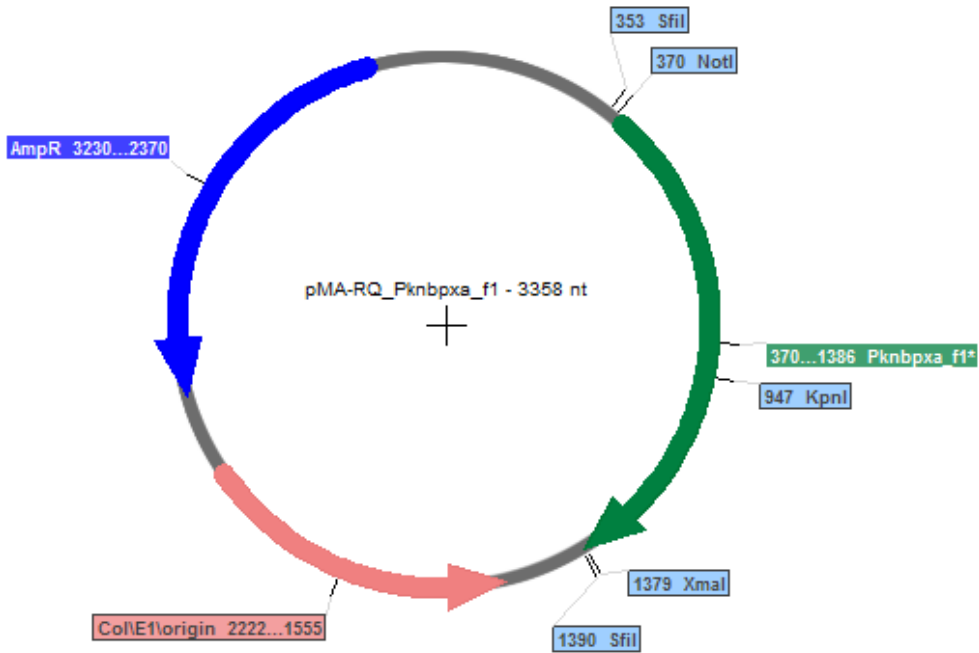
Appendix E: Synthetic *Pknbpxa* generation and validation



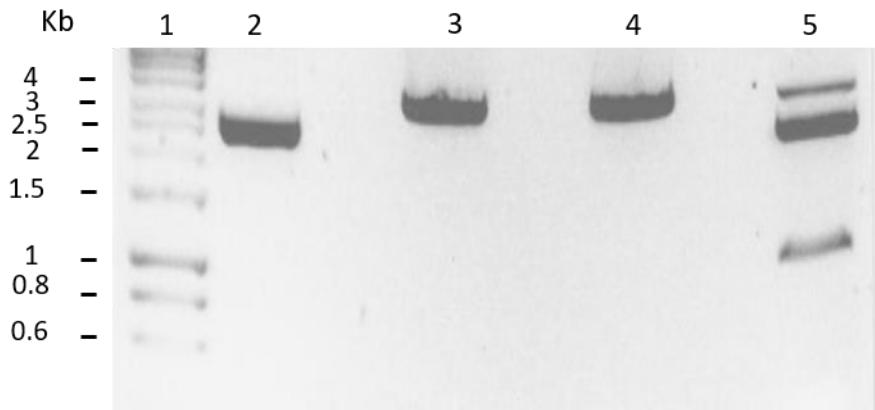
Schematic of gene synthesis (image adapted from IDT technologies; <http://www.idtdna.com/pages/decoded/decoded-articles/core-concepts/decoded/2012/09/21/assembly-pcr-for-novel-gene-synthesis>, (Last accessed 10/9/17))

pMA-RQ_Pknbpxa_f1 restriction digest with *NotI* and *XmaI*

pMA-RQ_Pknbpxa_f1 plasmid map



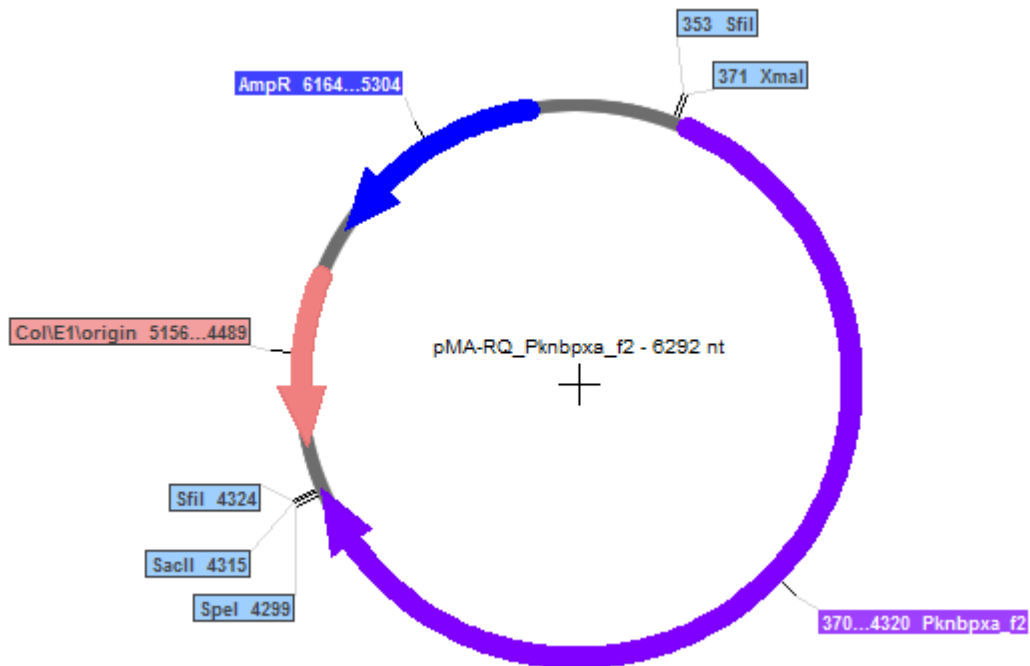
pMA-RQ_Pknbpxa_f1 restriction digest to isolate *Pknbpxa_f1*.



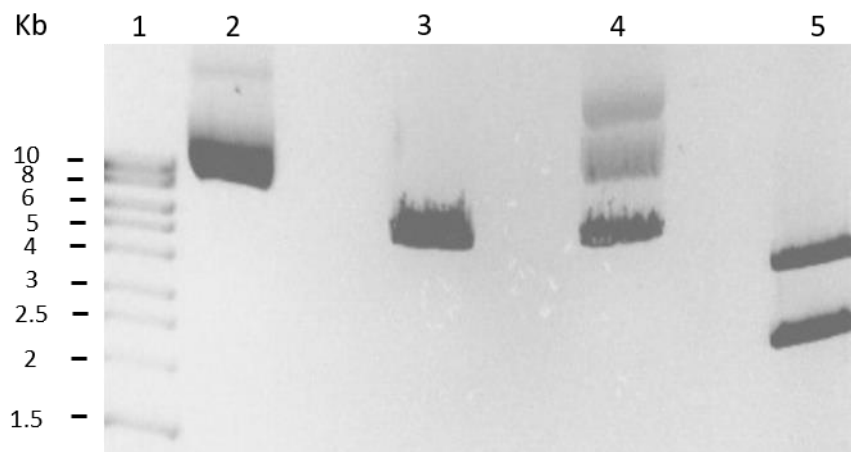
Lane 2 uncut pMA-RQ_Pknbpxa_f1, lane 3 digestion with *NotI*, lane 4 pMA-RQ_Pknbpxa_f1 digestion with *XmaI*, lane 5 double digest of pMA-RQ_Pknbpxa_f1 using *NotI* and *XmaI*. The two single digests (lanes 3 and 4) linearised the 3 kb plasmid, the double digest excised the 1 kb *Pknbpxa_f1* (lane5)

pMA-RQ_Pknbpxa_f2 restriction digest with XmaI and SacII

pMA-RQ_Pknbpxa_f2 plasmid map



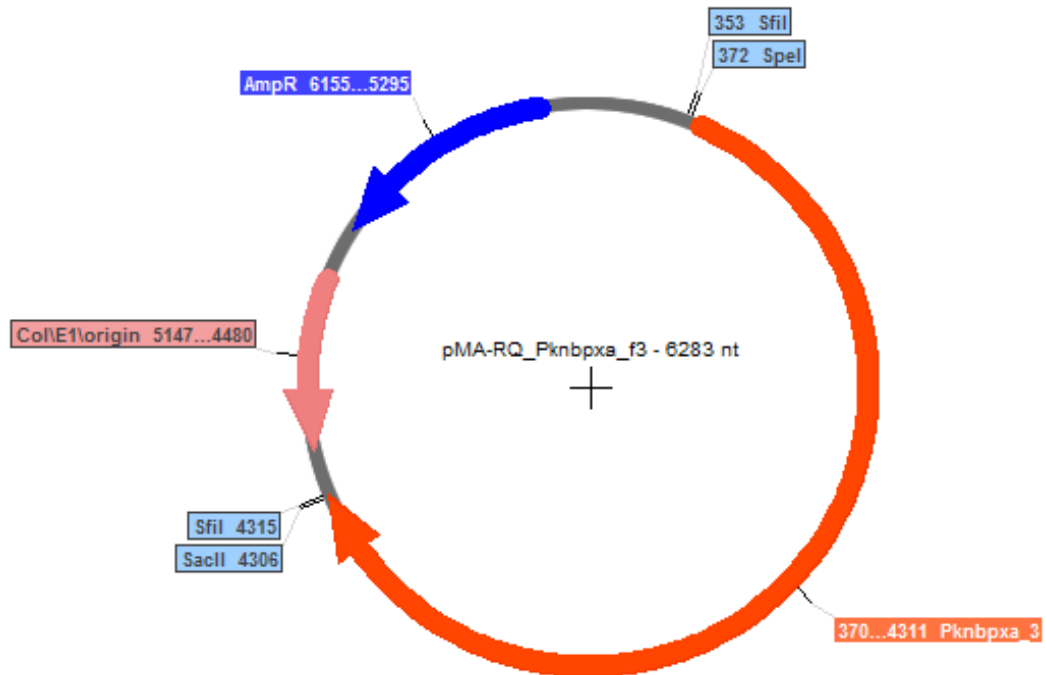
pMA-RQ_Pknbpxa_f2 restriction digest to isolate Pknbpxa_f2.



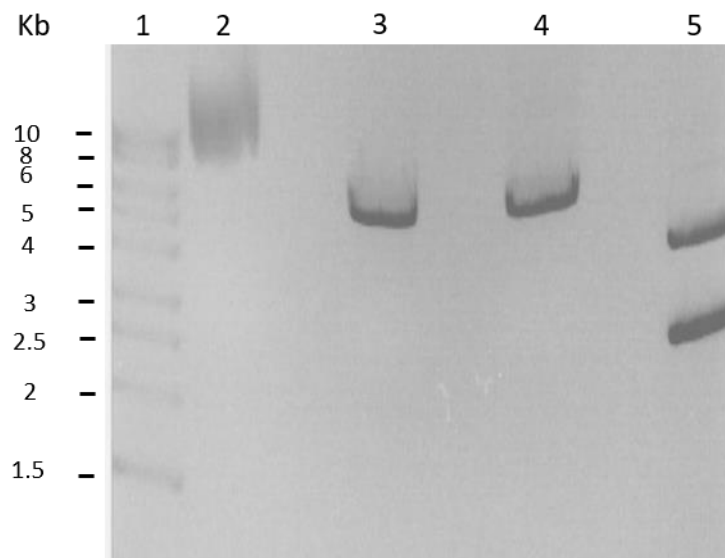
Lane 2 uncut pMA-RQ_Pknbpxa_f2, lane 3 digestion with XmaI, lane 4 pMA-RQ_Pknbpxa_f2 digestion with SacII, lane 5 double digest of pMA-RQ_Pknbpxa_f2 using XmaI and SacII. The two single digests (lanes 3 and 4) linearised the 6 kb plasmid, the double digest excised the 4 kb Pknbpxa_f2 (lane5)

pMA-RQ_*Pknbpxa_f3* restriction digest with *SpeI* and *SacII*

pMA-RQ_*Pknbpxa_f3* plasmid map



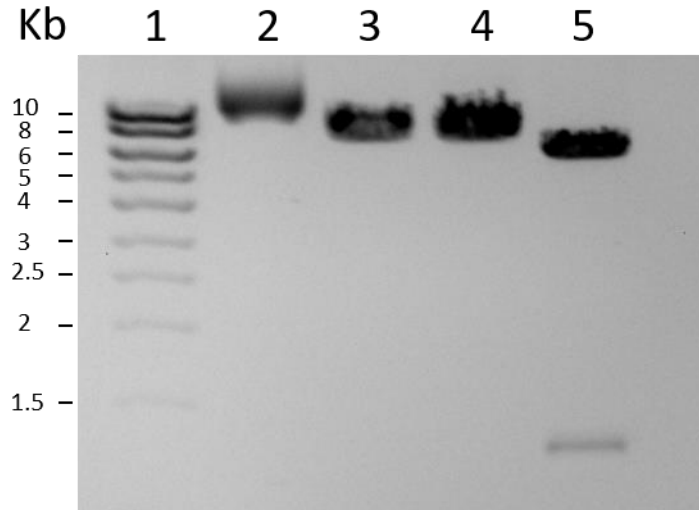
pMA-RQ_*Pknbpxa_f3* restriction digest to isolate *Pknbpxa_f3*.



Lane 2 uncut pMA-RQ_*Pknbpxa_f3*, lane 3 digestion with *SpeI*, lane 4 pMA-RQ_*Pknbpxa_f3* digestion with *SacII*, lane 5 double digest of pMA-RQ_*Pknbpxa_f3* using *SpeI* and *SacII*. The two single digests (lanes 3 and 4) linearised the 6 kb plasmid, the double digest excised the 4 kb *Pknbpxa_f3* (lane5)

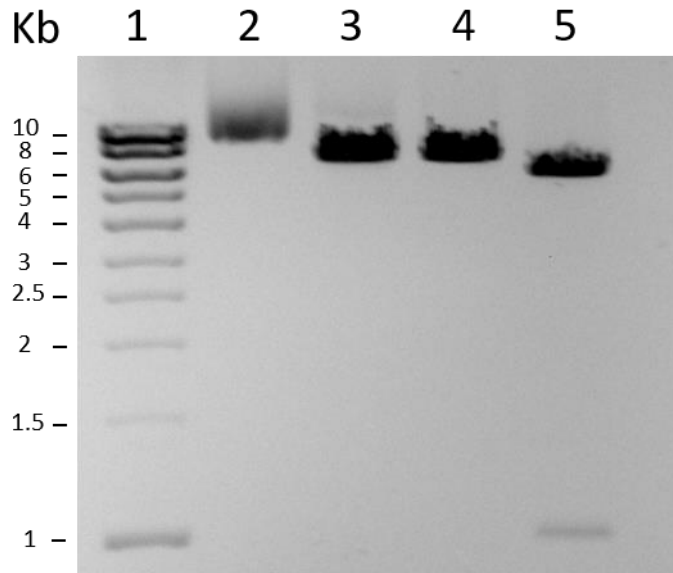
Appendix F: Cloning validation, Restriction digests and Sequencing results

Pk_{con}GFP restriction digest to remove PkHSP70 promoter.



Lane 2 uncut Pk_{con}GFP, lane 3 Pk_{con}GFP digestion with *NotI*, lane 4 Pk_{con}GFP digestion with *XmaI*, lane 5 double digest of Pk_{con}GFP using *NotI* and *XmaI*. The two single digests (lanes 3 and 4) linearised the 7.3 kb plasmid, the double digest excised the PkHSP70 promoter (lane5). The two single digests (lanes 3 and 4) linearised the 7.3 kb plasmid, the double digest excised the HSP70 promoter of 1.3 kb (lane5)

Pk_{con}GFP_ *Pknbpxa_f1* restriction digest to validate *Pknbpxa_f1* ligation.



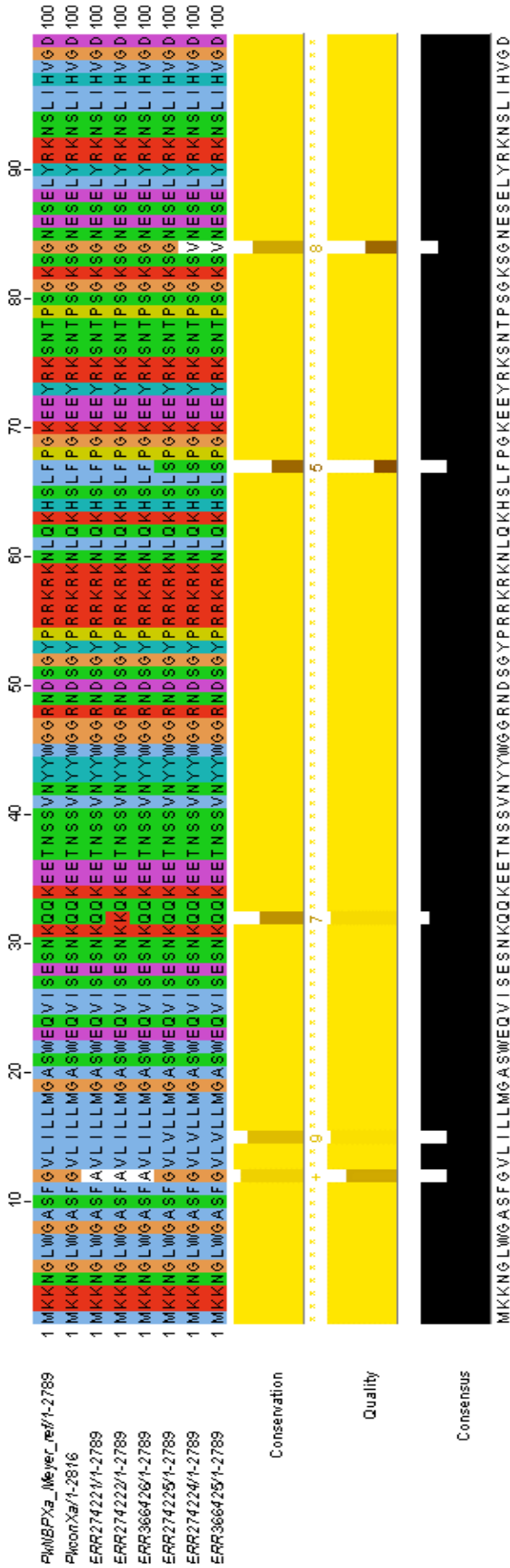
Lane 2 uncut Pk_{con}GFP_ *Pknbpxa_f1*, lane 3 Pk_{con}GFP_ *Pknbpxa_f1* digestion with *NotI*, lane 4 Pk_{con}GFP_ *Pknbpxa_f1* digestion with *XmaI*, lane 5 double digest of Pk_{con}GFP_ *Pknbpxa_f1* using *NotI* and *XmaI*. The two single digests (lanes 3 and 4) linearised the 7.3 kb plasmid, the double digest excised the *Pknbpxa_f1* fragment of 1 kb (lane5)

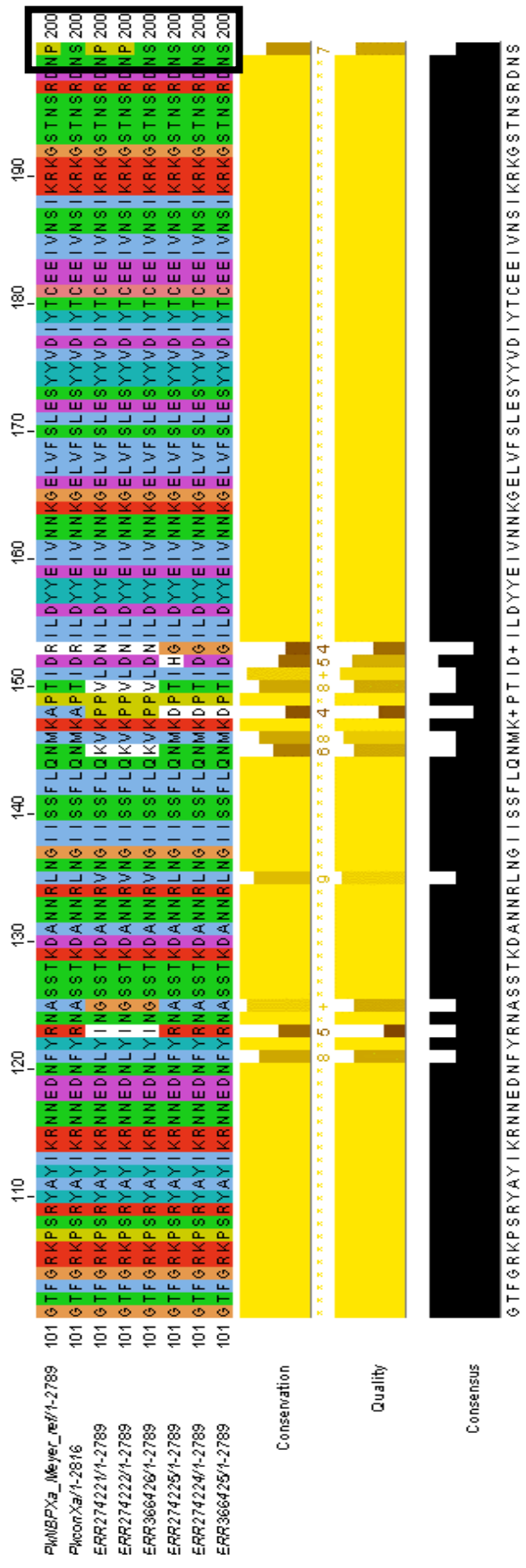

```
Seq_1  841  AAAATAACAGCGAAAACGCC  860
        |||
Seq_2  841  AAAATAACAGCGAAAACGCC  860
```


Seq_1	361	AGCGAAGAAAACTGGCCAAATGTAAAAGCGAAAGCCCGATTGATGAAAAAGCCTATATT	420
Seq_2	361	AGCGAAGAAAACTGGCCAAATGTAAAAGCGAAAGCCCGATTGATGAAAAAGCCTATATT	420
Seq_1	421	CTGAACAACGAAAAAAGCAAACCGCCTATATGAACGTGAAACTGAATCTGGAAGTGGTG	480
Seq_2	421	CTGAACAACGAAAAAAGCAAACCGCCTATATGAACGTGAAACTGAATCTGGAAGTGGTG	480
Seq_1	481	GAAAGCAATCTGCGTCAGATCGAAAATGTAAAGAAAGCATGAACAACATCCTGGAAAAA	540
Seq_2	481	GAAAGCAATCTGCGTCAGATCGAAAATGTAAAGAAAGCATGAACAACATCCTGGAAAAA	540
Seq_1	541	TCCACCAATCTGAAAAACAGCATTCTGGGTGCAAGCATCATTGAAAATAACAATAGCGTG	600
Seq_2	541	TCCACCAATCTGAAAAACAGCATTCTGGGTGCAAGCATCATTGAAAATAACAATAGCGTG	600
Seq_1	601	GATGTGCTGAAAAAAGAAGAGGTGCATTATATGCAGTACCTGAAAAATATCGAGAACGAG	660
Seq_2	601	GATGTGCTGAAAAAAGAAGAGGTGCATTATATGCAGTACCTGAAAAATATCGAGAACGAG	660
Seq_1	661	AAAAACGCATGATGGACGAAAAATCGAATGTGGATGTGATCCATGATAACGTCTGAAA	720
Seq_2	661	AAAAACGCATGATGGACGAAAAATCGAATGTGGATGTGATCCATGATAACGTCTGAAA	720

Seq_1	361	AATTATGAACATTTTATTTTTGTTTCAGAAAAAAAAAACTTTACACACATAAAAATGGCTA	420
Seq_2	361	AATTATGAACATTTTATTTTTGTTTCAGAAAAAAAAAACTTTACACACATAAAAATGGCTA	420
Seq_1	421	GTATGAATAGCCATATTTTATATAAAATTAATCCTATGAATTTATGACCATATTA AAAAT	480
Seq_2	421	GTATGAATAGCCATATTTTATATAAAATTAATCCTATGAATTTATGACCATATTA AAAAT	480
Seq_1	481	TTAGATATTTATGGAACATAATATGTTTGAAACAATAAGACAAAATTATTATTATTATTA	540
Seq_2	481	TTAGATATTTATGGAACATAATATGTTTGAAACAATAAGACAAAATTATTATTATTATTA	540
Seq_1	541	TTATTTTACTGTTATAAATTATGTTGTCT-CTTCAATGATTCATAAATAGTTGGACTTGA	599
Seq_2	541	TTATTTTACTGTTATAAATTATGT-GTCTCCTTCAATGATTCATAAATAGTTGGACTTGA	599
Seq_1	600	TTTTTAAAATGTTTATAAATATGATTAGCATAGTTAAATAAAAAAAGTTGAAAAATTA AAA	659
Seq_2	600	TTTTTAAAATGTTTATAAATATGATTAGCATAGTTAAATAAAAAAAGTTGAAAAATTA AAA	659
Seq_1	660	AAAAACATATAAACACAAATGATGTTTTTTCCTTCAATTCGATATCATATAGC	713
Seq_2	660	AAAAACATATAAACACAAATGATGTTTTTTCCTTCAATTCGATATCATATAGC	713

Appendix G: Alignment of PkNBPXa clinical sequences





P1N8P2a_Meyer_ref/1-2789 201 GDEDPEKGGDKDNNHNSGDKEDSMIKKLYDMMELLRMSCFSIKSELDGKINSLEYADTEGNEQVSGTSSKTYKLI EDEYVNC LKNNSENAKMIISNTMK 300
 P1N8P2a_Meyer_ref/1-2816 201 GDDPEKGGDKDNNYNSGAKEDAMIKKLYDMMELLRMPCFSIKSELDQRKINSLEYADTEDEEEVSGTSSKTYKLI EDEYVNC LKNNSENAKMIISNTMK 300
 ERR2742241-2789 201 GDDPEKGGDKDNNYNSGAKEDAMIKKLYDMMELLRMPCFSIKSELDQRKINSLEYADTEDEEEVSGTSSKTYKLI EDEYVNC LKNNSENAKMIISNTMK 300
 ERR2742241-2789 201 GDDPEKGGDKDNNYNSGAKEDAMIKKLYDMMELLRMPCFSIKSELDQRKINSLEYADTEDEEEVSGTSSKTYKLI EDEYVNC LKNNSENAKMIISNTMK 300
 ERR3664261-2789 201 GDDPEKGGDKDNNYNSGAKEDAMIKKLYDMMELLRMPCFSIKSELDQRKINSLEYADTEDEEEVSGTSSKTYKLI EDEYVNC LKNNSENAKMIISNTMK 300
 ERR2742251-2789 201 GDDPEKGGDKDNNHNSGDKEDSMIKKLYDMMELLRMSCFSIKSELDGKINSLEYADTEGNEQVSGTSSKTYKLI EDEYVNC LKNNSENAKMIISNTMK 300
 ERR2742241-2789 201 GDDPEKGGDKDNNHNSGDKEDSMIKKLYDMMELLRMSCFSIKSELDGKINSLEYADTEGNEQVSGTSSKTYKLI EDEYVNC LKNNSENAKMIISNTMK 300
 ERR3664251-2789 201 GDDPEKGGDKDNNHNSGDKEDSMIKKLYDMMELLRMSCFSIKSELDGKINSLEYADTEGNEQVSGTSSKTYKLI EDEYVNC LKNNSENAKMIISNTMK 300

Conservation

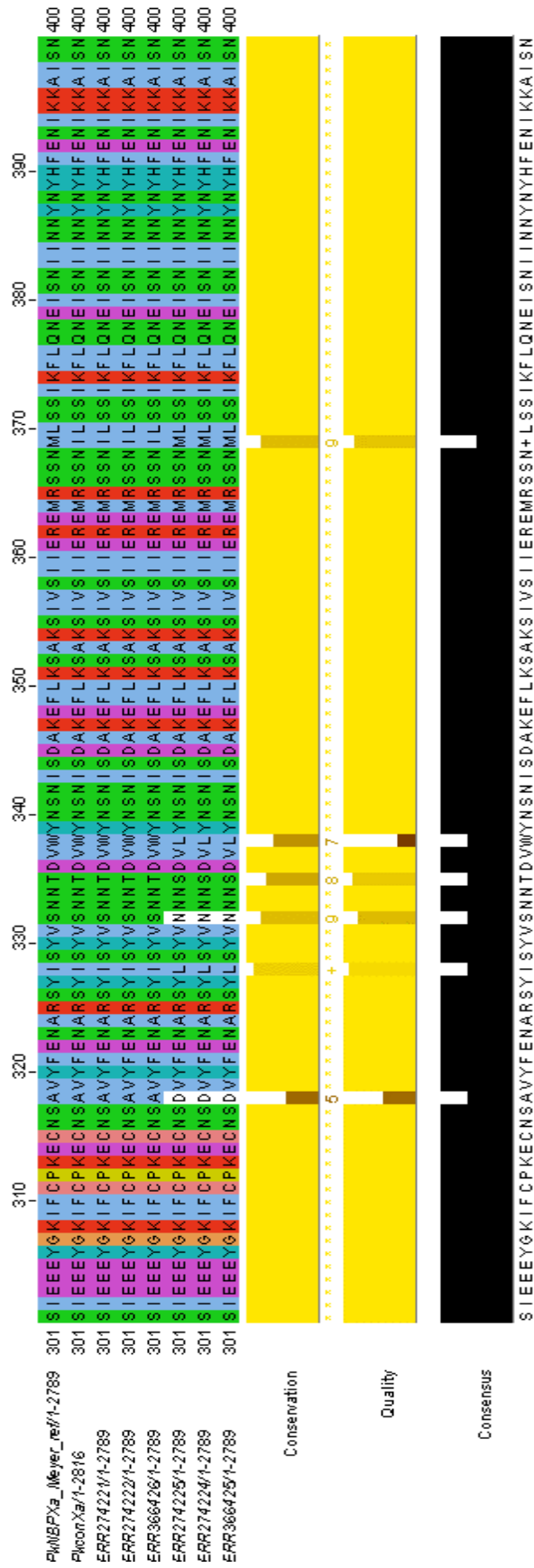


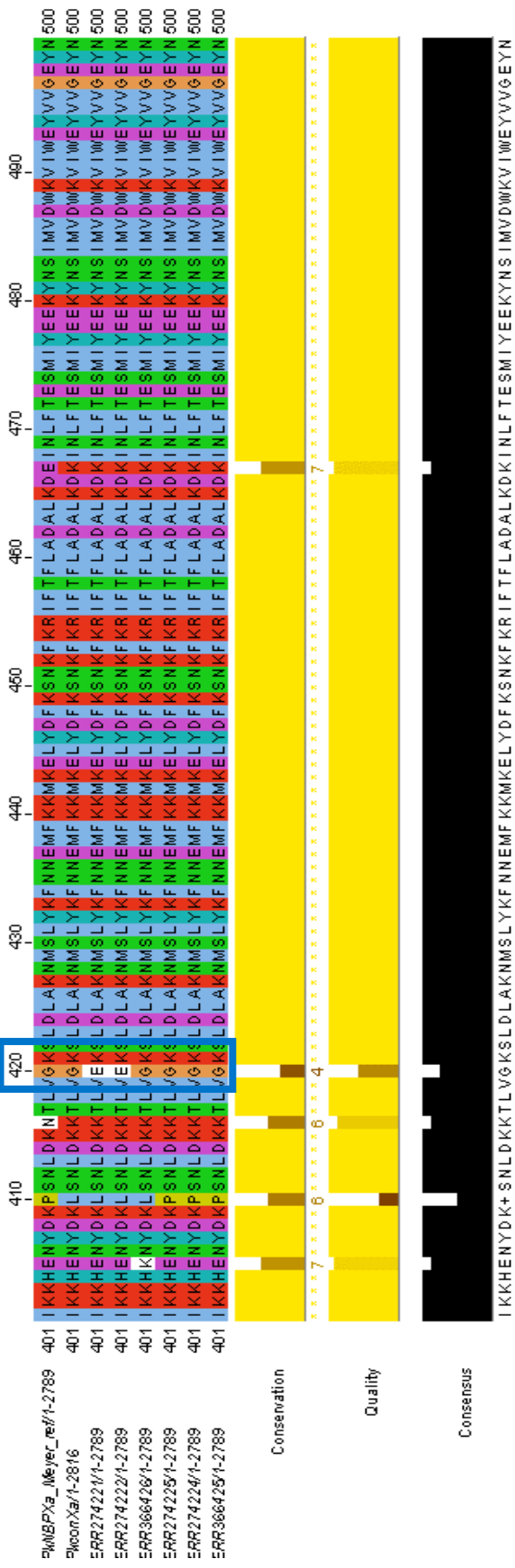
Quality

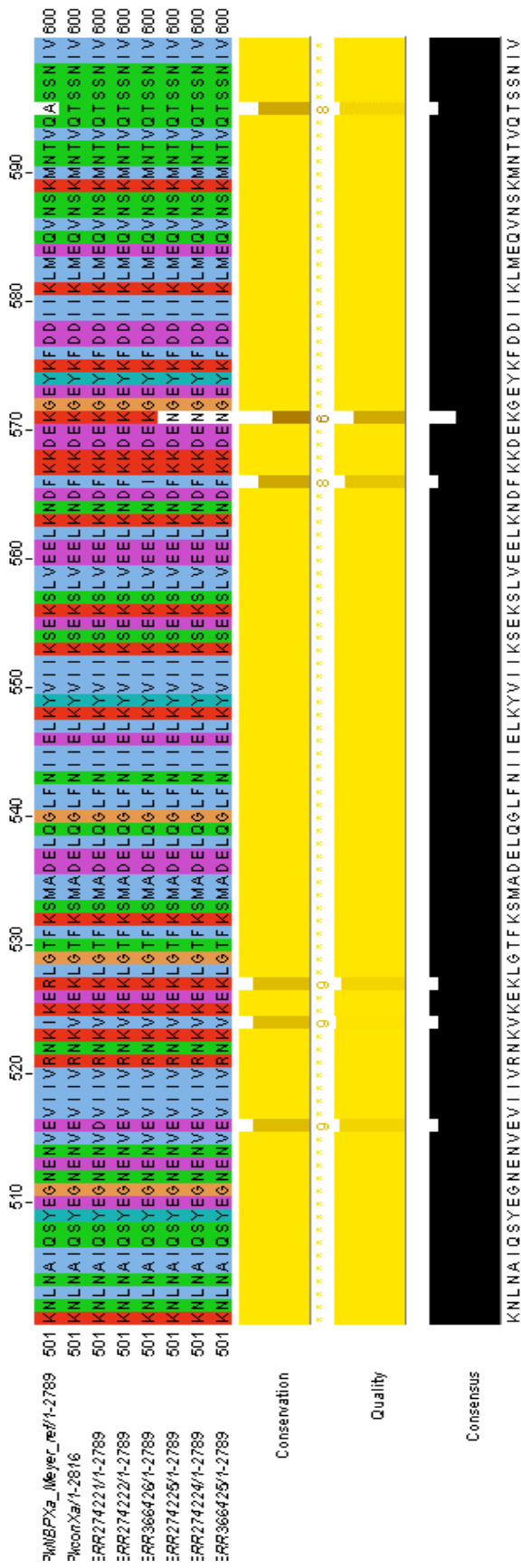


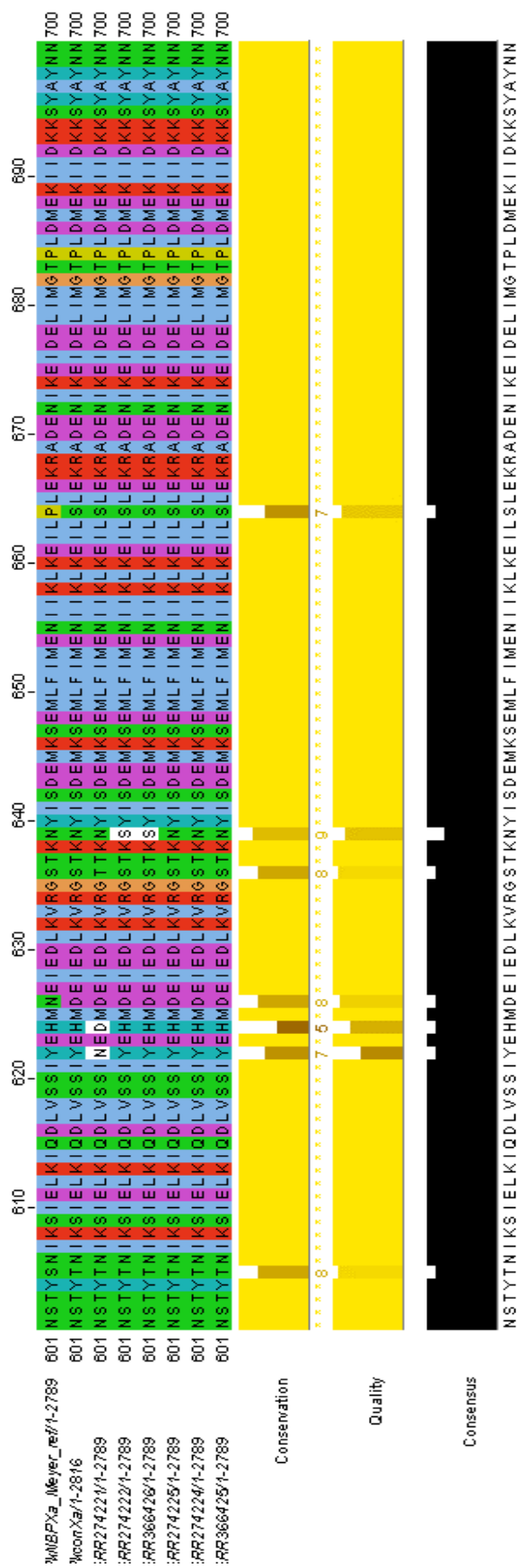
Consensus

GDDDPEKGGDKDNN+NSG+KED+MIKKLYDMMELLRM+CFSIKSELDGKINSLEYADTE+NE+VSGTSSKTYKLI EDEYVNC LKNNSENAKMIISNTMK











P1NBPXa_I_Meyer_ref/1-2789 801 DLKSVYDKLKVSIAEYTAEKRAIEEDRAVILKREEEFFGKVVYDKDDMLDVKDAYTNFLKHKDNFFKRNNDVKEALKVVRI NFLYYISMPEKY 900
 P1conXa/1-2816 801 DLKSVYDKLKVSIAEYTAEKRAIEEDRAVILKREEEFFGKVVYDKDDMLDVKDAYTNFLKHKDNFFKRNNDVKEALKVVRI NFLYYISMPEKY 900
 ERR274221/1-2789 801 DLKSVYDKLKVSIAEYTAEKRAIEEDRAVILKREEEFFGKVVYDKDDMLDVKDAYTNFLKHKDNFFKRNNDVKEALKVVRI NFLYYISMPEKY 900
 ERR274222/1-2789 801 DLKSVYDKLKVSIAEYTAEKRAIEEDRAVILKREEEFFGKVVYDKDDMLDVKDAYTNFLKHKDNFFKRNNDVKEALKVVRI NFLYYISMPEKY 900
 ERR366426/1-2789 801 DLKSVYDKLKVSIAEYTAEKRAIEEDRAVILKREEEFFGKVVYDKDDMLDVKDAYTNFLKHKDNFFKRNNDVKEALKVVRI NFLYYISMPEKY 900
 ERR274225/1-2789 801 DLKSVYDKLKVSIAEYTAEKRAIEEDRAVILKREEEFFGKVVYDKDDMLDVKDAYTNFLKHKDNFFKRNNDVKEALKVVRI NFLYYISMPEKY 900
 ERR274224/1-2789 801 DLKSVYDKLKVSIAEYTAEKRAIEEDRAVILKREEEFFGKVVYDKDDMLDVKDAYTNFLKHKDNFFKRNNDVKEALKVVRI NFLYYISMPEKY 900
 ERR366425/1-2789 801 DLKSVYDKLKVSIAEYTAEKRAIEEDRAVILKREEEFFGKVVYDKDDMLDVKDAYTNFLKHKDNFFKRNNDVKEALKVVRI NFLYYISMPEKY 900



Conservation

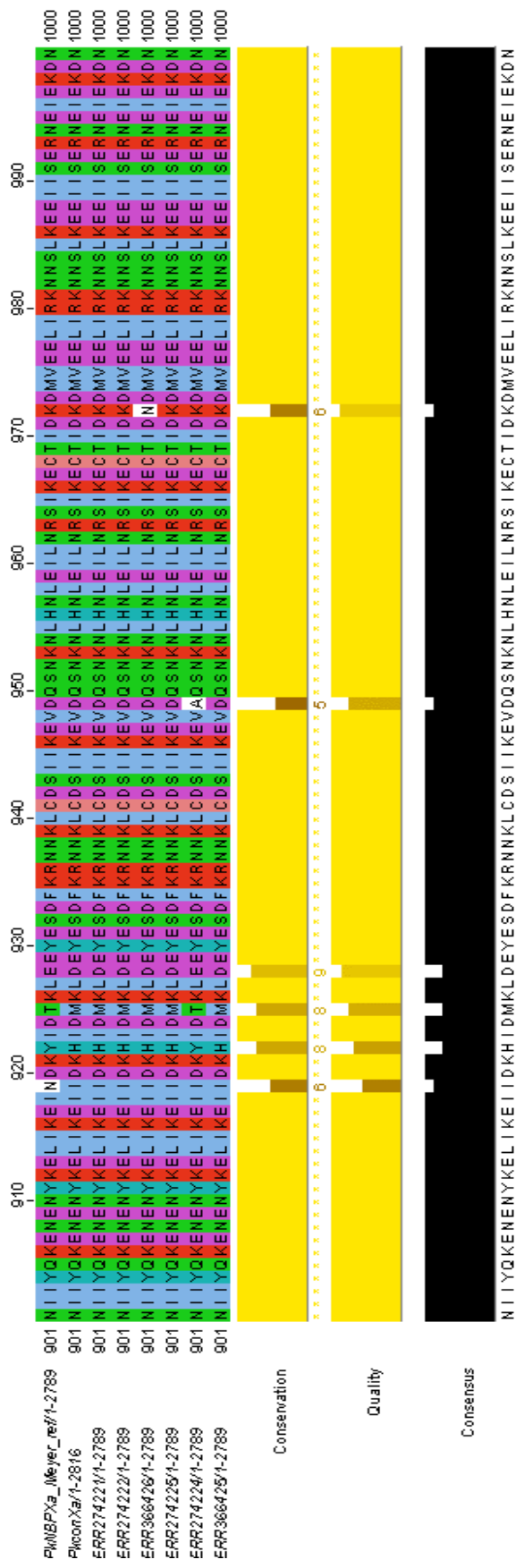


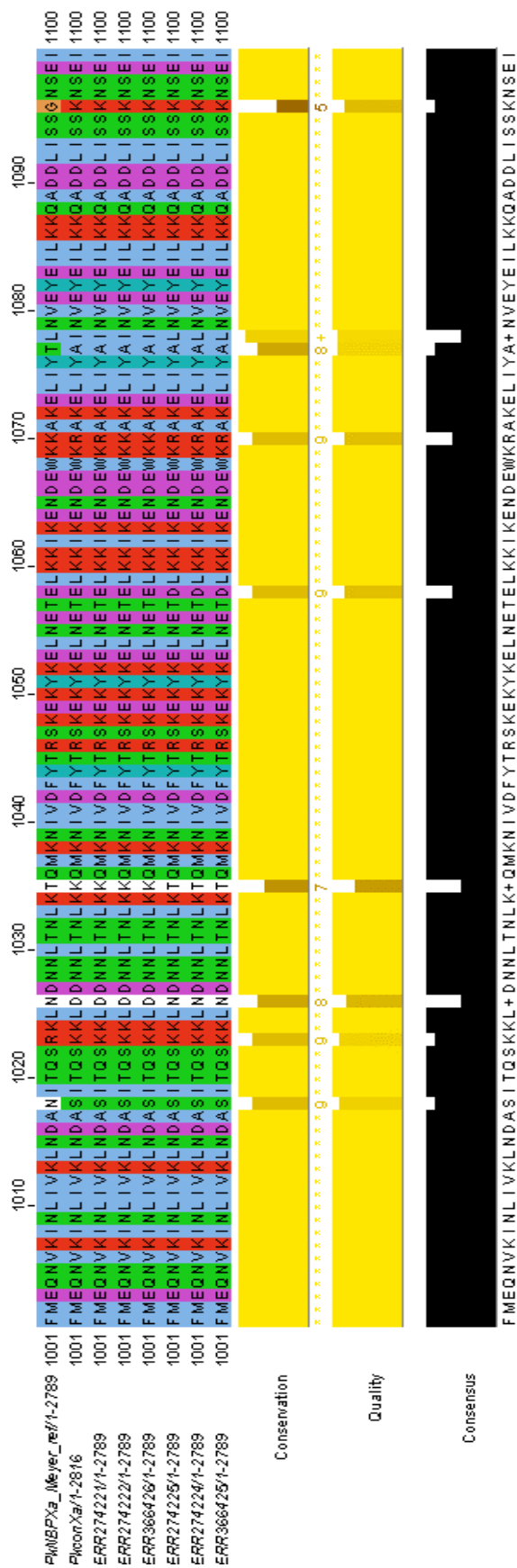
Quality

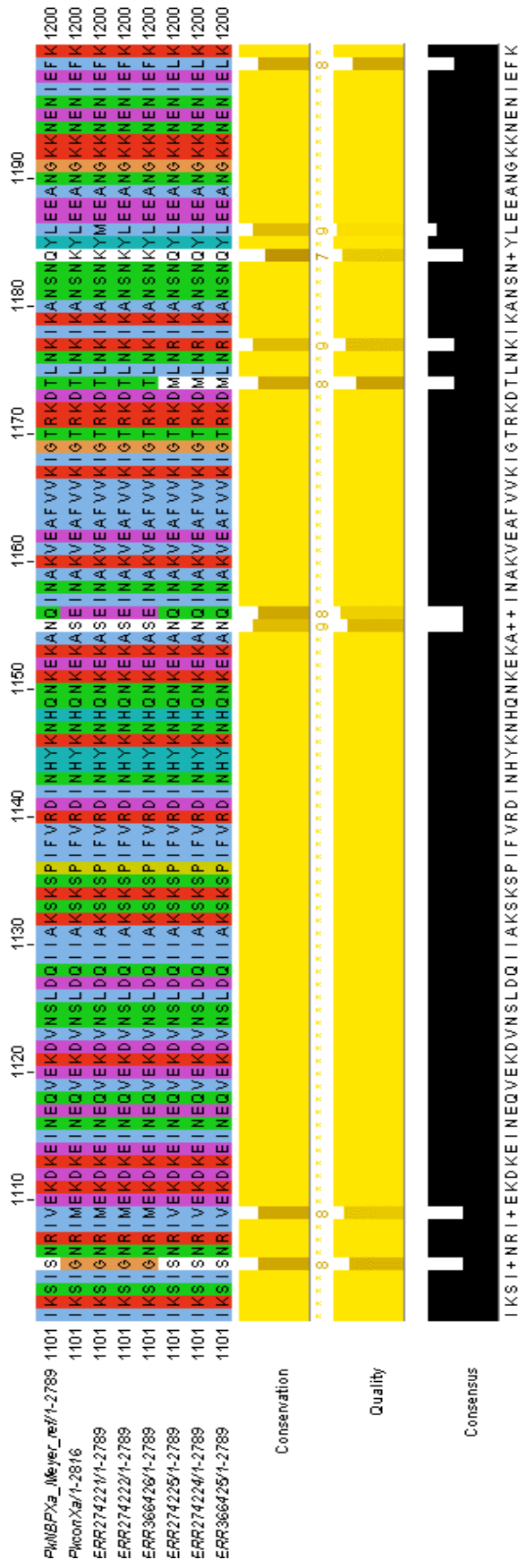


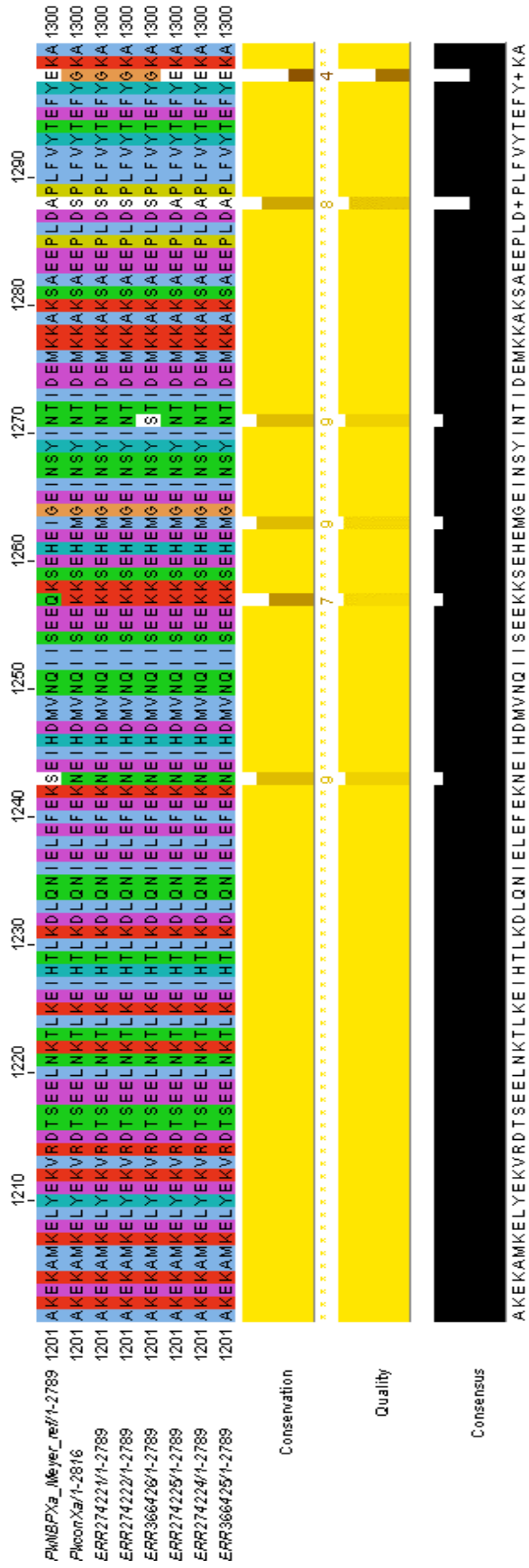
Consensus

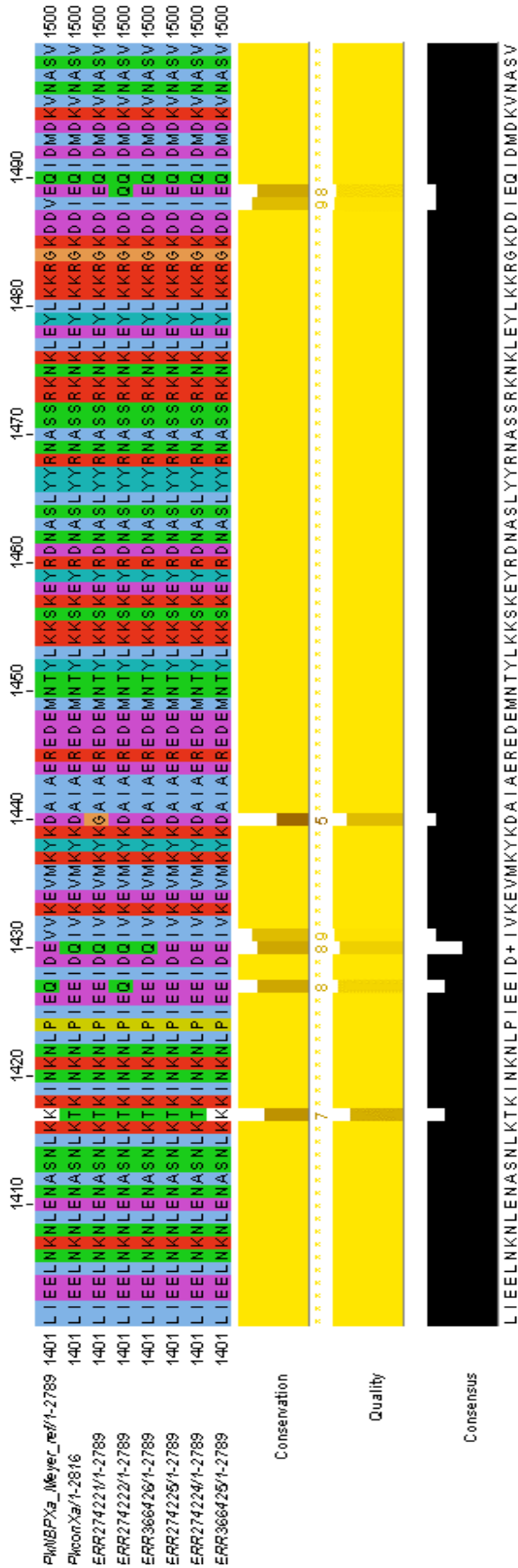
DLKSVYDKLKVSIAEYTAEKRAIEEDRAVILKREEEFFGKVVYDKDDMLDVKDAYTNFLKHKDNFFKRNNDVKEALKVVRI NFLYYISMPEKY
 DLKSVYDKLKVSIAEYTAEKRAIEEDRAVILKREEEFFGKVVYDKDDMLDVKDAYTNFLKHKDNFFKRNNDVKEALKVVRI NFLYYISMPEKY
 DLKSVYDKLKVSIAEYTAEKRAIEEDRAVILKREEEFFGKVVYDKDDMLDVKDAYTNFLKHKDNFFKRNNDVKEALKVVRI NFLYYISMPEKY
 DLKSVYDKLKVSIAEYTAEKRAIEEDRAVILKREEEFFGKVVYDKDDMLDVKDAYTNFLKHKDNFFKRNNDVKEALKVVRI NFLYYISMPEKY
 DLKSVYDKLKVSIAEYTAEKRAIEEDRAVILKREEEFFGKVVYDKDDMLDVKDAYTNFLKHKDNFFKRNNDVKEALKVVRI NFLYYISMPEKY
 DLKSVYDKLKVSIAEYTAEKRAIEEDRAVILKREEEFFGKVVYDKDDMLDVKDAYTNFLKHKDNFFKRNNDVKEALKVVRI NFLYYISMPEKY
 DLKSVYDKLKVSIAEYTAEKRAIEEDRAVILKREEEFFGKVVYDKDDMLDVKDAYTNFLKHKDNFFKRNNDVKEALKVVRI NFLYYISMPEKY

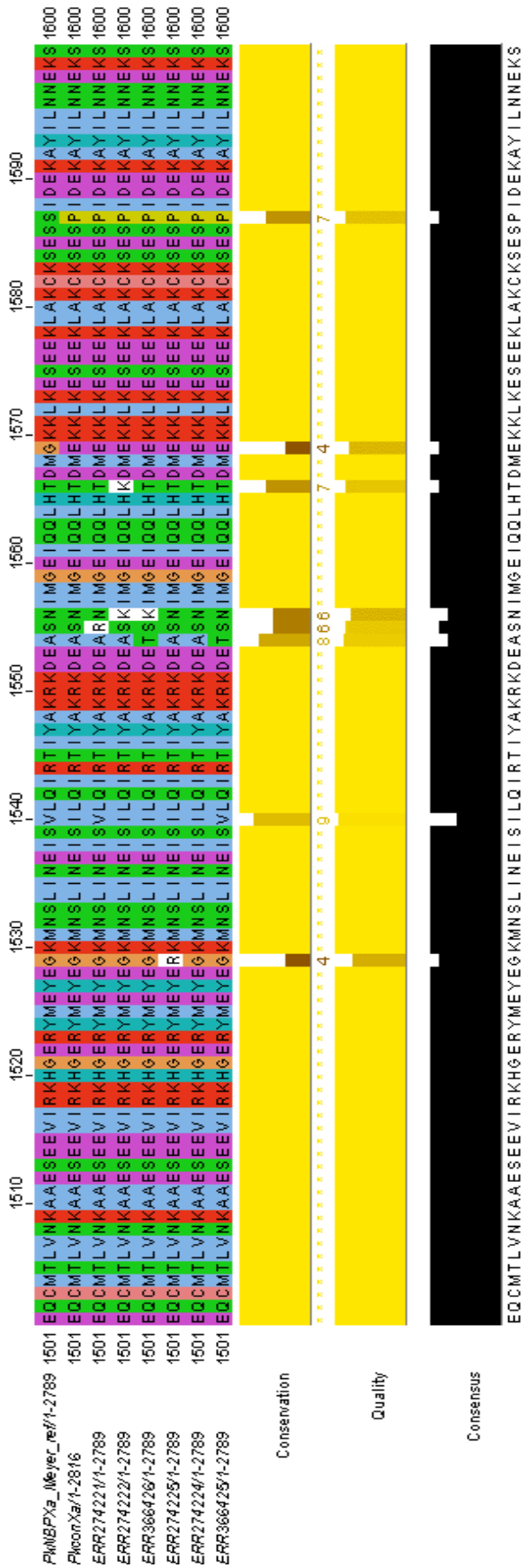


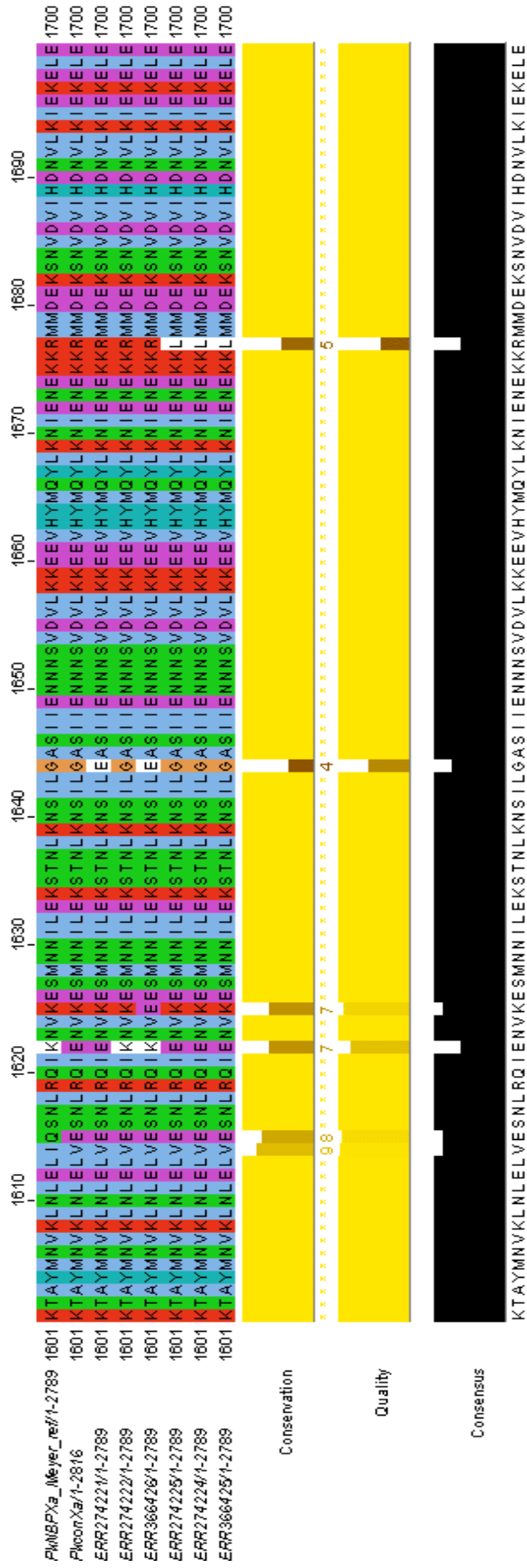


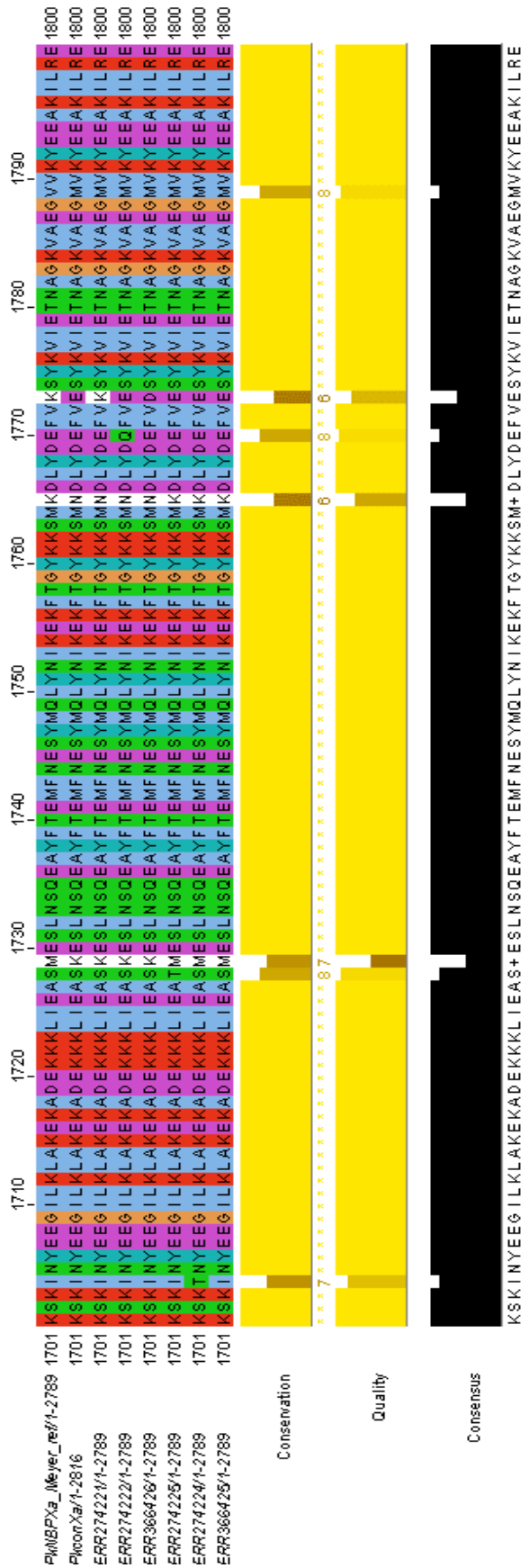


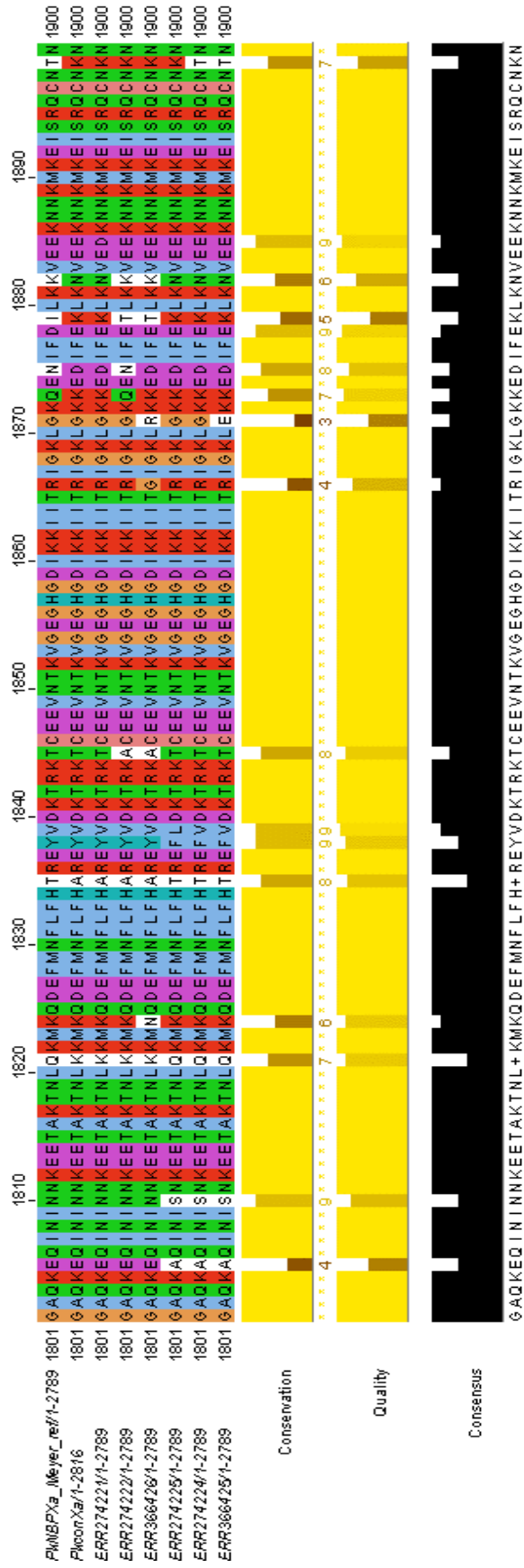


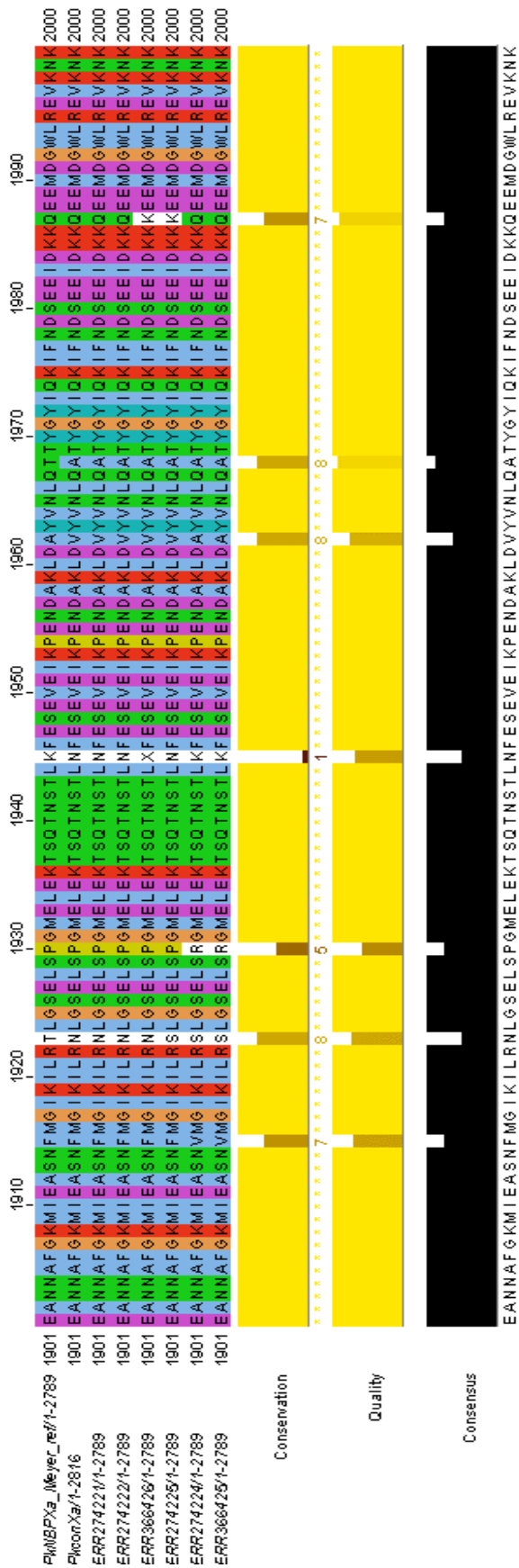


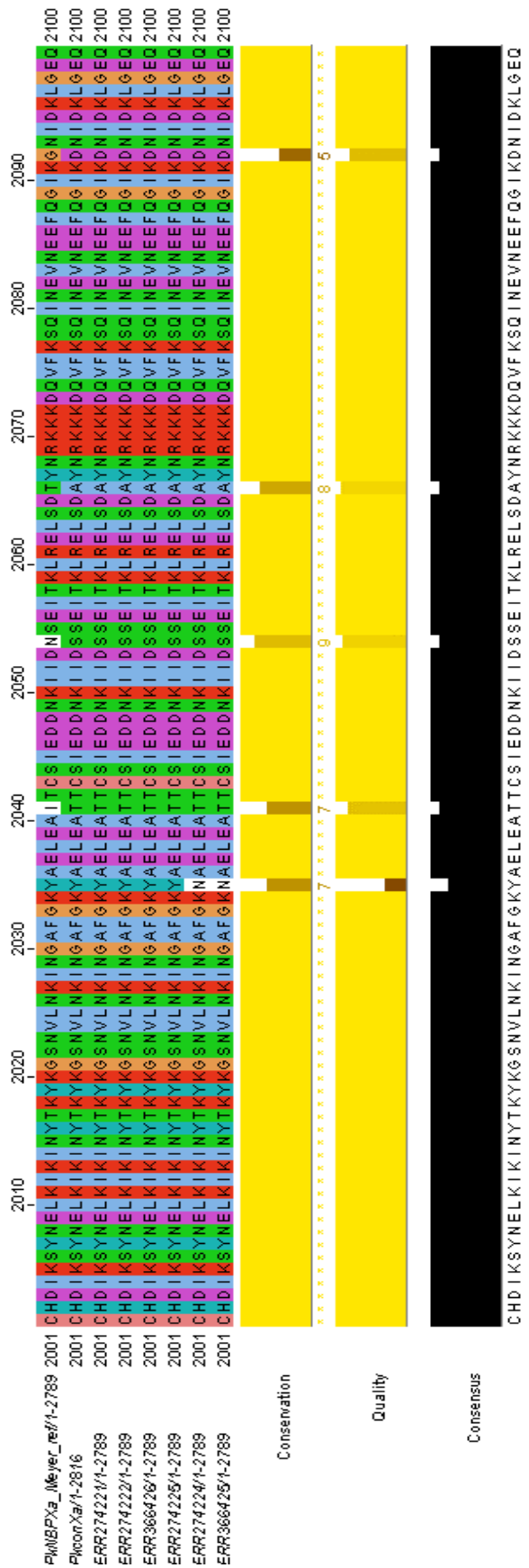


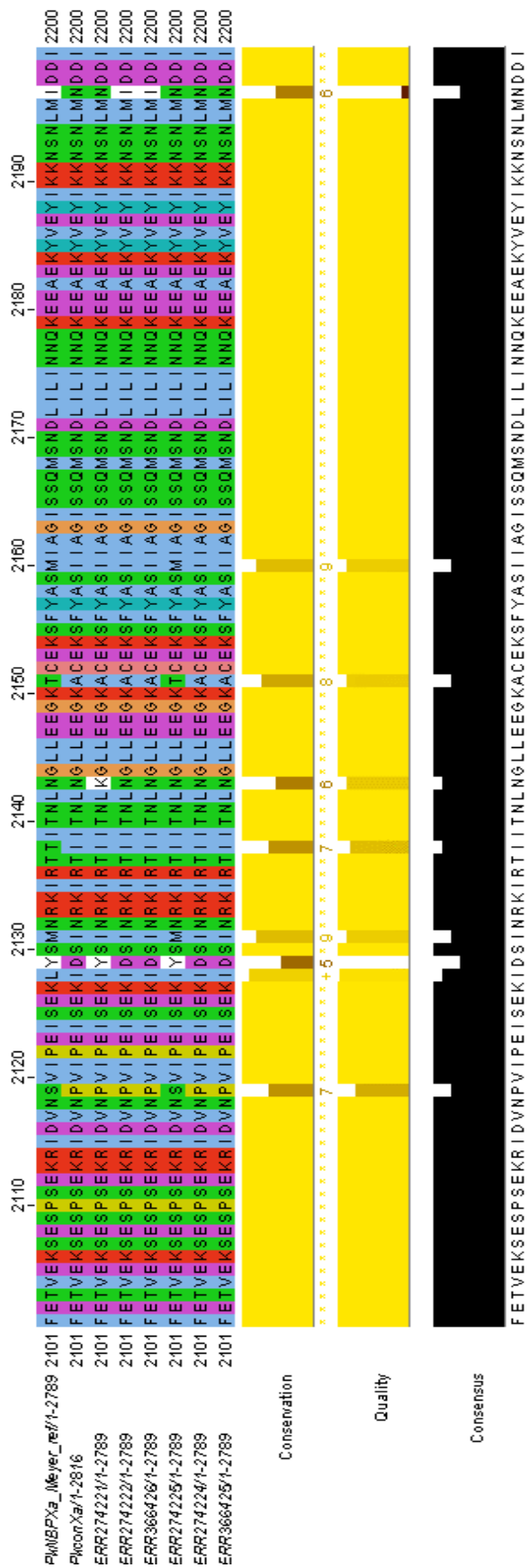


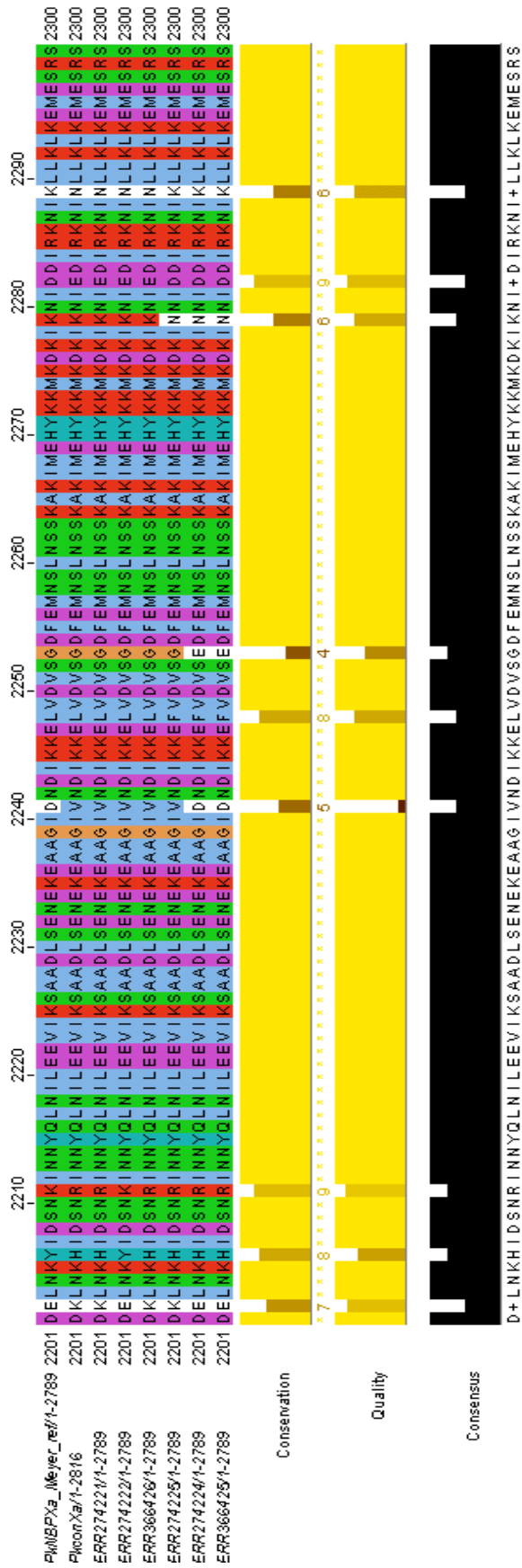


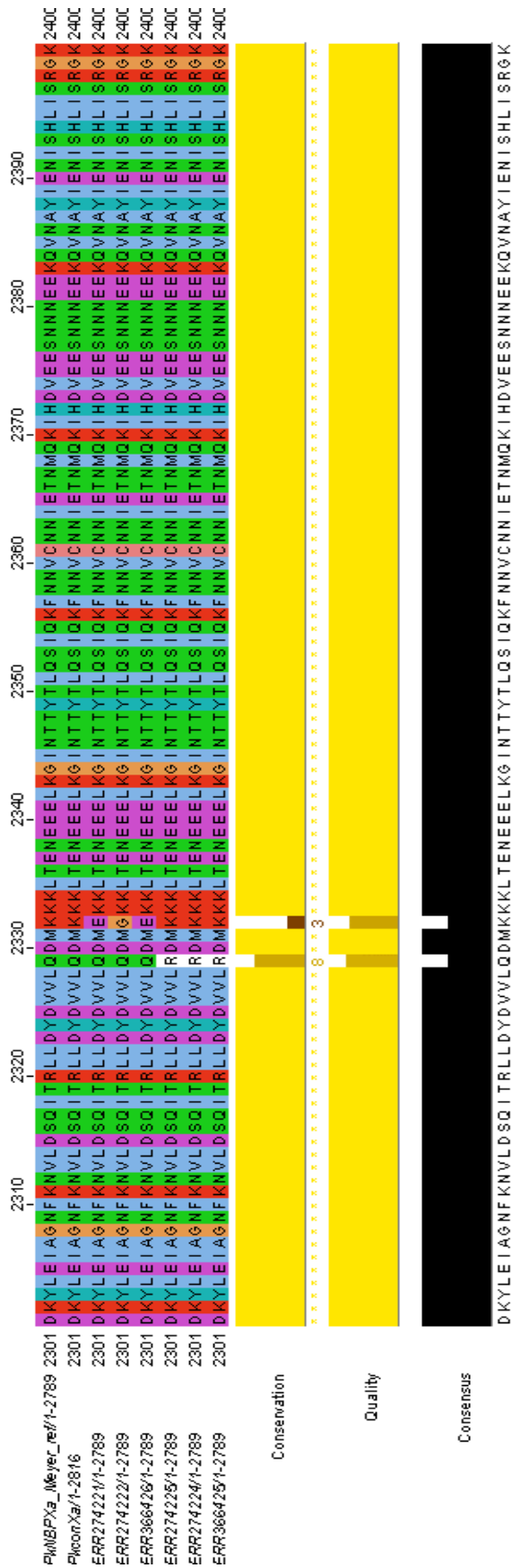


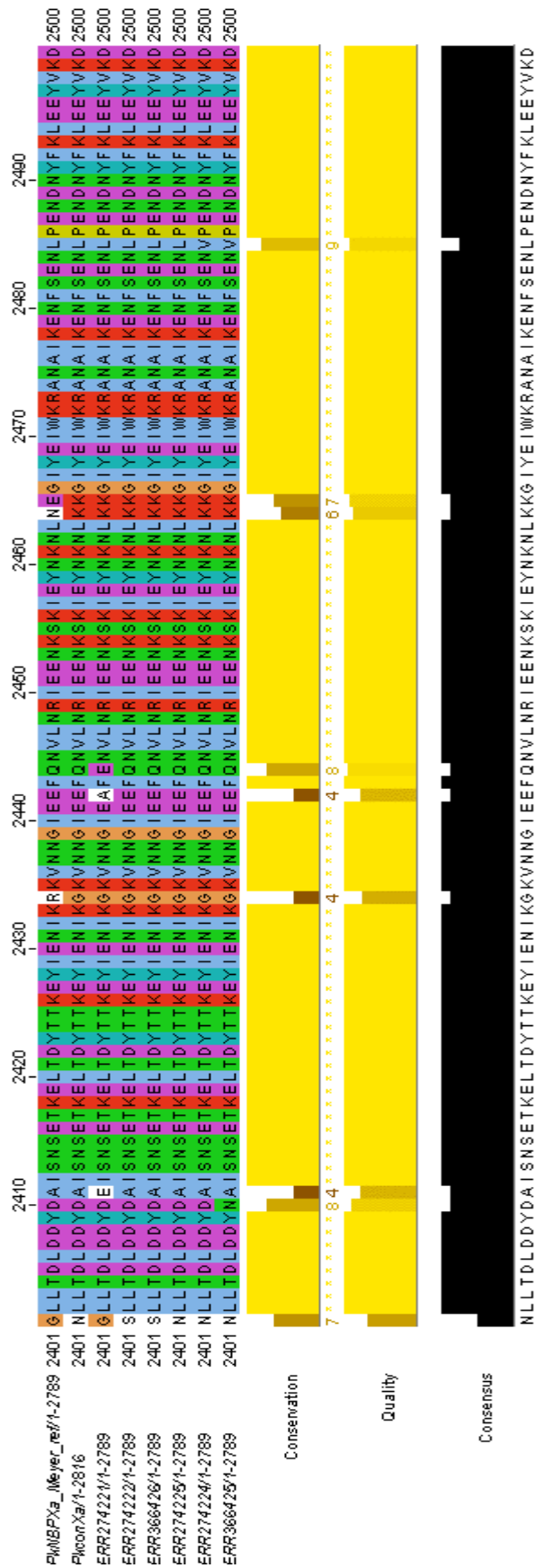


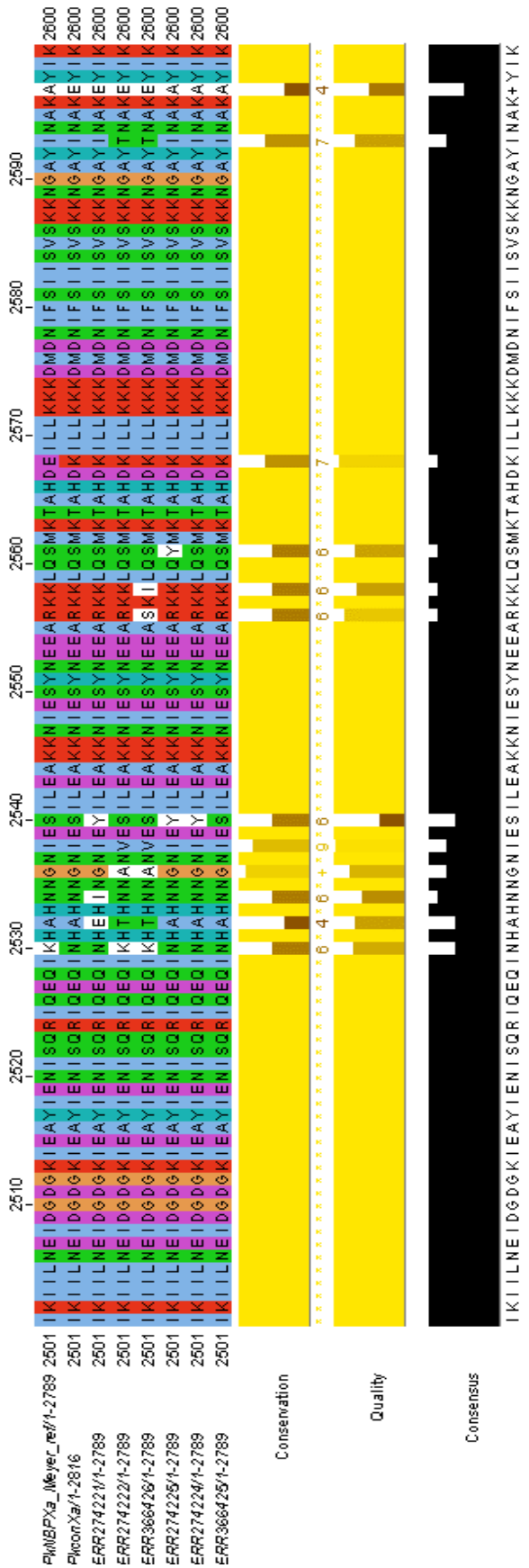


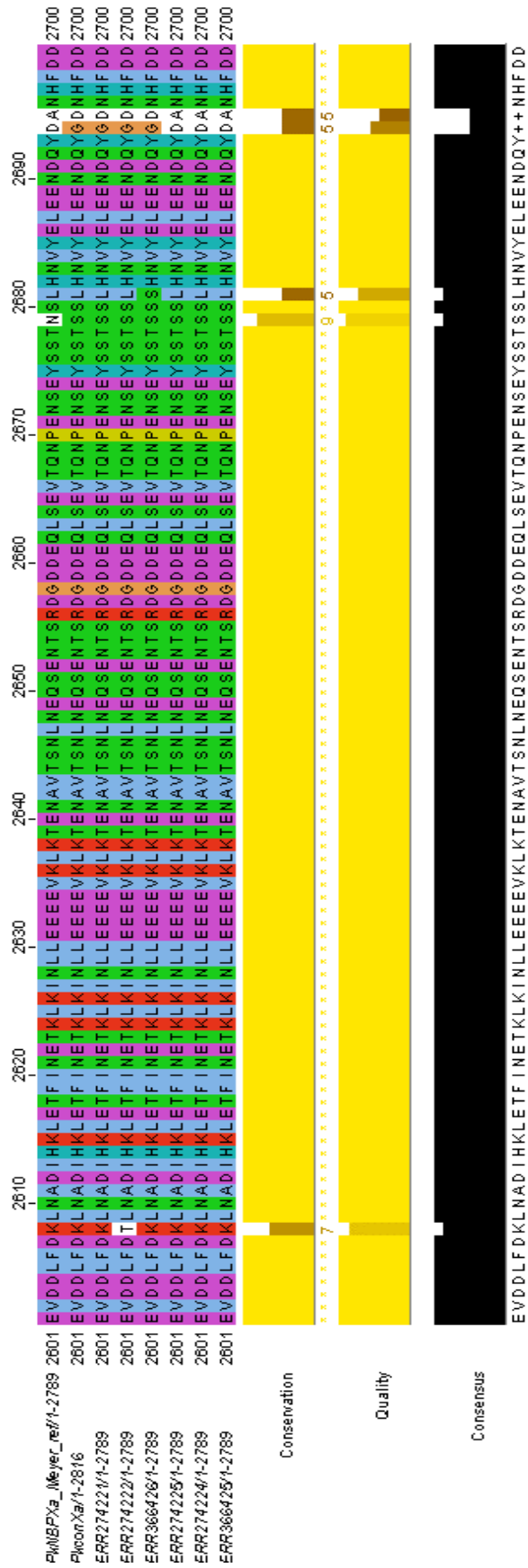


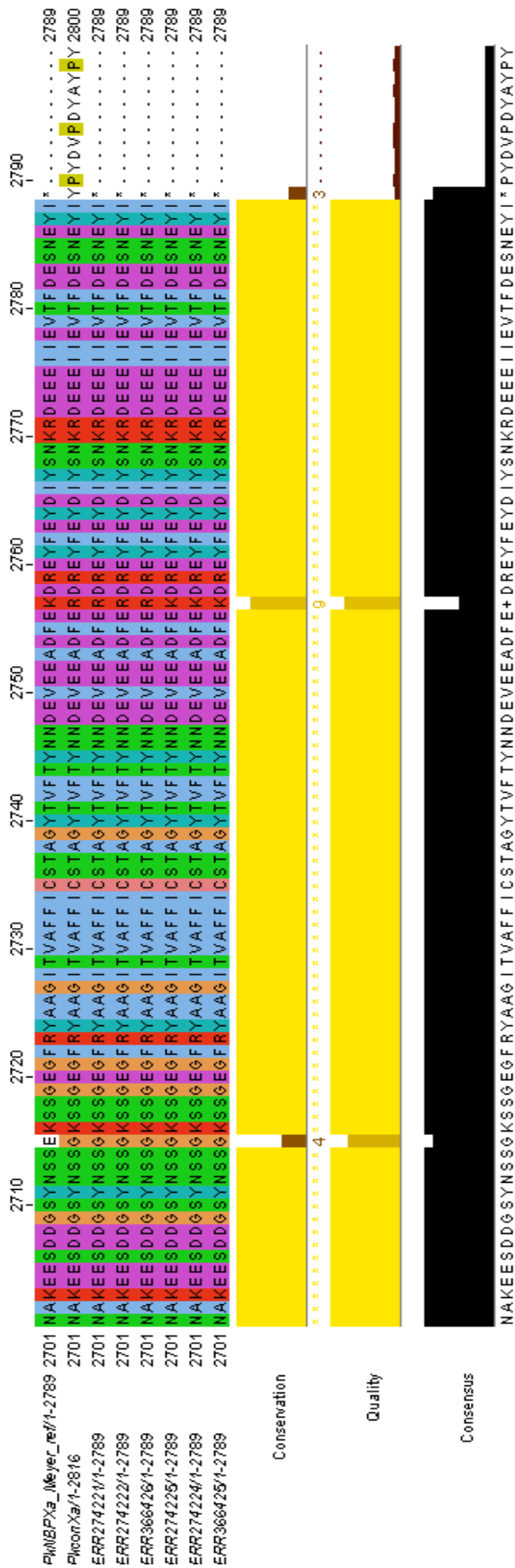


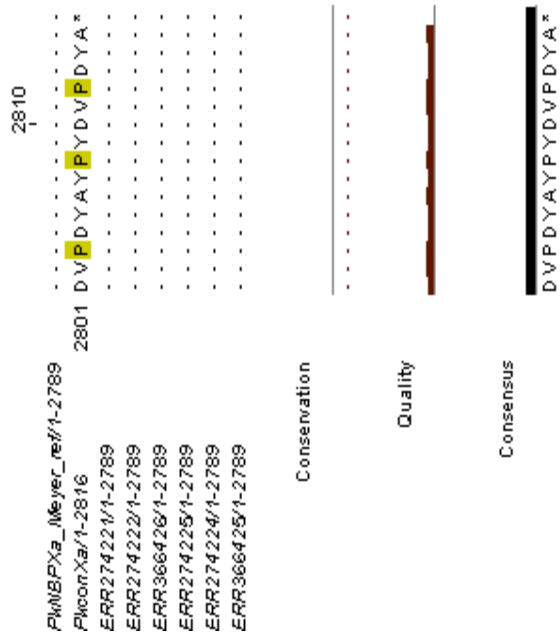












Genome sequences, and
PknBpXa sequences obtained
 from Pinheiro *et al.*, 2015,
<http://www.ebi.ac.uk/ena/data/view/PRJEB1405>.

Appendix H: Site Directed Mutagenesis Validation

pMA-RQ_Pknbpxa_f1: ag382cc mutation, sequence alignment

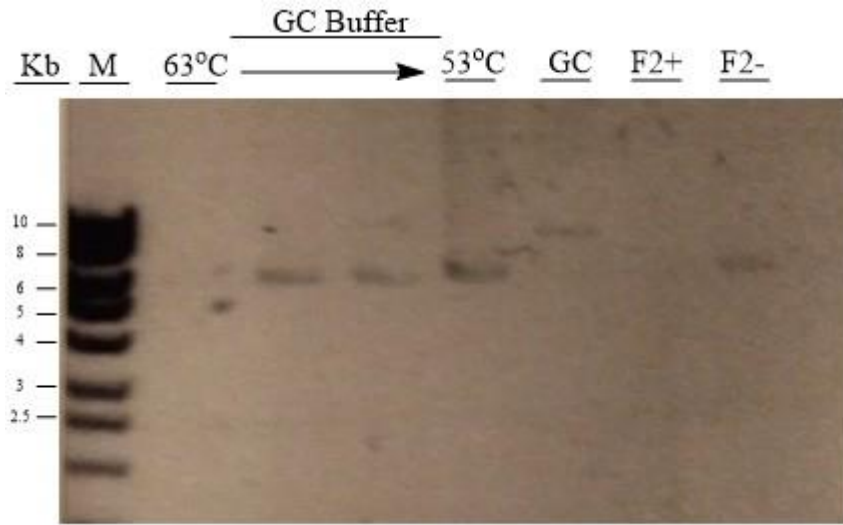
Alignment of Sequence_1: [R-XmaI] with Sequence_2: [pMA-RQ_Pknbpxa_f2]

Similarity : 581/583 (99.66 %) **S200P ag382cc**

```
Seq_1 1      G R N R Q N P L * I K R I D R D R V E W 60
TAGGCCGAAATCGGCAAAATCCCTTATAAATCAAAGAATAGACCGAGATAGGGTTGAGT
Seq_2 1      G R N R Q N P L * I K R I D R D R V E W 60
TAGGCCGAAATCGGCAAAATCCCTTATAAATCAAAGAATAGACCGAGATAGGGTTGAGT
Seq_1 61      P L Q G A P I R H S G C A T V G K G V S 120
GGCCGCTACAGGGCGCTCCCATTCGCCATTCAGGCTGCGCAACTGTTGGGAAGGGCGTTT
Seq_2 61      P L Q G A P I R H S G C A T V G K G V S 120
GGCCGCTACAGGGCGCTCCCATTCGCCATTCAGGCTGCGCAACTGTTGGGAAGGGCGTTT
Seq_1 121     V R A S S L L R Q L A K G G C A A R R L 180
CGGTGCGGGCCTCTTCGCTATTACGCCAGCTGGCGAAAGGGGGATGTGCTGCAAGGCGAT
Seq_2 121     V R A S S L L R Q L A K G G C A A R R L 180
CGGTGCGGGCCTCTTCGCTATTACGCCAGCTGGCGAAAGGGGGATGTGCTGCAAGGCGAT
Seq_1 181     S W V T P G F S Q S R R C K T T A S E R 240
TAAGTTGGGTAACGCCAGGGTTTTCCAGTCACGACGTTGTAAAACGACGGCCAGTGAGC
Seq_2 181     S W V T P G F S Q S R R C K T T A S E R 240
TAAGTTGGGTAACGCCAGGGTTTTCCAGTCACGACGTTGTAAAACGACGGCCAGTGAGC
Seq_1 241     D V I R L T I G R I G G R P S R P H S R 300
GCGACGTAATACGACTCACTATAGGGCGAATTGGCGGAAGGCCGTCAAGGCCGATTCCC
Seq_2 241     D V I R L T I G R I G G R P S R P H S R 300
GCGACGTAATACGACTCACTATAGGGCGAATTGGCGGAAGGCCGTCAAGGCCGATTCCC
Seq_1 301     D N P G D D D P E K K G D K D N N Y N S 360
GGGATAATCCCGGTGATGATGATCCGGAAAAAAGGCGATAAAGACAACAACATAACA
Seq_2 301     D N S G D D D P E K K G D K D N N Y N S 360
GGGATAATAGCGGTGATGATGATCCGGAAAAAAGGCGATAAAGACAACAACATAACA
Seq_1 361     G A K E D A M I K K L Y D N M E L L R M 420
GCGGTGCAAAAGAAGATGCCATGATCAAAAACTGTATGATAACATGGAAGCTGCTGCGTA
Seq_2 361     G A K E D A M I K K L Y D N M E L L R M 420
GCGGTGCAAAAGAAGATGCCATGATCAAAAACTGTATGATAACATGGAAGCTGCTGCGTA
Seq_1 421     P C F S I K S E L Q R K I N S L E Y A Q 480
TGCCGTGCTTTAGCATTAAAAGCGAACTGCAGCGTAAAATCAACAGCCTGGAATATGCAC
Seq_2 421     P C F S I K S E L Q R K I N S L E Y A Q 480
TGCCGTGCTTTAGCATTAAAAGCGAACTGCAGCGTAAAATCAACAGCCTGGAATATGCAC
Seq_1 481     T E D N E E V S G T S N S K T Y K L I E 540
AGACCGAAGATAATGAAGAAGTTAGCGGCACCAGCAATAGCAAAACCTATAAACTGATCG
Seq_2 481     T E D N E E V S G T S N S K T Y K L I E 540
AGACCGAAGATAATGAAGAAGTTAGCGGCACCAGCAATAGCAAAACCTATAAACTGATCG
```

```
      D E Y V N C L K N N S E N X
Seq_1 541 AGGATGAGTATGTGAACTGCCTGAAAAATAACAGCGAAAACGC 583
      |||
Seq_2 541 AGGATGAGTATGTGAACTGCCTGAAAAATAACAGCGAAAACGC 583
      D E Y V N C L K N N S E N X
```


pMA-RQ_Pknbpxa_f1: gt1043ag mutation generation



Site Directed Mutagenesis of the pMA-RQ_Pknbpxa_f2-1043ag plasmid. The PCR reaction was carried out using GC buffer compatible with the Phusion polymerase. A temperature gradient was used to identify the optimal temperature allowing primer binding. GC denotes a control pcr reaction using primers specific for a 10 Kb Lambda DNA amplicon. F2+ denotes 100 ng of neat pMA-RQ_Pknbpxa_f2 plasmid used as template for the PCR reaction digested with DpnI. F2- denotes 100 ng of neat pMA-RQ_Pknbpxa_f2 used as template for the PCR. Molecular weight marker was Hyperladder 1 Kb, and agarose gels were stained with SYBR Safe.

pMA-RQ_Pknbpxa_f1: gt1043ag mutation, sequence alignment

Alignment of Sequence_1: [F-SDM_XA_gt1043ag] with Sequence_2: [pMA-RQ_Pknbpxa_f2] G420E gt1043ag

Similarity : 1151/1153 (99.83 %)

```

          I L S S I K F L Q N E I S N I I N N Y N
Seq_1  1   ATATCCTGAGCAGCATCAAATTTCTGCAAAACGAAATCAGCAACATCATCAACAACACTACA  60
          |||
Seq_2  1   ATATCCTGAGCAGCATCAAATTTCTGCAAAACGAAATCAGCAACATCATCAACAACACTACA  60
          I L S S I K F L Q N E I S N I I N N Y N

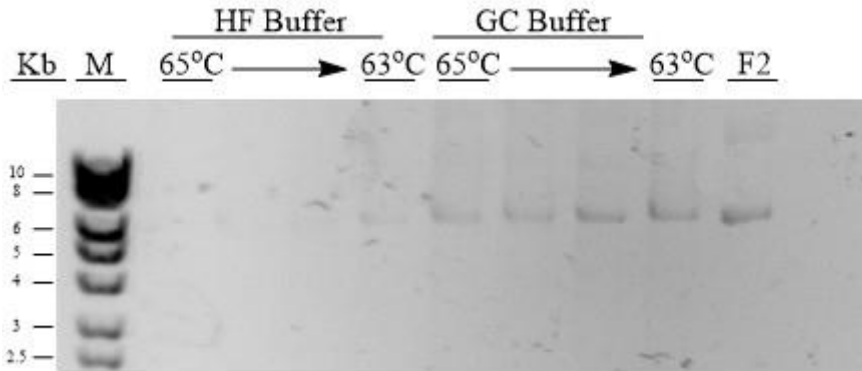
          Y H F E N I K K A I S N I K K H E N Y D
Seq_1  61  ACTACCACTTCGAGAACATCAAAAAAGCCATTAGCAATATCAAAAAACACGAGAACTACG  120
          |||
Seq_2  61  ACTACCACTTCGAGAACATCAAAAAAGCCATTAGCAATATCAAAAAACACGAGAACTACG  120
          Y H F E N I K K A I S N I K K H E N Y D

          K L S N L D K K T L V E K S L D L A K N
Seq_1  121 ATAAACTGAGCAACCTGGACAAAAAACCTGGTTGAGAAAAGCCTGGATCTGGCCAAAA  180
          |||
Seq_2  121 ATAAACTGAGCAACCTGGACAAAAAACCTGGTTGGTAAAAGCCTGGATCTGGCCAAAA  180
          K L S N L D K K T L V G K S L D L A K N

          M S L Y K F N N E M F K K M K E L Y D F
Seq_1  181 ATATGAGCCTGTATAAATTCACAACGAGATGTTCAAAAAATGAAAGAGCTGTACGATT  240
          |||
Seq_2  181 ATATGAGCCTGTATAAATTCACAACGAGATGTTCAAAAAATGAAAGAGCTGTACGATT  240
          M S L Y K F N N E M F K K M K E L Y D F
    
```

		K S N K F K R I F T F L A D A L K D K I	
Seq_1	241	TCAAAAGCAACAAATTCAAACGCATCTTCACCTTTCTGGCAGATGCACTGAAAGACAAAA	300
Seq_2	241	TCAAAAGCAACAAATTCAAACGCATCTTCACCTTTCTGGCAGATGCACTGAAAGACAAAA	300
		K S N K F K R I F T F L A D A L K D K I	
		N L F T E S M I Y E E K Y N S I M V D W	
Seq_1	301	TTAACCTGTTTACCGAGAGCATGATCTATGAAGAGAAAATACAACAGCATCATGGTGGACT	360
Seq_2	301	TTAACCTGTTTACCGAGAGCATGATCTATGAAGAGAAAATACAACAGCATCATGGTGGACT	360
		N L F T E S M I Y E E K Y N S I M V D W	
		K V I W E Y V V G E Y N K N L N A I Q S	
Seq_1	361	GGAAAGTGATTTGGGAATATGTTGTGGGCGAGTACAATAAAAAACCTGAATGCAATTCAGA	420
Seq_2	361	GGAAAGTGATTTGGGAATATGTTGTGGGCGAGTACAATAAAAAACCTGAATGCAATTCAGA	420
		K V I W E Y V V G E Y N K N L N A I Q S	
		Y E G N E N V E V I I V R N K V K E K L	
Seq_1	421	GCTATGAGGGCAATGAAAACGTGGAAGTTATTATCGTGCGCAACAAAGTAAAAGAAAAAC	480
Seq_2	421	GCTATGAGGGCAATGAAAACGTGGAAGTTATTATCGTGCGCAACAAAGTAAAAGAAAAAC	480
		Y E G N E N V E V I I V R N K V K E K L	
		G T F K S M A D E L Q G L F N I I E L K	
Seq_1	481	TGGGCACCTTTAAAAGCATGGCCGATGAACTGCAGGGTCTGTTTAATATCATCGAGCTGA	540
Seq_2	481	TGGGCACCTTTAAAAGCATGGCCGATGAACTGCAGGGTCTGTTTAATATCATCGAGCTGA	540

pMA-RQ_Pknbpxa_f1: g1982a mutation generation



Site Directed Mutagenesis of the pMA-RQ_Pknbpxa_f2-1982a plasmid. The PCR reaction was carried out with the GC buffer compatible with the Phusion polymerase. A temperature gradient from 67°C to 63°C was used to allowing primer binding. F2 denotes 100 ng of neat pMA-RQ_Pknbpxa_f2 plasmid used as template for the PCR reaction. Molecular weight marker was Hyperladder 1 Kb, and agarose gels were stained with SYBR Safe.

pMA-RQ_Pknbpxa_f1: g1982a mutation, sequence alignment

Alignment of Sequence_1: [F-SDM_XA_g1982a] with Sequence_2: [pMA-RQ_Pknbpxa_f2] **S733N g1982a**

Similarity : 1103/1104 (99.91 %)

```

Seq_1 1      N I K M I I K D I Y K D D L K K F V Q E      60
CAACATCAAAATGATTATCAAAGACATCTATAAAGATGATCTGAAAAAATTCGTGCAAGA
|
Seq_2 1      CAACATCAAAATGATTATCAAAGACATCTATAAAGATGATCTGAAAAAATTCGTGCAAGA      60
N I K M I I K D I Y K D D L K K F V Q E

Seq_1 61      I S R N M E K Y T D S I D N S S S A D E      120
AATCAGCCGCAACATGGAAAAATACACCGATAGCATTGATAACAGCAGCAGCGCAGATGA
|
Seq_2 61      AATCAGCCGCAACATGGAAAAATACACCGATAGCATTGATAGCAGCAGCAGCGCAGATGA      120
I S R N M E K Y T D S I D S S S S A D E

Seq_1 121     L D D V L K G I K V D Y E K I K S M K Y      180
ACTGGATGATGTACTGAAAGGTATCAAAGTGGACTATGAGAAAATCAAAGCATGAAATA
|
Seq_2 121     ACTGGATGATGTACTGAAAGGTATCAAAGTGGACTATGAGAAAATCAAAGCATGAAATA      180
L D D V L K G I K V D Y E K I K S M K Y

Seq_1 181     D D I A E S V E N I T N M L K I I S D A      240
CGACGACATTGCCGAAAGCGTTGAAAATATCACCAACATGCTGAAAATTATCTCCGATGC
|
Seq_2 181     CGACGACATTGCCGAAAGCGTTGAAAATATCACCAACATGCTGAAAATTATCTCCGATGC      240
D D I A E S V E N I T N M L K I I S D A

Seq_1 241     R E E I L K I K F G E T N K K L T N S L      300
CCGTGAGGAAATCCTGAAAATCAAATTTGGTGAAACCAACAAAAAAGTACCAATAGCCT
|
Seq_2 241     CCGTGAGGAAATCCTGAAAATCAAATTTGGTGAAACCAACAAAAAAGTACCAATAGCCT      300
R E E I L K I K F G E T N K K L T N S L

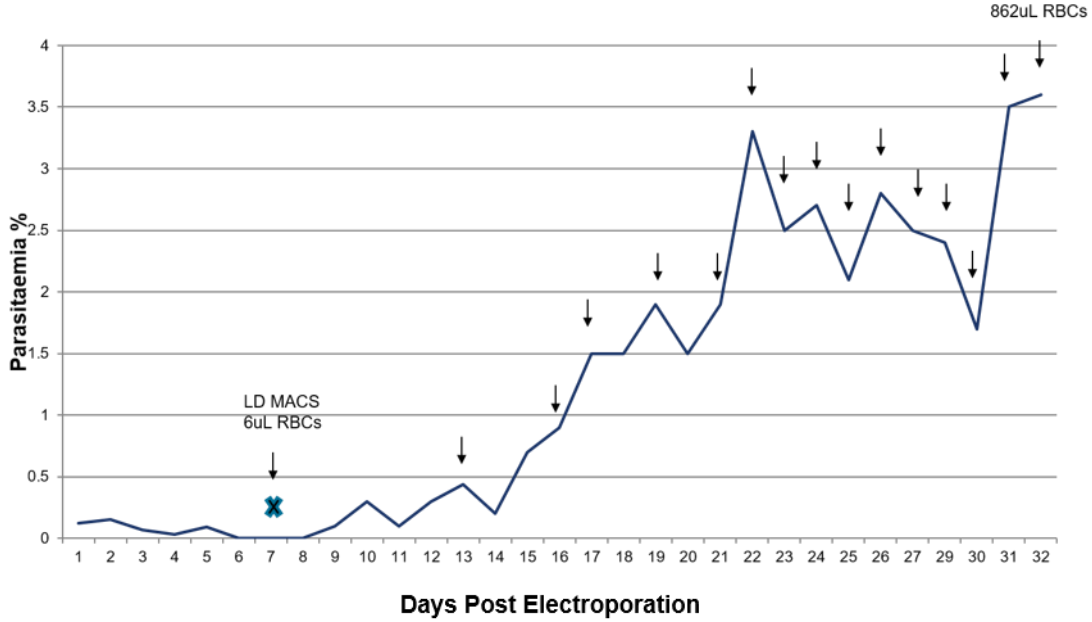
Seq_1 301     E Q L K S V Y D K L K V S I A E Y T A E      360
GGAACAGCTGAAAAGCGTTTATGACAAACTGAAAGTTAGCATTGCCGAATACACCGCAGA
|
Seq_2 301     GGAACAGCTGAAAAGCGTTTATGACAAACTGAAAGTTAGCATTGCCGAATACACCGCAGA      360
E Q L K S V Y D K L K V S I A E Y T A E

```

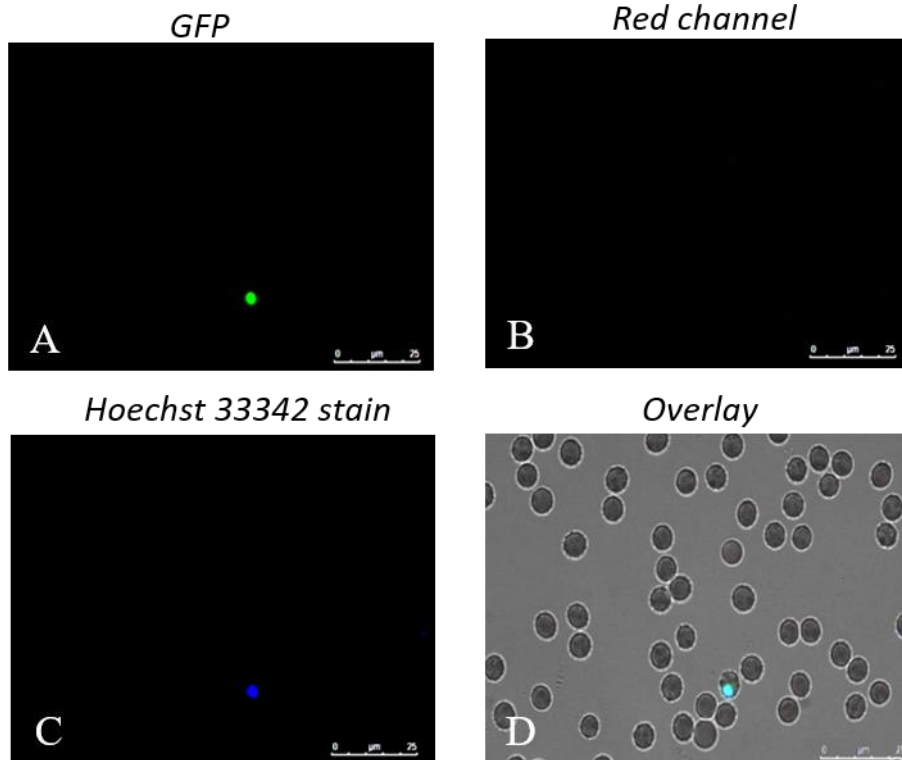
		K R K I E E D R A V I L K R E E E F F G	
Seq_1	361	AAAACGTAAAATTGAAGAAGATCGCGCAGTTATCCTGAAACGCGAAGAAGAATTTTTTCGG	420
Seq_2	361	AAAACGTAAAATTGAAGAAGATCGCGCAGTTATCCTGAAACGCGAAGAAGAATTTTTTCGG	420
		K R K I E E D R A V I L K R E E E F F G	
		K V Y D K D D D M L D V K D A Y T N F L	
Seq_1	421	CAAAGTGTATGACAAAGATGATGATATGCTGGATGTGAAAGATGCGTATAACCAACTTCCT	480
Seq_2	421	CAAAGTGTATGACAAAGATGATGATATGCTGGATGTGAAAGATGCGTATAACCAACTTCCT	480
		K V Y D K D D D M L D V K D A Y T N F L	
		K H K D N F F K N R N N V F E E F H T T	
Seq_1	481	GAAACATAAAGATAACTTTTTCAAAAACCGCAACAACGTTCGAAGAATTTACACCAC	540
Seq_2	481	GAAACATAAAGATAACTTTTTCAAAAACCGCAACAACGTTCGAAGAATTTACACCAC	540
		K H K D N F F K N R N N V F E E F H T T	
		K E A L K V V R I N F L Y Y I S M P E K	
Seq_1	541	CAAAGAAGCGCTGAAAGTTGTTTCGTATTAACTTTCTGTACTACATCAGCATGCCGAAAA	600
Seq_2	541	CAAAGAAGCGCTGAAAGTTGTTTCGTATTAACTTTCTGTACTACATCAGCATGCCGAAAA	600
		K E A L K V V R I N F L Y Y I S M P E K	
		Y N I I Y Q K E N E N Y K E L I K E I I	
Seq_1	601	ATACAACATCATCTATCAGAAAGAGAACGAGAATTACAAAGAACTGATCAAAGAGATCAT	660
Seq_2	601	ATACAACATCATCTATCAGAAAGAGAACGAGAATTACAAAGAACTGATCAAAGAGATCAT	660
		Y N I I Y Q K E N E N Y K E L I K E I I	
		D K H I D M K L D E Y E S D F K R N N K	
Seq_1	661	CGATAAACACATCGACATGAAACTGGACGAATATGAGAGCGATTTCAAACGGAATAACAA	720
Seq_2	661	CGATAAACACATCGACATGAAACTGGACGAATATGAGAGCGATTTCAAACGGAATAACAA	720
		D K H I D M K L D E Y E S D F K R N N K	

Appendix I: Growth Monitoring of Tf11.4 *Pk_{con}Pknbpxa_f1-3*

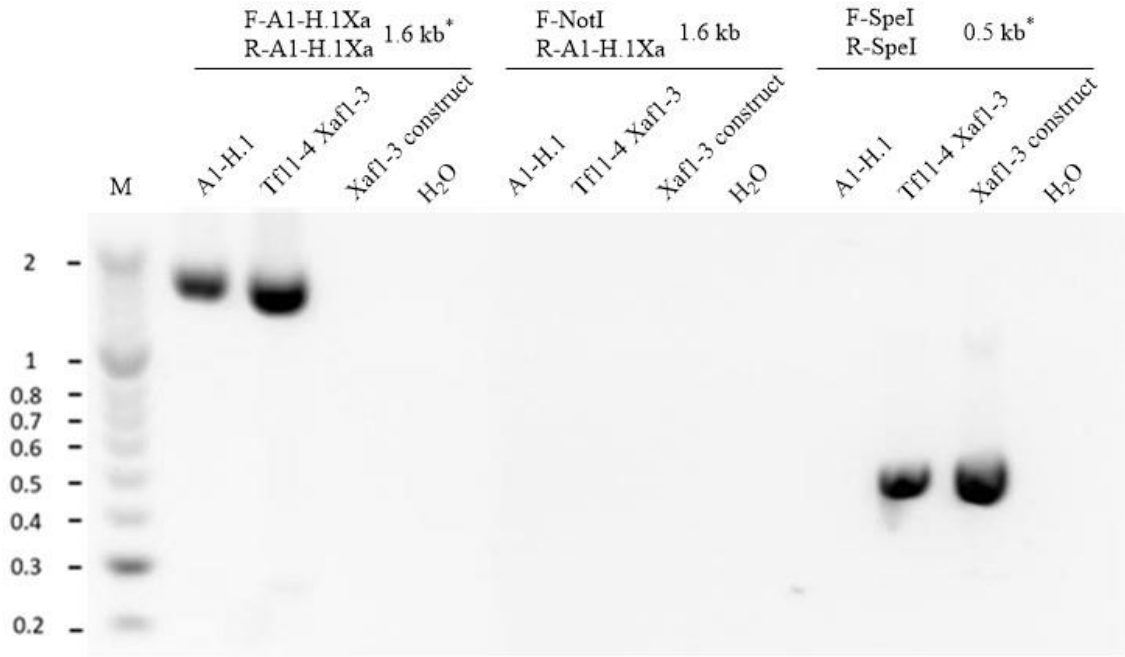
Monitoring of the Tf11.4 Transfection following LD MACs synchronisation



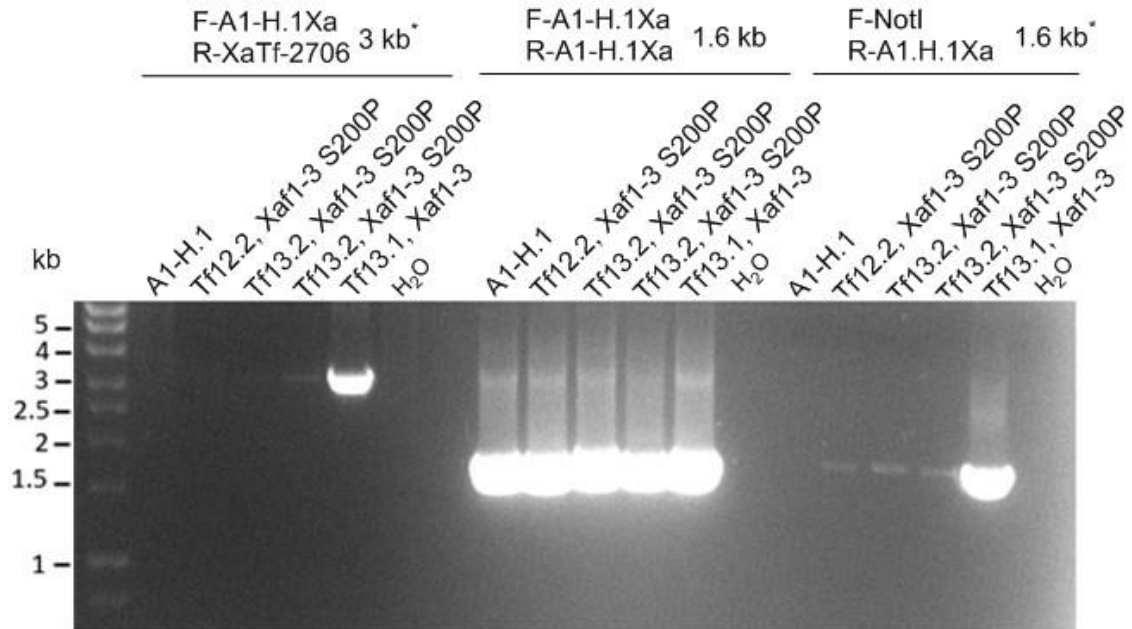
Live cell immunofluorescence of Tf11.5 (*Pk_{con}p230pGFP* control) prior to loss of the culture. Cells were stained with Hoechst 33342 (1 µg/mL). Slides were imaged on a Leica epifluorescent DM5500 microscope using a DFC5500 digital camera (Leica).



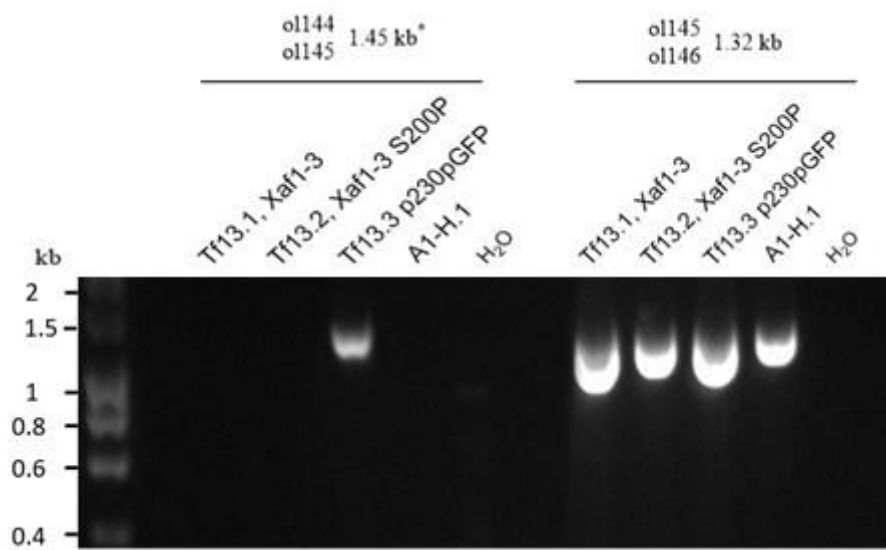
Appendix J: Uncropped Integration PCR gel images



Uncropped gel image of Figure 4.14



Uncropped gel image of Figure 4.16



Uncropped gel image of Figure 4.17

Appendix K: Publications

Ahmed, A. M., et al. (2014). "Disease progression in *Plasmodium knowlesi* malaria is linked to variation in invasion gene family members." *PLoS Negl Trop Dis* 8(8): e3086.

Millar, S. B. and J. Cox-Singh (2015). "Human infections with *Plasmodium knowlesi*--zoonotic malaria." *Clin Microbiol Infect* 21(7): 640-648.

Pinheiro, M. M., et al. (2015). "*Plasmodium knowlesi* genome sequences from clinical isolates reveal extensive genomic dimorphism." *PLoS One* 10(4): e0121303.

References

- . Available: <http://www.ebi.ac.uk/ena/data/view/PRJEB1405>.
- ABKARIAN, M., MASSIERA, G., BERRY, L., ROQUES, M. & BRAUN-BRETON, C. 2011. A novel mechanism for egress of malarial parasites from red blood cells. *Blood*, 117, 4118-24.
- ACHAN, J., TALISUNA, A. O., ERHART, A., YEKA, A., TIBENDERANA, J. K., BALIRAINÉ, F. N., ROSENTHAL, P. J. & D'ALESSANDRO, U. 2011. Quinine, an old anti-malarial drug in a modern world: role in the treatment of malaria. *Malar J*, 10, 144.
- ADAMS, J. H., HUDSON, D. E., TORII, M., WARD, G. E., WELLEMS, T. E., AIKAWA, M. & MILLER, L. H. 1990. The Duffy receptor family of Plasmodium knowlesi is located within the micronemes of invasive malaria merozoites. *Cell*, 63, 141-53.
- ADAMS, J. H., SIM, B. K., DOLAN, S. A., FANG, X., KASLOW, D. C. & MILLER, L. H. 1992. A family of erythrocyte binding proteins of malaria parasites. *Proc Natl Acad Sci U S A*, 89, 7085-9.
- AHMED, A. M., PINHEIRO, M. M., DIVIS, P. C., SINER, A., ZAINUDIN, R., WONG, I. T., LU, C. W., SINGH-KHAIRA, S. K., MILLAR, S. B., LYNCH, S., WILLMANN, M., SINGH, B., KRISHNA, S. & COX-SINGH, J. 2014. Disease progression in Plasmodium knowlesi malaria is linked to variation in invasion gene family members. *PLoS Negl Trop Dis*, 8, e3086.
- ALEXANDER, D. L., MITAL, J., WARD, G. E., BRADLEY, P. & BOOTHROYD, J. C. 2005. Identification of the moving junction complex of Toxoplasma gondii: a collaboration between distinct secretory organelles. *PLoS Pathog*, 1, e17.
- ALLEN, L. K., HATFIELD, J. M. & MANYAMA, M. 2013. Reducing microscopy-based malaria misdiagnosis in a low-resource area of Tanzania. *Tanzan J Health Res*, 15, 26-32.
- AMBERG-JOHNSON, K., HARI, S. B., GANESAN, S. M., LORENZI, H. A., SAUER, R. T., NILES, J. C. & YEH, E. 2017. Small molecule inhibition of apicomplexan FtsH1 disrupts plastid biogenesis in human pathogens. *Elife*, 6.
- ANTINORI, S., GALIMBERTI, L., MILAZZO, L. & CORBELLINO, M. 2012. Biology of human malaria plasmodia including Plasmodium knowlesi. *Mediterr J Hematol Infect Dis*, 4, e2012013.
- ASHLEY, E. A., DHORDA, M., FAIRHURST, R. M., AMARATUNGA, C., LIM, P., SUON, S., SRENG, S., ANDERSON, J. M., MAO, S., SAM, B., SOPHA, C., CHUOR, C. M., NGUON, C., SOVANNAROTH, S., PUKRITTAYAKAMEE, S., JITTAMALA, P., CHOTIVANICH, K., CHUTASMIT, K., SUCHATSOONTHORN, C., RUNCHAROEN, R., HIEN, T. T., THUY-NHIEN, N. T., THANH, N. V., PHU, N. H., HTUT, Y., HAN, K. T., AYE, K. H., MOKUOLU, O. A., OLAOSEBIKAN, R. R., FOLARANMI, O. O., MAYXAY, M., KHANTHAVONG, M., HONGVANTHONG, B., NEWTON, P. N., ONYAMBOKO, M. A., FANELLO, C. I., TSHEFU, A. K., MISHRA, N., VALECHA, N., PHYO, A. P., NOSTEN, F., YI, P., TRIPURA, R., BORRMANN, S., BASHRAHEIL, M., PESHU, J., FAIZ, M. A., GHOSE, A., HOSSAIN, M. A., SAMAD, R., RAHMAN, M. R., HASAN, M. M., ISLAM,

- A., MIOTTO, O., AMATO, R., MACINNIS, B., STALKER, J., KWIATKOWSKI, D. P., BOZDECH, Z., JEEYAPANT, A., CHEAH, P. Y., SAKULTHAEW, T., CHALK, J., INTHARABUT, B., SILAMUT, K., LEE, S. J., VIHOKHERN, B., KUNASOL, C., IMWONG, M., TARNING, J., TAYLOR, W. J., YEUNG, S., WOODROW, C. J., FLEGG, J. A., DAS, D., SMITH, J., VENKATESAN, M., PLOWE, C. V., STEPNIIEWSKA, K., GUERIN, P. J., DONDORP, A. M., DAY, N. P., WHITE, N. J. & TRACKING RESISTANCE TO ARTEMISININ, C. 2014. Spread of artemisinin resistance in *Plasmodium falciparum* malaria. *N Engl J Med*, 371, 411-23.
- ASSEFA, S., LIM, C., PRESTON, M. D., DUFFY, C. W., NAIR, M. B., ADROUB, S. A., KADIR, K. A., GOLDBERG, J. M., NEAFSEY, D. E., DIVIS, P., CLARK, T. G., DURAISINGH, M. T., CONWAY, D. J., PAIN, A. & SINGH, B. 2015. Population genomic structure and adaptation in the zoonotic malaria parasite *Plasmodium knowlesi*. *Proc Natl Acad Sci U S A*, 112, 13027-32.
- AUBURN, S., CAMPINO, S., CLARK, T. G., DJIMDE, A. A., ZONGO, I., PINCHES, R., MANSKE, M., MANGANO, V., ALCOCK, D., ANASTASI, E., MASLEN, G., MACINNIS, B., ROCKETT, K., MODIANO, D., NEWBOLD, C. I., DOUMBO, O. K., OUEDRAOGO, J. B. & KWIATKOWSKI, D. P. 2011. An effective method to purify *Plasmodium falciparum* DNA directly from clinical blood samples for whole genome high-throughput sequencing. *PLoS One*, 6, e22213.
- BACHMANN, A., ESSER, C., PETTER, M., PREDEHL, S., VON KALCKREUTH, V., SCHMIEDEL, S., BRUCHHAUS, I. & TANNICH, E. 2009. Absence of erythrocyte sequestration and lack of multicopy gene family expression in *Plasmodium falciparum* from a splenectomized malaria patient. *PLoS One*, 4, e7459.
- BAER, K., KLOTZ, C., KAPPE, S. H., SCHNIEDER, T. & FREVERT, U. 2007. Release of hepatic *Plasmodium yoelii* merozoites into the pulmonary microvasculature. *PLoS Pathog*, 3, e171.
- BAKER, R. P., WIJETILAKA, R. & URBAN, S. 2006. Two *Plasmodium* rhomboid proteases preferentially cleave different adhesins implicated in all invasive stages of malaria. *PLoS Pathog*, 2, e113.
- BALDWIN, M. R., LI, X., HANADA, T., LIU, S. C. & CHISHTI, A. H. 2015. Merozoite surface protein 1 recognition of host glycophorin A mediates malaria parasite invasion of red blood cells. *Blood*, 125, 2704-11.
- BANNISTER, L. H., BUTCHER, G. A., DENNIS, E. D. & MITCHELL, G. H. 1975. Studies on the structure and invasive behaviour of merozoites of *Plasmodium knowlesi*. *Trans R Soc Trop Med Hyg*, 69, 5.
- BANNISTER, L. H. & DLUZEWSKI, A. R. 1990. The ultrastructure of red cell invasion in malaria infections: a review. *Blood Cells*, 16, 257-92; discussion 293-7.
- BARAGANA, B., HALLYBURTON, I., LEE, M. C., NORCROSS, N. R., GRIMALDI, R., OTTO, T. D., PROTO, W. R., BLAGBOROUGH, A. M., MEISTER, S., WIRJANATA, G., RUECKER, A., UPTON, L. M., ABRAHAM, T. S., ALMEIDA, M. J., PRADHAN, A., PORZELLE, A., LUKSCH, T., MARTINEZ, M. S., LUKSCH, T., BOLSCHER, J. M., WOODLAND, A., NORVAL, S., ZUCCOTTO, F., THOMAS, J., SIMEONS, F., STOJANOVSKI, L., OSUNA-CABELLO, M., BROCK, P. M.,

- CHURCHER, T. S., SALA, K. A., ZAKUTANSKY, S. E., JIMENEZ-DIAZ, M. B., SANZ, L. M., RILEY, J., BASAK, R., CAMPBELL, M., AVERY, V. M., SAUERWEIN, R. W., DECHERING, K. J., NOVIYANTI, R., CAMPO, B., FREARSON, J. A., ANGULO-BARTUREN, I., FERRER-BAZAGA, S., GAMO, F. J., WYATT, P. G., LEROY, D., SIEGL, P., DELVES, M. J., KYLE, D. E., WITTLIN, S., MARFURT, J., PRICE, R. N., SINDEN, R. E., WINZELER, E. A., CHARMAN, S. A., BEBREVSKA, L., GRAY, D. W., CAMPBELL, S., FAIRLAMB, A. H., WILLIS, P. A., RAYNER, J. C., FIDOCK, D. A., READ, K. D. & GILBERT, I. H. 2015. A novel multiple-stage antimalarial agent that inhibits protein synthesis. *Nature*, 522, 315-20.
- BARBER, B. E., WILLIAM, T., GRIGG, M. J., MENON, J., AUBURN, S., MARFURT, J., ANSTEY, N. M. & YEO, T. W. 2013. A prospective comparative study of knowlesi, falciparum, and vivax malaria in Sabah, Malaysia: high proportion with severe disease from Plasmodium knowlesi and Plasmodium vivax but no mortality with early referral and artesunate therapy. *Clin Infect Dis*, 56, 383-97.
- BARGIERI, D. Y., ANDENMATTEN, N., LAGAL, V., THIBERGE, S., WHITELAW, J. A., TARDIEUX, I., MEISSNER, M. & MENARD, R. 2013. Apical membrane antigen 1 mediates apicomplexan parasite attachment but is dispensable for host cell invasion. *Nat Commun*, 4, 2552.
- BARTHOLDSON, S. J., CROSNIER, C., BUSTAMANTE, L. Y., RAYNER, J. C. & WRIGHT, G. J. 2013. Identifying novel Plasmodium falciparum erythrocyte invasion receptors using systematic extracellular protein interaction screens. *Cell Microbiol*, 15, 1304-12.
- BARTOLONI, A. & ZAMMARCHI, L. 2012. Clinical aspects of uncomplicated and severe malaria. *Mediterr J Hematol Infect Dis*, 4, e2012026.
- BATCHELOR, J. D., MALPEDE, B. M., OMATTAGE, N. S., DEKOSTER, G. T., HENZLER-WILDMAN, K. A. & TOLIA, N. H. 2014. Red blood cell invasion by Plasmodium vivax: structural basis for DBP engagement of DARC. *PLoS Pathog*, 10, e1003869.
- BAUM, J., CHEN, L., HEALER, J., LOPATICKI, S., BOYLE, M., TRIGLIA, T., EHLGEN, F., RALPH, S. A., BEESON, J. G. & COWMAN, A. F. 2009. Reticulocyte-binding protein homologue 5 - an essential adhesin involved in invasion of human erythrocytes by Plasmodium falciparum. *Int J Parasitol*, 39, 371-80.
- BAUM, J., GILBERGER, T. W., FRISCHKNECHT, F. & MEISSNER, M. 2008. Host-cell invasion by malaria parasites: insights from Plasmodium and Toxoplasma. *Trends Parasitol*, 24, 557-63.
- BECK, J. R., CHEN, A. L., KIM, E. W. & BRADLEY, P. J. 2014. RON5 is critical for organization and function of the Toxoplasma moving junction complex. *PLoS Pathog*, 10, e1004025.
- BEESON, J. G., AMIN, N., KANJALA, M. & ROGERSON, S. J. 2002. Selective accumulation of mature asexual stages of Plasmodium falciparum-infected erythrocytes in the placenta. *Infect Immun*, 70, 5412-5.
- BEESON, J. G., DREW, D. R., BOYLE, M. J., FENG, G., FOWKES, F. J. & RICHARDS, J. S. 2016. Merozoite surface proteins in red blood cell invasion, immunity and vaccines against malaria. *FEMS Microbiol Rev*, 40, 343-72.

- BESTEIRO, S., MICHELIN, A., PONCET, J., DUBREMETZ, J. F. & LEBRUN, M. 2009. Export of a *Toxoplasma gondii* rhoptry neck protein complex at the host cell membrane to form the moving junction during invasion. *PLoS Pathog*, 5, e1000309.
- BLACKMAN, M. J. & HOLDER, A. A. 1992. Secondary processing of the *Plasmodium falciparum* merozoite surface protein-1 (MSP1) by a calcium-dependent membrane-bound serine protease: shedding of MSP133 as a noncovalently associated complex with other fragments of the MSP1. *Mol Biochem Parasitol*, 50, 307-15.
- BOISSIERE, A., ARNATHAU, C., DUPERRAY, C., BERRY, L., LACHAUD, L., RENAUD, F., DURAND, P. & PRUGNOLLE, F. 2012. Isolation of *Plasmodium falciparum* by flow-cytometry: implications for single-trophozoite genotyping and parasite DNA purification for whole-genome high-throughput sequencing of archival samples. *Malar J*, 11, 163.
- BRANCUCCI, N. M., WITMER, K., SCHMID, C. & VOSS, T. S. 2014. A var gene upstream element controls protein synthesis at the level of translation initiation in *Plasmodium falciparum*. *PLoS One*, 9, e100183.
- BRAY, R. S. & GARNHAM, P. C. 1982. The life-cycle of primate malaria parasites. *Br Med Bull*, 38, 117-22.
- BRIGHT, A. T., TEWHEY, R., ABELES, S., CHUQUIYAURI, R., LLANOS-CUENTAS, A., FERREIRA, M. U., SCHORK, N. J., VINETZ, J. M. & WINZELER, E. A. 2012. Whole genome sequencing analysis of *Plasmodium vivax* using whole genome capture. *BMC Genomics*, 13, 262.
- BROWN, I. N., BROWN, K. N. & HILLS, L. A. 1968. Immunity to malaria: the antibody response to antigenic variation by *Plasmodium knowlesi*. *Immunology*, 14, 127-38.
- BROWN, K. N. & BROWN, I. N. 1965. Immunity to malaria: antigenic variation in chronic infections of *Plasmodium knowlesi*. *Nature*, 208, 1286-8.
- BURDA, P. C., CALDELARI, R. & HEUSSLER, V. T. 2017. Manipulation of the Host Cell Membrane during *Plasmodium* Liver Stage Egress. *MBio*, 8.
- BUSHELL, E., GOMES, A. R., SANDERSON, T., ANAR, B., GIRLING, G., HERD, C., METCALF, T., MODRZYNSKA, K., SCHWACH, F., MARTIN, R. E., MATHER, M. W., MCFADDEN, G. I., PARTS, L., RUTLEDGE, G. G., VAIDYA, A. B., WENGELNIK, K., RAYNER, J. C. & BILLKER, O. 2017. Functional Profiling of a *Plasmodium* Genome Reveals an Abundance of Essential Genes. *Cell*, 170, 260-272 e8.
- BUSTAMANTE, L. Y., BARTHOLDSON, S. J., CROSNIER, C., CAMPOS, M. G., WANAGURU, M., NGUON, C., KWIATKOWSKI, D. P., WRIGHT, G. J. & RAYNER, J. C. 2013. A full-length recombinant *Plasmodium falciparum* PfrH5 protein induces inhibitory antibodies that are effective across common PfrH5 genetic variants. *Vaccine*, 31, 373-9.
- BUTCHER, G. A. & MITCHELL, G. H. 2016. The role of *Plasmodium knowlesi* in the history of malaria research. *Parasitology*, 1-12.
- CARLTON, J. M., ADAMS, J. H., SILVA, J. C., BIDWELL, S. L., LORENZI, H., CALER, E., CRABTREE, J., ANGIUOLI, S. V., MERINO, E. F., AMEDEO, P., CHENG, Q., COULSON, R. M., CRABB, B. S., DEL PORTILLO, H. A., ESSIEN, K., FELDBLYUM, T. V., FERNANDEZ-BECERRA, C., GILSON, P. R., GUEYE, A. H., GUO, X., KANG'A, S., KOUIJ, T. W., KORSINCZKY, M.,

- MEYER, E. V., NENE, V., PAULSEN, I., WHITE, O., RALPH, S. A., REN, Q., SARGEANT, T. J., SALZBERG, S. L., STOECKERT, C. J., SULLIVAN, S. A., YAMAMOTO, M. M., HOFFMAN, S. L., WORTMAN, J. R., GARDNER, M. J., GALINSKI, M. R., BARNWELL, J. W. & FRASER-LIGGETT, C. M. 2008. Comparative genomics of the neglected human malaria parasite *Plasmodium vivax*. *Nature*, 455, 757-63.
- CARLTON, J. M., ANGIUOLI, S. V., SUH, B. B., KOOIJ, T. W., PERTEA, M., SILVA, J. C., ERMOLAEVA, M. D., ALLEN, J. E., SELENGUT, J. D., KOO, H. L., PETERSON, J. D., POP, M., KOSACK, D. S., SHUMWAY, M. F., BIDWELL, S. L., SHALLOM, S. J., VAN AKEN, S. E., RIEDMULLER, S. B., FELDBLYUM, T. V., CHO, J. K., QUACKENBUSH, J., SEDEGAH, M., SHOAIABI, A., CUMMINGS, L. M., FLORENS, L., YATES, J. R., RAINE, J. D., SINDEN, R. E., HARRIS, M. A., CUNNINGHAM, D. A., PREISER, P. R., BERGMAN, L. W., VAIDYA, A. B., VAN LIN, L. H., JANSE, C. J., WATERS, A. P., SMITH, H. O., WHITE, O. R., SALZBERG, S. L., VENTER, J. C., FRASER, C. M., HOFFMAN, S. L., GARDNER, M. J. & CARUCCI, D. J. 2002. Genome sequence and comparative analysis of the model rodent malaria parasite *Plasmodium yoelii yoelii*. *Nature*, 419, 512-9.
- CARTER, V., NACER, A. M., UNDERHILL, A., SINDEN, R. E. & HURD, H. 2007. Minimum requirements for ookinete to oocyst transformation in *Plasmodium*. *Int J Parasitol*, 37, 1221-32.
- CARVER, T., HARRIS, S. R., BERRIMAN, M., PARKHILL, J. & MCQUILLAN, J. A. 2012. Artemis: an integrated platform for visualization and analysis of high-throughput sequence-based experimental data. *Bioinformatics*, 28, 464-9.
- CENTERS FOR DISEASE, C. A. P. 2017. Available: <https://www.cdc.gov/malaria/about/biology/> [Accessed 20/3 2017].
- CHAKRAVORTY, S. J., HUGHES, K. R. & CRAIG, A. G. 2008. Host response to cytoadherence in *Plasmodium falciparum*. *Biochem Soc Trans*, 36, 221-8.
- CHAN, E. R., MENARD, D., DAVID, P. H., RATSIMBASOA, A., KIM, S., CHIM, P., DO, C., WITKOWSKI, B., MERCEREAU-PUJALON, O., ZIMMERMAN, P. A. & SERRE, D. 2012. Whole genome sequencing of field isolates provides robust characterization of genetic diversity in *Plasmodium vivax*. *PLoS Negl Trop Dis*, 6, e1811.
- CHAVCHICH, M., VAN BREDA, K., ROWCLIFFE, K., DIAGANA, T. T. & EDSTEIN, M. D. 2016. The Spiroindolone KAE609 Does Not Induce Dormant Ring Stages in *Plasmodium falciparum* Parasites. *Antimicrob Agents Chemother*, 60, 5167-74.
- CHEN, E., SALINAS, N. D., HUANG, Y., NTUMNGIA, F., PLASENCIA, M. D., GROSS, M. L., ADAMS, J. H. & TOLIA, N. H. 2016. Broadly neutralizing epitopes in the *Plasmodium vivax* vaccine candidate Duffy Binding Protein. *Proc Natl Acad Sci U S A*, 113, 6277-82.
- CHEN, L., LOPATICKI, S., RIGLAR, D. T., DEKIWADIA, C., UBOLDI, A. D., THAM, W. H., O'NEILL, M. T., RICHARD, D., BAUM, J., RALPH, S. A. & COWMAN, A. F. 2011. An EGF-like protein forms a complex with PfRh5 and is required for invasion of human erythrocytes by *Plasmodium falciparum*. *PLoS Pathog*, 7, e1002199.

- CHIN, W., CONTACOS, P. G., COATNEY, G. R. & KIMBALL, H. R. 1965. A Naturally Acquired Quotidian-Type Malaria in Man Transferable to Monkeys. *Science*, 149, 865.
- CHIN, W., CONTACOS, P. G., COLLINS, W. E., JETER, M. H. & ALPERT, E. 1968. Experimental mosquito-transmission of *Plasmodium knowlesi* to man and monkey. *Am J Trop Med Hyg*, 17, 355-8.
- CHITNIS, C. E., CHAUDHURI, A., HORUK, R., POGO, A. O. & MILLER, L. H. 1996. The domain on the Duffy blood group antigen for binding *Plasmodium vivax* and *P. knowlesi* malarial parasites to erythrocytes. *J Exp Med*, 184, 1531-6.
- CHOKEJINDACHAI, W. & CONWAY, D. J. 2009. Case-control approach to identify *Plasmodium falciparum* polymorphisms associated with severe malaria. *PLoS One*, 4, e5454.
- CLAESSENS, A., HAMILTON, W. L., KEKRE, M., OTTO, T. D., FAIZULLABHOY, A., RAYNER, J. C. & KWIATKOWSKI, D. 2014. Generation of antigenic diversity in *Plasmodium falciparum* by structured rearrangement of Var genes during mitosis. *PLoS Genet*, 10, e1004812.
- COATNEY, G. R., COLLINS, W. E. & CONTACOS, P. G. 1971. *The Primate Malaria*, U.S. National Institute of Allergy and Infectious Disease.
- COHUET, A., HARRIS, C., ROBERT, V. & FONTENILLE, D. 2010. Evolutionary forces on Anopheles: what makes a malaria vector? *Trends Parasitol*, 26, 130-6.
- COLLINS, C. R., DAS, S., WONG, E. H., ANDENMATTEN, N., STALLMACH, R., HACKETT, F., HERMAN, J. P., MULLER, S., MEISSNER, M. & BLACKMAN, M. J. 2013a. Robust inducible Cre recombinase activity in the human malaria parasite *Plasmodium falciparum* enables efficient gene deletion within a single asexual erythrocytic growth cycle. *Mol Microbiol*, 88, 687-701.
- COLLINS, C. R., HACKETT, F., ATID, J., TAN, M. S. Y. & BLACKMAN, M. J. 2017. The *Plasmodium falciparum* pseudoprotease SERA5 regulates the kinetics and efficiency of malaria parasite egress from host erythrocytes. *PLoS Pathog*, 13, e1006453.
- COLLINS, C. R., HACKETT, F., STRATH, M., PENZO, M., WITHERS-MARTINEZ, C., BAKER, D. A. & BLACKMAN, M. J. 2013b. Malaria parasite cGMP-dependent protein kinase regulates blood stage merozoite secretory organelle discharge and egress. *PLoS Pathog*, 9, e1003344.
- COLLINS, W. E., CONTACOS, P. G. & GUINN, E. G. 1967. Studies on the transmission of simian malaras. II. Transmission of the H strain of *Plasmodium knowlesi* by *Anopheles balabacensis balabacensis*. *J Parasitol*, 53, 841-4.
- COUNIHAN, N. A., KALANON, M., COPPEL, R. L. & DE KONING-WARD, T. F. 2013. *Plasmodium* rhoptry proteins: why order is important. *Trends Parasitol*, 29, 228-36.
- COWMAN, A. F., BERRY, D. & BAUM, J. 2012. The cellular and molecular basis for malaria parasite invasion of the human red blood cell. *J Cell Biol*, 198, 961-71.
- COWMAN, A. F. & CRABB, B. S. 2006. Invasion of red blood cells by malaria parasites. *Cell*, 124, 755-66.
- COX-SINGH, J. 2012. Zoonotic malaria: *Plasmodium knowlesi*, an emerging pathogen. *Curr Opin Infect Dis*, 25, 530-6.
- COX-SINGH, J. & CULLETON, R. 2015. *Plasmodium knowlesi*: from severe zoonosis to animal model. *Trends Parasitol*, 31, 232-8.

- COX-SINGH, J., DAVIS, T. M., LEE, K. S., SHAMSUL, S. S., MATUSOP, A., RATNAM, S., RAHMAN, H. A., CONWAY, D. J. & SINGH, B. 2008. Plasmodium knowlesi malaria in humans is widely distributed and potentially life threatening. *Clin Infect Dis*, 46, 165-71.
- COX-SINGH, J., HIU, J., LUCAS, S. B., DIVIS, P. C., ZULKARNAEN, M., CHANDRAN, P., WONG, K. T., ADEM, P., ZAKI, S. R., SINGH, B. & KRISHNA, S. 2010. Severe malaria - a case of fatal Plasmodium knowlesi infection with post-mortem findings: a case report. *Malar J*, 9, 10.
- COX-SINGH, J., SINGH, B., DANESHVAR, C., PLANCHE, T., PARKER-WILLIAMS, J. & KRISHNA, S. 2011. Anti-inflammatory cytokines predominate in acute human Plasmodium knowlesi infections. *PLoS One*, 6, e20541.
- COX, F. E. 2010. History of the discovery of the malaria parasites and their vectors. *Parasit Vectors*, 3, 5.
- CRAIG, A. G., GRAU, G. E., JANSE, C., KAZURA, J. W., MILNER, D., BARNWELL, J. W., TURNER, G., LANGHORNE, J. & PARTICIPANTS OF THE HINXTON RETREAT MEETING ON ANIMAL MODELS FOR RESEARCH ON SEVERE, M. 2012. The role of animal models for research on severe malaria. *PLoS Pathog*, 8, e1002401.
- CROSNIER, C., BUSTAMANTE, L. Y., BARTHOLDSON, S. J., BEI, A. K., THERON, M., UCHIKAWA, M., MBOUP, S., NDIR, O., KWIATKOWSKI, D. P., DURAISINGH, M. T., RAYNER, J. C. & WRIGHT, G. J. 2011. Basigin is a receptor essential for erythrocyte invasion by Plasmodium falciparum. *Nature*, 480, 534-7.
- CULVENOR, J. G., DAY, K. P. & ANDERS, R. F. 1991. Plasmodium falciparum ring-infected erythrocyte surface antigen is released from merozoite dense granules after erythrocyte invasion. *Infect Immun*, 59, 1183-7.
- CUNHA, C. B. & CUNHA, B. A. 2008. Brief history of the clinical diagnosis of malaria: from Hippocrates to Osler. *J Vector Borne Dis*, 45, 194-9.
- DANESHVAR, C., DAVIS, T. M., COX-SINGH, J., RAFA'EE, M. Z., ZAKARIA, S. K., DIVIS, P. C. & SINGH, B. 2009. Clinical and laboratory features of human Plasmodium knowlesi infection. *Clin Infect Dis*, 49, 852-60.
- DAS, S., HERTRICH, N., PERRIN, A. J., WITHERS-MARTINEZ, C., COLLINS, C. R., JONES, M. L., WATERMEYER, J. M., FOBES, E. T., MARTIN, S. R., SAIBIL, H. R., WRIGHT, G. J., TREECK, M., EPP, C. & BLACKMAN, M. J. 2015. Processing of Plasmodium falciparum Merozoite Surface Protein MSP1 Activates a Spectrin-Binding Function Enabling Parasite Egress from RBCs. *Cell Host Microbe*, 18, 433-44.
- DEL PORTILLO, H. A., FERRER, M., BRUGAT, T., MARTIN-JAULAR, L., LANGHORNE, J. & LACERDA, M. V. 2012. The role of the spleen in malaria. *Cell Microbiol*, 14, 343-55.
- DEMBELE, L., FRANETICH, J. F., LORTHIOIS, A., GEGO, A., ZEEMAN, A. M., KOCKEN, C. H., LE GRAND, R., DEREUDDRE-BOSQUET, N., VAN GEMERT, G. J., SAUERWEIN, R., VAILLANT, J. C., HANNOUN, L., FUCHTER, M. J., DIAGANA, T. T., MALMQUIST, N. A., SCHERF, A., SNOUNOU, G. & MAZIER, D. 2014. Persistence and activation of malaria hypnozoites in long-term primary hepatocyte cultures. *Nat Med*, 20, 307-12.

- DIVIS, P. C., SHOKOPLES, S. E., SINGH, B. & YANOW, S. K. 2010. A TaqMan real-time PCR assay for the detection and quantitation of *Plasmodium knowlesi*. *Malar J*, 9, 344.
- DLUZEWSKI, A. R., LING, I. T., HOPKINS, J. M., GRAINGER, M., MARGOS, G., MITCHELL, G. H., HOLDER, A. A. & BANNISTER, L. H. 2008. Formation of the food vacuole in *Plasmodium falciparum*: a potential role for the 19 kDa fragment of merozoite surface protein 1 (MSP1(19)). *PLoS One*, 3, e3085.
- DOOLAN, D. L., DOBANO, C. & BAIRD, J. K. 2009. Acquired immunity to malaria. *Clin Microbiol Rev*, 22, 13-36, Table of Contents.
- DOUGLAS, A. D., BALDEVIANO, G. C., LUCAS, C. M., LUGO-ROMAN, L. A., CROSNIER, C., BARTHOLDSON, S. J., DIOUF, A., MIURA, K., LAMBERT, L. E., VENTOCILLA, J. A., LEIVA, K. P., MILNE, K. H., ILLINGWORTH, J. J., SPENCER, A. J., HJERRILD, K. A., ALANINE, D. G., TURNER, A. V., MOORHEAD, J. T., EDGEL, K. A., WU, Y., LONG, C. A., WRIGHT, G. J., LESCANO, A. G. & DRAPER, S. J. 2015. A PfrH5-based vaccine is efficacious against heterologous strain blood-stage *Plasmodium falciparum* infection in aotus monkeys. *Cell Host Microbe*, 17, 130-9.
- DOUGLAS, A. D., WILLIAMS, A. R., ILLINGWORTH, J. J., KAMUYU, G., BISWAS, S., GOODMAN, A. L., WYLLIE, D. H., CROSNIER, C., MIURA, K., WRIGHT, G. J., LONG, C. A., OSIER, F. H., MARSH, K., TURNER, A. V., HILL, A. V. & DRAPER, S. J. 2011. The blood-stage malaria antigen PfrH5 is susceptible to vaccine-inducible cross-strain neutralizing antibody. *Nat Commun*, 2, 601.
- DOUGLAS, A. D., WILLIAMS, A. R., KNUEPFER, E., ILLINGWORTH, J. J., FURZE, J. M., CROSNIER, C., CHOUDHARY, P., BUSTAMANTE, L. Y., ZAKUTANSKY, S. E., AWUAH, D. K., ALANINE, D. G., THERON, M., WORTH, A., SHIMKETS, R., RAYNER, J. C., HOLDER, A. A., WRIGHT, G. J. & DRAPER, S. J. 2014. Neutralization of *Plasmodium falciparum* merozoites by antibodies against PfrH5. *J Immunol*, 192, 245-58.
- DOUSE, C. H., GREEN, J. L., SALGADO, P. S., SIMPSON, P. J., THOMAS, J. C., LANGSLEY, G., HOLDER, A. A., TATE, E. W. & COTA, E. 2012. Regulation of the *Plasmodium* motor complex: phosphorylation of myosin A tail-interacting protein (MTIP) loosens its grip on MyoA. *J Biol Chem*, 287, 36968-77.
- DOWSE, T. J., KOUSSIS, K., BLACKMAN, M. J. & SOLDATI-FAVRE, D. 2008. Roles of proteases during invasion and egress by *Plasmodium* and *Toxoplasma*. *Subcell Biochem*, 47, 121-39.
- DURASINGH, M. T., MAIER, A. G., TRIGLIA, T. & COWMAN, A. F. 2003a. Erythrocyte-binding antigen 175 mediates invasion in *Plasmodium falciparum* utilizing sialic acid-dependent and -independent pathways. *Proc Natl Acad Sci U S A*, 100, 4796-801.
- DURASINGH, M. T., TRIGLIA, T., RALPH, S. A., RAYNER, J. C., BARNWELL, J. W., MCFADDEN, G. I. & COWMAN, A. F. 2003b. Phenotypic variation of *Plasmodium falciparum* merozoite proteins directs receptor targeting for invasion of human erythrocytes. *EMBO J*, 22, 1047-57.
- DVORAK, J. A., MILLER, L. H., WHITEHOUSE, W. C. & SHIROISHI, T. 1975. Invasion of erythrocytes by malaria merozoites. *Science*, 187, 748-50.
- DVORIN, J. D., BEI, A. K., COLEMAN, B. I. & DURASINGH, M. T. 2010. Functional diversification between two related *Plasmodium falciparum*

- merozoite invasion ligands is determined by changes in the cytoplasmic domain. *Mol Microbiol*, 75, 990-1006.
- EGAN, A. F., FABUCCI, M. E., SAUL, A., KASLOW, D. C. & MILLER, L. H. 2002. Aotus New World monkeys: model for studying malaria-induced anemia. *Blood*, 99, 3863-6.
- EYLES, D. E., HOO, C. C., WARREN, M. & SANDOSHAM, A. A. 1963. Plasmodium Falciparum Resistant to Chloroquine in Cambodia. *Am J Trop Med Hyg*, 12, 840-3.
- FATIH, F. A., SENER, A., AHMED, A., WOON, L. C., CRAIG, A. G., SINGH, B., KRISHNA, S. & COX-SINGH, J. 2012. Cytoadherence and virulence - the case of Plasmodium knowlesi malaria. *Malar J*, 11, 33.
- FIGTREE, M., LEE, R., BAIN, L., KENNEDY, T., MACKERTICH, S., URBAN, M., CHENG, Q. & HUDSON, B. J. 2010. Plasmodium knowlesi in human, Indonesian Borneo. *Emerg Infect Dis*, 16, 672-4.
- FONAGER, J., FRANKE-FAYARD, B. M., ADAMS, J. H., RAMESAR, J., KLOP, O., KHAN, S. M., JANSE, C. J. & WATERS, A. P. 2011. Development of the piggyBac transposable system for Plasmodium berghei and its application for random mutagenesis in malaria parasites. *BMC Genomics*, 12, 155.
- FRANCIA, M. E. & STRIEPEN, B. 2014. Cell division in apicomplexan parasites. *Nat Rev Microbiol*, 12, 125-36.
- FRANCIS, S. E., SULLIVAN, D. J., JR. & GOLDBERG, D. E. 1997. Hemoglobin metabolism in the malaria parasite Plasmodium falciparum. *Annu Rev Microbiol*, 51, 97-123.
- FRANKE-FAYARD, B., JANSE, C. J., CUNHA-RODRIGUES, M., RAMESAR, J., BUSCHER, P., QUE, I., LOWIK, C., VOSHOL, P. J., DEN BOER, M. A., VAN DUINEN, S. G., FEBBRAIO, M., MOTA, M. M. & WATERS, A. P. 2005. Murine malaria parasite sequestration: CD36 is the major receptor, but cerebral pathology is unlinked to sequestration. *Proc Natl Acad Sci U S A*, 102, 11468-73.
- FREEMAN, R. R., TREJDOSIEWICZ, A. J. & CROSS, G. A. 1980. Protective monoclonal antibodies recognising stage-specific merozoite antigens of a rodent malaria parasite. *Nature*, 284, 366-8.
- FULTON, J. D. & GRANT, P. T. 1956. The sulphur requirements of the erythrocytic form of Plasmodium knowlesi. *Biochem J*, 63, 274-82.
- GALAWAY, F., DROUGHT, L. G., FALA, M., CROSS, N., KEMP, A. C., RAYNER, J. C. & WRIGHT, G. J. 2017. P113 is a merozoite surface protein that binds the N terminus of Plasmodium falciparum RH5. *Nat Commun*, 8, 14333.
- GALINSKI, M. R., LAPP, S. A., PETERSON, M. S., AY, F., JOYNER, C. J., KG, L. E. R., FONSECA, L. L., VOIT, E. O. & MAHPIC, C. 2017. Plasmodium knowlesi: a superb in vivo nonhuman primate model of antigenic variation in malaria. *Parasitology*, 1-16.
- GALINSKI, M. R., MEDINA, C. C., INGRAVALLO, P. & BARNWELL, J. W. 1992. A reticulocyte-binding protein complex of Plasmodium vivax merozoites. *Cell*, 69, 1213-26.
- GARDNER, M. J., HALL, N., FUNG, E., WHITE, O., BERRIMAN, M., HYMAN, R. W., CARLTON, J. M., PAIN, A., NELSON, K. E., BOWMAN, S., PAULSEN, I. T., JAMES, K., EISEN, J. A., RUTHERFORD, K., SALZBERG, S. L., CRAIG, A., KYES, S., CHAN, M. S., NENE, V., SHALLOM, S. J., SUH, B.,

- PETERSON, J., ANGIUOLI, S., PERTEA, M., ALLEN, J., SELENGUT, J., HAFT, D., MATHER, M. W., VAIDYA, A. B., MARTIN, D. M., FAIRLAMB, A. H., FRAUNHOLZ, M. J., ROOS, D. S., RALPH, S. A., MCFADDEN, G. I., CUMMINGS, L. M., SUBRAMANIAN, G. M., MUNGALL, C., VENTER, J. C., CARUCCI, D. J., HOFFMAN, S. L., NEWBOLD, C., DAVIS, R. W., FRASER, C. M. & BARRELL, B. 2002. Genome sequence of the human malaria parasite *Plasmodium falciparum*. *Nature*, 419, 498-511.
- GARNHAM, P. C. C. 1966. *Malaria Parasites and Other Haemosporidia*, Oxford Blackwell Scientific Publications.
- GAUR, D., FURUYA, T., MU, J., JIANG, L. B., SU, X. Z. & MILLER, L. H. 2006. Upregulation of expression of the reticulocyte homology gene 4 in the *Plasmodium falciparum* clone Dd2 is associated with a switch in the erythrocyte invasion pathway. *Mol Biochem Parasitol*, 145, 205-15.
- GERALD, N., MAHAJAN, B. & KUMAR, S. 2011. Mitosis in the human malaria parasite *Plasmodium falciparum*. *Eukaryot Cell*, 10, 474-82.
- GHORBAL, M., GORMAN, M., MACPHERSON, C. R., MARTINS, R. M., SCHERF, A. & LOPEZ-RUBIO, J. J. 2014. Genome editing in the human malaria parasite *Plasmodium falciparum* using the CRISPR-Cas9 system. *Nat Biotechnol*, 32, 819-21.
- GIADOM, B., DE VEER, G. E., VAN HENS BROEK, M. B., CORRAH, P. T., JAFFAR, S. & GREENWOOD, B. M. 1996. A comparative study of parenteral chloroquine, quinine and pyrimethamine-sulfadoxine in the treatment of Gambian children with complicated, non-cerebral malaria. *Ann Trop Paediatr*, 16, 85-91.
- GILSON, P. R. & CRABB, B. S. 2009. Morphology and kinetics of the three distinct phases of red blood cell invasion by *Plasmodium falciparum* merozoites. *Int J Parasitol*, 39, 91-6.
- GILSON, P. R., NEBL, T., VUKCEVIC, D., MORITZ, R. L., SARGEANT, T., SPEED, T. P., SCHOFIELD, L. & CRABB, B. S. 2006. Identification and stoichiometry of glycosylphosphatidylinositol-anchored membrane proteins of the human malaria parasite *Plasmodium falciparum*. *Mol Cell Proteomics*, 5, 1286-99.
- GIOVANNINI, D., SPATH, S., LACROIX, C., PERAZZI, A., BARGIERI, D., LAGAL, V., LEBUGLE, C., COMBE, A., THIBERGE, S., BALDACCI, P., TARDIEUX, I. & MENARD, R. 2011. Independent roles of apical membrane antigen 1 and rhoptry neck proteins during host cell invasion by apicomplexa. *Cell Host Microbe*, 10, 591-602.
- GISSELBERG, J. E., DELLIBOVI-RAGHEB, T. A., MATTHEWS, K. A., BOSCH, G. & PRIGGE, S. T. 2013. The suf iron-sulfur cluster synthesis pathway is required for apicoplast maintenance in malaria parasites. *PLoS Pathog*, 9, e1003655.
- GOEL, S., PALMKVIST, M., MOLL, K., JOANNIN, N., LARA, P., AKHOURI, R. R., MORADI, N., OJEMALM, K., WESTMAN, M., ANGELETTI, D., KJELLIN, H., LEHTIO, J., BLIXT, O., IDESTROM, L., GAHMBERG, C. G., STORRY, J. R., HULT, A. K., OLSSON, M. L., VON HEIJNE, G., NILSSON, I. & WAHLGREN, M. 2015. RIFINs are adhesins implicated in severe *Plasmodium falciparum* malaria. *Nat Med*, 21, 314-7.

- GOEL, V. K., LI, X., CHEN, H., LIU, S. C., CHISHTI, A. H. & OH, S. S. 2003. Band 3 is a host receptor binding merozoite surface protein 1 during the *Plasmodium falciparum* invasion of erythrocytes. *Proc Natl Acad Sci U S A*, 100, 5164-9.
- GRAEWE, S., RANKIN, K. E., LEHMANN, C., DESCHERMEIER, C., HECHT, L., FROEHLKE, U., STANWAY, R. R. & HEUSSLER, V. 2011. Hostile takeover by *Plasmodium*: reorganization of parasite and host cell membranes during liver stage egress. *PLoS Pathog*, 7, e1002224.
- GRECH, K., MARTINELLI, A., PATHIRANA, S., WALLIKER, D., HUNT, P. & CARTER, R. 2002. Numerous, robust genetic markers for *Plasmodium chabaudi* by the method of amplified fragment length polymorphism. *Mol Biochem Parasitol*, 123, 95-104.
- GRURING, C., MOON, R. W., LIM, C., HOLDER, A. A., BLACKMAN, M. J. & DURAISINGH, M. T. 2014. Human red blood cell-adapted *Plasmodium knowlesi* parasites: a new model system for malaria research. *Cell Microbiol*, 16, 612-20.
- GRUSZCZYK, J., LIM, N. T., ARNOTT, A., HE, W. Q., NGUITRAGOOL, W., ROOBSOONG, W., MOK, Y. F., MURPHY, J. M., SMITH, K. R., LEE, S., BAHLO, M., MUELLER, I., BARRY, A. E. & THAM, W. H. 2016. Structurally conserved erythrocyte-binding domain in *Plasmodium* provides a versatile scaffold for alternate receptor engagement. *Proc Natl Acad Sci U S A*, 113, E191-200.
- GUIZETTI, J. & SCHERF, A. 2013. Silence, activate, poise and switch! Mechanisms of antigenic variation in *Plasmodium falciparum*. *Cell Microbiol*, 15, 718-26.
- GUNALAN, K., GAO, X., LIEW, K. J. & PREISER, P. R. 2011. Differences in erythrocyte receptor specificity of different parts of the *Plasmodium falciparum* reticulocyte binding protein homologue 2a. *Infect Immun*, 79, 3421-30.
- GUNALAN, K., GAO, X., YAP, S. S., HUANG, X. & PREISER, P. R. 2013. The role of the reticulocyte-binding-like protein homologues of *Plasmodium* in erythrocyte sensing and invasion. *Cell Microbiol*, 15, 35-44.
- GUNALAN, K., LO, E., HOSTETLER, J. B., YEWHALAW, D., MU, J., NEAFSEY, D. E., YAN, G. & MILLER, L. H. 2016. Role of *Plasmodium vivax* Duffy-binding protein 1 in invasion of Duffy-null Africans. *Proc Natl Acad Sci U S A*, 113, 6271-6.
- HALE, V. L., WATERMEYER, J. M., HACKETT, F., VIZCAY-BARRENA, G., VAN OOIJ, C., THOMAS, J. A., SPINK, M. C., HARKIOLAKI, M., DUKE, E., FLECK, R. A., BLACKMAN, M. J. & SAIBIL, H. R. 2017. Parasitophorous vacuole poration precedes its rupture and rapid host erythrocyte cytoskeleton collapse in *Plasmodium falciparum* egress. *Proc Natl Acad Sci U S A*, 114, 3439-3444.
- HARVEY, K. L., YAP, A., GILSON, P. R., COWMAN, A. F. & CRABB, B. S. 2014. Insights and controversies into the role of the key apicomplexan invasion ligand, Apical Membrane Antigen 1. *Int J Parasitol*, 44, 853-7.
- HAYTON, K., GAUR, D., LIU, A., TAKAHASHI, J., HENSCHEN, B., SINGH, S., LAMBERT, L., FURUYA, T., BOUTTENOT, R., DOLL, M., NAWAZ, F., MU, J., JIANG, L., MILLER, L. H. & WELLEMS, T. E. 2008. Erythrocyte binding protein PfRH5 polymorphisms determine species-specific pathways of *Plasmodium falciparum* invasion. *Cell Host Microbe*, 4, 40-51.

- HERRERA, S., PERLAZA, B. L., BONELO, A. & AREVALO-HERRERA, M. 2002. Aotus monkeys: their great value for anti-malaria vaccines and drug testing. *Int J Parasitol*, 32, 1625-35.
- HESTER, J., CHAN, E. R., MENARD, D., MERCEREAU-PUJALON, O., BARNWELL, J., ZIMMERMAN, P. A. & SERRE, D. 2013. De novo assembly of a field isolate genome reveals novel Plasmodium vivax erythrocyte invasion genes. *PLoS Negl Trop Dis*, 7, e2569.
- HIETANEN, J., CHIM-ONG, A., CHIRAMANEWONG, T., GRUSZCZYK, J., ROOBSOONG, W., THAM, W. H., SATTABONGKOT, J. & NGUITRAGOOL, W. 2015. Gene Models, Expression Repertoire, and Immune Response of Plasmodium vivax Reticulocyte Binding Proteins. *Infect Immun*, 84, 677-85.
- HOLDER, A. A. & FREEMAN, R. R. 1981. Immunization against blood-stage rodent malaria using purified parasite antigens. *Nature*, 294, 361-4.
- HOPP, C. S., BOWYER, P. W. & BAKER, D. A. 2012. The role of cGMP signalling in regulating life cycle progression of Plasmodium. *Microbes Infect*, 14, 831-7.
- HULDEN, L. & HULDEN, L. 2011. Activation of the hypnozoite: a part of Plasmodium vivax life cycle and survival. *Malar J*, 10, 90.
- HUNT, P., MARTINELLI, A., FAWCETT, R., CARLTON, J., CARTER, R. & WALLIKER, D. 2004. Gene synteny and chloroquine resistance in Plasmodium chabaudi. *Mol Biochem Parasitol*, 136, 157-64.
- HUNT, P., MARTINELLI, A., MODRZYNSKA, K., BORGES, S., CREASEY, A., RODRIGUES, L., BERALDI, D., LOEWE, L., FAWCETT, R., KUMAR, S., THOMSON, M., TRIVEDI, U., OTTO, T. D., PAIN, A., BLAXTER, M. & CRAVO, P. 2010. Experimental evolution, genetic analysis and genome re-sequencing reveal the mutation conferring artemisinin resistance in an isogenic lineage of malaria parasites. *BMC Genomics*, 11, 499.
- HURWITZ, E. S., JOHNSON, D. & CAMPBELL, C. C. 1981. Resistance of Plasmodium falciparum malaria to sulfadoxine-pyrimethamine ('Fansidar') in a refugee camp in Thailand. *Lancet*, 1, 1068-70.
- HVIID, L. & JENSEN, A. T. 2015. PfEMP1 - A Parasite Protein Family of Key Importance in Plasmodium falciparum Malaria Immunity and Pathogenesis. *Adv Parasitol*, 88, 51-84.
- JAMBOU, R., EL-ASSAAD, F., COMBES, V. & GRAU, G. E. 2011. In vitro culture of Plasmodium berghei-ANKA maintains infectivity of mouse erythrocytes inducing cerebral malaria. *Malar J*, 10, 346.
- JANSE, C. J., CAMARGO, A., DEL PORTILLO, H. A., HERRERA, S., KUMLIEN, S., MONS, B., THOMAS, A. & WATERS, A. P. 1994. Removal of leucocytes from Plasmodium vivax-infected blood. *Ann Trop Med Parasitol*, 88, 213-6.
- JANSE, C. J., RAMESAR, J. & WATERS, A. P. 2006. High-efficiency transfection and drug selection of genetically transformed blood stages of the rodent malaria parasite Plasmodium berghei. *Nat Protoc*, 1, 346-56.
- JANSE, C. J. & WATERS, A. P. 2007. The exoneme helps malaria parasites to break out of blood cells. *Cell*, 131, 1036-8.
- JANSSEN, C. S., BARRETT, M. P., LAWSON, D., QUAIL, M. A., HARRIS, D., BOWMAN, S., PHILLIPS, R. S. & TURNER, C. M. 2001. Gene discovery in Plasmodium chabaudi by genome survey sequencing. *Mol Biochem Parasitol*, 113, 251-60.

- JEFFERY, G. M. 1962. Survival of trophozoites of *Plasmodium berghei* and *Plasmodium gallinaceum* in glycerolized whole blood at low temperatures. *J Parasitol*, 48, 601-6.
- JESLYN, W. P., HUAT, T. C., VERNON, L., IRENE, L. M., SUNG, L. K., JARROD, L. P., SINGH, B. & CHING, N. L. 2011. Molecular epidemiological investigation of *Plasmodium knowlesi* in humans and macaques in Singapore. *Vector Borne Zoonotic Dis*, 11, 131-5.
- JIANG, N., CHANG, Q., SUN, X., LU, H., YIN, J., ZHANG, Z., WAHLGREN, M. & CHEN, Q. 2010. Co-infections with *Plasmodium knowlesi* and other malaria parasites, Myanmar. *Emerg Infect Dis*, 16, 1476-8.
- JIN, Y., KEBAIER, C. & VANDERBERG, J. 2007. Direct microscopic quantification of dynamics of *Plasmodium berghei* sporozoite transmission from mosquitoes to mice. *Infect Immun*, 75, 5532-9.
- JIRAM, A. I., VYTHILINGAM, I., NOORAZIAN, Y. M., YUSOF, Y. M., AZAHARI, A. H. & FONG, M. Y. 2012. Entomologic investigation of *Plasmodium knowlesi* vectors in Kuala Lipis, Pahang, Malaysia. *Malar J*, 11, 213.
- JONGWUTIWES, S., BUPPAN, P., KOSUVIN, R., SEETHAMCHAI, S., PATTANAWONG, U., SIRICHAISINTHOP, J. & PUTAPORNTIP, C. 2011. *Plasmodium knowlesi* Malaria in humans and macaques, Thailand. *Emerg Infect Dis*, 17, 1799-806.
- JONGWUTIWES, S., PUTAPORNTIP, C., IWASAKI, T., SATA, T. & KANBARA, H. 2004. Naturally acquired *Plasmodium knowlesi* malaria in human, Thailand. *Emerg Infect Dis*, 10, 2211-3.
- JOSLING, G. A. & LLINAS, M. 2015. Sexual development in *Plasmodium* parasites: knowing when it's time to commit. *Nat Rev Microbiol*, 13, 573-87.
- KAESTLI, M., COCKBURN, I. A., CORTES, A., BAEA, K., ROWE, J. A. & BECK, H. P. 2006. Virulence of malaria is associated with differential expression of *Plasmodium falciparum* var gene subgroups in a case-control study. *J Infect Dis*, 193, 1567-74.
- KALANON, M. & MCFADDEN, G. I. 2010. Malaria, *Plasmodium falciparum* and its apicoplast. *Biochem Soc Trans*, 38, 775-82.
- KARIUKI, M. M., LI, X., YAMODO, I., CHISHTI, A. H. & OH, S. S. 2005. Two *Plasmodium falciparum* merozoite proteins binding to erythrocyte band 3 form a direct complex. *Biochem Biophys Res Commun*, 338, 1690-5.
- KAUSHANSKY, A., MIKOLAJCZAK, S. A., VIGNALI, M. & KAPPE, S. H. 2014. Of men in mice: the success and promise of humanized mouse models for human malaria parasite infections. *Cell Microbiol*, 16, 602-11.
- KE, H., SIGALA, P. A., MIURA, K., MORRISEY, J. M., MATHER, M. W., CROWLEY, J. R., HENDERSON, J. P., GOLDBERG, D. E., LONG, C. A. & VAIDYA, A. B. 2014. The heme biosynthesis pathway is essential for *Plasmodium falciparum* development in mosquito stage but not in blood stages. *J Biol Chem*, 289, 34827-37.
- KHIM, N., SIV, S., KIM, S., MUELLER, T., FLEISCHMANN, E., SINGH, B., DIVIS, P. C., STEENKESTE, N., DUVAL, L., BOUCHIER, C., DUONG, S., ARIEY, F. & MENARD, D. 2011. *Plasmodium knowlesi* infection in humans, Cambodia, 2007-2010. *Emerg Infect Dis*, 17, 1900-2.
- KLAASSEN, C. H., JEUNINK, M. A., PRINSEN, C. F., RUERS, T. J., TAN, A. C., STROBBE, L. J. & THUNNISSEN, F. B. 2003. Quantification of human DNA

- in feces as a diagnostic test for the presence of colorectal cancer. *Clin Chem*, 49, 1185-7.
- KOCKEN, C. H., OZWARA, H., VAN DER WEL, A., BEETSMA, A. L., MWENDA, J. M. & THOMAS, A. W. 2002. Plasmodium knowlesi provides a rapid in vitro and in vivo transfection system that enables double-crossover gene knockout studies. *Infect Immun*, 70, 655-60.
- KORIR, C. C. & GALINSKI, M. R. 2006. Proteomic studies of Plasmodium knowlesi SICA variant antigens demonstrate their relationship with P. falciparum EMP1. *Infect Genet Evol*, 6, 75-9.
- KOUSSIS, K., WITHERS-MARTINEZ, C., YEOH, S., CHILD, M., HACKETT, F., KNUEPFER, E., JULIANO, L., WOEHLBIER, U., BUJARD, H. & BLACKMAN, M. J. 2009. A multifunctional serine protease primes the malaria parasite for red blood cell invasion. *EMBO J*, 28, 725-35.
- KOVACS, S. D., RIJKEN, M. J. & STERGACHIS, A. 2015. Treating severe malaria in pregnancy: a review of the evidence. *Drug Saf*, 38, 165-81.
- KRAEMER, S. M. & SMITH, J. D. 2006. A family affair: var genes, PfEMP1 binding, and malaria disease. *Curr Opin Microbiol*, 9, 374-80.
- KUNG, S. H., RETCHLESS, A. C., KWAN, J. Y. & ALMEIDA, R. P. 2013. Effects of DNA size on transformation and recombination efficiencies in Xylella fastidiosa. *Appl Environ Microbiol*, 79, 1712-7.
- LAISHRAM, D. D., SUTTON, P. L., NANDA, N., SHARMA, V. L., SOBTI, R. C., CARLTON, J. M. & JOSHI, H. 2012. The complexities of malaria disease manifestations with a focus on asymptomatic malaria. *Malar J*, 11, 29.
- LANGHORNE, J. & COHEN, S. 1979. Plasmodium knowlesi in the marmoset (Callithrix jacchus). *Parasitology*, 78, 67-76.
- LAPP, S. A., GERALDO, J. A., CHIEN, J. T., AY, F., PAKALA, S. B., BATUGEDARA, G., HUMPHREY, J., MA, H. C., DE, B. J., LE ROCH, K. G., GALINSKI, M. R. & KISSINGER, J. C. 2017. PacBio assembly of a Plasmodium knowlesi genome sequence with Hi-C correction and manual annotation of the SICAv var gene family. *Parasitology*, 1-14.
- LAVERAN, C. L. 1982. Classics in infectious diseases: A newly discovered parasite in the blood of patients suffering from malaria. Parasitic etiology of attacks of malaria: Charles Louis Alphonse Laveran (1845-1922). *Rev Infect Dis*, 4, 908-11.
- LAVSTSEN, T., SALANTI, A., JENSEN, A. T., ARNOT, D. E. & THEANDER, T. G. 2003. Sub-grouping of Plasmodium falciparum 3D7 var genes based on sequence analysis of coding and non-coding regions. *Malar J*, 2, 27.
- LEE, K. S., DIVIS, P. C., ZAKARIA, S. K., MATUSOP, A., JULIN, R. A., CONWAY, D. J., COX-SINGH, J. & SINGH, B. 2011. Plasmodium knowlesi: reservoir hosts and tracking the emergence in humans and macaques. *PLoS Pathog*, 7, e1002015.
- LI, H. 2011. Improving SNP discovery by base alignment quality. *Bioinformatics*, 27, 1157-8.
- LI, H., HANDSAKER, B., WYSOKER, A., FENNELL, T., RUAN, J., HOMER, N., MARTH, G., ABECASIS, G., DURBIN, R. & GENOME PROJECT DATA PROCESSING, S. 2009. The Sequence Alignment/Map format and SAMtools. *Bioinformatics*, 25, 2078-9.

- LI, J. & HAN, E. T. 2012. Dissection of the Plasmodium vivax reticulocyte binding-like proteins (PvRBPs). *Biochem Biophys Res Commun*, 426, 1-6.
- LIBRADO, P. & ROZAS, J. 2009. DnaSP v5: a software for comprehensive analysis of DNA polymorphism data. *Bioinformatics*, 25, 1451-2.
- LIM, C., HANSEN, E., DESIMONE, T. M., MORENO, Y., JUNKER, K., BEI, A., BRUGNARA, C., BUCKEE, C. O. & DURAISINGH, M. T. 2013. Expansion of host cellular niche can drive adaptation of a zoonotic malaria parasite to humans. *Nat Commun*, 4, 1638.
- LIN, C. S., UBOLDI, A. D., EPP, C., BUJARD, H., TSUBOI, T., CZABOTAR, P. E. & COWMAN, A. F. 2016. Multiple Plasmodium falciparum Merozoite Surface Protein 1 Complexes Mediate Merozoite Binding to Human Erythrocytes. *J Biol Chem*, 291, 7703-15.
- LOBO, C. A., RODRIGUEZ, M., REID, M. & LUSTIGMAN, S. 2003. Glycophorin C is the receptor for the Plasmodium falciparum erythrocyte binding ligand PfEBP-2 (baebl). *Blood*, 101, 4628-31.
- LOPATICKI, S., MAIER, A. G., THOMPSON, J., WILSON, D. W., THAM, W. H., TRIGLIA, T., GOUT, A., SPEED, T. P., BEESON, J. G., HEALER, J. & COWMAN, A. F. 2011. Reticulocyte and erythrocyte binding-like proteins function cooperatively in invasion of human erythrocytes by malaria parasites. *Infect Immun*, 79, 1107-17.
- LU, J., TONG, Y., PAN, J., YANG, Y., LIU, Q., TAN, X., ZHAO, S., QIN, L. & CHEN, X. 2016. A redesigned CRISPR/Cas9 system for marker-free genome editing in Plasmodium falciparum. *Parasit Vectors*, 9, 198.
- LUBIS, I. N., WIJAYA, H., LUBIS, M., LUBIS, C. P., DIVIS, P. C., BESHIR, K. B. & SUTHERLAND, C. J. 2017. Contribution of Plasmodium knowlesi to multi-species human malaria infections in North Sumatera, Indonesia. *J Infect Dis*.
- LUCHAVEZ, J., ESPINO, F., CURAMENG, P., ESPINA, R., BELL, D., CHIODINI, P., NOLDER, D., SUTHERLAND, C., LEE, K. S. & SINGH, B. 2008. Human Infections with Plasmodium knowlesi, the Philippines. *Emerg Infect Dis*, 14, 811-3.
- MAENO, Y., CULLETON, R., QUANG, N. T., KAWAI, S., MARCHAND, R. P. & NAKAZAWA, S. 2016. Plasmodium knowlesi and human malaria parasites in Khan Phu, Vietnam: Gametocyte production in humans and frequent co-infection of mosquitoes. *Parasitology*, 1-9.
- MAHDAVI, S. A., RAEESI, A., FARAJI, L., YOUSSEFI, M. R. & RAHIMI, M. T. 2014. Malaria or flu? A case report of misdiagnosis. *Asian Pac J Trop Biomed*, 4, S56-8.
- MAIER, A. G., BAUM, J., SMITH, B., CONWAY, D. J. & COWMAN, A. F. 2009. Polymorphisms in erythrocyte binding antigens 140 and 181 affect function and binding but not receptor specificity in Plasmodium falciparum. *Infect Immun*, 77, 1689-99.
- MAIER, A. G., DURAISINGH, M. T., REEDER, J. C., PATEL, S. S., KAZURA, J. W., ZIMMERMAN, P. A. & COWMAN, A. F. 2003. Plasmodium falciparum erythrocyte invasion through glycophorin C and selection for Gerbich negativity in human populations. *Nat Med*, 9, 87-92.
- MARCHAND, R. P., CULLETON, R., MAENO, Y., QUANG, N. T. & NAKAZAWA, S. 2011. Co-infections of Plasmodium knowlesi, P. falciparum, and P. vivax

- among Humans and Anopheles dirus Mosquitoes, Southern Vietnam. *Emerg Infect Dis*, 17, 1232-9.
- MARKUS, M. B. 2015. Do hypnozoites cause relapse in malaria? *Trends Parasitol*, 31, 239-45.
- MAYER, D. C., COFIE, J., JIANG, L., HARTL, D. L., TRACY, E., KABAT, J., MENDOZA, L. H. & MILLER, L. H. 2009. Glycophorin B is the erythrocyte receptor of Plasmodium falciparum erythrocyte-binding ligand, EBL-1. *Proc Natl Acad Sci U S A*, 106, 5348-52.
- MAYER, D. C., MU, J. B., FENG, X., SU, X. Z. & MILLER, L. H. 2002. Polymorphism in a Plasmodium falciparum erythrocyte-binding ligand changes its receptor specificity. *J Exp Med*, 196, 1523-8.
- MAYER, D. C., MU, J. B., KANEKO, O., DUAN, J., SU, X. Z. & MILLER, L. H. 2004. Polymorphism in the Plasmodium falciparum erythrocyte-binding ligand JESEBL/EBA-181 alters its receptor specificity. *Proc Natl Acad Sci U S A*, 101, 2518-23.
- MCCOUBRIE, J. E., MILLER, S. K., SARGEANT, T., GOOD, R. T., HODDER, A. N., SPEED, T. P., DE KONING-WARD, T. F. & CRABB, B. S. 2007. Evidence for a common role for the serine-type Plasmodium falciparum serine repeat antigen proteases: implications for vaccine and drug design. *Infect Immun*, 75, 5565-74.
- MCFADDEN, G. I. & YEH, E. 2017. The apicoplast: now you see it, now you don't. *Int J Parasitol*, 47, 137-144.
- MELNIKOV, A., GALINSKY, K., ROGOV, P., FENNELL, T., VAN TYNE, D., RUSS, C., DANIELS, R., BARNES, K. G., BOCHICCHIO, J., NDIAYE, D., SENE, P. D., WIRTH, D. F., NUSBAUM, C., VOLKMAN, S. K., BIRREN, B. W., GNIRKE, A. & NEAFSEY, D. E. 2011. Hybrid selection for sequencing pathogen genomes from clinical samples. *Genome Biol*, 12, R73.
- MENARD, R., TAVARES, J., COCKBURN, I., MARKUS, M., ZAVALA, F. & AMINO, R. 2013. Looking under the skin: the first steps in malarial infection and immunity. *Nat Rev Microbiol*, 11, 701-12.
- MENDES, C., DIAS, F., FIGUEIREDO, J., MORA, V. G., CANO, J., DE SOUSA, B., DO ROSARIO, V. E., BENITO, A., BERZOSA, P. & AREZ, A. P. 2011. Duffy negative antigen is no longer a barrier to Plasmodium vivax--molecular evidences from the African West Coast (Angola and Equatorial Guinea). *PLoS Negl Trop Dis*, 5, e1192.
- MERCIER, C., ADJOGLE, K. D., DAUBENER, W. & DELAUW, M. F. 2005. Dense granules: are they key organelles to help understand the parasitophorous vacuole of all apicomplexa parasites? *Int J Parasitol*, 35, 829-49.
- MESHNICK, S. R. & DOBSON, M. J. 2001. The History of Antimalarial Drugs. In: ROSENTHAL, P. J. (ed.) *Antimalarial Chemotherapy: Mechanisms of Action, Resistance, and New Directions in Drug Discovery*. Totowa, NJ: Humana Press.
- MEYER, E. V., SEMENYA, A. A., OKENU, D. M., DLUZEWSKI, A. R., BANNISTER, L. H., BARNWELL, J. W. & GALINSKI, M. R. 2009. The reticulocyte binding-like proteins of P. knowlesi locate to the micronemes of merozoites and define two new members of this invasion ligand family. *Mol Biochem Parasitol*, 165, 111-21.
- MILLER, L. H., BARUCH, D. I., MARSH, K. & DOUMBO, O. K. 2002. The pathogenic basis of malaria. *Nature*, 415, 673-9.

- MILLER, L. H., FREMOUNT, H. N. & LUSE, S. A. 1971. Deep vascular schizogony of *Plasmodium knowlesi* in *Macaca mulatta*. Distribution in organs and ultrastructure of parasitized red cells. *Am J Trop Med Hyg*, 20, 816-24.
- MILLER, L. H., MASON, S. J., CLYDE, D. F. & MCGINNISS, M. H. 1976. The resistance factor to *Plasmodium vivax* in blacks. The Duffy-blood-group genotype, FyFy. *N Engl J Med*, 295, 302-4.
- MILLER, L. H., MASON, S. J., DVORAK, J. A., MCGINNISS, M. H. & ROTHMAN, I. K. 1975. Erythrocyte receptors for (*Plasmodium knowlesi*) malaria: Duffy blood group determinants. *Science*, 189, 561-3.
- MOGOLLON, C. M., VAN PUL, F. J., IMAI, T., RAMESAR, J., CHEVALLEY-MAUREL, S., DE ROO, G. M., VELD, S. A., KROEZE, H., FRANKE-FAYARD, B. M., JANSE, C. J. & KHAN, S. M. 2016. Rapid Generation of Marker-Free *P. falciparum* Fluorescent Reporter Lines Using Modified CRISPR/Cas9 Constructs and Selection Protocol. *PLoS One*, 11, e0168362.
- MOON, R. W., HALL, J., RANGKUTI, F., HO, Y. S., ALMOND, N., MITCHELL, G. H., PAIN, A., HOLDER, A. A. & BLACKMAN, M. J. 2013. Adaptation of the genetically tractable malaria pathogen *Plasmodium knowlesi* to continuous culture in human erythrocytes. *Proc Natl Acad Sci U S A*, 110, 531-6.
- MOON, R. W., SHARAF, H., HASTINGS, C. H., HO, Y. S., NAIR, M. B., RCHIAD, Z., KNUEPFER, E., RAMAPRASAD, A., MOHRING, F., AMIR, A., YUSUF, N. A., HALL, J., ALMOND, N., LAU, Y. L., PAIN, A., BLACKMAN, M. J. & HOLDER, A. A. 2016. Normocyte-binding protein required for human erythrocyte invasion by the zoonotic malaria parasite *Plasmodium knowlesi*. *Proc Natl Acad Sci U S A*, 113, 7231-6.
- MORENO-PEREZ, D. A., RUIZ, J. A. & PATARROYO, M. A. 2013. Reticulocytes: *Plasmodium vivax* target cells. *Biol Cell*, 105, 251-60.
- MORRIS, T., ROBERTSON, B. & GALLAGHER, M. 1996. Rapid reverse transcription-PCR detection of hepatitis C virus RNA in serum by using the TaqMan fluorogenic detection system. *J Clin Microbiol*, 34, 2933-6.
- MORRISSETTE, N. S. & SIBLEY, L. D. 2002. Cytoskeleton of apicomplexan parasites. *Microbiol Mol Biol Rev*, 66, 21-38; table of contents.
- MOSS 2008. The history of malaria and its control. *International Encyclopedia of Public Health*. Elsevier Inc.
- MURPHY, J. R., WEISS, W. R., FRYAUFF, D., DOWLER, M., SAVRANSKY, T., STOYANOV, C., MURATOVA, O., LAMBERT, L., ORR-GONZALEZ, S., ZELESKI, K. L., HINDERER, J., FAY, M. P., JOSHI, G., GWADZ, R. W., RICHIE, T. L., VILLASANTE, E. F., RICHARDSON, J. H., DUFFY, P. E. & CHEN, J. 2014. Using infective mosquitoes to challenge monkeys with *Plasmodium knowlesi* in malaria vaccine studies. *Malar J*, 13, 215.
- NACER, A., WALKER, K. & HURD, H. 2008. Localisation of laminin within *Plasmodium berghei* oocysts and the midgut epithelial cells of *Anopheles stephensi*. *Parasit Vectors*, 1, 33.
- NAING, C., WHITTAKER, M. A., NYUNT WAI, V. & MAK, J. W. 2014. Is *Plasmodium vivax* malaria a severe malaria?: a systematic review and meta-analysis. *PLoS Negl Trop Dis*, 8, e3071.
- NAKA, I., PATARAPOTIKUL, J., HANANANTACHAI, H., IMAI, H. & OHASHI, J. 2014. Association of the endothelial protein C receptor (PROCR) rs867186-G allele with protection from severe malaria. *Malar J*, 13, 105.

- NERY, S., DEANS, A. M., MOSOBO, M., MARSH, K., ROWE, J. A. & CONWAY, D. J. 2006. Expression of Plasmodium falciparum genes involved in erythrocyte invasion varies among isolates cultured directly from patients. *Mol Biochem Parasitol*, 149, 208-15.
- NEWBOLD, C., CRAIG, A., KYES, S., ROWE, A., FERNANDEZ-REYES, D. & FAGAN, T. 1999. Cytoadherence, pathogenesis and the infected red cell surface in Plasmodium falciparum. *Int J Parasitol*, 29, 927-37.
- NIANG, M., BEI, A. K., MADNANI, K. G., PELLY, S., DANKWA, S., KANJEE, U., GUNALAN, K., AMALADOSS, A., YEO, K. P., BOB, N. S., MALLERET, B., DURAISINGH, M. T. & PREISER, P. R. 2014. STEVOR is a Plasmodium falciparum erythrocyte binding protein that mediates merozoite invasion and rosetting. *Cell Host Microbe*, 16, 81-93.
- O'DONNELL, R. A., HACKETT, F., HOWELL, S. A., TREECK, M., STRUCK, N., KRNAJSKI, Z., WITHERS-MARTINEZ, C., GILBERGER, T. W. & BLACKMAN, M. J. 2006. Intramembrane proteolysis mediates shedding of a key adhesin during erythrocyte invasion by the malaria parasite. *J Cell Biol*, 174, 1023-33.
- OGUIKE, M. C., BETSON, M., BURKE, M., NOLDER, D., STOTHARD, J. R., KLEINSCHMIDT, I., PROIETTI, C., BOUSEMA, T., NDOUNGA, M., TANABE, K., NTEGE, E., CULLETON, R. & SUTHERLAND, C. J. 2011. Plasmodium ovale curtisi and Plasmodium ovale wallikeri circulate simultaneously in African communities. *Int J Parasitol*, 41, 677-83.
- OLIVIERI, A., COLLINS, C. R., HACKETT, F., WITHERS-MARTINEZ, C., MARSHALL, J., FLYNN, H. R., SKEHEL, J. M. & BLACKMAN, M. J. 2011. Juxtamembrane shedding of Plasmodium falciparum AMA1 is sequence independent and essential, and helps evade invasion-inhibitory antibodies. *PLoS Pathog*, 7, e1002448.
- ONDITI, F. I., NYAMONGO, O. W., OMWANDHO, C. O., MAINA, N. W., MALOBA, F., FARAH, I. O., KING, C. L., MOORE, J. M. & OZWARA, H. S. 2015. Parasite accumulation in placenta of non-immune baboons during Plasmodium knowlesi infection. *Malar J*, 14, 118.
- ORD, R. L., CALDEIRA, J. C., RODRIGUEZ, M., NOE, A., CHACKERIAN, B., PEABODY, D. S., GUTIERREZ, G. & LOBO, C. A. 2014. A malaria vaccine candidate based on an epitope of the Plasmodium falciparum RH5 protein. *Malar J*, 13, 326.
- ORLANDI, P. A., KLOTZ, F. W. & HAYNES, J. D. 1992. A malaria invasion receptor, the 175-kilodalton erythrocyte binding antigen of Plasmodium falciparum recognizes the terminal Neu5Ac(alpha 2-3)Gal- sequences of glycophorin A. *J Cell Biol*, 116, 901-9.
- ORR, R. Y., PHILIP, N. & WATERS, A. P. 2012. Improved negative selection protocol for Plasmodium berghei in the rodent malarial model. *Malar J*, 11, 103.
- OSIER, F. H., MACKINNON, M. J., CROSNIER, C., FEGAN, G., KAMUYU, G., WANAGURU, M., OGADA, E., MCDADE, B., RAYNER, J. C., WRIGHT, G. J. & MARSH, K. 2014. New antigens for a multicomponent blood-stage malaria vaccine. *Sci Transl Med*, 6, 247ra102.
- OTTO, T. D., BOHME, U., JACKSON, A. P., HUNT, M., FRANKE-FAYARD, B., HOEIJMAKERS, W. A., RELIGA, A. A., ROBERTSON, L., SANDERS, M., OGUN, S. A., CUNNINGHAM, D., ERHART, A., BILLKER, O., KHAN, S.

- M., STUNNENBERG, H. G., LANGHORNE, J., HOLDER, A. A., WATERS, A. P., NEWBOLD, C. I., PAIN, A., BERRIMAN, M. & JANSE, C. J. 2014a. A comprehensive evaluation of rodent malaria parasite genomes and gene expression. *BMC Biol*, 12, 86.
- OTTO, T. D., RAYNER, J. C., BOHME, U., PAIN, A., SPOTTISWOODE, N., SANDERS, M., QUAIL, M., OLLOMO, B., RENAUD, F., THOMAS, A. W., PRUGNOLLE, F., CONWAY, D. J., NEWBOLD, C. & BERRIMAN, M. 2014b. Genome sequencing of chimpanzee malaria parasites reveals possible pathways of adaptation to human hosts. *Nat Commun*, 5, 4754.
- OYOLA, S. O., ARIANI, C. V., HAMILTON, W. L., KEKRE, M., AMENGA-ETEGO, L. N., GHANSAH, A., RUTLEDGE, G. G., REDMOND, S., MANSKE, M., JYOTHI, D., JACOB, C. G., OTTO, T. D., ROCKETT, K., NEWBOLD, C. I., BERRIMAN, M. & KWIATKOWSKI, D. P. 2016. Whole genome sequencing of Plasmodium falciparum from dried blood spots using selective whole genome amplification. *Malar J*, 15, 597.
- OZWARA, H., LANGERMANS, J. A., MAAMUN, J., FARAH, I. O., YOLE, D. S., MWENDA, J. M., WEILER, H. & THOMAS, A. W. 2003. Experimental infection of the olive baboon (*Papio anubis*) with Plasmodium knowlesi: severe disease accompanied by cerebral involvement. *Am J Trop Med Hyg*, 69, 188-94.
- PAIN, A., BOHME, U., BERRY, A. E., MUNGALL, K., FINN, R. D., JACKSON, A. P., MOURIER, T., MISTRY, J., PASINI, E. M., ASLETT, M. A., BALASUBRAMANIAM, S., BORGWARDT, K., BROOKS, K., CARRET, C., CARVER, T. J., CHEREVACH, I., CHILLINGWORTH, T., CLARK, T. G., GALINSKI, M. R., HALL, N., HARPER, D., HARRIS, D., HAUSER, H., IVENS, A., JANSSEN, C. S., KEANE, T., LARKE, N., LAPP, S., MARTI, M., MOULE, S., MEYER, I. M., ORMOND, D., PETERS, N., SANDERS, M., SANDERS, S., SARGEANT, T. J., SIMMONDS, M., SMITH, F., SQUARES, R., THURSTON, S., TIVEY, A. R., WALKER, D., WHITE, B., ZUIDERWIJK, E., CHURCHER, C., QUAIL, M. A., COWMAN, A. F., TURNER, C. M., RAJANDREAM, M. A., KOCKEN, C. H., THOMAS, A. W., NEWBOLD, C. I., BARRELL, B. G. & BERRIMAN, M. 2008. The genome of the simian and human malaria parasite Plasmodium knowlesi. *Nature*, 455, 799-803.
- PASTERNAK, N. D. & DZIKOWSKI, R. 2009. PfEMP1: an antigen that plays a key role in the pathogenicity and immune evasion of the malaria parasite Plasmodium falciparum. *Int J Biochem Cell Biol*, 41, 1463-6.
- PEHRSON, C., MATHIESEN, L., HENO, K. K., SALANTI, A., RESENDE, M., DZIKOWSKI, R., DAMM, P., HANSSON, S. R., KING, C. L., SCHNEIDER, H., WANG, C. W., LAVSTSEN, T., THEANDER, T. G., KNUDSEN, L. E. & NIELSEN, M. A. 2016. Adhesion of Plasmodium falciparum infected erythrocytes in ex vivo perfused placental tissue: a novel model of placental malaria. *Malar J*, 15, 292.
- PEREZ-TOLEDO, K., ROJAS-MEZA, A. P., MANCIO-SILVA, L., HERNANDEZ-CUEVAS, N. A., DELGADILLO, D. M., VARGAS, M., MARTINEZ-CALVILLO, S., SCHERF, A. & HERNANDEZ-RIVAS, R. 2009. Plasmodium falciparum heterochromatin protein 1 binds to tri-methylated histone 3 lysine 9 and is linked to mutually exclusive expression of var genes. *Nucleic Acids Res*, 37, 2596-606.

- PFANDER, C., ANAR, B., SCHWACH, F., OTTO, T. D., BROCHET, M., VOLKMANN, K., QUAIL, M. A., PAIN, A., ROSEN, B., SKARNES, W., RAYNER, J. C. & BILLKER, O. 2011. A scalable pipeline for highly effective genetic modification of a malaria parasite. *Nat Methods*, 8, 1078-82.
- PINHEIRO, M. M., AHMED, M. A., MILLAR, S. B., SANDERSON, T., OTTO, T. D., LU, W. C., KRISHNA, S., RAYNER, J. C. & COX-SINGH, J. 2015. Plasmodium knowlesi genome sequences from clinical isolates reveal extensive genomic dimorphism. *PLoS One*, 10, e0121303.
- PRICE, R. N., UHLEMANN, A. C., BROCKMAN, A., MCGREADY, R., ASHLEY, E., PHAIPUN, L., PATEL, R., LAING, K., LOOAREESUWAN, S., WHITE, N. J., NOSTEN, F. & KRISHNA, S. 2004. Mefloquine resistance in Plasmodium falciparum and increased pfmdr1 gene copy number. *Lancet*, 364, 438-47.
- PRUDENCIO, M., RODRIGUEZ, A. & MOTA, M. M. 2006. The silent path to thousands of merozoites: the Plasmodium liver stage. *Nat Rev Microbiol*, 4, 849-56.
- RAHIMI, B. A., THAKKINSTIAN, A., WHITE, N. J., SIRIVICHAYAKUL, C., DONDORP, A. M. & CHOKEJINDACHAI, W. 2014. Severe vivax malaria: a systematic review and meta-analysis of clinical studies since 1900. *Malar J*, 13, 481.
- RAJAHRAM, G. S., BARBER, B. E., WILLIAM, T., MENON, J., ANSTEY, N. M. & YEO, T. W. 2012. Deaths due to Plasmodium knowlesi malaria in Sabah, Malaysia: association with reporting as Plasmodium malariae and delayed parenteral artesunate. *Malar J*, 11, 284.
- RAJAHRAM, G. S., BARBER, B. E., YEO, T. W., TAN, W. W. & WILLIAM, T. 2013. Case Report: Fatal Plasmodium Knowlesi Malaria Following an Atypical Clinical Presentation and Delayed Diagnosis. *Med J Malaysia*, 68, 71-72.
- RAYNER, J. C. 2008. The merozoite has landed: reticulocyte-binding-like ligands and the specificity of erythrocyte recognition. *Trends Parasitol*, 25, 104-106.
- RAYNER, J. C., GALINSKI, M. R., INGRAVALLO, P. & BARNWELL, J. W. 2000. Two Plasmodium falciparum genes express merozoite proteins that are related to Plasmodium vivax and Plasmodium yoelii adhesive proteins involved in host cell selection and invasion. *Proc Natl Acad Sci U S A*, 97, 9648-53.
- REDDY, K. S., AMLABU, E., PANDEY, A. K., MITRA, P., CHAUHAN, V. S. & GAUR, D. 2015. Multiprotein complex between the GPI-anchored CyRPA with PfRH5 and PfRipr is crucial for Plasmodium falciparum erythrocyte invasion. *Proc Natl Acad Sci U S A*, 112, 1179-84.
- RIGLAR, D. T., RICHARD, D., WILSON, D. W., BOYLE, M. J., DEKIWADIA, C., TURNBULL, L., ANGRISANO, F., MARAPANA, D. S., ROGERS, K. L., WHITCHURCH, C. B., BEESON, J. G., COWMAN, A. F., RALPH, S. A. & BAUM, J. 2011. Super-resolution dissection of coordinated events during malaria parasite invasion of the human erythrocyte. *Cell Host Microbe*, 9, 9-20.
- RIGLAR, D. T., WHITEHEAD, L., COWMAN, A. F., ROGERS, K. L. & BAUM, J. 2016. Localisation-based imaging of malarial antigens during erythrocyte entry reaffirms a role for AMA1 but not MTRAP in invasion. *J Cell Sci*, 129, 228-42.
- RODRIGUEZ, M., LUSTIGMAN, S., MONTERO, E., OKSOV, Y. & LOBO, C. A. 2008. PfRH5: a novel reticulocyte-binding family homolog of plasmodium

- falciparum that binds to the erythrocyte, and an investigation of its receptor. *PLoS One*, 3, e3300.
- ROOBSOONG, W., THARINJAROEN, C. S., RACHAPHAEW, N., CHOBSON, P., SCHOFIELD, L., CUI, L., ADAMS, J. H. & SATTABONGKOT, J. 2015. Improvement of culture conditions for long-term in vitro culture of *Plasmodium vivax*. *Malar J*, 14, 297.
- ROTTMANN, M., MCNAMARA, C., YEUNG, B. K., LEE, M. C., ZOU, B., RUSSELL, B., SEITZ, P., PLOUFFE, D. M., DHARIA, N. V., TAN, J., COHEN, S. B., SPENCER, K. R., GONZALEZ-PAEZ, G. E., LAKSHMINARAYANA, S. B., GOH, A., SUWANARUSK, R., JEGLA, T., SCHMITT, E. K., BECK, H. P., BRUN, R., NOSTEN, F., RENIA, L., DARTOIS, V., KELLER, T. H., FIDOCK, D. A., WINZELER, E. A. & DIAGANA, T. T. 2010. Spiroindolones, a potent compound class for the treatment of malaria. *Science*, 329, 1175-80.
- ROUGEMONT, M., VAN SAANEN, M., SAHLI, R., HINRIKSON, H. P., BILLE, J. & JATON, K. 2004. Detection of four *Plasmodium* species in blood from humans by 18S rRNA gene subunit-based and species-specific real-time PCR assays. *J Clin Microbiol*, 42, 5636-43.
- ROWE, A., OBEIRO, J., NEWBOLD, C. I. & MARSH, K. 1995. *Plasmodium falciparum* rosetting is associated with malaria severity in Kenya. *Infect Immun*, 63, 2323-6.
- RUECKER, A., SHEA, M., HACKETT, F., SUAREZ, C., HIRST, E. M., MILUTINOVIC, K., WITHERS-MARTINEZ, C. & BLACKMAN, M. J. 2012. Proteolytic activation of the essential parasitophorous vacuole cysteine protease SERA6 accompanies malaria parasite egress from its host erythrocyte. *J Biol Chem*, 287, 37949-63.
- RUTLEDGE, G. G., BOHME, U., SANDERS, M., REID, A. J., COTTON, J. A., MAIGA-ASCOFARE, O., DJIMDE, A. A., APINJOH, T. O., AMENGA-ETEGO, L., MANSKE, M., BARNWELL, J. W., RENAUD, F., OLLOMO, B., PRUGNOLLE, F., ANSTEY, N. M., AUBURN, S., PRICE, R. N., MCCARTHY, J. S., KWIATKOWSKI, D. P., NEWBOLD, C. I., BERRIMAN, M. & OTTO, T. D. 2017. *Plasmodium malariae* and *P. ovale* genomes provide insights into malaria parasite evolution. *Nature*, 542, 101-104.
- RYAN, J. R., STOUTE, J. A., AMON, J., DUNTON, R. F., MTALIB, R., KOROS, J., OWOUR, B., LUCKHART, S., WIRTZ, R. A., BARNWELL, J. W. & ROSENBERG, R. 2006. Evidence for transmission of *Plasmodium vivax* among a duffy antigen negative population in Western Kenya. *Am J Trop Med Hyg*, 75, 575-81.
- SAHAR, T., REDDY, K. S., BHARADWAJ, M., PANDEY, A. K., SINGH, S., CHITNIS, C. E. & GAUR, D. 2011. *Plasmodium falciparum* reticulocyte binding-like homologue protein 2 (PfrRH2) is a key adhesive molecule involved in erythrocyte invasion. *PLoS One*, 6, e17102.
- SCHMIDT, L. H. 1973. Infections with *Plasmodium falciparum* and *Plasmodium vivax* in the owl monkey--model systems for basic biological and chemotherapeutic studies. *Trans R Soc Trop Med Hyg*, 67, 446-74.
- SEMENYA, A. A., TRAN, T. M., MEYER, E. V., BARNWELL, J. W. & GALINSKI, M. R. 2012. Two functional reticulocyte binding-like (RBL) invasion ligands of

- zoonotic *Plasmodium knowlesi* exhibit differential adhesion to monkey and human erythrocytes. *Malar J*, 11, 228.
- SERMWITTAYAWONG, N., SINGH, B., NISHIBUCHI, M., SAWANGJAROEN, N. & VUDDHAKUL, V. 2012. Human *Plasmodium knowlesi* infection in Ranong province, southwestern border of Thailand. *Malar J*, 11, 36.
- SHELBY, J. P., WHITE, J., GANESAN, K., RATHOD, P. K. & CHIU, D. T. 2003. A microfluidic model for single-cell capillary obstruction by *Plasmodium falciparum*-infected erythrocytes. *Proc Natl Acad Sci U S A*, 100, 14618-22.
- SHEN, B. & SIBLEY, L. D. 2012. The moving junction, a key portal to host cell invasion by apicomplexan parasites. *Curr Opin Microbiol*, 15, 449-55.
- SHEN, B. & SIBLEY, L. D. 2014. Toxoplasma aldolase is required for metabolism but dispensable for host-cell invasion. *Proc Natl Acad Sci U S A*, 111, 3567-72.
- SIEVERS, F., WILM, A., DINEEN, D., GIBSON, T. J., KARPLUS, K., LI, W., LOPEZ, R., MCWILLIAM, H., REMMERT, M., SODING, J., THOMPSON, J. D. & HIGGINS, D. G. 2011. Fast, scalable generation of high-quality protein multiple sequence alignments using Clustal Omega. *Mol Syst Biol*, 7, 539.
- SILMON DE MONERRI, N. C., FLYNN, H. R., CAMPOS, M. G., HACKETT, F., KOUSSIS, K., WITHERS-MARTINEZ, C., SKEHEL, J. M. & BLACKMAN, M. J. 2011. Global identification of multiple substrates for *Plasmodium falciparum* SUB1, an essential malarial processing protease. *Infect Immun*, 79, 1086-97.
- SIM, B. K., CHITNIS, C. E., WASNIOWSKA, K., HADLEY, T. J. & MILLER, L. H. 1994. Receptor and ligand domains for invasion of erythrocytes by *Plasmodium falciparum*. *Science*, 264, 1941-4.
- SINGH, A. P., OZWARA, H., KOCKEN, C. H., PURI, S. K., THOMAS, A. W. & CHITNIS, C. E. 2005. Targeted deletion of *Plasmodium knowlesi* Duffy binding protein confirms its role in junction formation during invasion. *Mol Microbiol*, 55, 1925-34.
- SINGH, B., KIM SUNG, L., MATUSOP, A., RADHAKRISHNAN, A., SHAMSUL, S. S., COX-SINGH, J., THOMAS, A. & CONWAY, D. J. 2004. A large focus of naturally acquired *Plasmodium knowlesi* infections in human beings. *Lancet*, 363, 1017-24.
- SINNIS, P. & ZAVALA, F. 2012. The skin: where malaria infection and the host immune response begin. *Semin Immunopathol*, 34, 787-92.
- SOWUNMI, A., OKUBOYEJO, T. M., GBOTOSHO, G. O. & HAPPI, C. T. 2011. Risk factors for *Plasmodium falciparum* hyperparasitaemia in malarious children. *BMC Infect Dis*, 11, 268.
- SRINIVASAN, P., BEATTY, W. L., DIOUF, A., HERRERA, R., AMBROGGIO, X., MOCH, J. K., TYLER, J. S., NARUM, D. L., PIERCE, S. K., BOOTHROYD, J. C., HAYNES, J. D. & MILLER, L. H. 2011. Binding of *Plasmodium* merozoite proteins RON2 and AMA1 triggers commitment to invasion. *Proc Natl Acad Sci U S A*, 108, 13275-80.
- SRINIVASAN, P., YASGAR, A., LUCI, D. K., BEATTY, W. L., HU, X., ANDERSEN, J., NARUM, D. L., MOCH, J. K., SUN, H., HAYNES, J. D., MALONEY, D. J., JADHAV, A., SIMEONOV, A. & MILLER, L. H. 2013. Disrupting malaria parasite AMA1-RON2 interaction with a small molecule prevents erythrocyte invasion. *Nat Commun*, 4, 2261.

- SRIPRAWAT, K., KAEWPONGSRI, S., SUWANARUSK, R., LEIMANIS, M. L., LEK-UTHAI, U., PHYO, A. P., SNOUNOU, G., RUSSELL, B., RENIA, L. & NOSTEN, F. 2009. Effective and cheap removal of leukocytes and platelets from *Plasmodium vivax* infected blood. *Malar J*, 8, 115.
- STAFFORD, W. H., BLACKMAN, M. J., HARRIS, A., SHAI, S., GRAINGER, M. & HOLDER, A. A. 1994. N-terminal amino acid sequence of the *Plasmodium falciparum* merozoite surface protein-1 polypeptides. *Mol Biochem Parasitol*, 66, 157-60.
- STALLMACH, R., KAVISHWAR, M., WITHERS-MARTINEZ, C., HACKETT, F., COLLINS, C. R., HOWELL, S. A., YEOH, S., KNUEPFER, E., ATID, A. J., HOLDER, A. A. & BLACKMAN, M. J. 2015. *Plasmodium falciparum* SERA5 plays a non-enzymatic role in the malarial asexual blood-stage lifecycle. *Mol Microbiol*, 96, 368-87.
- STANWAY, R. R., MUELLER, N., ZOBIAK, B., GRAEWE, S., FROEHLKE, U., ZESSIN, P. J., AEPFELBACHER, M. & HEUSSLER, V. T. 2011. Organelle segregation into *Plasmodium* liver stage merozoites. *Cell Microbiol*, 13, 1768-82.
- STUBBS, J., SIMPSON, K. M., TRIGLIA, T., PLOUFFE, D., TONKIN, C. J., DURAISINGH, M. T., MAIER, A. G., WINZELER, E. A. & COWMAN, A. F. 2005. Molecular mechanism for switching of *P. falciparum* invasion pathways into human erythrocytes. *Science*, 309, 1384-7.
- SULLIVAN, D. J., JR., GLUZMAN, I. Y., RUSSELL, D. G. & GOLDBERG, D. E. 1996. On the molecular mechanism of chloroquine's antimalarial action. *Proc Natl Acad Sci U S A*, 93, 11865-70.
- SUNDARARAMAN, S. A., PLENDERLEITH, L. J., LIU, W., LOY, D. E., LEARN, G. H., LI, Y., SHAW, K. S., AYOUBA, A., PEETERS, M., SPEEDE, S., SHAW, G. M., BUSHMAN, F. D., BRISSON, D., RAYNER, J. C., SHARP, P. M. & HAHN, B. H. 2016. Genomes of cryptic chimpanzee *Plasmodium* species reveal key evolutionary events leading to human malaria. *Nat Commun*, 7, 11078.
- TA, T. H., HISAM, S., LANZA, M., JIRAM, A. I., ISMAIL, N. & RUBIO, J. M. 2014. First case of a naturally acquired human infection with *Plasmodium cynomolgi*. *Malar J*, 13, 68.
- TACHIBANA, S., SULLIVAN, S. A., KAWAI, S., NAKAMURA, S., KIM, H. R., GOTO, N., ARISUE, N., PALACPAC, N. M., HONMA, H., YAGI, M., TOUGAN, T., KATAKAI, Y., KANEKO, O., MITA, T., KITA, K., YASUTOMI, Y., SUTTON, P. L., SHAKHBATYAN, R., HORII, T., YASUNAGA, T., BARNWELL, J. W., ESCALANTE, A. A., CARLTON, J. M. & TANABE, K. 2012. *Plasmodium cynomolgi* genome sequences provide insight into *Plasmodium vivax* and the monkey malaria clade. *Nat Genet*, 44, 1051-5.
- TAN, C. H., VYTHILINGAM, I., MATUSOP, A., CHAN, S. T. & SINGH, B. 2008. Bionomics of *Anopheles latens* in Kapit, Sarawak, Malaysian Borneo in relation to the transmission of zoonotic simian malaria parasite *Plasmodium knowlesi*. *Malar J*, 7, 52.
- TAO, Z. Y., XIA, H., CAO, J. & GAO, Q. 2011. Development and evaluation of a prototype non-woven fabric filter for purification of malaria-infected blood. *Malar J*, 10, 251.

- TARDIEUX, I. & BAUM, J. 2016. Reassessing the mechanics of parasite motility and host-cell invasion. *J Cell Biol*, 214, 507-15.
- TARR, S. J., MOON, R. W., HARDEGE, I. & OSBORNE, A. R. 2014. A conserved domain targets exported PHISTb family proteins to the periphery of Plasmodium infected erythrocytes. *Mol Biochem Parasitol*, 196, 29-40.
- TAWK, L., LACROIX, C., GUEIRARD, P., KENT, R., GORGETTE, O., THIBERGE, S., MERCEREAU-PUJALON, O., MENARD, R. & BARALE, J. C. 2013. A Key Role for Plasmodium Subtilisin-like SUB1 Protease in Egress of Malaria Parasites from Host Hepatocytes. *J Biol Chem*, 288, 33336-46.
- TAYLOR, H. M., GRAINGER, M. & HOLDER, A. A. 2002. Variation in the expression of a Plasmodium falciparum protein family implicated in erythrocyte invasion. *Infect Immun*, 70, 5779-89.
- THAM, W. H., LIM, N. T., WEISS, G. E., LOPATICKI, S., ANSELL, B. R., BIRD, M., LUCET, I., DORIN-SEMBLAT, D., DOERIG, C., GILSON, P. R., CRABB, B. S. & COWMAN, A. F. 2015. Plasmodium falciparum Adhesins Play an Essential Role in Signalling and Activation of Invasion into Human Erythrocytes. *PLoS Pathog*, 11, e1005343.
- THAM, W. H., WILSON, D. W., LOPATICKI, S., SCHMIDT, C. Q., TETTEH-QUARCOO, P. B., BARLOW, P. N., RICHARD, D., CORBIN, J. E., BEESON, J. G. & COWMAN, A. F. 2010. Complement receptor 1 is the host erythrocyte receptor for Plasmodium falciparum PfRh4 invasion ligand. *Proc Natl Acad Sci U S A*, 107, 17327-32.
- TRAGER, W. & JENSEN, J. B. 1976. Human malaria parasites in continuous culture. *Science*, 193, 673-5.
- TRAMPUZ, A., JEREB, M., MUZLOVIC, I. & PRABHU, R. M. 2003. Clinical review: Severe malaria. *Crit Care*, 7, 315-23.
- TREECK, M., STRUCK, N. S., HAASE, S., LANGER, C., HERRMANN, S., HEALER, J., COWMAN, A. F. & GILBERGER, T. W. 2006. A conserved region in the EBL proteins is implicated in microneme targeting of the malaria parasite Plasmodium falciparum. *J Biol Chem*, 281, 31995-2003.
- TRIGLIA, T., THAM, W. H., HODDER, A. & COWMAN, A. F. 2009. Reticulocyte binding protein homologues are key adhesins during erythrocyte invasion by Plasmodium falciparum. *Cell Microbiol*, 11, 1671-87.
- TSUKAMOTO, M., MIYATA, A. & MIYAGI, I. 1978. Surveys on Simian Malaria Parasites and Their Vector in Palawan Island, the Philippines. *Trop Med*, 20, 39-50.
- TUIKUE NDAM, N., MOUSSILIOU, A., LAVSTSEN, T., KAMALIDDIN, C., JENSEN, A. T. R., MAMA, A., TAHAR, R., WANG, C. W., JESPERSEN, J. S., ALAO, J. M., GAMAIN, B., THEANDER, T. G. & DELORON, P. 2017. Parasites Causing Cerebral Falciparum Malaria Bind Multiple Endothelial Receptors and Express EPCR and ICAM-1-Binding PfEMP1. *J Infect Dis*, 215, 1918-1925.
- TURNER, L., LAVSTSEN, T., BERGER, S. S., WANG, C. W., PETERSEN, J. E., AVRIL, M., BRAZIER, A. J., FREETH, J., JESPERSEN, J. S., NIELSEN, M. A., MAGISTRADO, P., LUSINGU, J., SMITH, J. D., HIGGINS, M. K. & THEANDER, T. G. 2013. Severe malaria is associated with parasite binding to endothelial protein C receptor. *Nature*, 498, 502-5.

- VENKATESAN, M., AMARATUNGA, C., CAMPINO, S., AUBURN, S., KOCH, O., LIM, P., UK, S., SOCHEAT, D., KWIATKOWSKI, D. P., FAIRHURST, R. M. & PLOWE, C. V. 2012. Using CF11 cellulose columns to inexpensively and effectively remove human DNA from Plasmodium falciparum-infected whole blood samples. *Malar J*, 11, 41.
- VOLLER, A., HAWKEY, C. M., RICHARDS, W. H. & RIDLEY, D. S. 1969. Human malaria (Plasmodium falciparum) in owl monkeys (Aotus trivirgatus). *J Trop Med Hyg*, 72, 153-60.
- VYTHILINGAM, I. 2010. Plasmodium knowlesi in humans: a review on the role of its vectors in Malaysia. *Trop Biomed*, 27, 1-12.
- VYTHILINGAM, I. & HIL, J. 2013. *Simian Malaria Parasites: Special Emphasis on Plasmodium knowlesi and Their Anopheles Vectors in Southeast Asia*.
- VYTHILINGAM, I., LIM, Y. A., VENUGOPALAN, B., NGUI, R., LEONG, C. S., WONG, M. L., KHAW, L., GOH, X., YAP, N., SULAIMAN, W. Y., JEFFERY, J., ZAWIAH, A. G., NOR ASZLINA, I., SHARMA, R. S., YEE LING, L. & MAHMUD, R. 2014. Plasmodium knowlesi malaria an emerging public health problem in Hulu Selangor, Selangor, Malaysia (2009-2013): epidemiologic and entomologic analysis. *Parasit Vectors*, 7, 436.
- VYTHILINGAM, I., NOORAZIAN, Y. M., HUAT, T. C., JIRAM, A. I., YUSRI, Y. M., AZAHARI, A. H., NORPARINA, I., NOORRAIN, A. & LOKMANHAKIM, S. 2008. Plasmodium knowlesi in humans, macaques and mosquitoes in peninsular Malaysia. *Parasit Vectors*, 1, 26.
- WAGNER, J. C., PLATT, R. J., GOLDFLESS, S. J., ZHANG, F. & NILES, J. C. 2014. Efficient CRISPR-Cas9-mediated genome editing in Plasmodium falciparum. *Nat Methods*, 11, 915-8.
- WAHLGREN, M., GOEL, S. & AKHOURI, R. R. 2017. Variant surface antigens of Plasmodium falciparum and their roles in severe malaria. *Nat Rev Microbiol*, 15, 479-491.
- WANAGURU, M., LIU, W., HAHN, B. H., RAYNER, J. C. & WRIGHT, G. J. 2013. RH5-Basigin interaction plays a major role in the host tropism of Plasmodium falciparum. *Proc Natl Acad Sci U S A*, 110, 20735-40.
- WANG, Q., FUJIOKA, H. & NUSSENZWEIG, V. 2005. Exit of Plasmodium sporozoites from oocysts is an active process that involves the circumsporozoite protein. *PLoS Pathog*, 1, e9.
- WATERHOUSE, A. M., PROCTER, J. B., MARTIN, D. M., CLAMP, M. & BARTON, G. J. 2009. Jalview Version 2--a multiple sequence alignment editor and analysis workbench. *Bioinformatics*, 25, 1189-91.
- WEISS, G. E., GILSON, P. R., TAECHALERTPAISARN, T., THAM, W. H., DE JONG, N. W., HARVEY, K. L., FOWKES, F. J., BARLOW, P. N., RAYNER, J. C., WRIGHT, G. J., COWMAN, A. F. & CRABB, B. S. 2015. Revealing the sequence and resulting cellular morphology of receptor-ligand interactions during Plasmodium falciparum invasion of erythrocytes. *PLoS Pathog*, 11, e1004670.
- WELLEMS, T. E. & PLOWE, C. V. 2001. Chloroquine-resistant malaria. *J Infect Dis*, 184, 770-6.
- WELLS, T. N., BURROWS, J. N. & BAIRD, J. K. 2010. Targeting the hypnozoite reservoir of Plasmodium vivax: the hidden obstacle to malaria elimination. *Trends Parasitol*, 26, 145-51.

- WERTHEIMER, S. P. & BARNWELL, J. W. 1989. Plasmodium vivax interaction with the human Duffy blood group glycoprotein: identification of a parasite receptor-like protein. *Exp Parasitol*, 69, 340-50.
- WHITE, N. J. 2011. The parasite clearance curve. *Malar J*, 10, 278.
- WHITE, N. J. 2017. Malaria parasite clearance. *Malar J*, 16, 88.
- WHITE, N. J., HIEN, T. T. & NOSTEN, F. H. 2015. A Brief History of Qinghaosu. *Trends Parasitol*, 31, 607-10.
- WHITE, N. J., PUKRITTAYAKAMEE, S., PHYO, A. P., RUEANGWEERAYUT, R., NOSTEN, F., JITTAMALA, P., JEEYAPANT, A., JAIN, J. P., LEFEVRE, G., LI, R., MAGNUSSON, B., DIAGANA, T. T. & LEONG, F. J. 2014. Spiroindolone KAE609 for falciparum and vivax malaria. *N Engl J Med*, 371, 403-10.
- WHO. 2015. *World Malaria Report 2015* [Online]. Switzerland. Available: http://www.who.int/malaria/publications/world_malaria_report_2012/wmr2012_no_profiles.pdf [Accessed 19/3/17 2017].
- WHO. 2016. *World Malaria Report 2016* [Online]. Switzerland. Available: http://www.who.int/malaria/publications/world_malaria_report_2012/wmr2012_no_profiles.pdf [Accessed 19/3/17 2017].
- WILLIAM, T., MENON, J., RAJAHRAM, G., CHAN, L., MA, G., DONALDSON, S., KHOO, S., FREDERICK, C., JELIP, J., ANSTEY, N. M. & YEO, T. W. 2011. Severe Plasmodium knowlesi malaria in a tertiary care hospital, Sabah, Malaysia. *Emerg Infect Dis*, 17, 1248-55.
- WILLMANN, M., AHMED, A., SINDER, A., WONG, I. T., WOON, L. C., SINGH, B., KRISHNA, S. & COX-SINGH, J. 2012. Laboratory markers of disease severity in Plasmodium knowlesi infection: a case control study. *Malar J*, 11, 363.
- WILSON, R. J., FARRANT, J. & WALTER, C. A. 1977. Preservation of intraerythrocytic forms of malarial parasites by one-step and two-step cooling procedures. *Bull World Health Organ*, 55, 309-15.
- WITMER, K., SCHMID, C. D., BRANCUCCI, N. M., LUAH, Y. H., PREISER, P. R., BOZDECH, Z. & VOSS, T. S. 2012. Analysis of subtelomeric virulence gene families in Plasmodium falciparum by comparative transcriptional profiling. *Mol Microbiol*, 84, 243-59.
- WONGSRICHANALAI, C. & MESHNICK, S. R. 2008. Declining artesunate-mefloquine efficacy against falciparum malaria on the Cambodia-Thailand border. *Emerg Infect Dis*, 14, 716-9.
- WORLD HEALTH ORGANISATION, W. 2012. *Management of Severe Malaria - a practical handbook*.
- WRIGHT, K. E., HJERRILD, K. A., BARTLETT, J., DOUGLAS, A. D., JIN, J., BROWN, R. E., ILLINGWORTH, J. J., ASHFIELD, R., CLEMMENSEN, S. B., DE JONGH, W. A., DRAPER, S. J. & HIGGINS, M. K. 2014. Structure of malaria invasion protein RH5 with erythrocyte basigin and blocking antibodies. *Nature*, 515, 427-30.
- WUNDERLICH, J., ROHRBACH, P. & DALTON, J. P. 2012. The malaria digestive vacuole. *Front Biosci (Schol Ed)*, 4, 1424-48.
- WURTZ, N., MINT LEKWEIRY, K., BOGREAU, H., PRADINES, B., ROGIER, C., OULD MOHAMED SALEM BOUKHARY, A., HAFID, J. E., OULD AHMEDOU SALEM, M. S., TRAPE, J. F., BASCO, L. K. & BRIOLANT, S.

2011. Vivax malaria in Mauritania includes infection of a Duffy-negative individual. *Malar J*, 10, 336.
- YAP, A., AZEVEDO, M. F., GILSON, P. R., WEISS, G. E., O'NEILL, M. T., WILSON, D. W., CRABB, B. S. & COWMAN, A. F. 2014. Conditional expression of apical membrane antigen 1 in Plasmodium falciparum shows it is required for erythrocyte invasion by merozoites. *Cell Microbiol*, 16, 642-56.
- YEOH, S., O'DONNELL, R. A., KOUSSIS, K., DLUZEWSKI, A. R., ANSELL, K. H., OSBORNE, S. A., HACKETT, F., WITHERS-MARTINEZ, C., MITCHELL, G. H., BANNISTER, L. H., BRYANS, J. S., KETTLEBOROUGH, C. A. & BLACKMAN, M. J. 2007. Subcellular discharge of a serine protease mediates release of invasive malaria parasites from host erythrocytes. *Cell*, 131, 1072-83.
- YUSUF, N. A., GREEN, J. L., WALL, R. J., KNUEPFER, E., MOON, R. W., SCHULTE-HUXEL, C., STANWAY, R. R., MARTIN, S. R., HOWELL, S. A., DOUSE, C. H., COTA, E., TATE, E. W., TEWARI, R. & HOLDER, A. A. 2015. The Plasmodium Class XIV Myosin, MyoB, Has a Distinct Subcellular Location in Invasive and Motile Stages of the Malaria Parasite and an Unusual Light Chain. *J Biol Chem*, 290, 12147-64.
- ZHANG, C., XIAO, B., JIANG, Y., ZHAO, Y., LI, Z., GAO, H., LING, Y., WEI, J., LI, S., LU, M., SU, X. Z., CUI, H. & YUAN, J. 2014. Efficient editing of malaria parasite genome using the CRISPR/Cas9 system. *MBio*, 5, e01414-14.